MECHANISMS OF FILLER FLOCCULATION WITH PEO/COFACTOR DUAL-COMPONENT FLOCCULANTS

By

CHEN LU, B. ENG.

A Thesis

Submitted to the School of Graduate Studies

in Partial Fulfillment of the Requirements

for the Degree

Doctor of Philosophy

McMaster University

MECHANISMS OF FILLER FLOCCULATION WITH PEO/COFACTOR DUAL-COMPONENT FLOCCULANTS

DOCTOR OF PHILOSOPHY (2003) McMaster University

(Chemical Engineering) Hamilton, Ontario, Canada

TITLE: Mechanisms of Filler Flocculation with PEO/Cofactor Dual-component Flocculants

AUTHOR: Chen Lu, B. Eng. (Tianjin University)

SUPERVISOR: Professor Robert H. Pelton

NUMBER OF PAGES: vii, 199

Abstract

High molecular weight poly(ethylene oxide) (PEO) is used in papermaking as a flocculant to incorporate fines and fillers into papers. PEO flocculation is more effective in the presence of cofactors, which are phenolic polymers capable of forming aqueous complexes with PEO. In this work, two types of model cofactors were developed to study the PEO/cofactor flocculation mechanism. The first type of cofactors were latex particles with polystyrene-core poly(vinyl phenol)-shell (PS-PVPh) prepared by the surfactant-free emulsion polymerization. It was found that PS-PVPh particles enhanced the ability of PEO to flocculate polystyrene latex. When composite particles were added after PEO, they bridged together PEO-coated particles and aggregates. When composite particles were added before PEO, they acted as bridging agents and adsorb PEO in an extended configuration ideal for flocculation.

The second type of cofactors developed were water soluble tyrosine-containing polypeptides (TCP). TCP cofactors had well-defined structures and were optically active. Therefore, many analytical techniques, such as NMR, light scattering, isothermal titration calorimetry, and circular dichroism, were able to be applied to study the PEO/TCP complex formation mechanism. By taking into account the complex formation mechanism, the complex bridging flocculation mechanism of Xiao et al. was extended to explain many flocculation mechanisms. According to the extended mechanism, PEO/TCP complexes function as bridges to couple filler particles. Meanwhile, the complexes undergo deactivation – this is a new concept developed in this work. The deactivated complexes lose the ability to couple fillers, preventing the flocculation from reaching completion. It was proposed that the deactivation was induced by the encapsulation of TCP phenolic groups by PEO.

Acknowledgements

My deepest thanks go to my supervisor, Professor Robert H. Pelton, for guiding me into the wonderful world of polymer and colloid chemistry, for priceless advice on almost every aspect of my life, and for supervision in completing this thesis.

I am also grateful to the following people for their kind support during the course of this thesis:

Professor Richard Epand and Professor Shiping Zhu, members of my supervisor committee, for access to their equipments and for critical discussions.

Professor Vettai Ananthanarayanan, Professor Truis Smith-Palmer, Professor John Valliant, Professor John Brennan for access to their equipments and for useful discussions.

Dr. Raquel Epand, Dr. Rongjuan Cong, Dr. Jin Zhang, and Professor Donald Hughes for their useful discussions.

Mr. Doug Keller, Mr. Paul Gatt, Mr. Gord Slater, and Ms. Justyna Derkach for their generous help.

Dr. Vasso Bartzoka, Ms. Nicole Chen, Ms. Wei Chen, Dr. Xiaonong Chen, Mr. Lou Diflavio, Mr. Todd Hoare, Ms. Jessie Hong, Mr. Hermann Kampermann, Mr. Karsten Koppe, Ms. Hong Li, Ms. Linda Li, Dr. Jun Liu, Ms. Atefeh Moghaddamzadeh, Ms. Elizabeth Srokowski, Dr. Jinggong Wong, Mr. Lixin Xu, Ms. Yaling Xu, Mr. Boxin Zhao, Ms. Li Zhu for their friendship and help.

The ONDEO-Nalco company, the Canadian Government's NSERC-CRD programs, the Ontario Graduate Scholarship Program, and Shell Canada for financial support.

Finally, my parents, my wife Juntao Xu, and my brother Xin Lu for their love and encouragement.

Table of Contents

Chapter 1 Introduction

The papermaking process involves the filtration of fiber suspension (pulp furnish) on the papermaking machine. A pulp furnish normally contains fibers, fines (fiber fragments), and fillers such as kaolin clay and precipitated calcium carbonate (PCC). Fillers are used to reduce cost and improve paper properties.[1] Due to the small size of fines and fillers, polymeric flocculants are often added to incorporate fines and fillers into the paper sheet. Common flocculants are high molecular weight cationic polymers that can adsorb on the surfaces of fines and fillers. The adsorbed polymers function as bridges to induce flocculation. The flocculated fines and fillers are easily entrapped in the paper sheet. At the same time, some of fines and fillers attach to the fiber surface through the adsorbed polymers.[2]

Newsprint and other mechanical pulp furnishes usually contain large amount of dissolved and colloidal substances, which interfere with cationic flocculants. To circumvent this problem, high molecular weight poly(ethylene oxide) (PEO) was introduced to replace cationic flocculants.[3] PEO is a crystalline, thermoplastic polymer with the general formula $X\text{-}(CH_2CH_2O)_n\text{-}Y$. At room temperature, PEO is completely miscible with water in all proportions.[4] However, flocculation was only achieved in the presence of cofactors that are phenolic polymers, capable of forming aqueous complexes with PEO.[5] Common cofactors are phenol formaldehyde resin[6, 7], kraft lignin[3], and poly(vinyl phenol)[8].

For the last two decades, many researchers have made contributions to understanding the mechanism of PEO/cofactor flocculation. However, PEO/cofactor flocculation is a complicated process due to the presence of many components. The explanations of many flocculation observations still remain unknown.

The overall objective of this work is to extend our understanding of PEO/cofactor flocculation. In this chapter, the reported research work on PEO/cofactor flocculation is reviewed and un-resolved issues are identified. Finally, the specific objectives and the outline of this thesis will be presented.

Literature Review

PEO/cofactor flocculation is a complicated process, involving many interactions, such as PEO/cofactor complex formation, the adsorption of the complex onto the surface of fibers and fillers, and flocculation.[5] For clarity, PEO/cofactor complex formation mechanisms will be reviewed first, and then flocculation mechanisms will be discussed.

PEO/Cofactor Complex Formation

PEO/cofactor complex formation involves interactions at three distance levels. The first distance scale corresponds to the size of one phenolic group and the interaction between the individual polymer segments. The second distance scale corresponds to the size of one cofactor molecule. The third distance scale corresponds to the overall complex structure (supermolecular structure). The following paragraphs summarize the key features of the interactions occurring at each level.

The major issues at the segmental level are the geometry of bonded segments and the corresponding energetics. From the earliest studies, hydrogen bonding between polyether oxygens and phenolic hydroxyl groups has been assumed to be the driving force for complex formation.[5] Figure 1 shows the proposed structure of the hydrogen bonding between PEO and phenol formaldehyde resin.[9] Stack et al. first proposed that hydrophobic interaction may exist between PEO and cofactor.[10] Recently, Cong et al. applied NMR to study the interaction between PEO and poly(vinyl phenol-co-potassium styrene sulfonate) (PKS). They found that PEO approaches phenolic groups from above or below the aromatic planes.[11] Furthermore, at pH 12, PKS binds to PEO even though most of the phenolic hydroxyl groups deprotonate. Cong et al. therefore proposed that both hydrogen-bonding and hydrophobic interaction exist during PEO/cofactor association.

The main issues at the polymer chain distance scale are the configurations of complexed cofactor and PEO molecules, the effects of cofactor molecular weight and microstructure on complex formation, and the effect of PEO molecular weight on complex formation. Stack et al. used molecular modeling to simulate the structure of PEO/phenolic resin. It was proposed that complexed PEO molecules adopt a zigzag conformation and every other ether oxygen forms hydrogen bonding with phenolic hydroxyl group.[9] Pelton et al. simulated the structure of PEO/poly(vinyl phenol) and found that every fourth or fifth ether oxygen forms hydrogen bonding with phenolic hydroxyl groups.[8] Stack et al. proposed that a minimum molecular weight is required for cofactor to bind to PEO.[9] Xiao et al. proposed that PEO of molecular weight 2000 Da may not bind to cofactor.[12] However, experimental evidence for the effects of PEO and cofactor molecular weight on binding affinity is lacking.

The main issues at the overall complex scale are the molar mass and the size of the complex. For the last two decades, the supermolecular structure of PEO/cofactor complexes has been studied by many researchers to gain insight about PEO/cofactor flocculation mechanism. It was found that the complexes ranged from water soluble complexes involving a few PEO molecules[13, 14] to macroscopic visible precipitates[12, 15, 9]. In addition, increasing PEO molecular weight may increase the size of PEO/cofactor complexes.[13] The complexes between PEO and sulfonated kraft lignins adopted a more extended structure than PEO.[14] On the other hand, the complexes between PEO and phenol formaldehyde resins adopted a more compact structure than PEO.[10] It is generally agreed that cofactor molecules function as cross-linkers to couple PEO molecules.[16]

Flocculation Mechanism

Three mechanisms have been proposed in the literature to explain PEO/cofactor flocculation. Lindström et al. proposed a mechanism called network flocculation.[15, 17] According to the network flocculation mechanism, PEO and cofactor form a transit macroscopic network that can trap colloids mechanically. However, Xiao et al. found that the adsorption of PEO/cofactor complexes on the colloid surface is necessary for an effective flocculation.[18] Xiao et al.'s findings have been confirmed by Cong et al.[19] In a convincing paper, Xiao et al. proposed a mechanism called complex bridging flocculation

to explain many flocculation observations.[18] According to the complex bridging mechanism, PEO/cofactor complexes adsorb on the colloid surface and function as bridges to flocculate colloids. Furthermore, van de Ven and coworkers proposed a mechanism called association induced complex bridging flocculation.[14] Based on this mechanism, the complex formation between PEO and cofactor decreases the configurational entropy of PEO, facilitating the adsorption of the complexed PEO molecules on many surfaces. Thus, PEO/cofactor complexes can adsorb on cellulose surfaces, whereas neither PEO nor cofactor adsorbs.[20, 21]

Since the complex bridging flocculation mechanism is based on the conventional bridging flocculation mechanism induced by single-component flocculant, the conventional bridging mechanism will be reviewed in the following paragraphs. Then, the complex bridging mechanism will be discussed.

High molecular weight water soluble polymers are widely used to induce the aggregation of aqueous colloids.[22] The polymer can adsorb on a particle and form loops and tails, extending far beyond the electrical double layer of the particle.[23] Bridging flocculation occurs when the extended loops and tails adsorb on the bare surface of another particle.

Bridging flocculation is a kinetically controlled process. La Mer and coworkers first proposed that[24]:

$$-dN/dt \propto \theta(1-\theta) \qquad (1)$$

where N is the number concentration of primary particles, t is time, and θ is the degree of surface covered with adsorbed polymers. According to Equation 1, the highest flocculation rate occurs when half of the available surface is covered with adsorbed polymers.

However, flocculation experiments often show lower rates and extents of flocculation than expected from La Mer's theory. Recently, Gregory proposed that the adsorbed flocculant flattens (reconfigures) with time to give reduced or no flocculation.[25] In a convincing paper, Pelssers et al. showed that polystyrene latex flocculation with PEO displays deactivation by reconfiguration.[26] Figure 2 shows the schematic illustration of Gregory's bridging mechanism. Once polymers adsorb on the particle surface, polymer reconfiguration and particle collision occurs simultaneously. Bridging occurs by the adsorbed polymers extending beyond two electrical double layers. Over time the adsorbed polymers flatten to be within the electrical double layers, thus inhibiting bridging. Furthermore, if the polymer concentration is in excess of the concentration to saturate the available particle surface, flocculation will also compete with steric stabilization. A particle is sterically stabilized if its surface is saturated with adsorbed polymers.

Polymer reconfiguration and steric stabilization dictate that bridging flocculation is sensitive to both flocculant and particle concentration.[27] Bridging competes with polymer reconfiguration at low flocculant concentrations and competes with steric stabilization at high flocculant concentrations. The highest flocculation rate is thus

obtained at an intermediate flocculant concentration. Decreasing particle concentration decreases particle collision rate, leading to a decreased flocculation rate irrespective of flocculant concentration.

Complex bridging flocculation proceeds in a similar way as conventional bridging flocculation. Figure 3 shows the schematic illustration of the complex bridging flocculation of polystyrene latex (PS) by PEO and phenol formaldehyde resin (PFR) in the presence of wood fibers.[18] The phenolic resin is added first, and some of it will adsorb onto the surfaces of latex particles. PEO addition leads to the complexes formed between PEO and phenolic resin both in solution and on the latex particle surface. The dispersed complexes are not colloidally stable, and aggregation occurs capturing both dispersed complexes and latex particles in colloidal flocs (step 5). With time, rather large flocs are formed and deposit onto fiber surfaces. Figure 3 also shows the possible formation of a transit PEO/PFR network (step 6) and the mechanical entrapment of latex particles in the network (step 8). However, such mechanical entrapment was proposed to be insignificant to induce latex flocculation.

PEO/cofactor flocculation has many advantages over conventional bridging flocculation induced by PEO alone.[18] 1) When PEO is used alone, PEO flattens at the particle surface and reduces flocculation efficiency. In complex bridging flocculation, PEO can adsorb in multilayers, which are bound together with cofactor. The multilayers can grow far beyond the electrical double layer and remain active to flocculate particles. In another word, complex bridging flocculation is not sensitive to the reconfiguration of adsorbed polymer. 2) When PEO is used alone, steric stabilization competes with flocculation when PEO concentration is in excess of the concentration to saturate the available particle surface. In complex bridging flocculation, PEO adsorbs in multilayers and does not saturate the particle surface. 3) Goto et al. proposed that elastic PEO/cofactor complexes can survive the high shear rate in the papermaking process.[16]

Un-resolved Issues

PEO/cofactor flocculation is difficult to study because of the many possible interactions. The characterization of PEO/cofactor complexes is especially a challenge because they often form a macroscopic coacervate phase. Therefore, the explanations of many flocculation observations still remain elusive and a unified flocculation mechanism is still pursued by researchers. In the following paragraphs we will present some of the un-resolved issues.

Both hydrogen bonding and hydrophobic interaction have been assumed to be the driving force of PEO/cofactor association. However, no experimental evidence has been given in the literature to support both assumptions. Furthermore, many results suggest that neither hydrogen bonding nor hydrophobic interaction is the driving force of PEO/cofactor binding. Carignan et al. showed that water borne resins based on poly(sodium naphthalene sulfonate) contain no phenolic hydroxyl groups but are effective cofactors.[28] It was also found that poly(vinyl phenol) is a good cofactor, whereas more hydrophobic polymer polystyrene shows no affinity to PEO.[29]

PEO/cofactor interaction at the polymer chain level is not well understood. It is unknown whether the binding between PEO and cofactor is a reversible process or an irreversible process (high affinity binding). If it is a reversible process, bound polymer chains equilibrate with unbound polymer chains and a binding constant is required to describe the binding affinity. If it is a high affinity binding, all the added cofactor chains can bind to PEO until PEO is saturated and the binding is independent of the concentrations of PEO and cofactor. Since the adsorption of polymers at a solid/liquid interface is normally an irreversible process due to the polymer cooperative effect[23], we might expect the binding between PEO and cofactor is also an irreversible process. Furthermore, most commercial cofactors are phenolic resins with complicated structures and broad polydispersities, thus the effects of cofactor molecular weight and microstructure on PEO/cofactor binding remain unknown. Some researchers proposed that a minimum cofactor molecular weight is required for an effective binding.[9] However, no direct evidence has been shown to support such proposal.

PEO/cofactor complexes showed various supermolecular structures, ranging from water soluble complexes to macroscopic precipitates. Nonetheless, the mechanism that controls the supermolecular structure is unknown. Specifically, it is not known whether the supermolecular structure is controlled thermodynamically or kinetically.[30, 31] If it is controlled thermodynamically, it is independent of the mixing methods, such as the shear rate and the addition order of PEO/cofactor. If it is controlled kinetically, it depends on the mixing methods. Furthermore, PEO/cofactor flocculation extents depend on PEO molecular weight and the PEO/cofactor ratio.[32] Thus, it is of interest to investigate how PEO molecular weight and the PEO/cofactor ratio influence the complex supermolecular structure.

Complex bridging flocculation is generally accepted to be the mechanism of PEO/cofactor flocculation. However, many flocculation results cannot be explained by the proposed mechanism. The efficiency of PEO/cofactor flocculation increases with PEO molecular weight. The usual argument for the molecular weight dependence is that increasing polymer molecular weight decreases the reconfiguration rate of adsorbed polymers. However, the molecular weight sensitivity of PEO seems to be extreme. Recognizing that the molecular weight of PEO repeat unit is only 44 Da, PEO of molecular weight 1 MDa is extremely long and should be a good flocculant. However, 1 MDa PEO molecules are poor flocculants in the PEO phenolic resin system. Xiao et al. also pointed out that PEO/cofactor complexes adsorb in multilayers, extending far beyond the electrical double layer.[18] Thus, the reconfiguration argument cannot explain the PEO molecular weight effect.

PEO/cofactor flocculation extent also depends on many other experimental conditions, such as the shear rate, the ratio of PEO/cofactor, and the addition order of PEO/cofactor.[18] Increasing the shear rate can increase the flocculation extent. The best flocculation is often obtained at an intermediate PEO/cofactor ratio. Adding cofactor before PEO normally gives a higher flocculation extent than adding PEO before cofactor or adding a premixed PEO/cofactor complex. Recently, van de Ven et al. found that PEO solution history affects the flocculation rate. A poorly dissolved PEO solution with PEO

entanglements gives a higher flocculation rate than a well-dissolved PEO solution.[33] Nevertheless, no unified explanation has been proposed to explain the above flocculation results.

In summary, two important issues remain to be resolved. The first issue is to correlate the PEO/cofactor complex formation mechanism with the flocculation mechanism. PEO/cofactor complex formation is considered an essential step for an effective flocculation.[8] It seems necessary to incorporate the complex formation mechanism into the complex bridging flocculation mechanism. The second issue is the deactivation of flocculation. The extent of PEO/cofactor flocculation depends on many experimental conditions and rarely reaches one hundred percent. However, the mechanism that prevents flocculation from reaching completion is still unknown.

Objectives of This Work

The overall objectives of this work are to gain a better understanding of the PEO/cofactor flocculation mechanism and to extend our knowledge of colloid and surface chemistry. The specific objectives are:

1. To develop well-defined cofactors that are suitable for mechanistic studies. Most commercial cofactors are phenolic resins prepared by condensation polymerization. The complicated structures and the broad molecular weight distribution of such cofactors hinder the characterization of PEO/cofactor complexes.

2. To gain insights about the mechanism of PEO/cofactor complex formation. The characterization of PEO/cofactor complexes will be carried out at three distance scales. The first scale corresponds to one phenolic group, the second scale corresponds to one polymer chain, and the third scale corresponds to the overall complex structure (supermolecular structure).

3. To investigate the effect of soluble calcium ions on PEO/cofactor complex formation. Most of the PEO/cofactor complex characterizations reported in the literature were carried out in the absence of calcium ions.[34, 35] However, calcium ions are abundant in many pulp suspensions and it is known that calcium can interfere with PEO/cofactor flocculation. Therefore, it is necessary to characterize PEO/cofactor complexes in the presence of calcium ions.

4. To apply new methods to characterize PEO/cofactor complexes. Recently, light scattering[28], fluorescence photobleaching[13], and NMR[11] have been applied to study the complex supermolecular structure as well as the morphology of the bonded segments. However, new methods are required to investigate some other aspects of PEO/cofactor complexes, such as the energetics of complex formation and the structures of bonded cofactor molecules.

5. To extend the complex bridging flocculation mechanism by incorporating the PEO/cofactor complex formation mechanism. Specifically, flocculation tests will be carried out using the well-defined cofactors under various experimental conditions, such as shear rate, PEO molecular weight, PEO/cofactor ratio, and ionic strength. At the same

time, the structures of PEO/cofactor complexes will be characterized under the same experimental conditions. Flocculation results will then be correlated to the complex structures.

Thesis Outline

Chapter two describes the preparation and characterization of polystyrene – poly(vinylphenol) composite latex particles. This chapter describes the method of preparing a polystyrene-core poly(vinylphenol)-shell (PS-PVPh) particle, which will be used a model cofactor to study PEO/cofactor flocculation in the following chapters. The surface of cleaned core-shell particles had sufficient charged groups to stabilize the particle from pH 1 to 13. This chapter was published in Colloids and Surfaces A 2002, 201, 161.

Chapter three describes PEO flocculation of polystyrene-core poly(vinylphenol)-shell latex: an example of ideal bridging. This chapter describes the interaction between PEO and PS-PVPh particle cofactor. This chapter was published in Langmuir 2001, 17, 7770.

Chapter four describes PEO flocculation with phenolic microparticles. This chapter presents the flocculation results of PEO and PS-PVPh cofactor. The flocculation targets were polystyrene latex and precipitated calcium carbonate. This chapter was published in Journal of Colloid and Interface Science 2002, 254, 101.

Chapter five describes aqueous complex formation between poly(ethylene oxide) and tyrosine-containing polypeptides. In a preliminary note, we reported that tyrosine-containing polypeptides are effective model cofactors.[36] This chapter investigates the complex formation between PEO and tyrosine-containing polypeptides at segmental and polymer chain distance scales using capillary electrophoresis, NMR, isothermal titration calorimetry, and circular dichroism. This chapter was submitted for publication in Macromolecules.

Chapter six describes the supermolecular structures of PEO/tyrosine-containing polypeptide complexes. This chapter investigates the supermolecular structures of PEO/tyrosine-containing polypeptide complexes prepared under various experimental conditions, such as shear rate, PEO molecular weight, and ionic strength. A kinetics mechanism was proposed to explain the effects of the experimental conditions on the complex supermolecular structure. This chapter is in preparation for publication.

Chapter seven describes the flocculation of PCC by PEO/tyrosine-containing polypeptide. This chapter reports the flocculation results by PEO/tyrosine-containing polypeptide under various experimental conditions, such shear rate, PEO molecular weight, and ionic strength. Xiao et al.'s complex bridging flocculation mechanism was extended to account for the mechanism of PEO/peptide complex formation. This chapter is in preparation for publication.

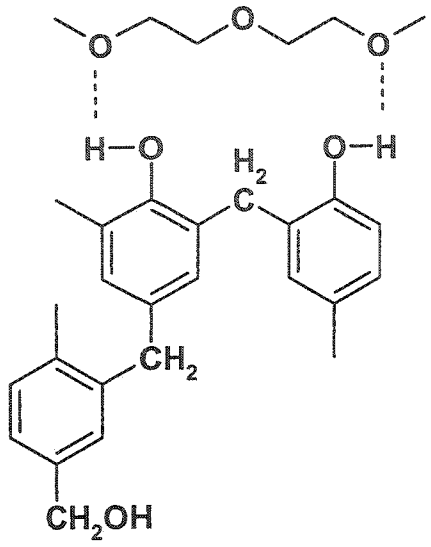

Figure 1. Schematic diagram of the hydrogen bonding formation between PEO and phenol formaldehyde resin.[9]

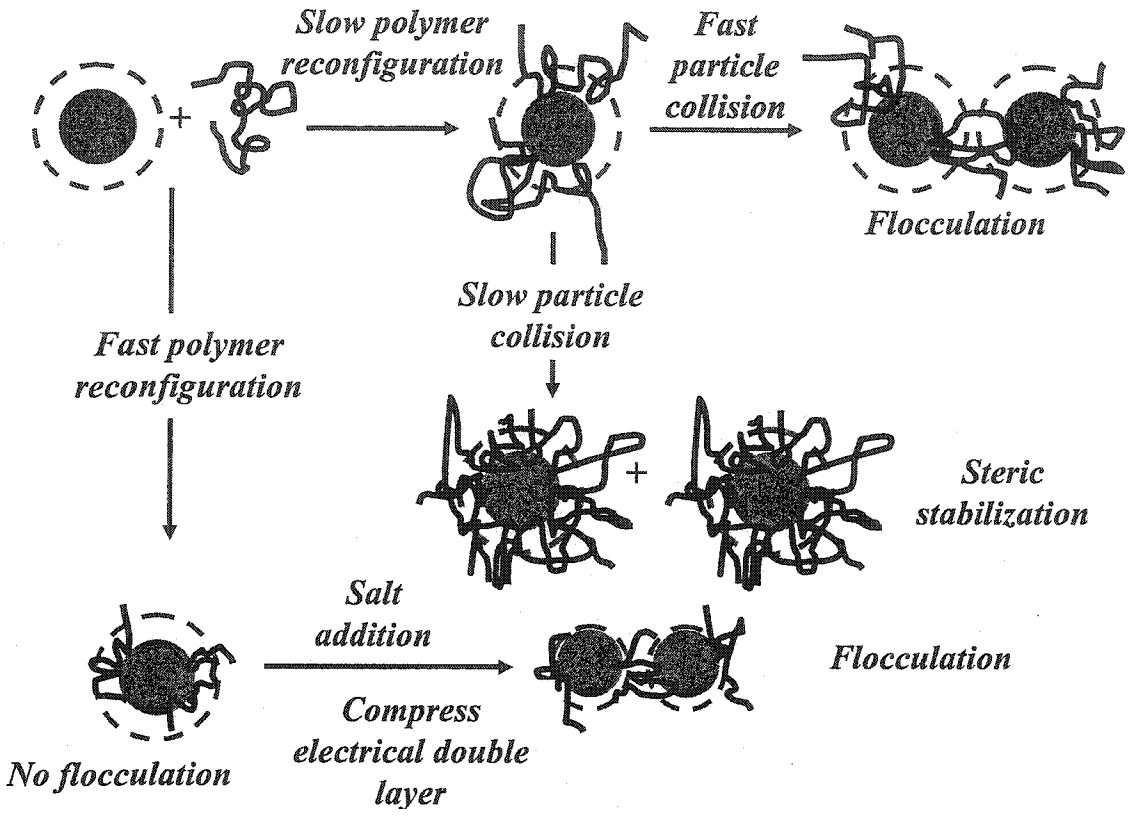

Figure 2. Schematic illustration of bridging flocculation mechanism.

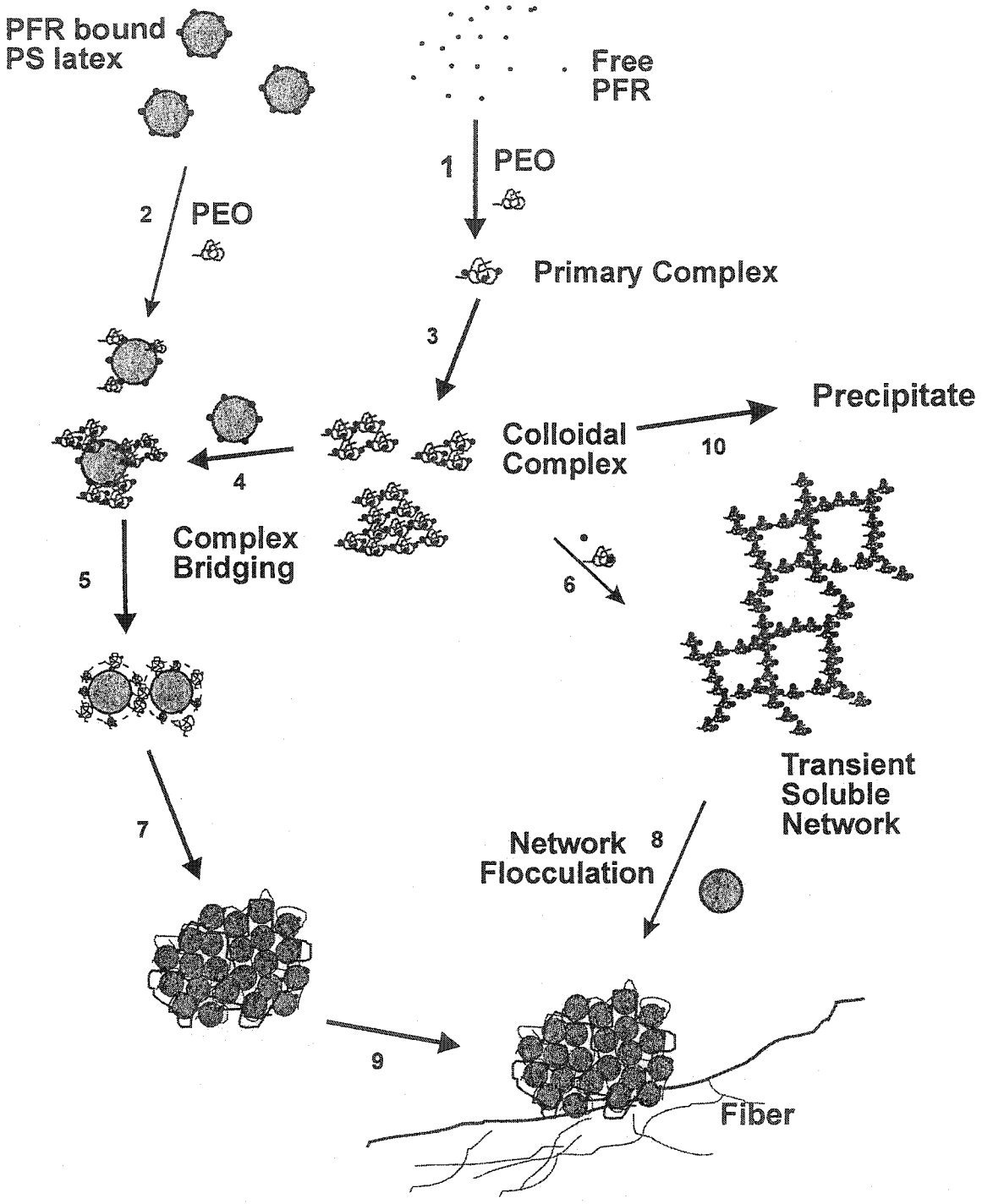

Figure 3. Proposed flocculation mechanism for latex with phenolic resin-PEO system in the presence of wood fibers.[18]

References

[1] Biermann, C. J. *Handbook of Pulping and Papermaking*, Academic Press: New York, 1996.

[2] Neimo, L. *Papermaking Chemistry*, Fapet Oy: Helsinki, 1999.

[3] Pelton, R. H.; Allen, L. H.; Nugent, H. M. *Svensk Papperstidning* **1980**, *83*, 251.

[4] Bailey, F. E., Jr.; Koleske, J. V. *Poly(ethylene oxide)*, Academic Press: New York, 1996.

[5] Pelton, R. H. *Polymer-Colloid Interactions in Pulp and Paper Manufacture*, in *Colloid-Polymer Interactions*, Farinato, R.; Dubin, P. Eds.; John Wiley & Sons, Inc.: New York.

[6] Carrard, J. P.; Pummer, H. *U.S. Patent* 4,070,236, 1973.

[7] Pelton, R. H.; Tay, C. H.; Allen, L. H., *Journal of Pulp and Paper Science* **1984**, *10*, 5.

[8] Pelton, R.; Xiao, H.; Brook, M. A.; Hamielec, A. *Langmuir* **1996**, *12*, 5756.

[9] Stack, K. R.; Dunn, L. A.; Roberts, N. K. *Colloids and Surfaces* **1991**, *61*, 205.

[10] Stack, K. R.; Dunn, L. A.; Roberts, N. K. *Journal of Wood Chemistry and Technology* **1993**, *13*, 283.

[11] Cong, R.; Bain, A. D.; Pelton, R. H. *Journal of Polymer Science B* **2000**, *38*, 1276.

[12] Xiao, H.; Pelton, R. H.; Hamielec, A. *Journal of Polymer Science* **1995**, *35*, 2605.

[13] Cong, R.; Pelton, R. H.; Russo, P.; Doucet, G. *Macromolecules* **2003**, *36*, 204.

[14] van de Ven, T. G. M. *Journal of Pulp and Paper Science* **1997**, *23*, J447.

[15] Lindström, T.; Glad-Nordmark, G. *Journal of Colloid and Interface Science* **1984**, *97*, 62.

[16] Goto, S.; Pelton, R. H. *Colloids and Surfaces* **1999**, *155*, 231.

[17] Wagberg, L.; Lindström, T. *Colloids and Surfaces* **1987**, 27, 29.

[18] Xiao, H.; Pelton, R. H.; Hamielec, A. *Journal of Pulp and Paper Science* **1996**, *22*, J475.

[19] Cong, R.; Pelton, R. H. *Journal of Colloid and Interface Science*, in press.

[20] van de Ven, T. G. M. ; Alince, B. *Journal of Pulp and Paper Science* **1996**, *22*, J257.

[21] Stack, K. R.; Dunn, L. A.; Roberts, N. K. *Colloids and Surfaces A* **1993**, *70*, 23.

[22] Dickinson, E.; Eriksson, L. *Advances in Colloid and Interface Science* **1991**, *34*, 1.

[23] Fleer, G. J.; Cohen Stuart, M. A.; Scheutjens, J. M. H. M.; Cosgrove, T.; Vincent, B. *Polymer at Interfaces*, Chapman & Hall: New York, 1993.

[24] Smellie, R. H., Jr.; La Mer, V. K. *Journal of Colloid Science* **1958**, *23*, 589.

---

[25] Gregory, J. *Colloids and Surfaces* **1988**, *31*, 231.

[26] Pelsser, E. G. M.; Cohen Stuart, M. A.; Fleer, G. *J. Colloids and Surfaces* **1989**, *38*, 15.

[27] Pelsser, E. G. M.; Cohen Stuart, M. A.; Fleer, G. J. *Journal of Chemical Society, Faraday Transaction* **1990**, *86*, 1355.

[28] Carignan, A.; Garnier, G.; van de Ven, T. G. M. *Journal of Pulp and Paper Science* **1998**, *24*, 94.

[29] Lu, C.; Pelton, R. H.; Richardson, R. ; Cosgrove, T. ; Dalnoki-Veress, K. "Neutron Reflection of the Adsorbed PEO layer at the Poly(vinyl phenol)/Water Interface," Private Communication.

[30] Dautzenberg, H. *Macromol. Symp.* **2000**, *162*, 1.

[31] Bakeev, K.N.; Izumrudov, V. A.; Kuchanov, S, I.; Zezin, A, B.; Kabanov, V. A. *Macromolecules* **1992**, *25*, 4249.

[32] Gibbs, A.; Pelton, R. H. *Journal of Pulp and Paper Science* **1999**, *25*, 267.

[33] Kratochvil, D.; Alince, B.; van de Ven, T. G. M. *Journal of Pulp and Paper Science* **1999**, *25*, 331.

[34] Gibbs, A.; Yang, Z.; Xiao, H.; Pelton, R. In *Fundamentals of Papermaking materials, Transactions of the Fundamental Research* Symposium, 11th, Cambridge, UK, 1997.

[35] Laivins, G.; Polverari, M.; Allen, L. *Journal of Pulp and Paper Science* **2001**, *27*, 190.

[36] Lu, C.; Pelton, R. H.; Valliant, J.; Bothwell, S. ; Stephenson, K. *Langmuir* **2002**, *18*, 4536.

Chapter 2 Preparation and Characterization of Polystyrene-poly(p-acetoxystyrene) and Polystyrene-poly(p-vinyl phenol) Composite Latex Particles

Abstract

Polystyrene-core poly(p-vinylphenol)-shell (PS-PVPh) latexes were prepared by the hydrolysis of polystyrene–core poly(p-acetoxystyrene)-shell (PS-PAS) latexes. Polymerization conditions required for uniform core/shell structures were identified. The latexes were made by surfactant-free aqueous emulsion polymerization which gave stable latexes and uniform particle size distributions. It was necessary to use divinylbenzene in the second stage of PS-PAS polymerization to prevent dissolution and removal of poly(p-vinyl phenol) during hydrolysis. Infrared spectroscopy, dynamic light scattering, electron microscopy, potentiometric and conductometric titration, disc centrifugation and electrophoresis were used to elucidate the structure of the shell layer. After hydrolysis, the PVPh shell contained approximately 59% water for 20 % divinylbenzene crosslinker and 76% water for 1% crosslinker. Cleaned core-shell particles bore sufficient negative charge to render the particles electrostatically stable over a wide pH range. Phenolic groups in the particle shell region dissociated in the pH range 10 to over 11.5.

Introduction

High molecular weight poly(ethylene oxide), (PEO), is employed in papermaking as a flocculant to incorporate fines and fillers into papers based on mechanical pulps. PEO is more effective in the presence of cofactors, which are polymers capable of forming aqueous complexes with PEO. Common cofactors are kraft lignin[1], phenol formaldehyde resin[2, 3], tannic acid[4] and poly(p-vinylphenol) (PVPh).[5, 6] All these cofactors have phenolic groups in their structures. This has lead to much discussion in the paper technology literature about the importance of hydrogen bonding between the polyether oxygens and the phenolic hydroxyl groups.[4, 7] Waterborne resins based on poly(sodium naphthalene sulfonate), which contains no phenolic hydroxyl groups but are effective cofactors, appear to be an exception.[8] All the reported cofactors are either water-soluble polymers or hydrogel particles. In this work we report the synthesis and characterization of novel latex-based cofactors.

The overall goal of this work was to determine whether colloidally dispersed particles bearing phenolic surface groups are effective cofactors or not. The specific objectives of the work described in this paper were to prepare and characterize polystyrene-core poly(p-vinyl phenol)-shell (PS-PVPh) composite particles. These materials have not been described before in the literature. Flocculation studies with the composite particles are described in a following paper.[9]

Core-shell particles are usually prepared by two-stage seeded growth emulsion polymerization. During the second stage polymerization, monomer 2 is introduced in the presence of seed polymer based on monomer1. When monomer 2 is a solvent for polymer 1, the swelling rate of the seed polymer 1 by the monomer 2 often appears to be rapid, giving an equilibrium swelling of seed polymer with monomer 2.[10, 11] After the addition of initiator, the monomer 2 is initiated in the water phase to form water-soluble oligomeric radicals. The radicals grow until they become insoluble and enter the monomer-swollen seed particles.[12] Unwanted secondary particles are observed when the oligoradicals have a high charge density. This is because electrostatic repulsion reduces the adsorption rate of highly charged oligoradicals onto the seed particles.[13]

The morphology of two-stage latex particles has been studied extensively by many investigators.[14, 15, 16] During the past 20 years there have been reports of composite particles which have been characterized as "core-shell," "inverted core/shell," "golf ball-like" and "hemispherical" structure[17, 18]. Many factors, including initiator[19] and surfactant[20] properties, can be used to control particle structures. In some cases particle morphology can be predicted by thermodynamic models which involve the minimization of the overall interfacial energies.[20] In other cases, the molecular weights of the seed and stage 2 polymers are usually quite high and the morphological structures present as intermediate conversions may be "frozen in" giving non-equilibrium particle structures. Many approaches for controlling composite particle morphology have been reported,

including controlled monomer feed[19], addition of other solvents[18] and varying the cross-linking degree of the seed particles.

Described in this work is the preparation of composite particles which were obtained by polymerizing p-acetoxystyrene (AS) in the presence of polystyrene (PS) seed particles. After the second stage polymerization, composite particles were hydrolyzed with sodium hydroxide at 70°C to convert poly(p-acetoxystyrene) (PAS) into poly(p-vinyl phenol) (PVPh). Infrared (IR), transmission electron microscopy (TEM), disc centrifugation, potentiometric and conductometric titration, dynamic light scattering and electrophoretic mobility measurements were employed to characterize the particle structures.

Experimental

Materials

Styrene from Aldrich Chemical Company was purified by distillation in a reduced-pressure nitrogen atmosphere. Divinylbenzene (DVB) and p-acetoxystyrene (AS) from Aldrich Chemical Company were used as received. Potassium persulfate (KPS), sodium hydroxide, sodium chloride and sodium dodecyl sulfate (SDS) from BDH were used as received. The water came from a Millipore Milli-Q system fitted with a Super C carbon cartridge, two ion-exchange cartridges, and an Organex Q cartridge.

The water-soluble two-component resin for transmission electron microcopy with brand name NANOPLAST FB 101 was obtained from Rolf Bachhuber. Component 1 is melamine resin, MME 7002 (hexamethylol-melamine-methyl ether, 70% in water, and 1% free formaldehyde) and component 2 is acid catalyst B 52 (p-tolulene sulfonic acid).

Methods

Polystyrene Latex Preparation

All polymerizations were carried out in a thermo-stated glass reactor, equipped with a glass paddle-type stirrer, and continuously purged with nitrogen. The agitation rate in all cases was 350 RPM.

Polystyrene (PS) latexes were prepared by a conventional surfactant-free batch process[21] in which water and monomer were first introduced into the reactor. After purging with nitrogen and allowing the solution to reach thermal equilibrium, an aqueous solution of potassium persulfate was added to initiate the polymerization, giving time zero of the reaction. The temperature was kept at 70°C. The recipes are shown in Table 1. For PS4, 0.15 g SDS was introduced into 300 mL water before the addition of 25 g styrene monomer. After 24 hours of reaction, the vessel was removed from the thermostat and allowed to stand for a few minutes. The latex was then decanted through

a filter packed with glass wool to remove coagulum. The latex was then cleaned by dialysis, using "well-boiled" dialysis tubing.

The Swelling of the Seed Polystyrene Particles by Acetoxystyrene Monomer

The swelling rate of seed PS latex by AS monomer was examined by the following procedure. 0.927 g AS monomer was added to 100 g stirred latex PS3 of 0.927 wt % at 25°C. At various time intervals, samples were withdrawn and added 0.001 mol/L NaCl solution. Particle sizes were measured by dynamic light scattering (details given below).

The Second Stage Polymerization

The recipes of the second stage polymerization are summarized in Table 2. AS monomer was added into the seed latex and the mixture was held at 70°C over a period of 4 hours. Except for samples CPS4, CPS6 and CPS7, DVB monomer was introduced with AS monomer to function as a cross-linking agent. Aqueous potassium persulfate was added to initiate the second stage polymerization.

The Third Stage - Hydrolysis

After 10 hours of reaction, sodium hydroxide was added to give a concentration of 0.5 mol/L to hydrolyze PAS at 70°C. After 4 hours of hydrolysis, CPS4, CPS6 and CPS7 were purified by four successive centrifugations (Beckman L7 Ultracentrifuge, 40,000 rpm and 30 min), decantations, and dispersions in water. The other latexes were cleaned by dialysis against water.

Latex Characterizations

Particle sizes were measured using a Lexel laser (wave length 514 nm) equipped with a BI-9000 AT Digital Correlator (Brookhaven). The light scattering was measured at a 90° angle and the particle sizes were calculated using the non-negatively constrained least squares (regularized) method using software BI9000AT version 6.1.

The particle size distributions of colloidal suspensions were also measured using a BI-DCP (Disc Centrifuge Photosedimentometer) Particle Sizer (Brookhaven Instrument Co.). For pure PS particles and PS-PAS composite particles, the BI-DCP was operated in the line-start mode. The sample was prepared by the following way. 5 mL methanol was initially mixed with 15 mL water and latex was added to give a concentration ranging from 100 to 400 mg/L. After the preparation of the sample, the BI-DCP was turned on and the rotation speed of the disc was set at 8000 RPM. 15 mL water and 1 mL methanol were injected into the spinning disc. For the final step, 0.2 mL sample was added into the disc and the data were collected and weight average diameters were recorded. For PS-PVPh composite particles, the BI-DCP was operated in the homogeneous mode in order to avoid swelling of the PVPh shell with methanol. The sample was prepared by adding

PS-PVPh latex into 20 mL water to give a concentration ranging from 10 to 50 mg/L. The BI-DCP operated with a disc rotation speed of 8000 RPM. About 12 mL sample was injected and the data was collected.

For composite particles, interpreting the BI-DCP data is complicated because the shell polymer density is different from the core polymer density. Thus, the particle density is a function of shell thickness, which is, in turn, a function of diameter. The following equation gives this relationship where ρ_c, ρ_1 and ρ_s are the densities of the composite particle, the core polymer and the shell polymer respectively, r_1 is the core particle radius and r_c is the composite particle radius.

$$\rho_c = \frac{\rho_1 r_1^3 + (r_c^3 - r_1^3)\rho_s}{r_c^3} \qquad (1)$$

For a given set of experimental conditions in the disk centrifuge, the following equation is valid where $\Delta\rho$ is the density difference between the particle and water, r is the particle radius and C is a constant which includes RPM, location of the detector, etc.

$$\Delta\rho r^2 = C \qquad (2)$$

When a DCP experiment was conducted with core-shell particles, the density of polystyrene (ρ_{ps}) was entered into the software which, in turn generated an apparent radius r_{app}. To get the correct radius equation 2 can be rewritten in the following form where ρ_w is the density of water. The left hand side denotes the actual composite particles whose radius and density are both unknown. The right hand side gives the apparent values for an equivalent polystyrene particle – the density is that of polystyrene and r_{app} comes from the experiment.

$$(\rho_c - \rho_w)r_c^2 = (\rho_{ps} - \rho_w)r_{app}^2 \qquad (3)$$

Simultaneous solution of equations 1 and 3 yield both the average particle diameter and density. The shell polymer density was based on its composition and the following pure polymer values. The density of PS is 1050 kg/m^3, the density of PVPh is 1190 kg/m^3 as measured by Xiao.[5] The density of PAS was estimated to be 1200 kg/m^3 at 25°C based on the density of 3.415 wt% PAS latex which was determined to be 1002 kg/m^3 using a DMA 45 Digital Density Meter (Anton Paar).[22] The corresponding density of PAS was calculated assuming no water penetration into PAS particles.

The hydrolysis degree of PAS was determined by infrared (IR) measurements (BIO-RAD FTS-40). The latex suspension was first dried and mixed with potassium bromide. The mixture was then pressed to make a thin film and an IR absorbency spectrum was obtained.

Potentiometric and conductometric titrations were carried out to characterize latex particle surfaces using an ABU93 Triburette Radiometer (Copenhagen) and a CDM 83 Conductivity meter (Copenhagen) controlled by Aliquot software (McMaster University). 0.1 mol/L NaOH was added first and the forward titration was stopped at pH 11.7; 0.1 mol/L HCl was then added until the pH reached 3 for the back titration. The corrected titration curve was obtained by subtracting the water-only curve from the suspension curve.[23]

Particle size and morphology were observed with transmission electron microscopy (TEM) and number average particle size was calculated based on the measurement of one hundred particles for each latex sample. For this, latex suspensions were diluted and a drop was placed onto a copper grid and allowed to dry at room temperature in a desiccator. Particle cross sections were observed by thin sections of particles embedded in NANOPLAST. In this procedure, the latex suspension was first mixed with MME 7002 resin and catalyst B 52 was introduced with a ratio of 10.0 g MME 7002 to 0.225 g B 52. The mixed resin was placed in a desiccator, dried at 40°C and subsequently hardened at 60°C for two days. The thin sections were cut with a diamond knife and observed with TEM without staining.

The electrophoretic mobility measurements in aqueous solution were made with a Coulter DELSA 440 SX using the software version 2.03. The suspension was prepared by dispersing 0.05 mL of latex suspension (0.942 wt %) into 0.001 mol/L NaCl aqueous solution, and the pH was adjusted by HCl/NaOH. A parabola method[24] was used for data analysis.

Results

Four PS latexes were prepared using recipes summarized in Table 1. A second stage polymerization (see Table 2) was employed to add a shell of PAS which was then hydrolyzed (Stage 3) by sodium hydroxide at 70°C to give a shell based on poly(p-vinyl phenol).

The ability of AS monomer to swell polystyrene seed latex at 25 °C was measured by dynamic light scattering and the results are summarized in Figure 1. The mass of added AC was equal to the mass of polystyrene. The swelling was a fast process and reached equilibrium in 30 minutes which agrees with Morton and Goodwin's results for polystyrene swelling with styrene.[10, 11] The amount of AS monomer absorbed into PS3 particles was calculated based on the increase in PS3 particle size. The swelling maximum in Figure 1 corresponded to an AS weight content of 30 % inside the seed particle leaving about half of the added AS in the aqueous phase.

Figure 2 shows the IR absorbance spectra for CPS1 before (top spectra) and after (bottom bottom spectra) the hydrolysis from the poly(acetoxystyrene) shell to the poly(vinyl phenol) shell. The shell also contains 20% crosslinker (DVB). For PS-PAS

composite latex, there is a large peak around 1760 cm^{-1}, which is the characteristic frequency of the C=O stretching in an ester group. This peak almost disappeared after the four hours of hydrolysis. An estimate based on the heights of the absorbance peak suggests that 80% of acetate groups had been cleaved to give phenolic groups. A similar analysis of CPS2 with 5% crosslinking showed that 90% of the acetate groups were hydrolyzed.

Table 3 summarizes the particle size results at the different stages measured by dynamic light scattering (DLS) and transmission electron microscopy (TEM). As shown in DLS experiments, all the particle sizes from CPS1 to CPS6 increased from the first stage (PS) to the second stage (PS-PAS). If cross-linking agent was added, the particle sizes increased again after hydrolysis (PS-PVPh). The more DVB was introduced, the less the particle size increased. For instance, the diameter of CPS2 (5% cross-linking degree) increased from 205 nm (PS-PAS) to 269 nm (PS-PVPh) after hydrolysis. By contrast, the diameter of CPS1 (20% cross-linking degree) only increased from 208 nm (PS-PAS) to 250 nm (PS-PVPh) after hydrolysis. Both CPS1 and CPS2 were prepared using the same seed PS particles and the same mass ratio of PS seed to AS monomer. In the case of CPS4 and CPS6 which contained no DVB, particle sizes became slightly smaller after hydrolysis. Presumably, some of the hydrolyzed PVPh surface polymer desorbed from the latex surface. By contrast, particle size results based on TEM showed no obvious particle size increase after hydrolysis for all the particles. It is possible that the diameter increase measured by DLS was associated with water swelling of the PVPh shell; this would not be observed in TEM.

The particle sizes of CPS1, CPS2, CPS3 and CPS5 measured by disc centrifugation are summarized in Table 4. The particle size results show a trend similar to those measured by DLS (Table 3). PS-PAS composite particles were larger than their PS seed particles and their sizes were even larger after hydrolysis. The more the cross-linking agent was added during the second stage polymerization, the less the particle sizes increased after hydrolysis.

Figure 3 shows the TEM photographs of CPS5 at different stages. The pure polystyrene particles showed a spherical shape and smooth surface. After the second stage polymerization, the particle size increased and the shape also became non-spherical. However, the particle surfaces were still as smooth as polystyrene and the size distribution was also quite uniform. No secondary particles were observed. After hydrolysis, the particle surface was no longer smooth; it had a fluffy appearance.

The TEM photographs of particle thin sections are shown in Figure 4. PS particles had a uniform cross section. By contrast, the images of PS-PVPh particles (both CPS2 and CPS5) in Figure 4b and 4c show a core-shell structure. The CPS5 PS-PVPh particle (Figure 4c) appeared to have PVPh lobes on the surface of the PS core. Perhaps the distribution of divinylbenzene (crosslinker) in the shell was not uniform giving a range of degrees of swelling after PAS was hydrolyzed to PVPh.

The TEM photographs of CPS6 and CPS7 after the third stage (PS-PVPh particle) are shown in Figure 5. For CPS7, the seed PS latex was used directly without cleaning. Thus SDS from the first stage polymerization was carried to the second stage polymerization. 1 g toluene was also added with CPS7 seed latex to help swell the seed particles. For CPS6, there was no extra addition of toluene and the seed latex was polymerized without SDS. All the other polymerization conditions were kept the same for these two samples. The morphology of CPS6 appeared to be similar to that of CPS5 (Figure 3), whereas CPS7 had a different morphology from the other composite particles. CPS7 particles appear to have two kinds of surfaces. The dark domains appear to be smoother than the bright domains. We speculate that the rough bright domains on the "golf ball-like" particles are PVPh whereas the smooth dark domains are polystyrene.

For PS-core PVPh-shell particles, water fractions in the particle shell layer were calculated based on the particle size changes. It was assumed that particles formed perfect core-shell morphology and the particle swelling after hydrolysis was induced by the absorption of water in the shell. As seen from Table 5, the water fractions calculated using DLS diameters are similar to those calculated using disc centrifuge diameters. When the cross-linking degree decreased from 20, 5 to 1%, the shell water content increased from 59, 72 to 76% according to DLS and from 57, 71 to 81% according to disc centrifugation. This suggests that the water fraction increased when decreasing the cross-linking degree in the particle shell region.

Conductometric and potentiometric titration curves for CSP2 PS-PVPh particles are shown in Figure 6. 0.1 mol/L NaOH standard solution was first added into latex suspension until the pH reached 11.7. 0.1 mol/L HCl standard solution was then introduced for the back titration and stopped at pH 3. Figure 6 shows the reverse titration curve. The conductometric curve indicates a small flat spot of about 0.05 meq in the pH range for carboxyl groups. The potentiometric curve was used to give titratable charge content as a function of pH and the result is shown in Figure 7 for two latexes. In order to construct Figure 7, the degree of ionization was assumed to be zero at pH 3 – thus the contribution of bound sulfate groups is not accounted for. There was a low (<2 meq/g) content of weak acid groups. Significant dissociation of the phenolic groups required pH values above 10.

Table 6 shows the electrophoretic mobility values of CPS2 PS-PVPh suspension as a function of pH. CPS2 PS-PVPh particles were suspended in 0.001 mol/L NaCl solution and the pH was varied by extra addition of HCl/NaOH. When the pH value was increased from 2.4 to 10.2, particle mobility decreased from -1.29×10^{8} m^2/Vs to -4.21×10^{8} m^2/Vs. This result is consistent with the titrations and suggests the presence of both strong and weak acid groups that stabilize the particles.

Discussion

Multistage polymerizations do not necessarily guarantee core-shell particles. However, since polyacetoxystyrene is more hydrophilic than polystyrene, the formation of PS-core PAS-shell latexes is thermodynamically favored.[20] After hydrolysis the particle morphology also depends upon the distribution of crosslinks in the shell and the degree of attachment to the polystyrene core. Comparing the internal structures of CPS2 and CPS5 core-shell particles, we found that a higher cross-linking degree in the shell favors more uniform core-shell morphology.

The electrical properties of the composite latexes require some comment. Surfactant free polystyrene latexes are known to have both strongly and weakly acidic surface groups. The strong acid groups are sulfates from the initiator and the weak groups appear to be carboxyls and benzoic acid moieties[25] which arise from oxidation of polystyrene.[26] There has been much speculation about the origin of the carboxyls which includes the contamination from dialysis tubing[27]. Both the potentiometric titration data and the mobility measurements suggest that similar groups are present on the surface of the composite particles. Indeed, these groups are required to give electrostatic stabilization of the latex particles. At high pH dissociated phenol groups also contribute to particle charge. The pK_a value of phenol is around 9.9, however, higher pH values were required to dissociate the PVPh shell because of the polyelectrolyte effect.

Conclusions

1. Latexes particles with PS-core and PVPh-shell were prepared by the surfactant-free emulsion polymerization of p-acetoxystyrene monomer in the presence of polystyrene seed particles followed by base hydrolysis. The hydrolysis degree varied due to the cross-linking degree in the particle shell region. For 5% cross-linking degree, 90% of PAS was converted to PVPh.

2. DVB crosslinker was required in the second stage polymerization in order to anchor the PVPh shell during hydrolysis. 5% DVB gave a much more uniform shell than 1% DVB.

3. The PVPh shell contained between 59% water with 20% corsslinker and 76% water with 1% crosslinker at neutral pH.

4. Cleaned core/shell particles bore sufficient electrically charged groups to stabilize the particles from pH 1 to 13.

Table 1. Recipes for polystyrene latex preparations which were carried out at 70°C.

Latex	Styrene (g)	H_2O (ml)	$K_2S_2O_8$ (g)	SDS (g)
PS1	4.5	300	0.05	0
PS2	5	300	0.06	0
PS3	9	300	0.09	0
PS4	25	300	0.25	0.15

Table 2. Recipes for the second stage polymerization, 70°C.

Sample	Seed (g) (Solid Content)	AS (g)	DVB (g)	AS+DVB/PS Mass Ratio	Toluene (g)	$K_2S_2O_8$ (g)
CPS1	PS1 100 g (0.816%)	1.632	0.408	2.5/1	0	0.020
CPS2	PS1 100 g (0.816%)	1.938	0.102	2.5/1	0	0.020
CPS3	PS2 100 g (0.927%)	1.835	0.019	2/1	0	0.019
CPS4	PS2 100 g (0.927%)	1.854	0	2/1	0	0.019
CPS5	PS3 100 g (2.14%)	2.119	0.021	1/1	0	0.020
CPS6	PS3 100g (2.14%)	0.856	0	0.4/1	0	0.009
CPS7	PS4 100 g (6.78%)	2.712	0	0.4/1	1	0.024

Table 3. Particle diameters determined at different stages using DLS and TEM. The DLS error limits show the standard deviations of the mean based on 5 measurements. The TEM error limits are the standard deviations of the distribution. The crosslinking degree is expressed as the weight percentage of DVB added with AS monomer.

Sample	Crosslinking Degree	Method	1st Stage (nm) PS Core	2nd Stage (nm) PS Core + PAS Shell	3rd stage (nm) PS Core + PVPh Shell
CPS1	20%	DLS	138 ± 7	208 ± 5	250 ± 3
		TEM	120 ± 5	180 ± 5	185 ± 5
CPS2	5%	DLS	138 ± 7	205 ± 7	269 ± 5
		TEM	120 ± 5	180 ± 5	185 ± 5
CPS3	1%	DLS	185 ± 1	250 ± 10	330 ± 10
		TEM	140 ± 5	195 ± 5	200 ± 5
CPS4	0	DLS	185 ± 1	255 ± 3	250 ± 4
		TEM	140 ± 5	190 ± 5	185 ± 5
CPS5	1%	DLS	440 ± 13	515 ± 24	590 ± 8
		TEM	324 ± 5	387 ± 5	390 ± 5
CPS6	0	DLS	440 ± 13	484 ± 4	466 ± 4
		TEM	324 ± 5	350 ± 5	345 ± 5
CPS7	0	DLS	310 ± 10		350 ± 7
		TEM	267 ± 5		270 ± 5

Table 4. Particle diameters measured by BI_DCP centrifugal particle sizer. See text for details.

Sample	PS Core	PS Core + PAS Shell	PS Core + PVPh Shell
CPS1	156 ± 10	205 ± 22	238 ± 22
CPS2	156 ± 10	203 ± 10	249 ± 10
CPS3	185 ± 20	226 ± 23	299 ± 23
CPS5	360 ± 16	422 ± 38	519 ± 38

Table 5. Water fractions in PS-PVPh particle shell region with different cross-linking degrees.

Sample	Cross-linking Degree	Method	Shell Region Water Fraction
CPS1	20%	DLS	59%
		DC	57%
CPS2	5%	DLS	72%
		DC	71%
CPS3	1%	DLS	76%
		DC	81%

Table 6. Electrophoretic mobility of CPS2 as a function of pH. The light scattering angle was chosen at 22.5°. [NaCl] = 0.001 mol/L, T= 25°C.

pH	Mobility ($m^2/Vs \times 10^8$)
2.4	-1.29 ± 0.08
6.2	-2.96 ± 0.09
8.4	-3.38 ± 0.06
9.6	-3.96 ± 0.14
10.2	-4.21 ± 0.12

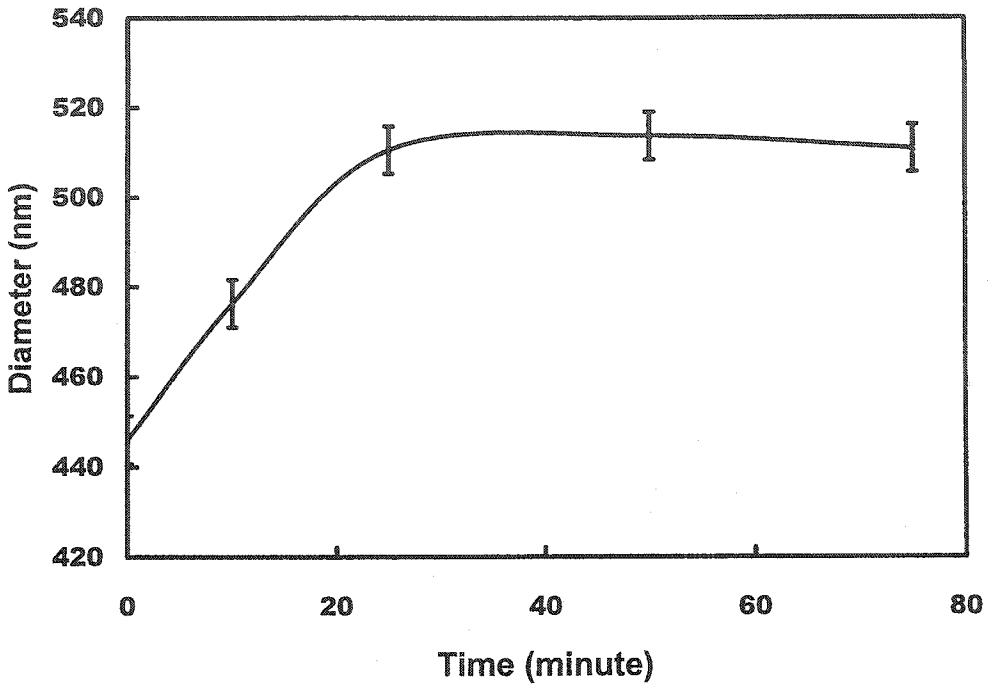

Figure 1. The increase of PS (PS3) particle diameter induced by the addition of AS monomer. PS/AS mass ratio was equal to 1. The samples were withdrawn at different time interval and particle sizes were measured three times at each point by DLS. The error bars show ± one standard deviation of the mean based on 15 measurements.

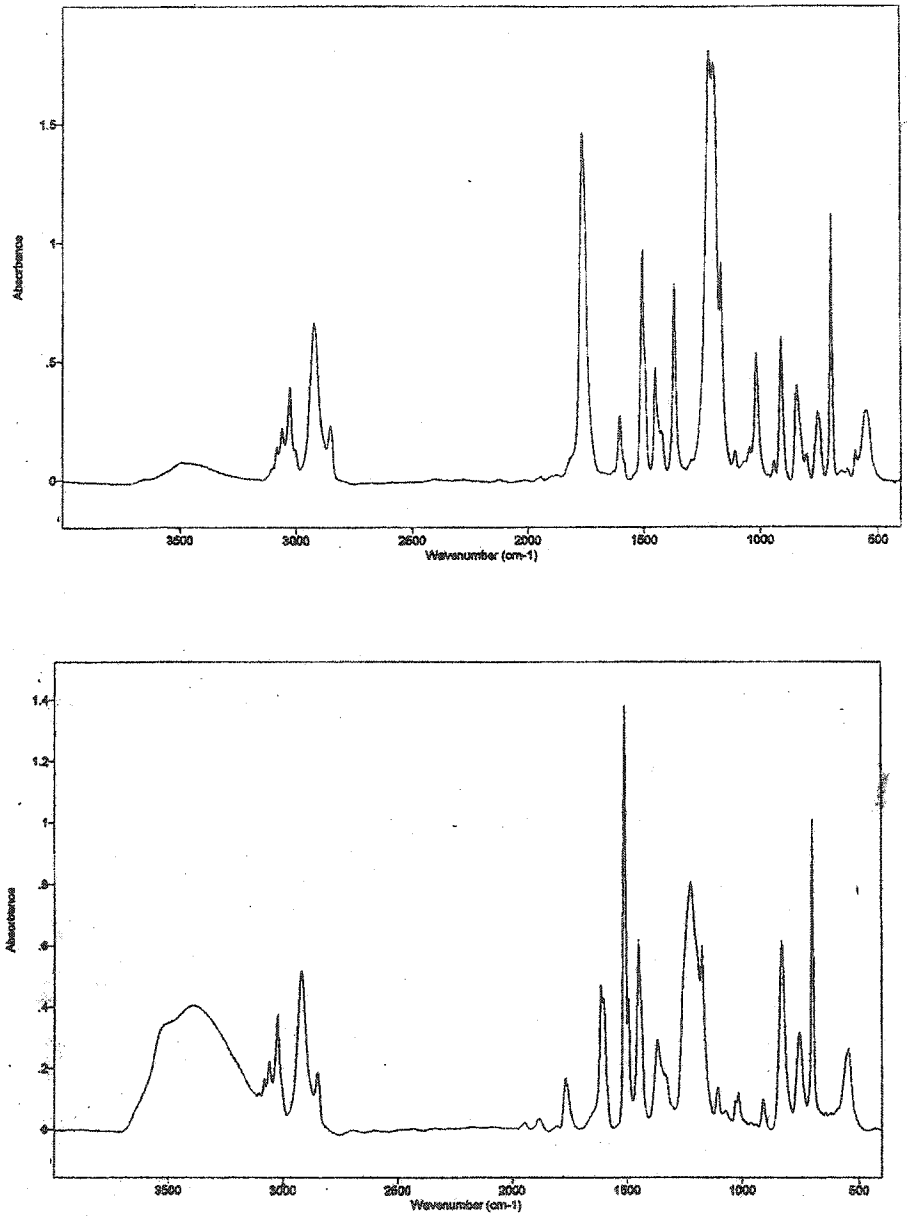

Figure 2. Infrared absorbance spectra of CPS1 (20% cross-linking). Top – second stage latex before hydrolysis (PS core + PAS shell), bottom – third stage latex after hydrolysis (PS core + PVPh shell).

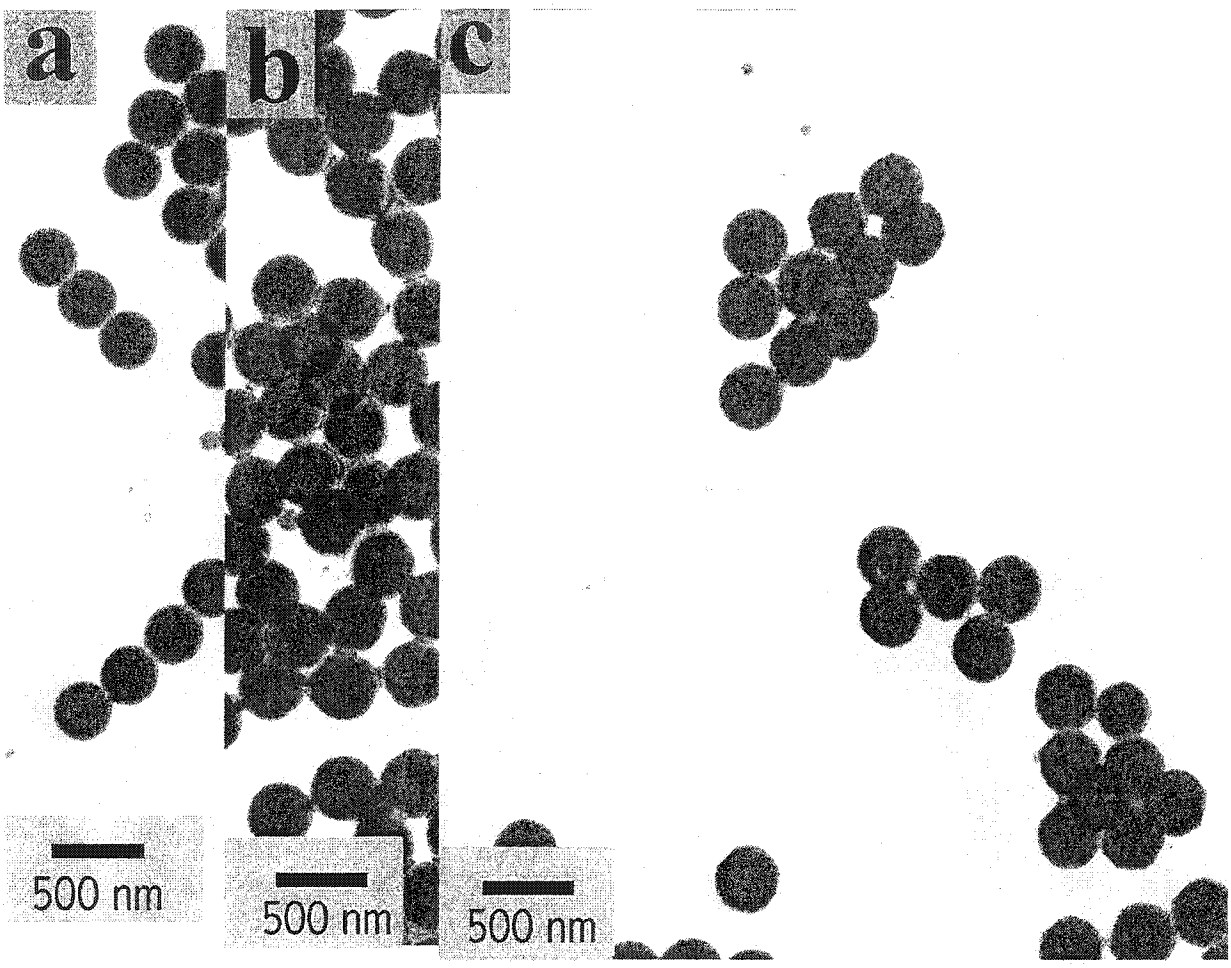

Figure 3. TEM images of CPS5 (1% cross-linking). (a) polystyrene seed particle, (b) second stage latex before hydrolysis (PS core + PAS shell), (c) third stage latex after hydrolysis (PS core + PVPh shell).

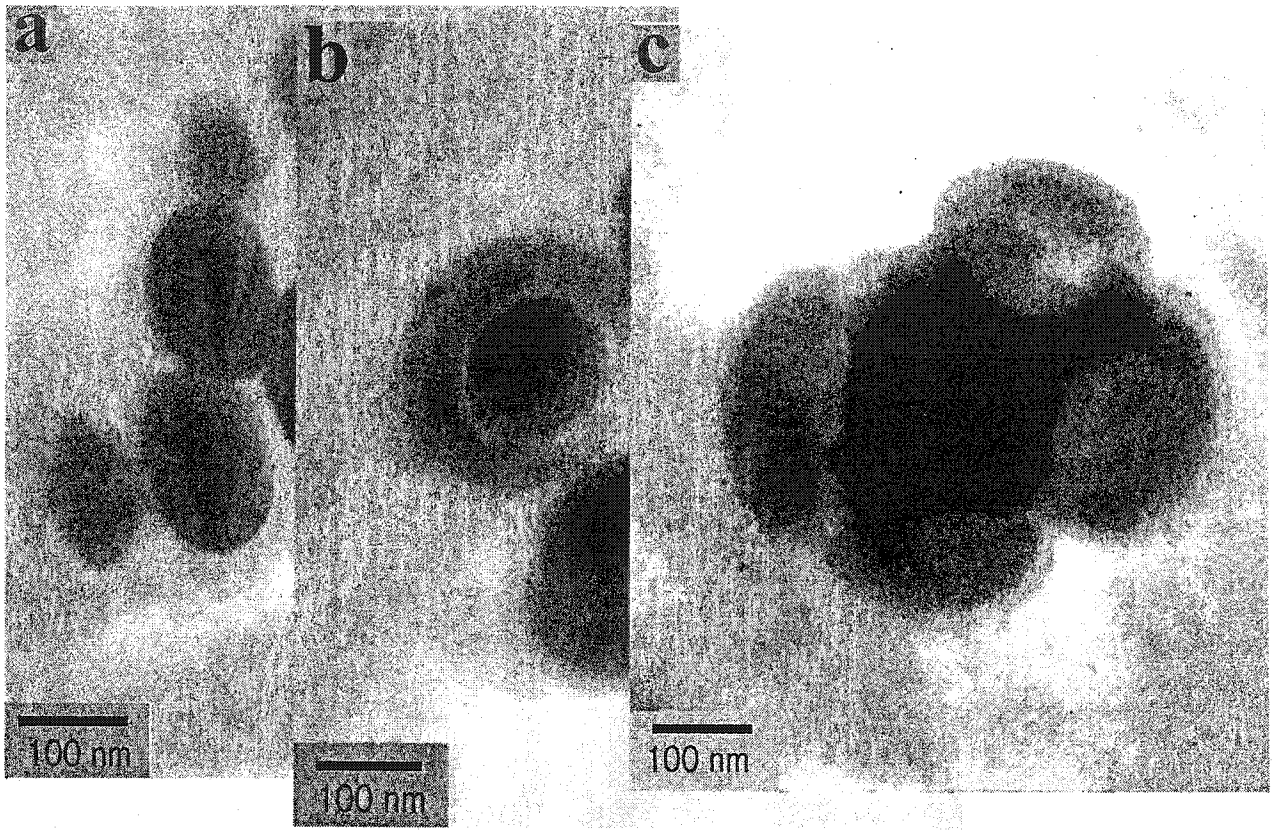

Figure 4. TEM images of particle cross-sections. (a) polystyrene seed particle of CPS2, (b) third stage latex of CPS2 (PS-PVPh), (c) third stage latex of CPS5 (PS-PVPh).

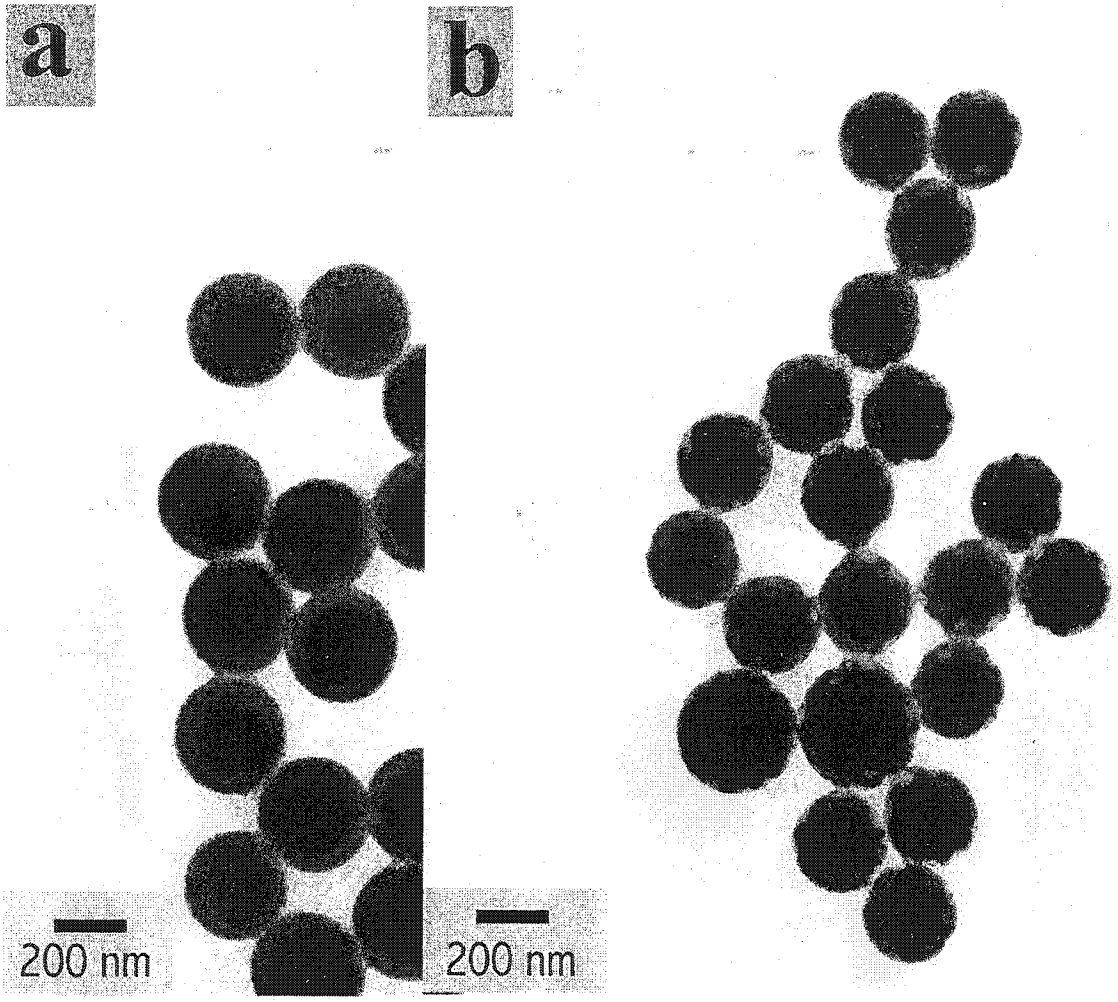

Figure 5. **(a) TEM images of CPS6 (no cross-linking) at the third stage (PS core + PVPh shell) ((AS + DVB)/PS = 0.4/1, no toluene and SDS). (b) TEM images of CPS7 (no cross-linking) at the third stage (PS core + PVPh shell) ((AS + DVB)/PS = 0.4/1, with toluene and SDS).**

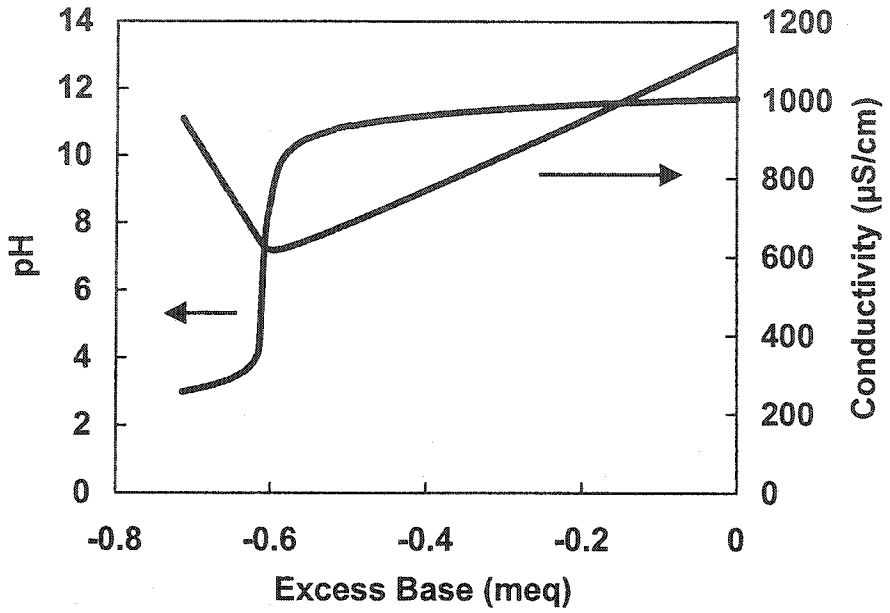

Figure 6. Potentiometric and conductometric titrations for CPS2 PS-PVPh latex. Initial total volume = 85 mL, particle concentration = 0.724 g/L.

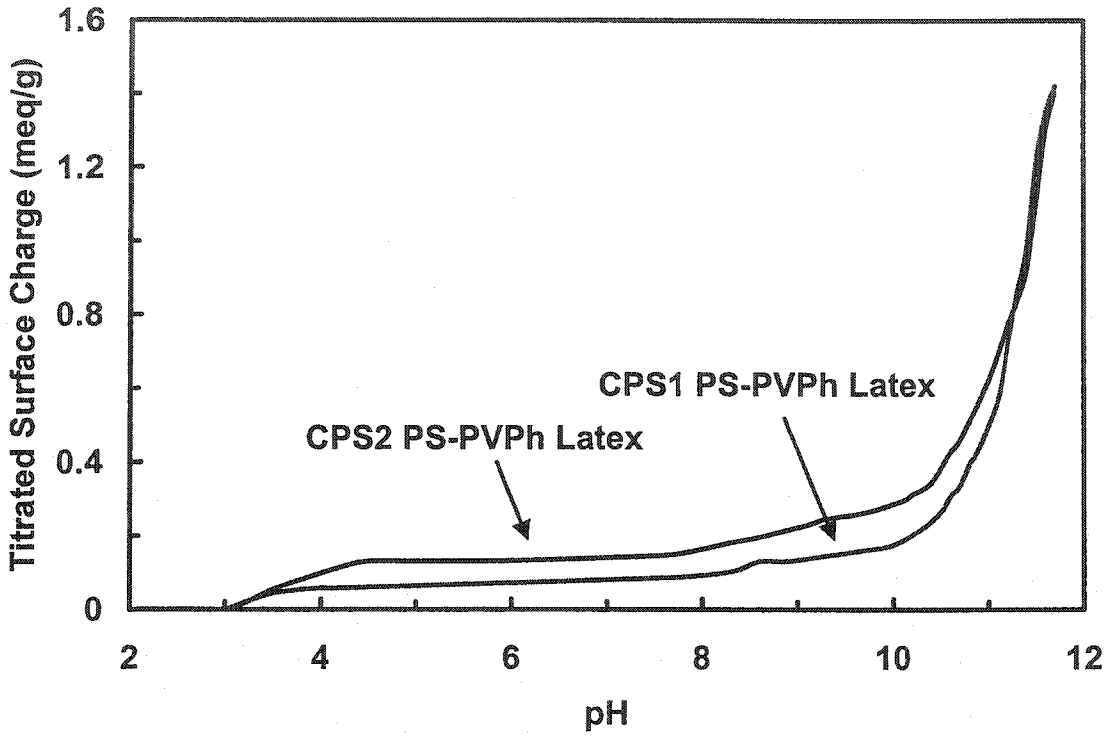

Figure 7. The titratable charge content of two composite latexes as functions of pH.

References

[1] Pelton, R. H.; Allen, L. H.; Nugent, H. M. *Svensk Papperstidn* **1980**, *83*, 251.

[2] Garrard, J. P.; Pummer, H. *US Patent* 1973: 4,070,236.

[3] Pelton, R. H.; Tay, C. H.; Allen, L. H. *J. Pulp and Paper Science* **1984**, *10*, 5.

[4] Lindström, T.; Glads-Nord-Mark, G. *Colloids & Surfaces* **1984**, *8*, 337.

[5] Pelton, R. H.; Xiao, H.; Brook, M. A.; Hamielec, A. *Langmuir* **1996**, *12*, 5756.

[6] Echt, E. *European Patent Application* 1994: 621 369 A1.

[7] Stack, K. R.; Dunn, L. A.; Roberts, N. K. *Journal of Wood Chemistry and Technology* **1993**, *13(2)*, 283.

[8] Carignan, A.; Garnier, G.; van de Ven, T. G. M. *J. Pulp Paper Sci.* **1998**, *24(3)*, 94.

[9] Lu, C.; Pelton, R. H. *Journal of Colloid and Interface Science* **2002**, *254*, 101.

[10] Goodwin, J. W.; Ottewill, R. H.; Harris, N. M.; Tabony, J. *J. Colloid Interface Sci.* **1980**, *78*, 253.

[11] Morton, M.; Kaizerman, S.; Altier, M. W. *J. Colloid Sci.* **1954**, *9*, 300.

[12] Maxwell, I. A.; Morrison, B. R.; Napper, D. H.; Gilbert, R. G. *Macromolecules* **1991**, *24*, 1629.

[13] EI-Aasser, M. S. In *Scientific Methods for the Study of Polymer Colloids and Their Applications, NATO Series*; Kluwer Academic Publishers: Netherlands 1990; Chapter 1, pp 1-127.

[14] Lee, D. I.; Ishikawa, T. *Journal of Polymer Science: Polymer chemistry Edition* **1983**, *21*, 147.

[15] Marion, P.; Beinert, G.; Juhué, D.; Lang, J. *Macromolecules* **1997**, *30*, 123.

[16] Winnik, M. A.; Zhao, C. *Langmuir* **1993**, *9*, 2053.

[17] Okubo, M.; Murakami, Y.; Fujiwara, T. *Colloid Polym. Sci.* **1996**, *274*, 520.

[18] Okubo, M.; Murakami, Y.; Fujiwara, T. *Colloid Polym. Sci.* **1998**, *276*, 186.

[19] Jönsson, Jan-Erik; Hassander, H.; Törnell, B. *Macromolecules* **1994**, *27*, 1932.

[20] Sundberg, D. C.; Casassa, A. P.; Pantazopoulos, J.; Muscato, M. R. *J. Appl. Polym. Sci.* **1990**, *41*, 1425.

[21] Goodwin, J. W.; Hearn, J.; Ho, C. C.; Ottewill, R. H. *Br. Polym. J.* **1973**, *5*, 347.

[22] Leopold, O. K.; Graz, H. S. *Instruction Manual for Calculating Digital Density Meter (DMA 45)*, Anton Paar K. G.

---

[23] Tan, J. S.; Gasper, S. P. *Macromolecules* **1973**, *6(5)*, 741.

[24] Pelton, R. H.; Miller, P.; McPhee, W.; Rajaram, S. *Colloids and Surfaces A: Physicochemical and Engineering Aspects* **1993**, *80*, 181.

[25] Goodall, A. R.; Hearn, J.; Wilkinson, M. C. *J. Polym. Sci., Polym. Chem. Ed.* **1979**, *17*, 1019.

[26] Yate, D, E.; Ottewill, R. H.; Goodwin, J. W. *J. Colloid Interfaces Sci.* **1977**, *62*, 356.

[27] Wilkinson, M. C.; Hearn, J.; Steward, P. A. *Advances in Colloid and Interface Science* **1999**, *81*, 77.

Chapter 3 PEO Flocculation of Polystyrene-core Poly(vinyl phenol)-shell Latex – An Example of Ideal Bridging

Abstract

The poly(ethylene oxide) (PEO) induced flocculation of polystyrene latex (PS) and polystyrene-core poly(p-vinyl phenol)-shell (PS-PVPh) latexes were compared. PEO gave much more effective flocculation of the core-shell particles and flocculation was observed over a much greater range of PEO concentrations. The core-shell particles were able to adsorb 6 to 7 times more PEO than comparable sized polystyrene latex. It is proposed that the efficient flocculation and the PEO high adsorption capacity of core-shell particles shows that adsorbed PEO molecules do not spread upon the poly(vinyl phenol) surface.

The polymer flattening model of Pelssers, Cohen Stuart and Fleer was extended to account for the available surface area when an adsorbed flocculant molecule spreads on a surface. The revised model, coupled with conventional kinetic expressions for flocculation and polymer adsorption, gave good predictions of a wide variety of flocculation behaviors.

Introduction

High molecular weight water-soluble polymers (flocculants) are widely used to induce the aggregation of aqueous colloids.[1] In most cases the flocculants are slightly cationic, to encourage adsorption, and are linear with molecular weights in the millions. Cationic copolymers of polyacrylamide are typical examples.

A number of models have been developed to relate flocculant adsorption isotherms to the optimum flocculant dosage [2,3,4,5,6]. La Mer's bridging concepts are the basis for most of these theories.[7] In bridging, the flocculant adsorbs onto a colloidal particle in sufficiently extended configuration so that the adsorbed macromolecule extends beyond the distance of the closest approach of a second particle. Bridging occurs when the adsorbed flocculant on one particle adsorbs onto a second one giving a doublet. La Mer pointed out that the highest flocculation efficiency should correspond to the situation where half of the available surface is covered with adsorbed flocculant. Although qualitatively simple, bridging is quantitatively complicated because polymer adsorption dynamics are coupled to particle collision dynamics.

Flocculation experiments frequently show lower rates and extents of flocculation than expected from bridging theory. There are a number of explanations including: a fraction of a the particle surface sites are "blocked" with other adsorbed material or are inactive [3,4,5,] hydrodynamic forces can irreversibly[8] destroy polymer bridges either by chain scission[9] or by transfer into an inactive form; and, adsorbed flocculant flattens (reconfigures) with time to give reduced or no flocculation.[10,11]

The flocculation of monodisperse, surfactant-free polystyrene latex with high molecular weight poly(ethylene oxide) (PEO) is an appealing experimental system. The latex surface has been well characterized, the particles are uniform spheres and electrostatics are not involved in polymer adsorption. However, this is a deviant system. In a convincing paper, Pelssers et al.[12] showed that polystyrene latex flocculation with PEO displays deactivation by spreading. The effects are greatest when the ionic strength is low (requiring thick bridging layers) and when the particle concentrations are low (lower collision frequency gives longer times for polymer spreading). Furthermore, they proposed that the spreading could be described by a 1-parameter model (Equation 17 as discussed in the following sections).[13]

The tendency for adsorbed flocculants to adsorb and then spread can be inhibited by pre-adsorbing ("site blocking") other polymers which occupy bare surface limiting the opportunity for adsorbed flocculant to spread. [4,14,15]

In view of all the possible complications in bridging flocculation there are few examples of ideal bridging. In such a system there should be no flocculant re-configuration, there should be no redispersion of flocs, and the flocculant concentration dependence should conform to the original concepts of Smellie and La Mer.

This paper makes two contributions to flocculation science. First, a new experimental system is described which appears to give ideal bridging flocculation; it is a polystyrene latex with a shell of poly(vinyl phenol) flocculated with PEO. Second, we present a model which extends Pelssers's treatment[13] of polymer flattening to give quantitative descriptions of flocculation kinetics for deviant systems such as the PEO flocculation of polystyrene latex.

Modeling Flocculation

Modeling Particle Aggregation

A model is developed in this section to predict the turbidity of an aggregating latex suspension. Consider a suspension of uniform colloidal particles with a concentration of N_1 particles per unit volume and assume that flocculation is initiated by flocculant addition at $t = 0$. The initial rate of flocculation is given by the following equation where k_{11} is the particle collision rate constant for two primary particles and E is the flocculation efficiency which gives the fraction of collisions leading to doublets.

$$-dN_1 / dt = k_{11} N_1^2 E \qquad (1)$$

Equation 1 can be extended to the following differential equation for the concentration of aggregates containing m primary particles.

$$dN_m / dt = \left[\frac{1}{2} \sum_{i=1}^{i=m-1} k_{i,m-i} N_i N_{m-i} - \sum_{i=1}^{\infty} k_{im} N_i N_m \right] E \qquad (2)$$

where N_m, N_i and N_j are the number concentrations of m-fold, i-fold and j-fold clusters respectively. Equation 2 is predicated on the assumption that aggregates do not break – that is, flocculation is irreversible.

A key assumption in our model is that singlets and doublets are mainly responsible for the turbidity of an aggregating latex suspension. For these we employed the following simplified versions of Equation 2 in which a single value of the particle aggregation rate constant appears in the right hand term. Since our simulations are for turbulent suspensions, this assumption means the collision frequency of larger aggregates is underestimated.

$$dN_1 / dt = -k_{11} N_1 E \sum_{j=1}^{\infty} N_j \qquad (3)$$

$$dN_2 / dt = \left[\frac{1}{2} k_{11} N_1^2 - k_{21} N_2 \sum_{j=1}^{\infty} N_j \right] E \qquad (4)$$

$$dN_3 / dt = \left[\frac{1}{2} k_{21} N_1 N_2 - k_{13} N_3 \sum_{m=1}^{\infty} N_m \right] E \qquad (5)$$

The total concentration of particles at any point in the flocculation process was required. For this we made the Smoluchowski approximation that k_{ij} was independent of aggregate size. This leads to the flollowing standard relationship for the time dependence of the total particle concentration.[16]

$$d\sum_{k=1}^{\infty} N_k / dt = -\frac{1}{2} k_1 E (\sum_{k=1}^{\infty} N_k)^2 \qquad (6)$$

Solution of these equations required specific values for k_{ij} and E. We employed the following variation of the classical expression for the coagulation rate constant k_1 following von Smoluchowski[17] and Saffman and Turner[18].

$$k_1 = \alpha_T \sqrt{\frac{8\pi}{15}} (r_i + r_j)^3 G \qquad (7)$$

where: r_i and r_j are the hydrodynamic radii of the particles i and j, respectively; G is the effective shear rate; α_T is the correction factor of shear coagulation[19] and can be assumed to be 1 for the bridging of PS particles by the flexible polymer as suggested in the literature.[20]

Smellie and La Mer proposed that E was related to the degree of surface covered with adsorbed flocculant, θ.[7] Hogg [2] gave the following equation which is a corrected version of the Smellie and La Mer expression.

$$E = 2\theta(1-\theta) \qquad (8)$$

Moudgil and coworkers considered three types of polymer adsorption sites on particle surfaces: active - those bearing adsorbed polymers capable of bridging; empty – those available for bridge adsorption; and, inactive – those sites which cannot bind bridging flocculant.[3, 4, 5] Equation 2 can be modified to the following form to account for the presence of inactive sites.

$$E = 2\theta_a \theta_e \qquad (9)$$

$$\theta_a = n_a / n_t \qquad (10)$$

$$\theta_e = n_e / n_t \qquad (11)$$

where n_a is the number of active polymers on one particle surface, n_t is the maximum number of polymers that can adsorb onto one particle surface, n_e is the number of empty sites on one particle surface and it is assumed that each polymer occupies one of particle surface sites.

The total capacity of the suspension to adsorb flocculant, n_t, was estimated from the PEO adsorption isotherm using Equation 12.

$$n_t = \Gamma_{\max} \alpha N_{av} / MW \qquad (12)$$

where N_{av} is the Avogadro number, α the surface area of one particle, MW the molecular weight of polymer and $\Gamma_{\max}$ the maximum adsorption capacity on the particle surface.

Equation 12 is not exact for the case of an adsorbing polymer which can spread. If adsorption occurs slowly from a very dilute suspension, the initially adsorbed polymer will spread which lowers the adsorption capacity. Recently, van Eijk and Cohen Stuart proposed a polymer adsorption kinetic model, which accounted for the reconfiguration of adsorbed polymer.[21] The model was cast in terms of the flux of polymer to the surface and analytical solutions were given for the case of constant flux which can be obtained in stagnation point flow.

The number of empty adsorption sites, n_e, was obtained by subtracting the number of adsorbed polymers on each particle, n_b, from the total number of sites per particle, n_t.

$$n_e = n_t - n_b \qquad (13)$$

The total number of occupied bonding sites, n_b, was obtained from the following material balance of polymer in solution where c_o is the initial polymer concentration, and c is the polymer concentration at time t.

$$n_b = (c_o - c) / N_0 \qquad (14)$$

Modeling Polymer Adsorption

The initial rate of flocculant adsorption is given by the following expression where k_p is the flocculant particle collision constant and N_0 and c_o are the initial concentration of primary particles and polymer molecules respectively.[10]

$$dc_0 / dt = -k_p N_0 c_0 \qquad (15)$$

The rate of polymer adsorption at longer times was assumed to be the following function of the fraction of available adsorption sites, θ_e, which is also a function of time.

$$dc / dt = -k_p N_0 c\theta_e \qquad (16)$$

Our model specifically accounts for the reconformation of active to inactive adsorbed flocculant. Pelssers,[13] proposed the following equation to account for spreading and deactivation.

$$dn_a / dt = k_p c - k_s n_a \qquad (17)$$

where k_s is the rate constant for the deactivation (spreading) of adsorbed polymers.

Schneider and coworkers[22] showed that polymers adsorbed at an early stage will flatten to a large extent, whereas a significant population of polymers that arrive later will adsorb with a low bound fraction. This indicates that the polymer deactivation rate depends upon the availability of empty sites (θ_e). Therefore, we modified Equation (20) to give the following expression.

$$dn_a / dt = (k_p c_c - k_s n_a)\theta_e \qquad (18)$$

Equations 3, 4, 6, 16 and 18 were solved simultaneously by the Rkadapt numerical method in MathCAD Version 2000 Professional. Two other numerical methods, rkfixed (Runge-Kutta method) and Bulstoer (Bulirsch-Stoer method) were also employed and they gave essentially the same results. The MathCAD convergence tolerance (TOL), which controls the precision to which integrals and derivatives are evaluated, was set as 10^{-8}.

Estimating Turbidly

The turbidity of a suspension is sum of the contributions of each type of particle[23, 24].

$$\tau = \sum N_i C_i \qquad (19)$$

where τ is turbidity and C_i is the scattering cross-section of i-fold aggregates. Pelssers et al's single particle counting results indicated that the most abundant species in flocculating suspensions were singlets and doubles[13]. Thus, only singlets and doublets were used to estimate turbidity and Equation 19 simplifies to give the following, where the relative turbidity, τ_r, is the turbidity divided by the turbidity of the stable suspension.

$$\tau_r = (N_1 C_1 + N_2 C_2) / N_0 C_1 \qquad (20)$$

where C_1 is given by

$$C_1 = Q_1 \pi r_1^2 \qquad (21)$$

and Q_1 is the non-dimensional scattering coefficient for primary particles. In the case of doublets, primary particles are assumed to be independent scatterers and the light scattered by each interferes with that scattered by its neighbors.[25] Consequently C_2 can be expressed as

$$C_2 = 2C_1\left[1 + \sin(2r_1 h)/2r_1 h\right] \qquad (22)$$

where h is given as

$$h = 4\pi/\lambda \qquad (23)$$

and λ is the wavelength of the incident light.

Experimental

Materials

PEO 309 with a weight average molecular weight of 8×10^6 Da (Polyox 309) and a weight average molecular weight of 1×10^5 Da (Polyox N-10) were obtained from Union Carbide. Solutions of concentrated PEO samples were prepared by mixing polymer (0.5 g/L) in water with mild agitation for 24 hours. Analytical grade tannic acid (Aldrich) was used without further purification.

Polystyrene (PS) latexes were prepared by a conventional surfactant-free batch process.[26] PS-core poly(p-vinylphenol)-shell (PS-PVPh) latexes were synthesized in our laboratory by hydrolyzing PS-core poly(p-acetoxystyrene)-shell latexes, which were prepared by two stage surfactant-free emulsion polymerization. In order to anchor the poly(p-vinylphenol) shell during hydrolysis, Divinylbenzene (DVB) was introduced with p-acetoxystyrene monomer for the second stage polymerization. Details of the preparation and characterization of core-shell latexes have been reported in the previous paper.[27] Table 1 lists the weight average particle diameters measured by a BI-DCP Particle Sizer (Brookhaven Instrument Co.) and intensity average particle diameters by dynamic light scattering (DLS) using a Lexel laser (wave length 514 nm) equipped with a BI-9000 AT digital correlator (Brookhaven). The light scattering was measured at a 90° angle and the particle sizes were calculated by the non-negatively constrained least squares (regularized) method using software BI9000AT version 6.1.

Table 2 shows the shell water fractions calculated from the changes in particle size, determined by DLS, with hydrolysis. For this analysis it was assumed that swelling only occurred in the shell region and that no polymer chains were removed in the

hydrolysis operation. The electrophoretic mobilities of the core-shell particles are shown in Table 3. The mobilities reflect the presence of sulfate groups originating from the persulfate initiator.

Methods

The degree to which suspensions of latex particles were flocculated was analyzed using a Photometric Dispersion Analyzer (PDA) (Rank Brothers, Cambridge, UK), the operation of which has been described previously.[24, 28] All of the experiments except otherwise mentioned were carried out in 0.001 mol/L NaCl solution and the total volume was kept at 200 mL. In a typical flocculation experiment, PEO was added 60 seconds after the addition of latex particles. The suspension was stirred at 475 rpm using a three-bladed propeller (55 mm diameter) and the extent of flocculation was monitored by circulating the suspension through PDA at a rate of 45 mL/min. After flocculation, DC output was converted to relative turbidity by the following relationship,

$$\tau_r = \ln\left(\frac{V_w}{V_t}\right) \Big/ \ln\left(\frac{V_w}{V_{t=0}}\right) \qquad (24)$$

where V_w is the output voltage for water, $V_{t=0}$ is the output voltage for latex suspension before the addition of PEO and V_t is the output voltage at time t. It can be assumed that the relative turbidity is roughly proportional to the fraction of un-flocculated particles. The higher the relative turbidity, the lower the flocculation extent. A more rigorous relationship between relative turbidity and un-flocculated particles was given in the above sections.

PEO equilibrium adsorption amount on the latex particle surfaces was measured by the tannic acid method.[29, 30] A linear calibration equation of the absorbency of PEO and tannic acid complex as a function of PEO concentration was obtained first in the following manner. PEO was dissolved in water to give a concentration of 0.5 g/L. Various amounts of PEO solution were added into a 50 mL volumetric flask containing 5 mL of 1 mol/L NaCl solution. 30 mL of water was then introduced and the volumetric flask was shaken up and down 20 times. 5 mL of 2 g/L tannic acid and more water were added to give a total volume of 50 mL. The volumetric flask was shaken another 20 times and let stand for 30 minutes at room temperature. The absorbency of PEO and tannic acid complex was measured with a HP8452A UV-Vis spectrophotometer (Hewlett-Packard) at a wavelength of 600 nm. In the PEO equilibrium absorption experiments, latex suspension was added into 0.001 mol/L NaCl solution to give a concentration of 0.2 g/L. Various amounts of PEO were added and the suspensions and allowed to stand for 4 days to reach adsorption equilibrium. The latex particles were extracted by spinning the suspension for 50 minutes at 50,000 rpm at 25°C. 15 mL of supernatant was transferred to a 50 mL volumetric flask. The amount of free PEO in the

supernatant was measured by the absorbency of PEO and tannic acid complex and the adsorbed PEO amount was calculated accordingly.

The change of the particle size of PS and PS-PVPh due to the adsorption of PEO N-10 ($MW=10^5$) was measured by DLS. In a typical experiment, PEO N-10 was added to latex suspension of 20 mg/L and the suspension was diluted by 0.001 mol/L NaCl solution. The light scattering was measured at a 90° angle and the particle sizes were calculated by the non-negatively constrained least squares (regularized) method using software BI9000AT version 6.1. Particle sizes were measured six times for each PEO concentration.

Results

In this work we compared the PEO-induced flocculation behavior of polystyrene latex with polystyrene-shell poly(vinyl phenol)-shell particles. The preparation and characterization of the particles has been described previously[27] and the properties are summarized in Tables 1 - 3. The core-shell particles are monodisperse with a shell thickness of around 60 nm with shell water contents varying between 60~80 wt% depending upon the concentration of crosslinking monomer used in the preparation. The following sections summarize the absorption and flocculation results.

Figure 1 shows the adsorption isotherms (25°C) for PEO 309 ($MW=8\times10^6$ Da) onto polystyrene latex and on three polystyrene-core poly(vinylphenol)-shell latexes. The maximum adsorption amount of PEO for the polystyrene particles PS1 (diameter 138 nm) was close to 0.98 mg/m^2, a value quoted in the literature.[30] By contrast the adsorption maximum for CPS3 was around 7.6 mg/m^2, which is more than six times greater. The other two PS-PVPh latexes with higher shell crosslink densities had slightly lower PEO adsorption capacities (CPS2 was 6.1 mg/m^2 and CPS1 was 6.2 mg/m^2). The shell cross-linker contents for CPS1, CPS2 and CPS3 were 20 wt%, 5 wt% and 1 wt% respectively. Thus, the very high PEO adsorption capacities were not very sensitive to the degree of crosslinking in the PVPh shells. It is difficult to rationalize these high adsorption densities in terms of the packing of individual PEO random coils. van de Ven explains high PEO adsorption densities by the presence of non-equilibrium entangled PEO in which two or more chains adsorb as a single species[31].

The core-shell particles are not hard spheres – the shells are more than half water. Dynamic light scattering was used to probe changes in shell structure upon the adsorption of medium molecular weight PEO N-10 ($MW=10^5$ Da) which was chosen to minimize flocculation. The results, summarized in Figure 2, show that the size of CPS2 decreased from 269 nm to 250 nm upon PEO adsorption. This indicates that PEO/PVPh complex formation caused the average shell water content to decrease from 72% to 64%. We do not know how far the adsorbed PEO penetrates into the poly(vinyl phenol) shell. However, the fact that the adsorption isotherm was nearly independent of crosslink

density (above) and that good flocculation was achieved (below), suggests that adsorbed PEO was mainly in the exterior parts of the shell.

It is noteworthy that in doing dynamic light scattering it was necessary to employ low core-shell latex particle concentrations to prevent flocculation. In standard flocculation experiments PEO N-10 (10,000 Da) gave a steady-state relative turbidity of 0.7. We believe that this is the first reported instance of such a low molecular weight PEO giving flocculation of latex in low ionic strength solution.

By contrast, the particle size of polystyrene latex PS2 did not change indicating that the adsorbed PEO layer on PS2 was less than our ability to measure changes in hydrodynamic thickness (i.e. less than 5 nm, the scale of the error bars).

Polystyrene latex was flocculated with high molecular weight PEO. Figure 3 shows the flocculation extent of PS5 as a function of time for three different PEO concentrations expressed as mass per square meter of latex surface. In all cases the minimum relative turbidity, a measure of the extent of flocculation, was greater than 0.5 indicating poor flocculation. The curve corresponding to the lowest PEO dose had a small positive slope at long times indicating slight floc redispersion whereas the other two curves suggested a slow approach to a steady state relative turbidity.

Some corresponding results for core-shell particle flocculation with PEO are shown in Figure 4. The intermediate PEO concentrations of 0.46 and 2.89 mg/m^2 gave nearly complete flocculation with no indication of redispersion whereas the lowest and the highest dosages gave slightly less flocculation.

The flocculation of the two types of latexes is directly compared in Figure 5 which shows the relative turbidities as function of PEO concentration at 200 s after the addition of PEO 309. Thus, this corresponds to maximum, steady state flocculation. The solid lines show the model predictions and will be discussed later. The experimental results indicate the maximum extent of flocculation. Polystyrene latex flocculation occurred over a narrow range of PEO concentrations – similar results have been reported before.[12] By contrast, the core-shell particles were more completely flocculated and good flocculation was observed over a much broader range of PEO dosages.

Figure 6 shows the effect of NaCl concentration on the flocculation of PS and PS-PVPh latex particles. For PS5, the relative turbidity at the steady state (200 s) decreased from 0.725 to 0.46 when NaCl concentration was increased from 0 to 0.005 mol/L. There was little subsequent improvement when NaCl concentration was increased from 0.005 to 0.1 mol/L – similar results have been reported before.[12] Core-shell latex CPS5 also showed electrolyte sensitivity over the same salt concentration range. As before, the extents of flocculation were much greater with the core-shell latex so there was little scope for further improvement with salt addition.

Discussion

It is our hypothesis that the extreme differences in the adsorption (see Figure 1) and in the flocculation behavior of polystyrene, compared with core-shell particles (see Figure 5), reflect the fact that PEO does not spread on the core-shell particle surface. To support this we present the following results of the modeling which indicates that PEO deactivation by spreading must be invoked to predict the PS data whereas spreading is not necessary for modeling the core-shell particle data.

Experimental particle sizes and adsorption maxima were employed for the modeling. In addition, PEO 309 was assumed to be a spherical particle in water with a radius of 210 nm.[13] The average shear rate, G (see Equation 7) was assumed to be 800 s^{-1} based on measurements in similar devices.[32]

The rate constant (k_s) of polymer deactivation (by reconfiguration) is the only completely arbitrary model parameter that must be assigned. It is generally accepted that the polymer adsorption rate is much greater than the particle collision rate.[10] Therefore, when polymer concentration is much below particle surface saturation concentration, the flocculation extent is mainly controlled by the competition between polymer deactivation and particle collision. By contrast, when the PEO dosage is much above the surface saturation concentration, the particle surfaces are saturated quickly and polymer deactivation is negligible. This indicates that flocculation is most sensitive to polymer deactivation rate at low polymer concentration. Thus, k_s was obtained by fitting the model to the experimental results for polystyrene for at a PEO dosage of 0.47 mg/m^2. Figure 7 shows both theoretical and experimental relative turbidity values as a function of time. The best fit corresponded to a k_s value of 0.52 s^{-1} which was used for all the polystyrene modeling. Note, that the curve for $k_s = 0$ was a poor fit indicating that surface deactivation was important.

The ability of the model to predict polystyrene flocculation under other conditions is illustrated in Figure 8. The experimental trends with changing PEO concentration were simulated; however, the experimental steady state relative turbidities were about 20% higher than the model predictions.

The model was also used to simulate the flocculation of core-shell latex CPS5. Figure 9 compares calculated and experimental results. Unlike polystyrene latex, realistic equilibrium extents of flocculation were predicted without invoking deactivation (i.e. $k_s = 0$). The model can roughly approximate flocculation rate at low and medium PEO concentration (0.10 and 0.46 mg/m^2). However computed initial flocculation rate results were much greater than the experimental results at high PEO concentration, suggesting the rate constants estimated by Equation 7 were too high. On the other hand, good estimates of the steady state extent of flocculation were obtained.

The overall ability of the model to predict steady-state turbidities is shown in Figure 5. The points are experimental results and the solid lines are computed results. The spreading constants, k_s, for each type of latex are shown beside the curves. All the other model parameters were based on measured quantities such as particles sizes, measured PEO adsorption maximums etc. Clearly, the model does a reasonable job of predicting a wide range of experimental behaviors.

The new feature of the present model is the extension of Pelssers et al.'s spreading model (Equation 17) to include the available surface area for spreading (Equation 18). Figure 10 shows the computed number of active polymers per particle, n_a, as functions of time for different polymer dosages as computed by Pelssers' original equation (Equation 6 in reference 13). This behavior is clearly unrealistic because at high polymer concentrations the active polymer concentration should not go to zero because there should be no spreading. By contrast, including the θ_e term (Equation 18) gives the results shown in Figure 11. At low PEO dosage there is a lot of available surface and the polymer completely deactivates with time. At high PEO dosage the number of active polymers becomes constant. Note, that under these conditions there is no flocculation since there are no bare surfaces to which the active chains can bridge.

Several assumptions were made for the modeling, and these are now considered. First, it was assumed that flocs were not disrupted by hydrodynamic forces. Except for one polystyrene curve in Figure 3, all the flocculation versus time curves were either horizontal or slightly decreasing at long times. By contrast, weak flocs tend to break apart giving significant increases in turbidity with time because floc destruction is partially irreversible.

Second, it was assumed that the hydrodynamic efficiency factor α_T was one. This is equivalent to assuming that the hydrodynamic factors are the same when considering the two types of latexes. The ranges of particle sizes were the same for both PS and PS-PVPh particles so this appears to be a reasonable assumption. Nevertheless, some of the differences in flocculation may reflect subtle hydrodynamic differences in the two types of particles.

Finally, the modeling of turbidity ignored triplets and bigger particles. This was done for computational convenience. In the direct single particle counting of PEO induced polystyrene flocs, Pelssers et al. mentioned that they did not observe triplets or larger particles. This is expected because the larger particles have very high collision diameters causing their number to become very small even in the early stages of flocculation.

Both the adsorption isotherms and the flocculation curves indicate that PEO does not spread on the core-shell particle surfaces in the timescale of the flocculation experiments. This is not an obvious conclusion. It is known that aqueous PEO forms stable complexes with linear, water-soluble copolymers of vinyl phenol in aqueous

solutions.[33] Recent NOESY NMR results indicate that complex formation arises from hydrophobic interactions between methylenes on PEO and aromatic rings.[34] Furthermore, it is known from theory that the extent to which adsorbing polymer coils collapse and spread upon an impermeable uniform surface increases with segment-surface adsorption energy.[35] If PEO-PVPh interactions are of similar magnitude as PEO-polystyrene, then we would predict spreading.

However, the PVPh shells are not uniform and impermeable. The shell region is a crosslinked network containing as much as 76% water (Table 3). Thus we propose that the crosslinked PVPh chains are swollen and mobile which should facilitate cooperative interactions with PEO leading to local regions of collapse (coacervation) of the complex. The observation that the adsorption of lower molecular PEO gives a measurable collapse in the shell thickness (Figure 2) supports this view.

Conclusions

1. The maximum PEO adsorption on PS-PVPh core-shell particle surfaces is over 6 times greater than that observed with polystyrene latex.

2. PS-PVPh core-shell particles are almost completely flocculated over a broad range of PEO concentrations in contrast to the behavior of polystyrene latex.

3. We propose that adsorbed PEO does not spread on the poly(vinyl phenol) particle shells giving ideal bridging flocculation and high adsorption capacities.

4. An extension of the spreading model of Pelssers et al. coupled to standard treatments of polymer adsorption kinetics and coagulation kinetics gives good predictions of the maximum extent of flocculation for polystyrene latex. It was not necessary to invoke spreading to simulate the core-shell particles flocculation curves.

Table 1. Particle diameters determined by dynamic light scattering (DLS) and disc centrifuge (DC). The DLS error limits show the standard deviations of the mean based on 5 measurements. The DC error limits are the standard deviations of the distribution. The cross-linking degree stands for the weight percentage of DVB added with p-acetoxystyrene monomer.

Latex	Sample Name	Cross-linking Degree	Diameter	Shell Thickness[27] (nm)
PS	PS1		138 ± 7	-
PS	PS2		185 ± 1	-
PS	PS5		535 ± 15	-
PS-PVPh	CPS1	20%	250 ± 3	56
PS-PVPh	CPS2	5%	269 ± 5	66
PS-PVPh	CPS3	1%	330 ± 10	73
PS-PVPh	CPS5	1%	590 ± 8	75

Table 2 The influence of PS-PVPh shell crosslink density (mass fraction of divinylbenzene) on swelling in water determined by DLS.

Sample	Cross-linking Degree	Shell Region Water Fraction
CPS1	20%	59%
CPS2	5%	72%
CPS3	1%	76%

Table 3 The influence of pH on the electrophoretic mobility of CPS2 core-shell latex. Measurements were made at a light scattering angle of 22.5°. [NaCl] = 0.001 mol/L, 25°C.

pH	Mobility ($m^2/Vs \times 10^8$)
2.4	-1.29 ± 0.08
6.2	-2.96 ± 0.09
8.4	-3.38 ± 0.06
9.6	-3.96 ± 0.14
10.2	-4.21 ± 0.12

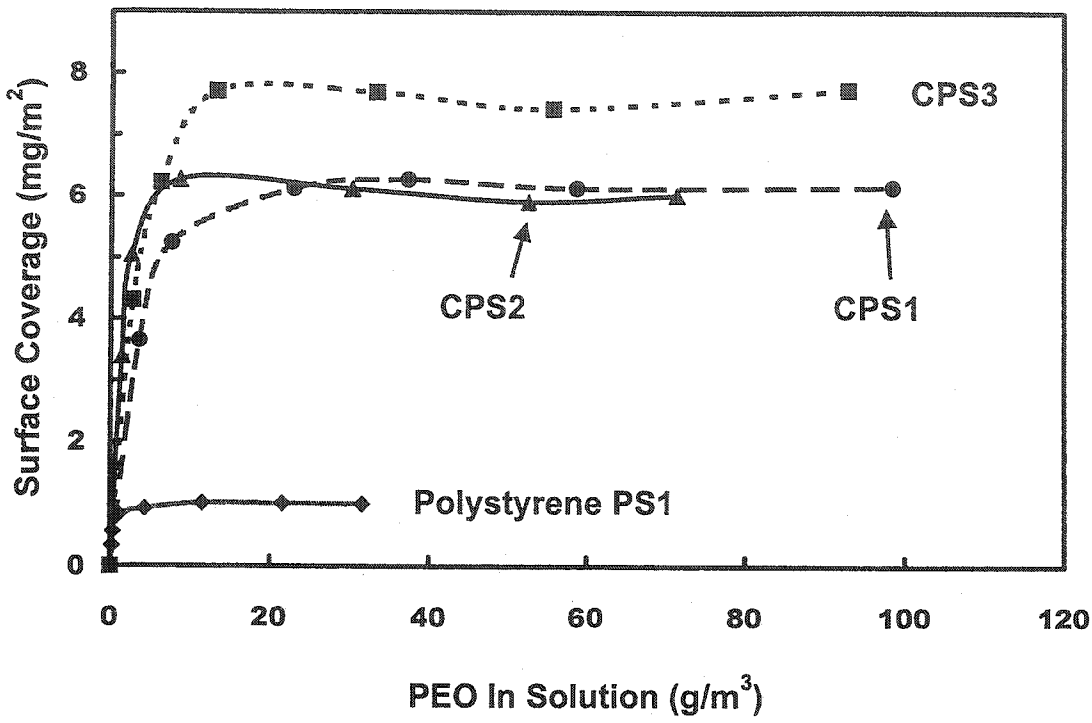

Figure 1. **PEO 309 (8×10^6 Da) adsorption isotherms (25°C) on polystyrene and core-shell particles. The latex concentrations were 0.2 g/L in 0.001 mol/L NaCl.**

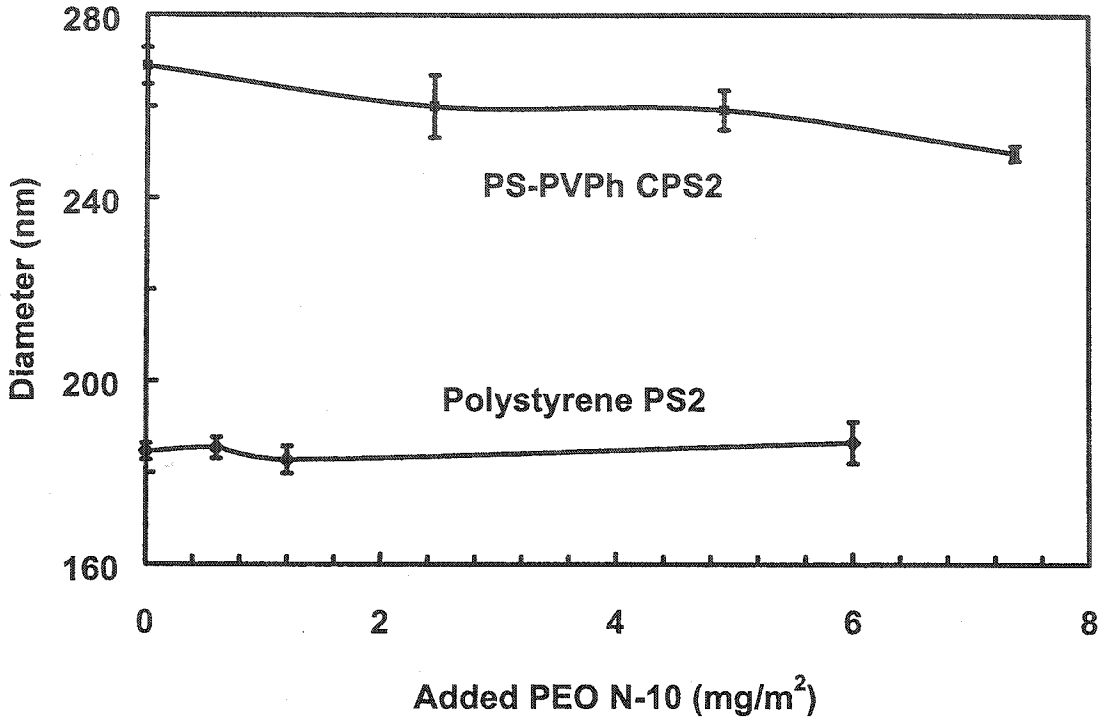

Figure 2. The influence of PEO N-10 (MW=10^5 Da) adsorption on the hydrodynamic particle size of polystyrene and core-shell latex in 0.001 mol/L NaCl solution. The error bars represent ± 1 standard deviation based on 6 DLS experiments.

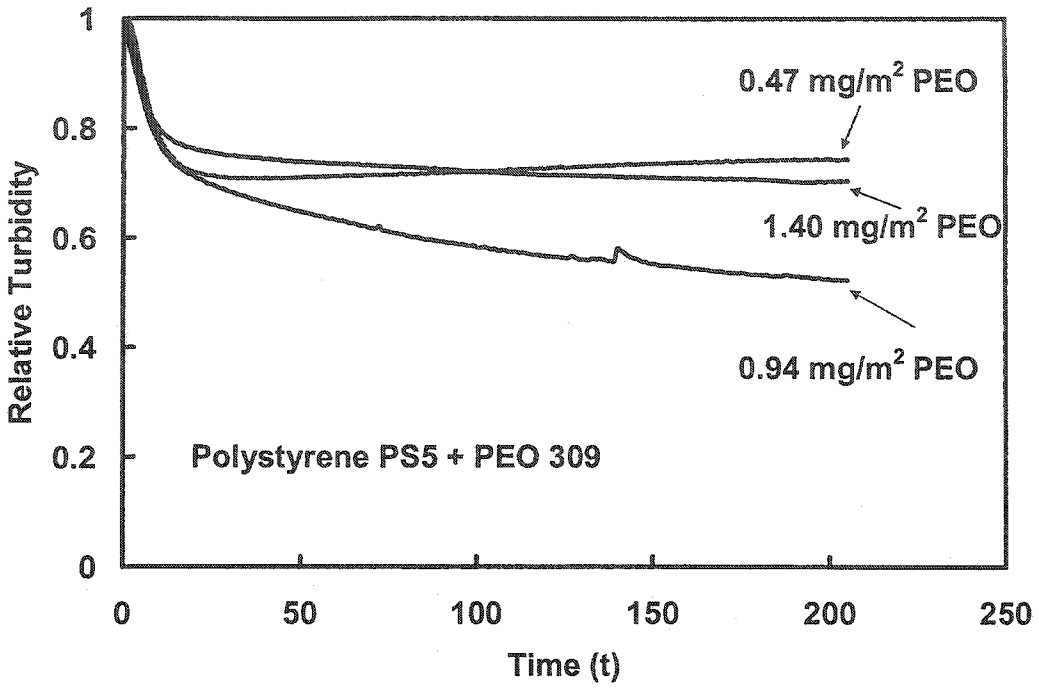

Figure 3. Relative turbidity of PS5 polystyrene latex as a function of time from the addition of PEO 309. The labels give the PEO concentration expressed as mass per latex surface area. [PS5] = 0.2 g/L; [NaCl] = 0.001 mol/L.

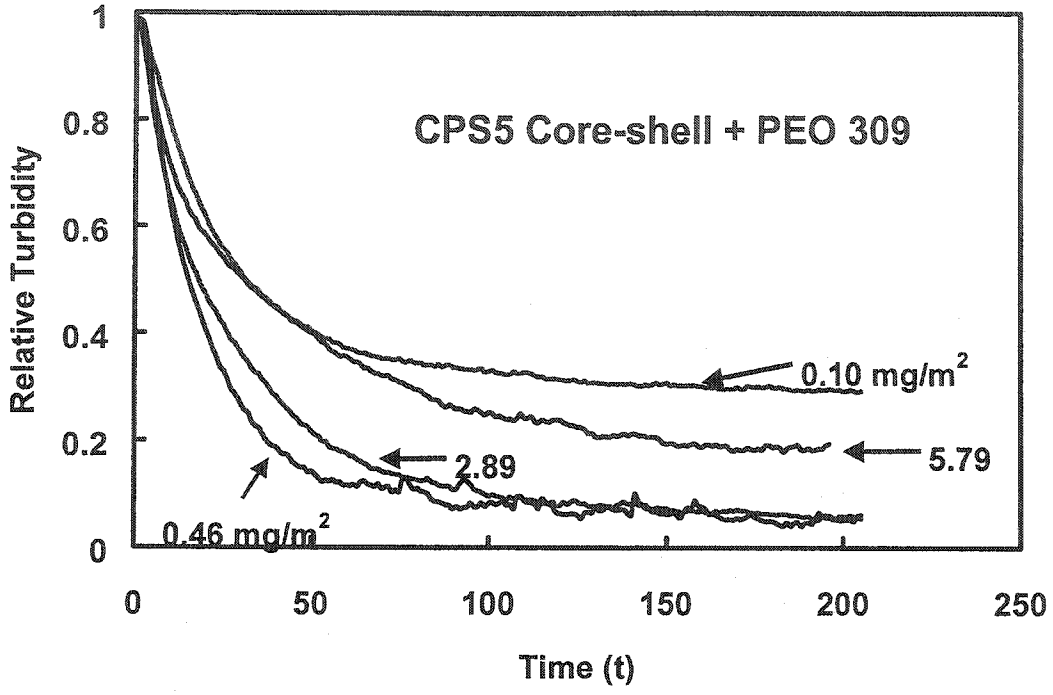

Figure 4. Core-shell latex CPS5 flocculation with PEO 309. The labels denote the PEO concentration. [CPS5] = 0.2 g/L; [NaCl] = 0.001 mol/L;

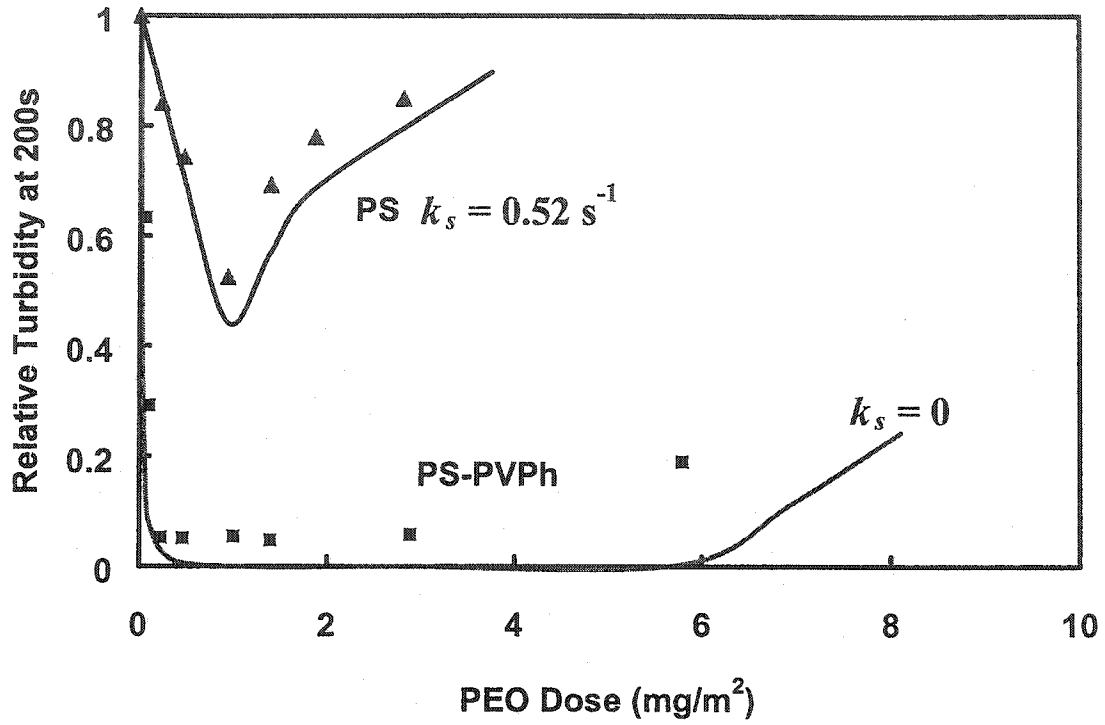

Figure 5. **The influence of PEO 309 dose on latex flocculation. The solid lines denote model results. [PS5] & [CPS5] = 0.2 g/L; [NaCl] = 0.001 mol/L.**

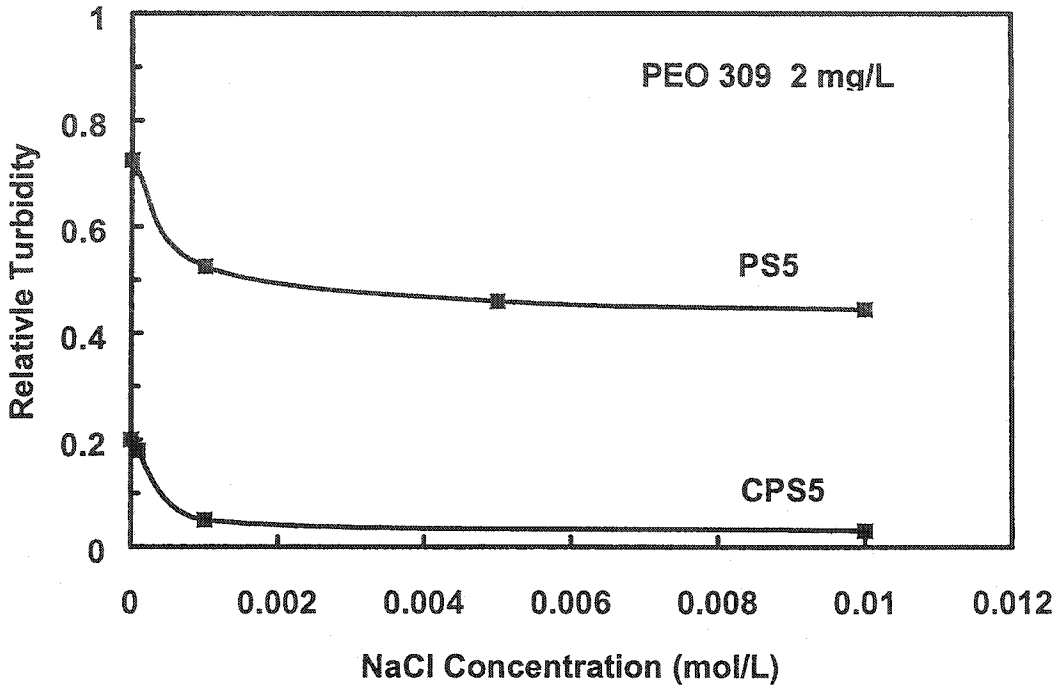

Figure 6. The effect of NaCl concentration on flocculation. [PS5] & [CPS5] = 0.2 g/L; [PEO] = 0.002 g/L.

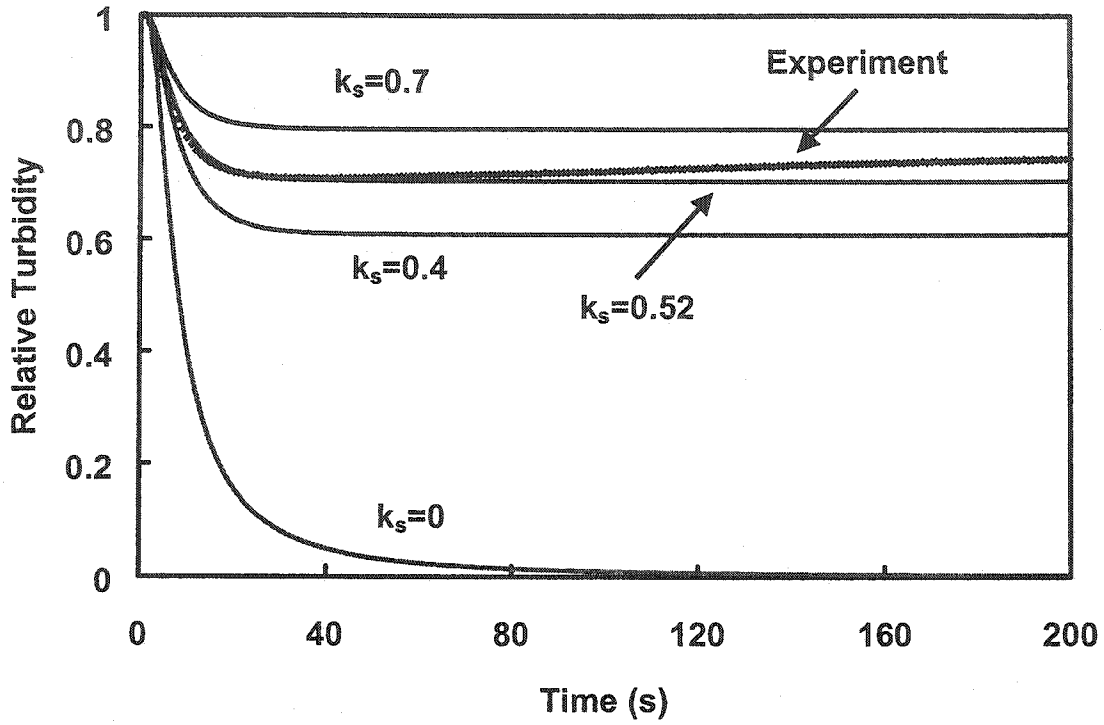

Figure 7. Fitting the deactivation rate constant, k_s, to a polystyrene flocculation curve. [PS5] = 0.2 g/L; [NaCl] = 0.001 mol/L; [PEO] = 0.001 g/L (0.47 mg/m^2). For the modeling, Γ_{max} = 1 mg/m^2, G = 800 s^{-1}.

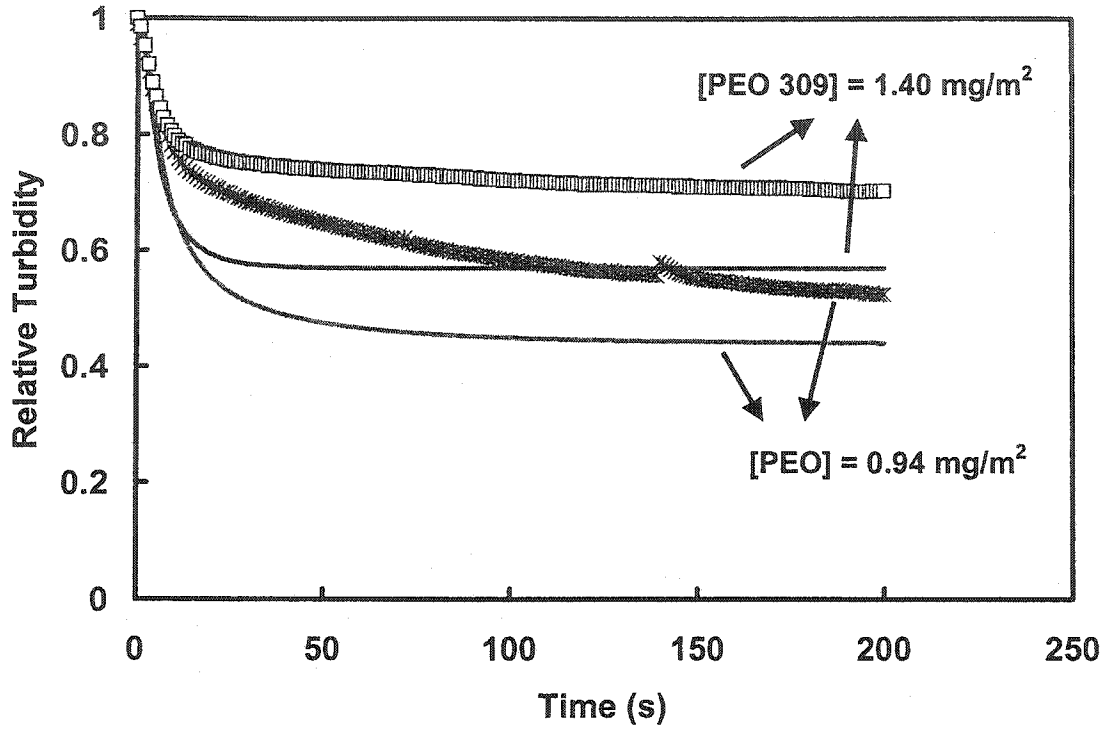

Figure 8. Relative turbidity of PS5 flocculated by PEO 309 at different concentrations. Solid lines represent the computed result and dotted lines represent the experimental result. [PS5] = 0.2 g/L; [NaCl] = 0.001 mol/L; PEO was added 60 seconds after the addition of PS5. Γ_{max} is postulated to be 1 mg/m^2 for PEO 309 on PS particle surface.

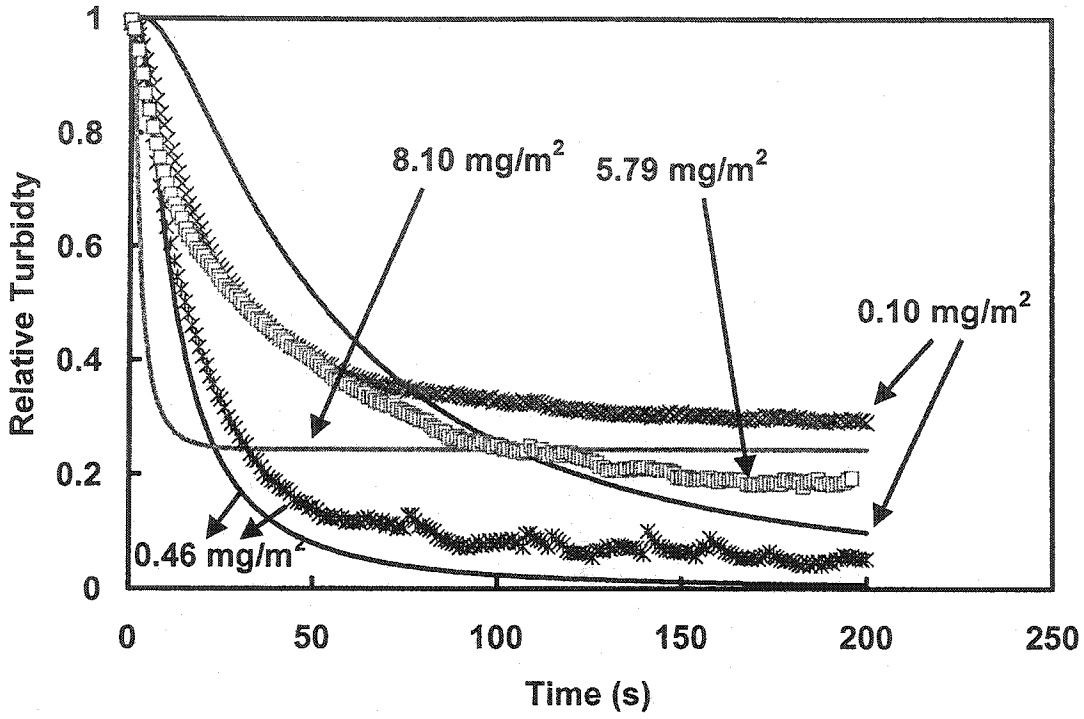

Figure 9. Computed relative turbidity of CPS5 flocculated by PEO 309 at different concentrations. Experimental conditions: [CPS5] = 0.2 g/L; [NaCl] = 0.001 mol/L; PEO was added 60 seconds after the addition of CPS5. Γ_{max} is postulated to be 6 mg/m^2 for PEO 309 on PVPh particle surface.

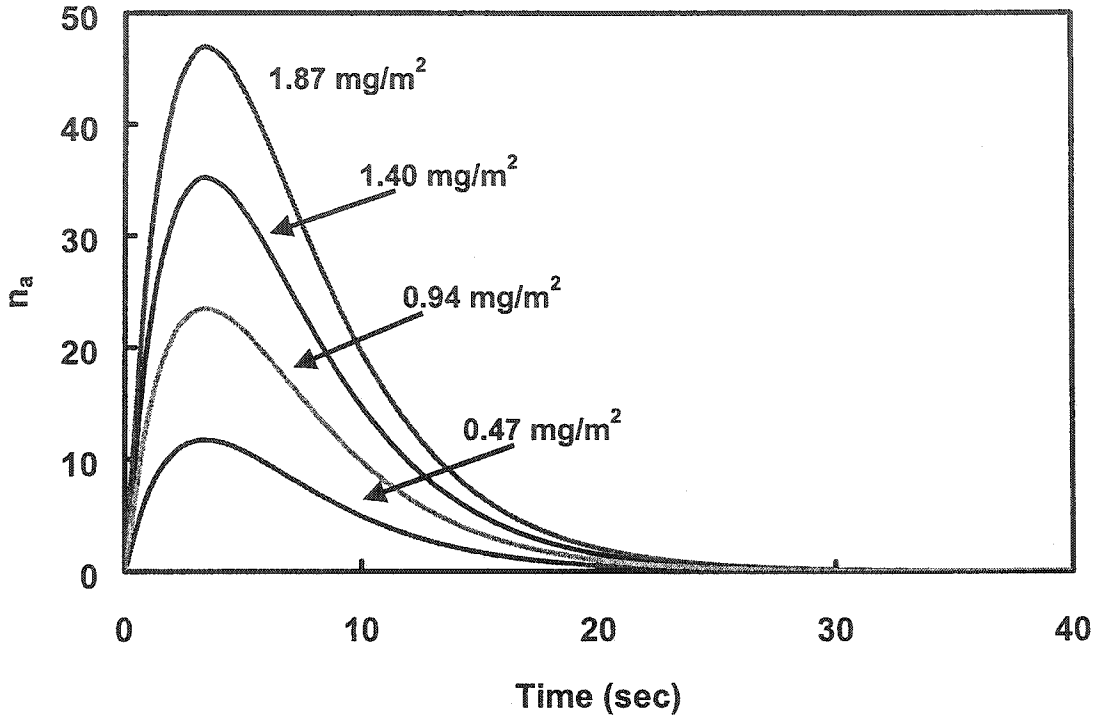

Figure 10. Computed change of the adsorbed active PEO 309 on the PS5 surface based on Equation 6 from reference 13. k_s = 1/3.4 s^{-1} (adapted from reference 13). [PS5] = 0.2 g/L.

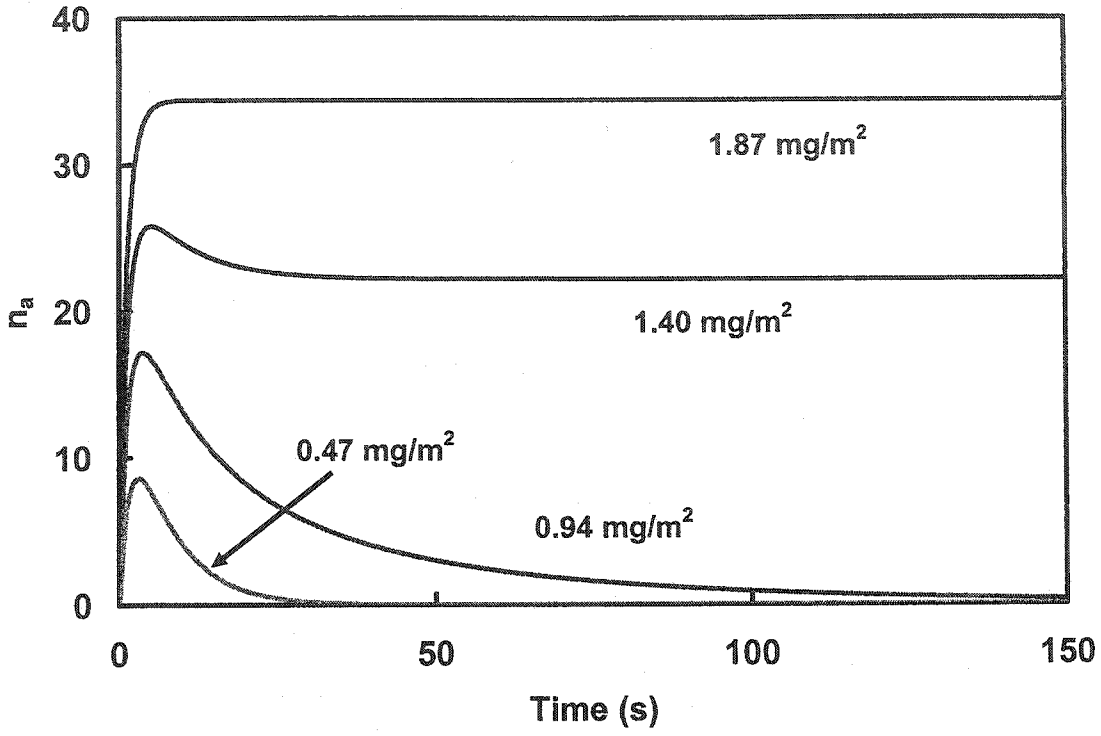

Figure 11. Computed change of the adsorbed active PEO 309 on the PS5 surface. [PS5] = 0.2 g/L. Γ_{max} is postulated to be 1 mg/m^2 for PEO 309 on PS particle surface.

References

1 Elimelech, M.; Gregory, J.; Jia, X.; Williams, R. A. Particle Deposition and Aggregation, Butterworth-Heinemann: Woburn, MA.,1995

2 Hogg, R. *J. Colloid Interface Sci.* **1984**, *102(1)*, 232-236.

3 Moudgil, B. M.; Shah, B. D.; Soto, H. S. *J. Colloid Interface Sci.* **1987**, *119(2)*, 466-473.

4 Behl, S.; Moudgil, B. M.; Prakash, T. S. *J. Colloid Interface Sci.* **1993**, *161*, 414-422.

5 Moudgil, B.M.; Behl, S. in *Flotation Science and Engineering*, Matis, K.A. Edi.; Marcel Dekker: New York, **1995**; p415.

6 Molski, A. *Colloid Polymer Sci.* **1989**, *267*, 371-375.

7 Smellie, R. H. Jr.; La Mer, V. K. *J. Colloid Sci.* **1958**, *23*, 589-599.

8 Pelton, R. H. *Colloids Surfaces* **1981**, *2*, 277-285.

9 Tanaka, H.; Ödberg, L. Wågberg, L.; Lindström, T. *J. Colloid Interface Sci.* **1990**, *134(1)*, 229-234.

10 Gregory, J. *Colloids and Surfaces* **1988**, *31*, 231- 253.

11 Gregory, J., *J. Colloid Interface Sci.* **1973**, *42*, 448-456.

12 Pelssers, E. G. M; Cohen Stuart, M. A.; Fleer, G. J. *Colloid Surfaces* 1989, 38, 15-25.

13 Pelssers, E. G. M.; Cohen Stuart, M. A.; Fleer, G. J. *J. Chem. Soc. Faraday Trans.* **1990**, *86(9)*, 1355-1361.

14 Stemme, S., Ödberg, L., *Colloids Surfaces* A **1999**, *157* 307-313.

15 Swerin, A.; Ödberg, L.; Wågberg, L. *Colloids Surfaces* A **1996**, *113*, 25-38

16 Overbeek, J. TH. G. Kinetics of Flocculation, in *Colloid Science, 1, Irreversible Systems*, Elsevier: Rotterdam, Netherlands, **1952**.

17 von Smoluchowski, M. *Z. Phys.* **1916**, *17*, 557-585.

18 Saffman, P. G.; Turner, J. S. *J. Fluid Mech.* **1956**, *1*, 16.

19 Adachi, Y. *Adv. Colloid and Interface Sci.* **1995**, *56*, 1-31.

20 Adachi, Y.; Wada, T. *J Colloid Interface Sci.* **2000**, *229*, 148-154.

21 van Eijk, M. C. P.; Cohen Stuart, M. A. *Langmuir* **1997**, *13*, 5447-5450.

22 Schneider, H. M.; Frantz, P.; Granick, S. Langmuir **1996**, *12*, 994-996.

23 Gregory, J. J. Colloid Interface Sci. **1985**, *105(2)*, 357-371.

[24] Gregory, J.; Nelson, D. W. in *Solid-Liquid Separation*, J. Gregory Ed.Ellis Horwood, Chichester, **1984**.

[25] Lips, A.; Smart, C.; Willis, E. *Trans. Faraday Soc.* **1971**, *67*, 2979-2988.

[26] Goodwin, J. W.; Hearn, J.; Ho, C. C.; Ottewill, R. H. Br. Polym. J. **1973**, *5*, 347-362.

[27] Lu, C.; Pelton, R. H. *Colloid Surfaces*, Submitted

[28] Gibbs, A.; Xiao, H.; Deng, Y.; Pelton, R. H. *Tappi* **1997**, *80(4)*, 163-170.

[29] Nuysink, J.; Koopal, L. K. *Talanta* **1982**, *29*, 495-501.

[30] Couture, L.; van de Ven, T. G. M. *Colloid Surfaces* **1991**, *54*, 245-260.

[31] Polverari, M.; van de Ven, T.G. *Colloids Surfaces A* **1994**, *86* 209—228.

[32] Tam Doo, P. A.; Kerekes, R. J.; Pelton, R. H. J. Pulp Paper Sci. **1984**, *10(4)*, 80-88.

[33] Pelton, R. H.; Xiao. H.; Brook, M. A.; Hamielec, A. *Langmuir* **1996**, *12*, 5756-5762.

[34] Cong, R.; Bain, A. D.; Pelton, R. H. *J. Polym. Sci.* **2000**, *38*, 1276-1284.

[35] Fleer, G. J.; Cohen Stuart, M. A.; Scheutjens, J. M. H.; Cosgrove, T.; Vincent, B. *Polymers at Interfaces*; Chapman &Hall: London, **1993**.

Chapter 4 PEO Flocculation with Phenolic Microparticles

Abstract

Polystyrene latex and precipitated calcium carbonate (PCC) with and without dextran sulfate pretreatment were flocculated by the consecutive addition of high molecular weight poly(ethylene oxide) and a novel composite latex microparticle consisting of a polystyrene core and a poly(p-vinylphenol) shell. Good flocculation of polystyrene latex and PCC was obtained, whereas the PCC coated with dextran sulfate was not flocculated. The interaction of the composite microparticle with the target colloids was governed by electrostatic forces whereas hydrogen bonding and hydrophobic interactions drove the PEO adsorption onto the composite particles.

Introduction

Fillers, such as precipitated calcium carbonate (PCC) and kaolin, are widely used in the paper industry to reduce cost and improve paper properties. Due to the small size of these colloidal particles, the papermaking process often involves the application of polymeric flocculants (retention aids) to promote the entrainment of colloidal fillers into the paper sheet during the filtration of the fiber suspension on the paper machine. For the last two decades, microparticle flocculants have been the dominant technology in the paper industry. The original microparticle system was cationic starch followed by colloidal silica.[1] High molecular weight cationic polyacrylamide followed by bentonite is also very popular. In both of these examples a polymeric flocculant is added first followed by an oppositely charged colloid. The popularity of microparticle-based flocculant systems reflects several practical benefits, such as significant reflocculation when the shear rate is lowered, efficient dewatering and reduced concentration dependence.[2, 3]

A detailed mechanism of microparticle flocculation was proposed first by Swerin et al.[4] who suggested that cationic polymer adsorbs onto the fiber and filler particle surfaces. Subsequent deposition of an anionic particle on the adsorbed polymer acts as a bridge causing flocculation. Wågberg and co-workers suggested that the type of surface on which the polymer first adsorbs is crutial for the effective flocculation by microparticle flocculants.[2] It was suggested that a highly negative surface charge gives a thinner adsorbed polymer layer, and thus decreasing bridging efficiency. Similar conclusions were more recently made by Asselman and co-workers.[5]

Here we report a new microparticle flocculant system based on a novel polystyrene-core poly(p-vinylphenol)-shell (PS-PVPh) composite latex which was used with high molecular weight poly(ethylene oxide) (PEO).[6, 7] The preparation and characterization of the composite microparticles was described in a previous publication.[8] The poly(vinyl phenol) shells consist of approximately 70% water. The core-shell particles display a negative electrophoretic mobility from sulfate groups and are colloidally stable from pH 2.4 to 11.5. Phenolic groups in the particle shell region dissociate in the pH range 10 to over 11.5. One of the most surprising properties of the composite particles is that the maximum PEO adsorption on PS-PVPh core-shell particle surfaces is over 6 times greater than that observed with polystyrene latex. From this observation we concluded that absorbed PEO has a very extended configuration when adsorbed on the phenolic surfaces. Finally, high molecular weight PEO induces flocculation of the composite particles. Kinetic measurements suggest simple bridging behavior.[9]

In this work we report the flocculation of three types of target colloids by the sequential addition of high molecular weight PEO and composite microparticles. In some cases good flocculation was observed. This system is interesting from a mechanistic perspective because the microparticle interactions with the bare target

colloids were electrostatic, whereas those with PEO resulted from hydrogen bonding and hydrophobic interactions.[10]

Experimental

Materials

Poly(ethylene oxide) (PEO) was used with a weight average molecular weight of 8×10^6 Da as specified by the supplier Union Carbide (Polyox 309). Stock solutions of PEO samples were prepared by mixing polymer (0.5 g/L) in water with mild agitation for 24 hours. Surfactant sodium dodecyl sulfate (SDS) from BDH was used without further purification. Precipitated calcium carbonate, PCC (Albacore HO®, Specialty Minerals Inc.), consists of aggregates of scalenohedral needles with a mean particle size of 1.34 μm (Brookhaven Disc Centrifuge), and a specific surface area of 12.0 m^2/g (nitrogen adsorption). Dextran sulfate (MW=10, 000) (DS) was purchased from Sigma as the sodium salt with an average of 2.3 sulfate groups per glucosyl residue. All work was performed with water from a Millipore Milli-Q system fitted with one Super C carbon cartridge, two ion-exchange cartridges, and one Organex Q cartridge.

Polystyrene (PS) core – PVPh shell latexes were synthesized in our laboratories. Details of the preparation and characterization of core-shell latexes have been reported elsewhere and the latex properties are summarized in Table 1.[8] Polystyrene latexes were prepared by a conventional surfactant-free batch process,[11] except PS latex PS8 (see Table 1), which was prepared with SDS to give smaller particles.

The particle sizes shown in Table 1 were measured using two techniques: 1. BI-DCP (Disc Centrifuge Photosedimentometer) particle sizer (Brookhaven Instrument Co.); 2. dynamic light scattering using a Lexel laser (wave length 514 nm) equipped with a BI-9000 AT digital correlator (Brookhaven). Light scattering was measured at a 90° angle and the particle sizes were calculated using the non-negatively constrained least squares (regularized) method.[9]

Procedure

Particle electrophoretic mobility was measured using a Brookhaven ZetaPALS at 25°C. All the samples were prepared in 0.001 mol/L NaCl and pH was adjusted by the addition of HCl or NaOH. Reported particle mobility was the average of 10 cycles. Each cycle contained 20 runs (scans). PEO adsorption isotherms were measured using the tannic acid method.[12, 13, 9] A linear calibration equation of the absorbency of PEO and tannic acid complex as a function of PEO concentration was obtained using with a HP8452A UV-Vis spectrophotometer (Hewlett-Packard) at a wavelength of 600 nm. In the PEO equilibrium absorption experiments, latex suspension was added into 0.001 mol/L NaCl solution to give a concentration of 0.2 g/L. Various amount of PEO was added and the suspension was let stand for 4 days to reach adsorption equilibrium. The latex particles were extracted by spinning the suspension for 50 minutes at 50,000 rpm at

25°C. 15 mL of supernatant was moved to 50 mL volumetric flask. The PEO concentration in the supernatant was measured by the absorbency of PEO and tannic acid complex and the corresponding adsorbed PEO amount was calculated from a mass balance.

The degree to which suspensions of latex particles or PCC were flocculated was analyzed using a flow turbidity sensor (Photometric Dispersion Analyzer (PDA), Rank Brothers, Cambridge, UK), the operation of which has been described previously.[14, 15] All the experiments were carried out in 0.001 mol/L NaCl and the pH values were adjusted by NaOH and HCl. The total volume was kept at 200 mL. In a typical flocculation experiment, latex particles or PCC, core-shell particles, PEO were added consecutively. The order of chemical addition and times between additions were varied. The suspension was stirred at 475 rpm using a three-bladed propeller (55 mm diameter) and the extent of flocculation was monitored by circulating the suspension through the PDA at a rate of 45 mL/min. The DC output of the PDA was converted to relative turbidity by the following relationship, where V_w is the output voltage for water, $V_{t=0}$ is the output voltage for the PCC suspension before flocculant addition and V_t is the output voltage at time t. It was assumed that the relative turbidity was proportional to the concentration of un-flocculated colloidal particles.

$$\tau_r = \ln\left(\frac{V_w}{V_t}\right) \Big/ \ln\left(\frac{V_w}{V_{t=0}}\right) \qquad (1)$$

Polystyrene flocs were dried at room temperature and floc structure was studied using scanning electron microscopy (SEM) and transmission electron microscopy (TEM).

Results

Some properties of the polystyrene-core poly(vinyl phenol)-shell composite latex particles as well as the polystyrene target colloids are summarized in Table 1. Figure 1 shows the electrophoretic mobilities of core-shell particles and PCC as a function of pH. CPS2 and CPS5 had the similar mobilities from pH 3.5 to 10.5. Both core-shell particles were negatively charged and became more negative with increasing pH. PCC showed slightly positive mobilities below pH 9.5, and slightly negative mobilities above pH 9.5.

PEO adsorption isotherms on both CPS2 and CPS5 were measured and are compared in Figure 2. Both types of core-shell particles had a PEO binding capacity of about 8 mg/m^2 which is about 8 times greater than that of clean polystyrene latex.[9]

Polystyrene Flocculation

Surfactant-free polystyrene latex is a hydrophobic, anionic charge stabilized colloid which is often used as a model target colloid in flocculation studies. Under conditions of low ionic strength, very high molecular weight PEO will only partially

flocculate polystyrene latex. [16, 17] In this work aqueous suspensions of surfactant-free polystyrene latex PS5 were flocculated by the sequential addition of PEO and composite particles. The extent of flocculation was estimated by relative turbidity measurements and Figure 3 shows examples of relative turbidity (τ_r) versus time curves. The first jump in relative turbidity occurred upon adding the polystyrene latex to the flocculation apparatus, which contained only dilute electrolyte. The times at which that happened and thus the absolute values along the time axis were arbitrary. Flocculation started with the subsequent addition of PEO, which caused the latex aggregation, giving a drop in relative turbidity. The subsequent addition of composite latex CPS5 revitalized the flocculation as seen by a second decrease in turbidity vs time curves. Note that initially there was a slight increase in turbidity upon the addition of CPS5, reflecting the contributions of the composite latex to the turbidity.

The extent of flocculation obtained by the sequential addition of PEO and composite microparticles was sensitive to PEO concentration (see Figure 3). The intermediate PEO concentration of 2 mg/L gave greater flocculation than did either 0.75 mg/L or 8 mg/L/. In previous work we showed that 2 mg/L PEO corresponded to PS5 surface coverage of 0.94 mg/m^2, which is close to saturation, 1 mg/m^2.[9] With 2 mg/L PEO alone the relative turbidity approached a steady state of $\tau_r \sim 0.5$. Under these conditions the un-flocculated latex was stabilized by an adsorbed layer of PEO. However, subsequent addition of composite latex CPS5 revitalized the flocculation.

By contrast, when the PEO concentration was 0.75 mg/L, the adsorbed PEO relaxed to a flatter conformation due to the relatively empty PS5 surface.[9] Under these conditions the partially flocculated PS5 could not be revitalized significantly by the addition of CPS5. Finally, when the PEO concentration was 8 mg/L (a large excess), the degree of flocculation was low. The addition of core-shell particles did not significantly revitalize flocculation because the composite particles were coated with the excess PEO which served to sterically stabilize the composite particles.

Examples of electron micrographs of the polystyrene-composite particle heteroflocs are shown in Figure 4. The SEM and TEM images seem to be consistent with a flocculation process where the smaller composite particles bridge together the polystyrene latex.

The role of composite particle concentration is illustrated in Figure 5 which shows the degree of latex flocculation 200 seconds after the PEO addition corresponding to steady-state flocculation, as a function of the mass ratio of composite particle CPS5 to PEO. In these experiments PS was first added into 0.001 M NaCl solution at pH 6.5 to give a concentration of 0.2 g/L. 0.002 g/L PEO was added 60 seconds after the addition of CPS5. The steady-state flocculation results were rather insensitive to CPS5/PEO ratios greater than 3 – this corresponds to a PS/CPS5 mass ratio of 33. The extent of steady-state flocculation was also insensitive to pH from 3 to 10 – see Table 3.

We propose that the high PEO adsorption capacity is an important feature of composite microparticle flocculants. As control experiments, the composite particles were replaced by small polystyrene latex particles. The results are summarized in Table 2, while the polystyrene latex properties are summarized in Table 1. The 440 nm and 260 nm latexes showed only slight improvements compared to adding no secondary microparticle. On the other hand, the 48 nm latex decreased the τ_r from 0.53 to 0.37 which is intermediate between no effect and the effect of the composite particles which gave a steady-state τ_r value of about 0.2 (eg. see Figure 3). It is also noteworthy that the secondary polystyrene particles listed in Table 1 were added at the same mass concentration so smaller particles gave much higher number concentrations and surface areas.

PCC Flocculation

Aqueous suspensions of precipitated calcium carbonate (PCC) were also flocculated by PEO in conjunction with core-shell latex particles. The PCC particles are positively charged aggregates of scalenohedral needles with a mean particle size of 1.34 μm at pH below 9.5. The following results reveal one difference compared with polystyrene latex flocculation. The PCC system is sensitive to the order of PEO and composite particle addition.

Figure 6 compares results from experiments in which polystyrene latex PS5 and composite particles CPS5 were used as the second component (i.e. as microparticles) to improve PCC flocculation by PEO. In the case of PS5, there was no flocculation at all. When CPS5 was introduced, the order of addition of PEO and composite particles played an important role. Relatively good flocculation was observed when CPS5 was added before PEO, whereas no flocculation was observed when the PEO was added first. Increasing CPS5 concentration from 0.02 g/L to 0.1 g/L showed no improvement in PCC flocculation when PEO was added first. Initial relative turbidity values above 1 reflect the fact that the latex particles scatter light and contribute to the measured turbidity.

PCC suspensions were also flocculated with composite particles CPS2 with a diameter of 269 nm, which is about half the diameter of the CPS5 used in the previous experiments. Figure 7 shows results for varying the order of addition and pH. As before (Figure 6) the best results were obtained when the composite particles were added before PEO. However, unlike the results for the larger CPS5, there was also significant flocculation when PEO was added before CPS2. This indicates that particle size of composite particles plays an important role in the flocculation. There was also some pH effect for the PEO-first experiments. Flocculation at pH 8.5 was greater than at pH 10.5.

PCC flocculation with PEO-CPS2 was particularly sensitive to mixing order even over small time scales. Figure 8 compares results when the sequential additions were only separated by 1 second. When CPS2 was added first, the relative turbidity dropped to 0.14 at steady state, which was close to that with a time interval of 60 seconds (Figure

4). By contrast, when PEO was added first, the relative turbidity dropped to 0.39, which was larger than that with the time interval of 60 seconds. Thus, the mixing order effects persist in the PCC system even when the time intervals are very small.

Summarized in Table 3 are results on the effect of pH values on PCC flocculation when CPS2 was added 60 seconds before PEO. Because calcium carbonate dissolves at low pH, the range was limited from 8.5 to 10.5 by extra addition of NaOH or HCl. At steady state, the flocculation results were not sensitive to pH.

PCC+DS Flocculation

Many industrial flocculants must function in the presence of significant quantities of anionic polyelectrolytes which can interfere both with cationic polymers and electrosterically stabilized colloids. Polystyrene latex and PCC are relatively easy colloids to flocculate and not very demonstrative of industrial systems. By contrast, we have shown that pretreatment of PCC with dextran sulfate gives a very difficult-to-flocculate, realistic target colloid.[18]

Figure 9 summarizes the flocculation behavior of PCC-dextran sulfate mixtures. The sequential addition of CPS2 and PEO (curve a) gave very poor flocculation of pretreated PCC. Only by adding high concentrations of CPS2 before the dextran sulfate was significant flocculation observed. Thus, we conclude that the composite particle flocculants are unlikely to be of commercial interest.

Discussion

This work describes the flocculation of three very different colloids, polystyrene latex, PCC, and PCC pretreated with dextran sulfate. PCC is a positively charged aggregate of needle shaped crystals, does not adsorb PEO, and is not flocculated by PEO alone. By contrast, polystyrene latex is negatively charged, smooth spherical particles and is partially flocculated by PEO alone. Finally, the dextran sulfate pretreated PCC is negatively charged and not flocculated by PEO. The negatively charged composite particles form weak (i.e. shear sensitive) aggregates with positive PCC. Electrostatic replusion prevents composite latex heterocoagulation with either the polystyrene latex or the dextran sulfate treated PCC.

Commercial microparticle flocculation systems are popular in papermaking, which is a particularly demanding flocculation application. The concept is that the flocculation of a colloidal suspension with polymers can be improved by the addition of a second colloid which helps the bridging process.[4] The activity of phenolic coated latex as a microparticle flocculant with PEO was evaluated in the three target colloids. The flocculation extent of PS and PCC upon PEO addition was increased in the presence of phenolic-coated latex.

The influence of the order of PEO and composite particle addition gives some insight into the mechanisms. In the case of polystyrene latex, the relative order of PEO and composite particle addition is not very important. If PEO is added first, the latex partially flocculates leaving a suspension of flocs and primary latex particles which are coated with PEO. Subsequent addition of composite particles gives further flocculation because of the high affinity of PEO, adsorbed on the polystyrene, for the phenolic surface on the composite particle. On the other hand, if the composite particles are added before the PEO, then the two types of colloids compete for PEO.

PEO does not adsorb onto PCC, thus PEO alone gives no flocculation. Similarly, the composite particles coated with PEO will not interact with PCC. The flocculation of PCC was only obtained when the composite particles were added before PEO. Under these conditions the negatively charged composite particles deposited onto the cationic PCC. Without PEO the aggregates were very weak and were easily redispersed. However, with PEO the aggregates were more extensive and shear resistant.

In summary, the interactions of the microparticles with the target colloids is mainly determined by electrostatic effects, whereas the microparticle/PEO interactions are hydrogen bonding and possible hydrophobic interaction. Compared with soluble phenolic polymer cofactors such as copolymers of vinyl phenol[19] or high tyrosine content polypeptides[20], the phenolic shell particles are not spectacular flocculants when used with PEO. On the other hand, they do illustrate the principles of microparticle flocculation in a case where the microparticle/flocculant interaction is not electrostatically driven.

Conclusions

1. Polystyrene-core poly(p-vinyl phenol)-shell composite particles enhance the ability of PEO to flocculate polystyrene latex. When composite particles are added after PEO, they bridge together PEO coated particles and aggregates. When composite particles are added before PEO, they act as bridging agents and adsorb PEO in an extended configuration ideal for flocculation.

2. The cationic PCC particles weakly bind to the negatively charged composite particles. Subsequent PEO adsorption strengthens the flocs so they can persist in turbulent flow.

3. Polystyrene-core poly(p-vinyl phenol)-shell composite particles are unlikely to be useful commercial flocculants because they cannot aggregate electro-sterically stabilized PCC pretreated with dextran sulfate.

Table 1. Particle diameters measured by dynamic light scattering (DLS) except PS5, which was measured by disc centrifuge (DC). The DLS error limits show the standard deviations of the mean based on 5 measurements. The DC error limits are the standard deviations of the distribution. The cross-linking degree stands for the weight percentage of divinylbenzene added with p-acetoxystyrene monomer.

Latex	Sample Name	Cross-linking Degree	Diameter	Shell Thickness (nm)	Shell region water fraction
PS	PS5	-	535 ± 15	-	-
PS	PS6	-	440 ± 10	-	-
PS	PS7	-	260 ± 8	-	-
PS	PS8*	-	48 ± 3	-	-
PS-PVPh	CPS2	5%	269 ± 5	66	72%
PS-PVPh	CPS5	1%	590 ± 8	75	76%
PS-PVPh	CPS6	0%	345 ± 5	21	-

*0.28 g SDS was introduced into 125 mL H_2O before the addition of styrene monomer during the polymerization process in order to decrease particle size. SDS was not removed before the flocculation experiments.

Table 2 **PS5 latex flocculation by PEO and smaller PS latex particles, PS6(440 nm), PS7 (260 nm) and PS8 (48 nm). Flocculation conditions: [PS5] = 0.2 g/L; [PEO] = 0.002 g/L; [smaller PS] = 0.008 g/L; [NaCl] = 0.001 mol/L; pH = 6.5; smaller PS latex was added 60 seconds before PEO. The flocculation was assumed to reach steady state 200 seconds later after the addition of PEO and the relative turbidity was measured.**

Sample	Particle Size of Smaller PS Particles (nm)	Relative Turbidity at Steady State
PEO		0.53
PEO + PS6	440 ± 10	0.53
PEO + PS7	260 ± 8	0.51
PEO + PS8	48 ± 3	0.37

Table 3. **The steady state turbidity (200 seconds after PEO addition) as a function of suspension pH. Experimental conditions for PS5: [PS5] = 0.2 g/L; [PEO] = 0.002 g/L; [CPS5] = 0.008 g/L; [NaCl] = 0.001 mol/L; CPS5 was added 60 seconds before PEO. Experimental conditions for PCC: [PCC] = 0.5 g/L; [PEO] = 0.005 g/L; [CPS2] = 0.02 g/L; [NaCl] = 0.001 mol/L; CPS2 was added 60 seconds before the addition of PEO. pH was adjusted by the addition of NaOH or HCl..**

PS5		PCC	
pH	Relative turbidity at 200 s	pH	Relative turbidity at 200 s
2.7	0.143	8.5	0.144
5.4	0.143	9.2	0.140
7.1	0.138	9.6	0.138
9.4	0.155	9.9	0.129
10.1	0.155	10.5	0.122

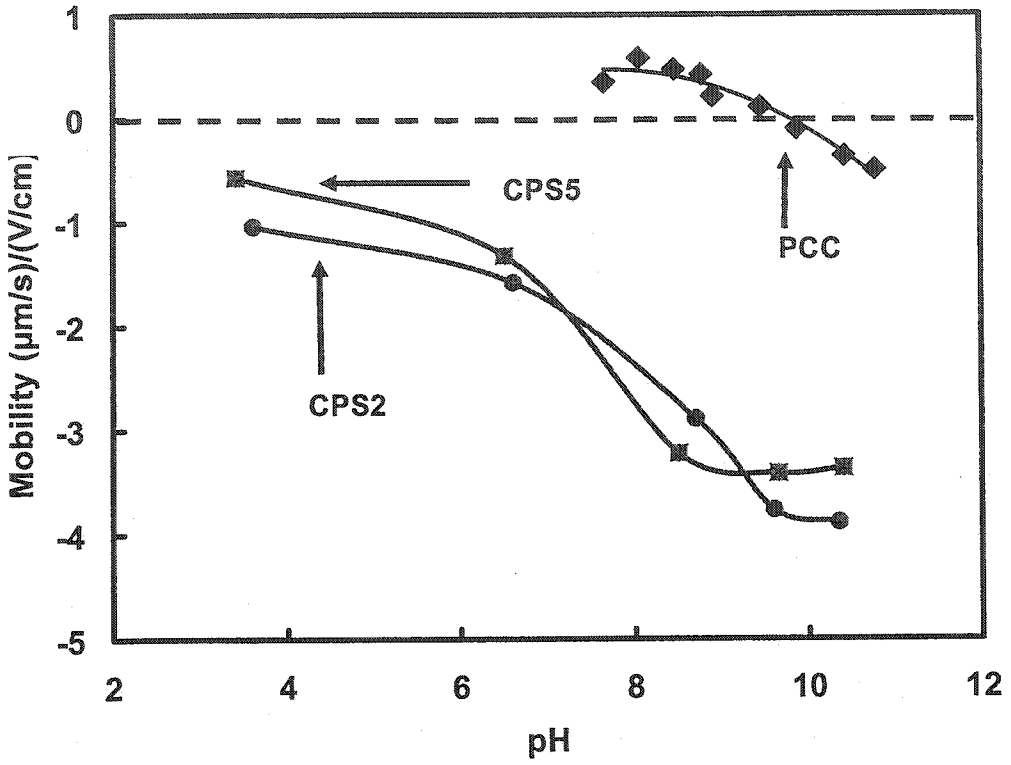

Figure 1. Electrophoretic mobility as a function of pH in 0.001 mol/L NaCl. pH was adjusted by the addition of HCl or NaOH.

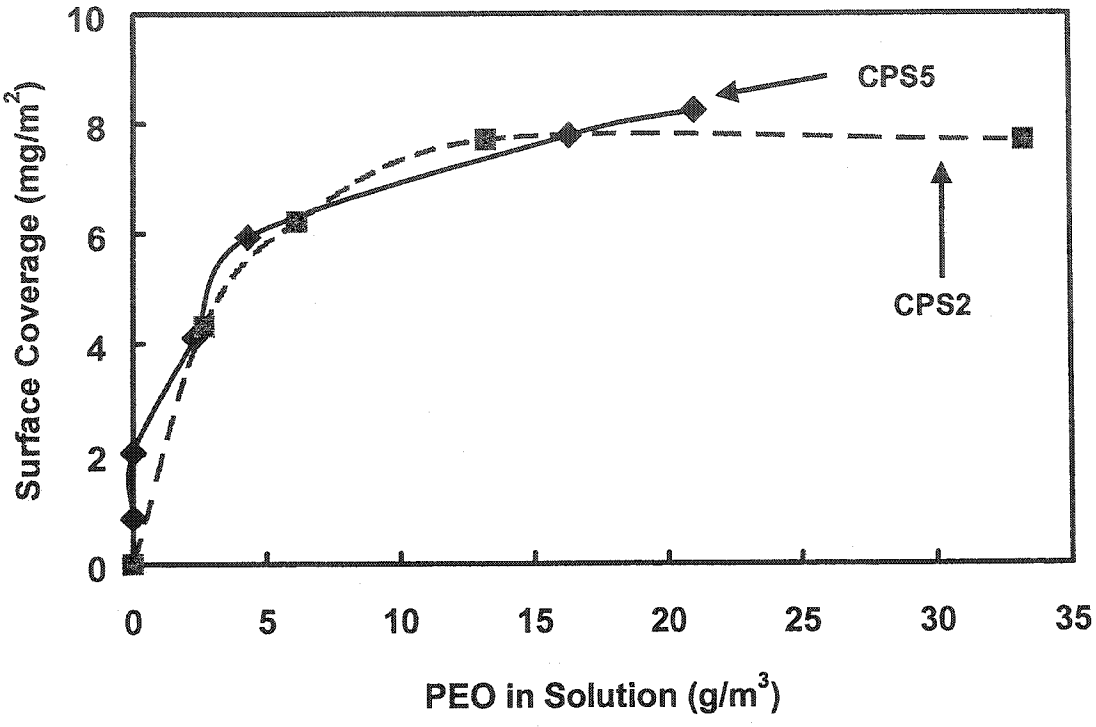

Figure 2. PEO 309 (MW=8×10^6) adsorption isotherms (25°C) on CPS2 and CPS5. The latex concentration was 0.2 g/L in 0.001 mol/L NaCl.

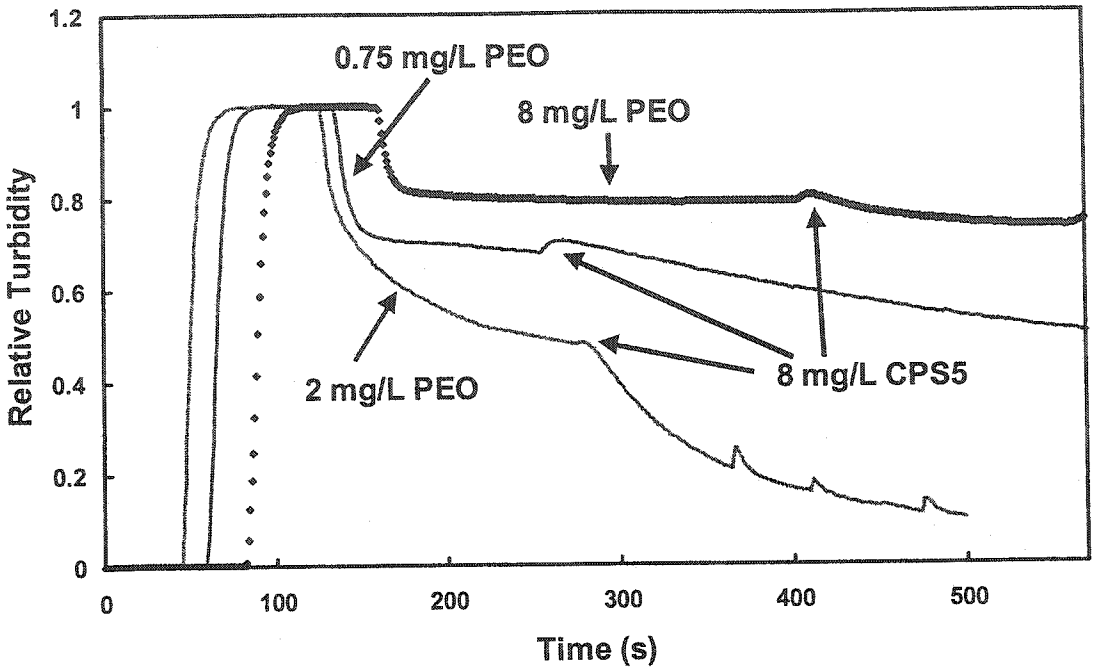

Figure 3 **PS5 Flocculation by PEO 309 and CPS5. Experimental conditions: [PS5] = 0.2 g/L; [NaCl] = 0.001 mol/L; pH = 6.5. The first jump of relative turbidity corresponds to the addition of PS5.**

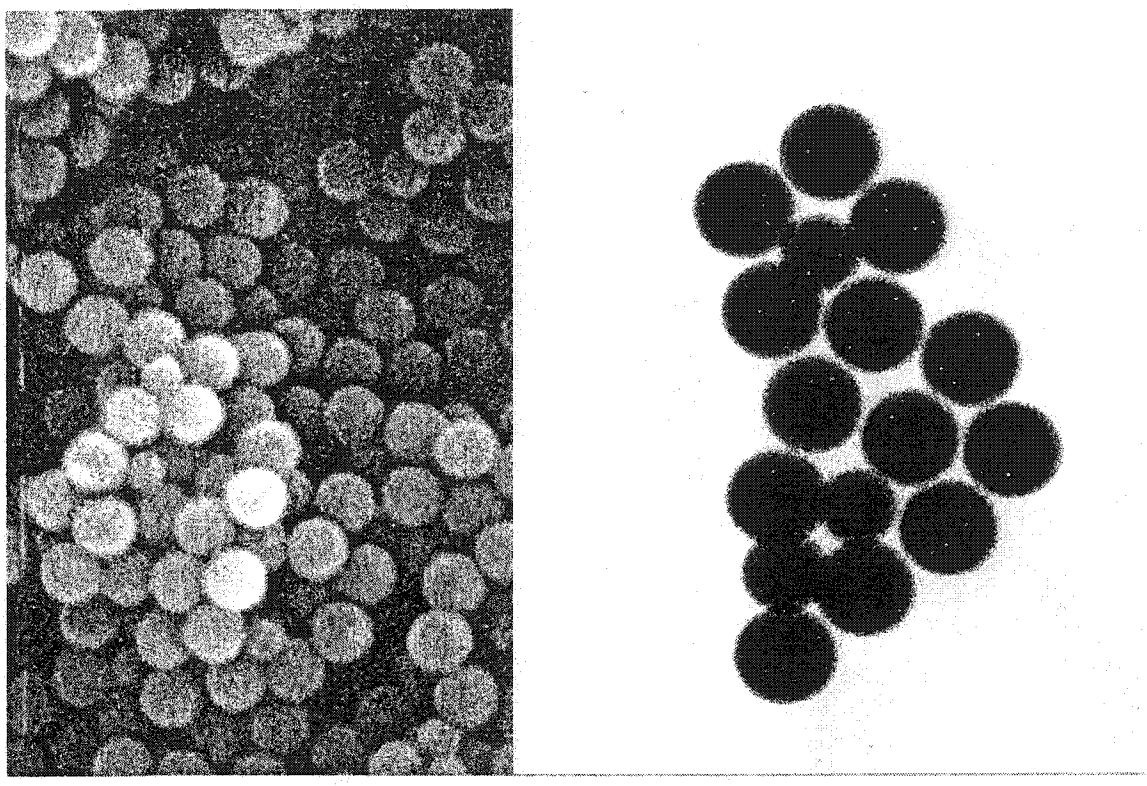

(a) (b)

Figure 4 (a) SEM micrograph of PS5 (500 nm) floc flocculated by PEO and CPS6 (345 nm) and (b) TEM micrograph of PS5 flocs formed by the addition of PEO and CPS5 (390 nm).

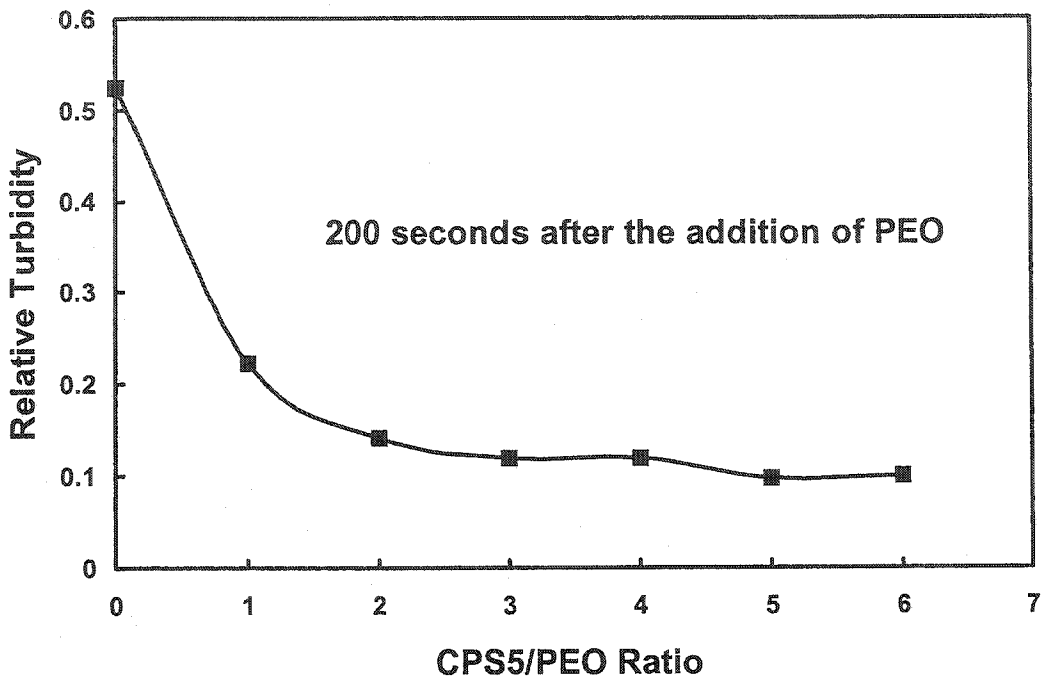

Figure 5 **The effect of CPS5/PEO mass ratio on latex PS5 flocculation. Experimental conditions: [PS5] = 0.2 g/L; [PEO] = 0.002 g/L; [NaCl] = 0.001 mol/L; pH = 6.5; and, CPS5 was added 60 seconds before PEO.**

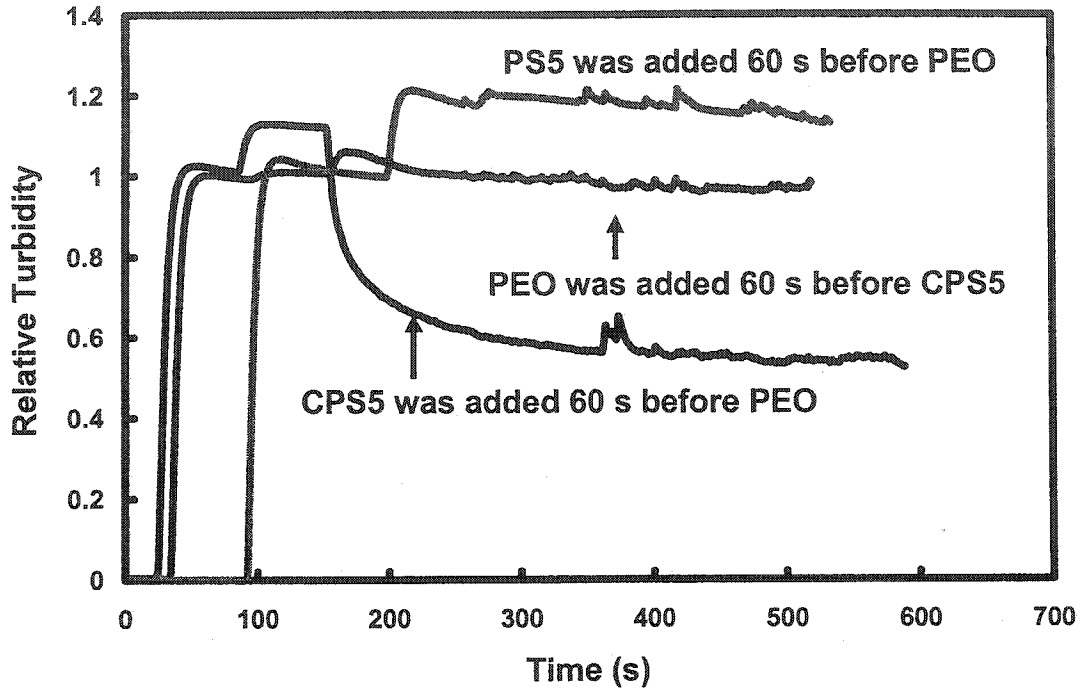

Figure 6 **The influence of addition order on PCC flocculation by mixtures of PEO and CPS5 (60 seconds between the additions of PEO and CPS5/PS5). Flocculation conditions: [PCC] = 0.5 g/L; [PEO] = 0.005 g/L; [CPS5/PS5] = 0.02 g/L; [NaCl] = 0.001 mol/L; pH = 8.5**

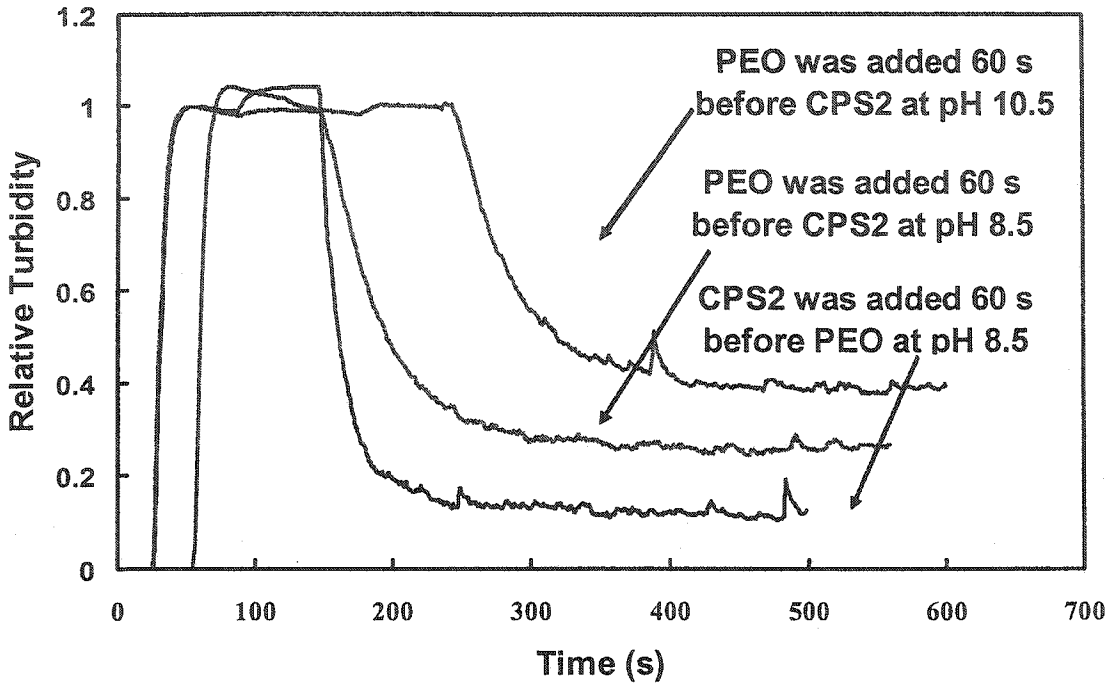

Figure 7 **PCC flocculation by mixtures of PEO and CPS2. Flocculation conditions: [PCC] = 0.5 g/L; [PEO] = 0.005 g/L; [CPS2] = 0.02 g/L; [NaCl] = 0.001 mol/L.**

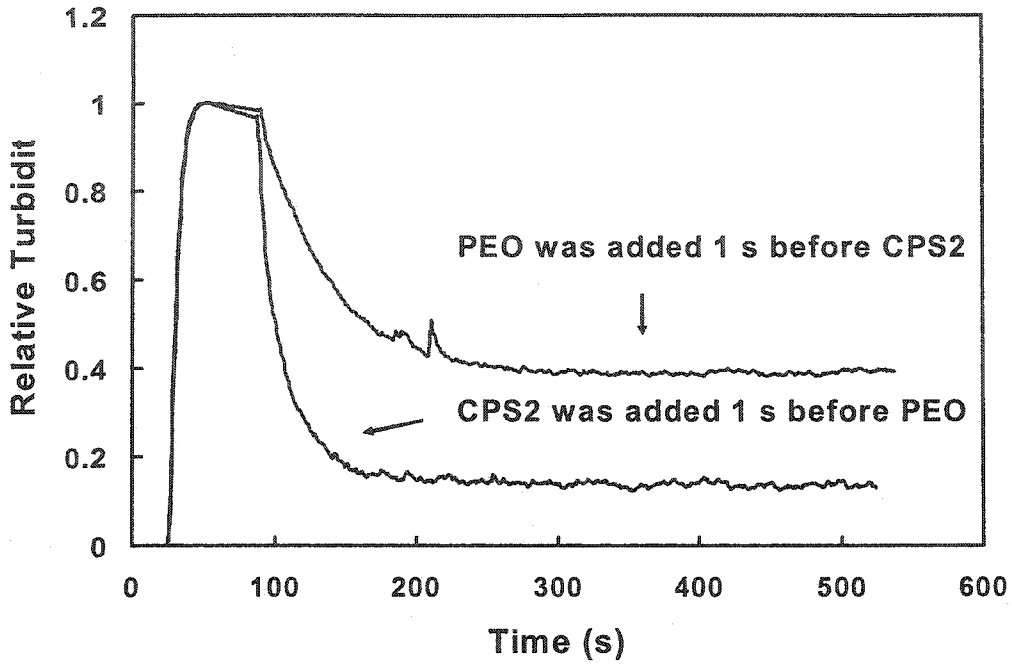

Figure 8 **PCC flocculation by mixtures of PEO and CPS2 (1 second between the additions of PEO and CPS2). Flocculation conditions: [PCC] = 0.5 g/L; [PEO] = 0.005 g/L; [CPS2] = 0.02 g/L; [NaCl] = 0.001 mol/L; pH = 8.5.**

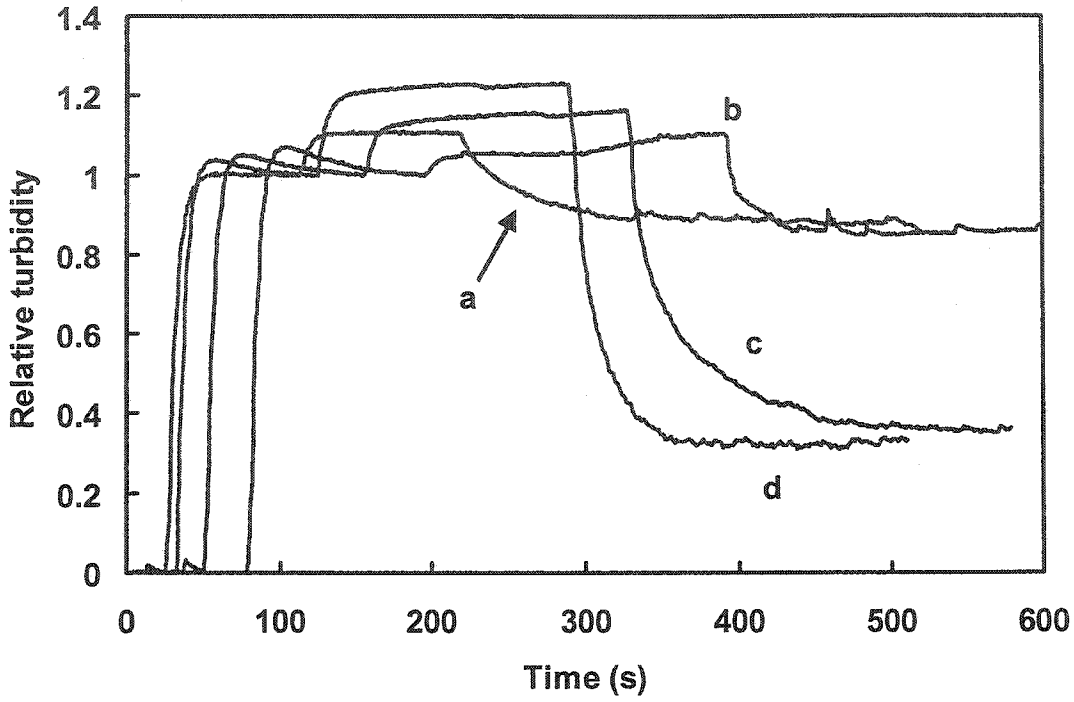

Figure 9. **Effect of dextran sulfate (DS) on PCC flocculation by PEO and CPS2. Flocculation conditions: [PCC] = 0.5 g/L; [PEO] = 0.005 g/L; [NaCl] = 0.001 mol/L; pH = 7.8; [DS] = 0.01 g/L. (a) DS was premixed with PCC; PEO was added 60 seconds after the addition of CPS2; [CPS2] = 0.06 g/L. (b)-(d) CPS2 was added 100 seconds before the addition of DS; PEO was added 100 seconds after DS. (b) [CPS2] = 0.02 g/L. (c) [CPS2] = 0.06 g/L. (d) [CPS2] = 0.1 g/L.**

References

---

[1] Sunden, O., Batelson, P.G., Johansson, H.E., Larsson, H.M., and, Svending, P.J., US. Patent 4,388,150 (1983).

[2] Wågberg, L., Björklund, M., Asell, I., Swerin, A., *Tappi* **79**, 157 (1996).

[3] Lindström, T., in Fundamentals of Papermaking; Trans. Ninth Fundamental Research Symposium (C. F. Baker and V. W. Pynton, Eds.), p. 311. Mechanical Engineering Publications Ltd., London, 1989.

[4] Swerin, A., and Odberg, L., *Nordic Pulp Paper Res. J.* **4**, 389 (1993).

[5] Asselman, T., Alince, B., Garnier, G., and van de Ven, T. G. M., *Nordic Pulp and Paper Research Journal* **5**, 515 (2000).

[6] van de Ven, T. G. M. *Journal of Pulp and Paper Science* **23**, 447 (1997).

[7] Gibbs, A.; Pelton, R. H. *Journal of Pulp and Paper Science* **25**, 267, 1999.

[8] Lu, C., and Pelton, R. H., *Colloid and Surfaces* **201**, 161 (2001).

[9] Lu, C., and Pelton, R. H., *Langmuir* **17**, 7770 (2001).

[10] Cong, R., Bain, A. D., Pelton, R. H. *J. Polym. Sci. B* **38**, 1276 (2000).

[11] Goodwin, J. W., Hearn, J., Ho, C. C. and Ottewill, R. H., *Br. Polym. J.* **5**, 347 (1973).

[12] Attia, Y. A., Rubio, J. *Br. Polym. J.* **7**, 135 (1975).

[13] Nuysink, J., Koopal, L. K. *Tananta* **29**, 495 (1982).

[14] Gregory, J., *J. Colloid and interface Sci.* **105**, 357 (1985)

[15] Gibbs, A., Xiao, H., Deng, Y. and Pelton, R. H., *Tappi* **80**, 163 (1997).

[16] Pelssers, E. G. M., Cohen Stuart, M. A., and Fleer, G. J., *Colloids and Surfaces* **38**, 15 (1989).

[17] Pelssers, E. G. M., Cohen Stuart, M. A., and Fleer, G. J., *J. Chem. Soc. Faraday Trans.* **86**, 1355 (1990).

[18] Cong, R., Smith-Palmer, T., and Pelton, R. H., *J. Pulp Paper Science* **27**, 379 (2001).

[19] Gibbs, A., Yang, Z., Xiao, H., and Pelton, R. H., *Tappi* **80**, 163 (1997).

[20] Lu, C., Pelton, R. H., Valliant, J. Bothwell, S., and Stephenson, K., *Langmuir* **18**, 4536 (2002).

Chapter 5 Aqueous Complex Formation between Poly(ethylene oxide) and Tyrosine-containing Polypeptides

Abstract

The aqueous complexes between tyrosine-containing water soluble polypeptides and poly(ethylene oxide) (PEO) were characterized using capillary electrophoresis, isothermal titration calorimetry, circular dichroism, and nuclear magnetic resonance. In the absence of soluble calcium, PEO partially binds to poly(Glu, Tyr) (1:1) which is an endothermic process and does not induce much change in the peptide CD spectra. Based on the observation that peptides with lower molecular weights or lower tyrosine contents do not interact with PEO, it is proposed that a block of at least four tyrosine groups in the polypeptide backbone are required for PEO binding.

In the presence of calcium ions, the binding of poly(Glu, Tyr) (1:1) with PEO was stoichiometric and irreversible. Based on changes in CD spectra, the initial large exotherms in the isothermal titrations were attributed to the folding of polypeptide chains upon complex formation. With calcium the requirement of tyrosine blocks for PEO binding was relaxed because of the association of phenolic groups in the folded polypeptide.

Introduction

Poly(ethylene oxide) (PEO) is arguably the most important synthetic nonionic water soluble polymer both in terms of scientific studies and industrial applications.[1] This report describes the results of a study of interactions responsible for aqueous complex formation between high molecular PEO and tyrosine-containing polypeptides (TCP). Our interest in these unusual systems stems from the fact that they serve as models for PEO complexes with synthetic water-borne phenolic polymers. The latter system is used as a flocculant to induce the deposition of filler particles onto wood pulp fibers in the papermaking process.[2, 3, 4] Although this specific industrial application is the source of our interest, we believe that the current results have broader ramifications because PEO is employed as a protein-resistant surface coating for biomaterials.[5]

There has been a number of reports describing complex formation between dilute PEO and synthetic phenolic polymers, which are called cofactors in the paper technology literature. This literature now summarized, however, most of the work described was hampered by the restriction that the phenolic polymers were polydisperse and poorly characterized.

Stack and coworkers studied PEO and phenol formaldehyde resin complex formation and proposed that PFR could bind to PEO when the molecular weight of the phenolic resin was above 500 Da. [6] Carignan et al. was the first group to apply light scattering to characterize the interactions between PEO and poly(sodium naphthalene sulphonate) and modified phenolic resin.[7] They showed that the binding of highly charged cofactors to PEO leads to the expansion of the PEO coils.

Pelton and coworkers were the first group to study PEO/cofactor interaction using well-defined vinyl polymer cofactors.[8, 9] A series of poly(vinyl phenol-co-styrene sulfonate potassium) samples of different phenolic content was prepared. Using fluorescence photo bleaching techniques, it was found that higher phenolic content led to larger complex size.[10] 2D NMR measurements on the same system showed that the protons on the bound PEO segments were above and below the aromatic residues. Both hydrophobic interaction and hydrogen bonding were proposed to be the driving forces between PEO and phenolic groups [11]

The PEO/cofactor complexes are difficult to study because they are kinetically controlled, they often aggregate to form a macroscopic coacervate phase and because the number of PEO segments and phenolic polymer segments which are actually bonded together is unknown. In this work we have employed simple tyrosine-containing polypeptides (TCP) as model cofactors. The polypeptides offer the advantage that circular dichroism can be used to monitor changes in configuration. Initial results from this project were reported in a note in which it was shown that some polypeptides formed PEO complexes which were effective colloidal flocculants.[12] The polypeptides poly(Glu, Tyr) (1:1) (note Glu is a glutamic acid residue and Tyr is a tyrosine residue) of high

molecular weight (36 kDa) and a high tyrosine content (50 mole%) induced efficient flocculation of precipitated calcium carbonate (a common papermaking filler), whereas similar copolymers with only 20 mole % tyrosine content did not. In this work, isothermal titration calorimetry, capillary electrophoresis, nuclear magnetic resonance spectroscopy (NMR), and circular dichroism were used to characterize PEO/TCP complexes.

Experimental

Materials

PEO 309(molecular weight (MW)=8 MDa), PEO N-12K (MW=1 MDa), PEO N-10 (MW=100 kDa), and polyethylene glycol (PEG) 5000 (MW=5 K Da) were obtained from Union Carbide. PEG 350 (MW=350 Da) was purchased from Aldrich. Random L-polypeptides were purchased from Sigma, who report that the L-peptides used were prepared by ring opening polymerization of α-amino acid-N-carboxyanhydrides.[13] The compositions and properties of the polypeptides are summarized in Table 1.

PEO stock solutions were prepared by dissolving polymer (1 g/L) in water with mild end-to-end rotation for 24 hours. Polypetide stock solutions were prepared by dissolving polypeptides (1 g/L) in water under gentle shaking for 10 minutes. Buffer solutions at different pH were prepared by mixing tris(hydroxymethyl)aminomethane (Tris) (Boehringer, Mannheim) and HCl (Anachemia). $CaCl_2$ salt was purchased from BDH. All work was performed with water from a Millipore Milli-Q system fitted with one Super C carbon cartridge, two ion-exchange cartridges, and one Organex Q cartridge.

Methods

NMR

NMR spectra were recorded using a Bruker DRX-500 spectrometer at 30°C. For one-dimensional proton NMR, a 6.7 μs pulse (90°) width was used, and a delay time of 2.5 s was inserted between successive acquisitions. 100 scans were carried out for each spectrum. Two-dimensional NOESY spectra were acquired in the phase-sensitive mode using the pulse sequence (90°-t_1-90° -τ-90° -ACQ) (t_1 and τ stand for the incremental delay time and mixing time, respectively). Mixing time was set at 0.1 s. Phase-sensitive data was obtained by using time proportional phase incrementation (TPPI). In the t_2 dimension, 2K data points were used with 4.401 kHz spectral width, 64 scans, and a 2.5 relaxation time delay. In the t_1 dimension, 256 FID's were zero-filled to produce a 1K×1K data matrix. H_2O proton peak at 4.72 ppm was pre-saturated with a 55 dB pulse to improve spectrum resolution.

Isothermal Titration Calorimetry

The heat of PEO/TCP interactions was measured by isothermal titration calorimetry. Thermal titrations were carried out using an ultra-sensitive isothermal titration calorimeter (VP-ITC) from MicroCal, LLC (Northampton, MA). In a typical experiment, peptide solutions and PEO solutions were first prepared by dissolving peptide and PEO in the Tris buffer solution. 0.001 M $CaCl_2$ was introduced into the buffer if specified. Before the titration, all the samples had been degassed using a MicroCal Thermo-Vac for five minutes. During the titration, the PEO solution was injected into the polypeptide solution at 30°C and stirred at 300 rpm. The differential power (baseline) between the sample cell and the reference cell was 5 μCal/sec. The heat needed to dilute the PEO solution in the buffer, was measured in a control experiment and found to be insignificant. Titration data was processed by MicroCal Origin version 5.0 and background titration heat was not subtracted.

Capillary Electrophoresis

Capillary electrophoresis was used to distinguish between free and PEO bound TCP. A Millipore capillary electrophoresis apparatus with a UV detector of wavelength 265 nm was fitted with a 64.5 cm fused silica capillary (75 μm diameter) and a data collection computer. In a typical experiment, the TCP was first mixed with $CaCl_2$ solution, if required, and the pH was adjusted to 8 using 0.05 mol/L Tris buffer. 30 seconds later, PEO was added in one injection and the solution was stirred for three minutes and then was siphoned into the capillary. The voltage across the capillary was regulated to 25 kV and the sample was eluted with 0.01 M Tris buffer at a pH of 8.

Circular Dichroism

TCP polypeptides are optically active and circular dichroism was used to probe changes in TCP configuration. The circular dichroism measurements were made with a Jasco J-600 spectropolarimeter fitted with a 0.5 cm quartz cell. Data was collected from 200 to 250 nm at 0.2 nm intervals with a time constant of 0.5 s. In a typical experiment, TCP was first mixed with pH buffer and $CaCl_2$ solution (if $CaCl_2$ was required). 30 seconds later, PEO was added in one shot. After 5 minutes of mixing, the complex solution was loaded into the quartz cell. Five CD spectra were recorded for each TCP sample and the average CD spectrum was reported. CD data was expressed in terms of mean residue ellipticity, $[\theta]$.

Results

The following paragraphs summarize the results of experiments aimed at characterizing the complexes formed between tyrosine-containing polypeptides (TCP) and PEO. Herein we use the term TCP to describe all the polypeptides, whereas the names, structures, and properties of the specific peptides are summarized in Table 1.

Many of the experiments were conducted in the presence of Ca^{2+} because it is present in many papermaking suspensions and because PEO/cofactor flocculation is often sensitive to the presence of soluble calcium ions.[8, 14, 15] In some cases calcium appears to improve flocculation, whereas in others it does not. Polypeptides PEY1, PEY4, and PEYA (see Table 1) are charged polyelectrolytes at neutral pH due to the presence of glutamic acid residues. It is well known that polyGlu has high affinity to Ca^{2+} in aqueous conditions at neutral pH.[16, 17, 18] In this work, "TCP(Ca^{2+})" is used to represent TCP in the presence of Ca^{2+}.

Capillary Electrophoresis

Figure 1 shows the capillary electrophoresis measurements of the PEO 309/PEY1 complexes in the absence of Ca^{2+}. In this work, the electrophoretic flow of the peptides opposed the electro-osmotic flow of buffer solution. Thus, the higher the electrophoretic mobility, the longer was the corresponding elution time. Curve (a) corresponds to PEY1 solution without PEO 309. The first sharp peak at around 4 minutes was the water peak, whereas the broad peak at around 8 minutes was assigned to PEY1. When PEO 309 was mixed with PEY1 (Curve b), a third peak was observed between the water peak and the PEY1 peak, and was assigned to PEO 309/PEY1 complex. PEO 309 is a very large uncharged molecule, thus the complexes with PEY1 will be much larger and will have a lower charge density than PEY1. Thus, the complexes are expected to have lower electrophoretic mobility and shorter elution time than PEY1. When the PEO 309/PEY mass ratio was raised from 1.5 to 6 (i.e. compare curves b and d), the electrophoretic mobility of the complexes decreased (i.e. faster elution).

We were surprised to observe a free PEY1 peak in the presence of such a large excess of PEO (Curve d). Results presented in subsequent sections will show that PEY1 was saturated with bound PEO when the total mass solution concentration ratio of PEO/PEY1 was around 0.18 (herein we call this the mass saturation ratio). Thus, a ratio of 6 represents a very large excess of PEO which might be expected to bind all of the PEY1. Since PEY1 has a distribution of both molecular weight and microstructure, it was possible that some PEY1 molecules could not bind to PEO 309 even when PEO 309 was present in great excess. The area under the peak was proportional to the mass of PEY1, the mass fraction of the un-bound PEY1 molecules was approximately 70%.

The presence of calcium ions promoted PEO/TCP complex formation. Figure 2 shows capillary electrophoresis results for PEO 309/PEY1(Ca^{2+}) complexes. With increasing concentration of PEO 309, the PEY1 peak decreased. At a PEO/PEY1(Ca^{2+}) mass ratio of 0.25, the PEY1 peak disappeared completely. Unlike the calcium-free experiments (Figure 1), there was no evidence of a peak corresponding to a PEO/PEY(Ca2+) complex. Our results to be published in a companion paper show that under these conditions the complexes are colloidally unstable and tend to aggregate to form macroscopic hydrogels[19] which are too large to enter the capillary. Based on the results in Figure 2, the mass saturation ratio of PEO/PEY(Ca^{2+}) is between 0.15 and 0.25,

which is close to the ratio of 0.20 obtained from isothermal titration calorimetry (see below).

NMR

Two-dimensional NOESY NMR is often used to elucidate the molecular structure of bio-molecules and synthetic polymers.[20] This technique is powerful because a cross-peak will occur in a two-dimensional NOESY spectrum if the distance between two protons is less than 0.45 nm.[21] Figure 3 and Figure 4 show the NOESY spectra of PEYA and PEY1 respectively. Integration of the one-dimensional proton peaks confirmed the molecular formula provided by Sigma. An interesting feature in these results is the e-g cross-peak in the PEY1 spectrum. This must arise from the close association of tyrosine moieties since the distance between the "e" proton (β phenolic proton of tyrosine) and "g" proton (3 position proton of tyrosine phenol) on an individual tyrosine is farther than 4.5 Å. No "e-g" cross-peak is shown on PEYA spectrum indicating the absence of tyrosine association. It is proposed in the discussion section that the presence of closely associated phenolic groups is required for PEO complex formation.

Isothermal Titration Calorimetry

In a typical isothermal titration calorimetry experiment, one reactant is gradually added to a solution and the resulting heat effect of each injection is recorded.[22] The results are expressed as a heat flow into the calorimeter so a positive heat reading indicates an endothermic reaction and a negative reading indicates an exothermic reaction. The reaction enthalpy, entropy, and binding constant can also be calculated from titration results involving well-defined processes.

Figure 5 shows TCP titration with PEO N-12K (MW=1 MDa) in the absence of Ca^{2+}. The quantity of added PEO (i.e. the X axis) is scaled to the mass of TCP in the titration. The corresponding heat flow (i.e. the Y axis) is scaled to the number of moles of polyether oxygens added with that injection. The titration curve for PEY4 (poly(Glu, Tyr) (4:1)) is a straight line, which suggests that there was no detectable interaction between PEY4 and PEO N-12K whereas PEY1 and PEYA gave heat effects. The association between PEY1 and PEO resulted in a positive titration curve, which indicates that the association was endothermic. The released reaction heat was highest at the beginning of the titration and gradually decreased to the baseline. The initial heat effect was around 67 cal per mole of injected C_2H_4O moieties. It was assumed that the complex formation was complete when the first derivative became zero which corresponded to a PEO/PEY1 mass ratio of 0.18.[23]

PEYA exhibits behavior between that of PEY4 and PEY1; the initial heat effect for the PEYA titration was only 38 cal/mole injection of C_2H_4O and PEO/PEYA binding ceased at a PEO/PEYA mass ratio of 0.07. The average number of tyrosine monomers on each TCP chain was calculated based on TCP weight average molecular weight. On

average, each PEY1 chain has 78 tyrosine residues whereas PEYA has 69 and PEY4 has only 51. Thus the heat effect seems to be related to the tyrosine content.

The presence of calcium ions influenced heat effects associated with complex formation. Figure 6 shows the TCP(Ca^{2+}) titrations with PEO N-12K. As with the calcium free experiments, no interaction was observed between PEY4(Ca^{2+}) and PEO. By contrast the shape of the PEY1(Ca^{2+}) titration curve was significantly different from the titration in the absence of calcium. The titration curve was initially negative (exothermic) and then gradually became positive (endothermic) at a PEO/PEY1(Ca^{2+}) mass ratio of 0.09. Therefore there were at least two effects caused by adding PEO to PEY1(Ca^{2+}) - one was exothermic and the other endothermic. PEY1(Ca^{2+}) was saturated with PEO when the PEO/PEY1(Ca^{2+}) mass ratio reached 0.20 which is slightly higher than 0.18, the calcium-free value.

The PEYA(Ca^{2+}) titration with PEO was also sensitive to the presence of calcium. The initial heat was 102 cal/mole injection of C_2H_4O, which was much higher than the 38 cal/mole injection of C_2H_4O for the PEYA titration. The titration curve increased to 120 cal/mole injection of C_2H_4O at a PEO/PEYA(Ca^{2+}) mass ratio of 0.08 and then decreased gradually to the baseline when the PEO/PEYA(Ca^{2+}) mass ratio was 0.20. Thus calcium ion enhances the affinity of PEYA to PEO.

Figure 7 shows three PEY1(Ca^{2+}) titrations corresponding to the initial PEY1(Ca^{2+}) concentrations of 0.4 g/L, 03 g/L, and 0.2 g/L. The three titration curves almost overlap which is consistent with the notion of high affinity binding.[24]

Figure 8 shows the influence of PEO molecular weight on PEY1 titrations in the absence of calcium. There was no interaction between PEG 350 and PEY1. Furthermore, the heat effects assocated with 5000 Da PEO were much less than those from 100,000 Da PEO. Therefore, under the conditions of these experiments, the results in Figure 8 show that the minimum PEO molecular weight producing measurable heat effects when mixed with PEY1 was between 350 and 5000 Da.

PEO molecular weight effects were also investigated in the presence of calcium ions. Figure 9 shows PEY1(Ca^{2+}) titrations with four PEOs. As with the calcium-free results, there was no interaction between PEG 350 and PEY1(Ca^{2+}). 5000 Da PEO gave only an exotherm whereas the two high molecular weight PEOs (10^5 and 10^6 Da) showed initial exotherms followed by endotherms. The highest molecular weight PEO gave the highest endothermic response.

Figure 10 shows the pH effect on PKY1 (poly(Lys, Tyr) (1:1)) titration with PEO N-12K (MW=1 MDa). PKY1 is a positively charged tyrosine-containing polypeptide with amine groups along the polymer chain. PEO/PKY1 binding was endothermic when the pH was 8. However, it became exothermic when the pH was 1.7. At the intermediate pH of 7.2, an exothermic interaction was initially observed and was followed by an endothermic interaction much like the PEY1 case in calcium.

It was proposed that the hydrophobic interaction between PEO and the phenolic groups on the cofactor is the driving force for the association between PEO and a cofactor.[11] To test this, PKF1 was titrated with PEO N-12K and the result is also shown in Figure 10. The phenylalanine moieties on PKF1 are more hydrophobic than the tyrosine moieties on PKY1. However, PKF1 did not bind to PEO N-12K, suggesting that hydrophobic interactions do not dominate complex formation.

Circular Dichroism

In general, the average configuration of polypeptides can be derived from CD spectra and the results are usually expressed as a fraction of three fundamental structures: the random coil, the α-helix, and the β-sheet. However, the presence of a large fraction of tyrosine moieties can distort the far UV CD spectrum of the peptides and make the peptide structure derivation invalid.[25] In this work, CD was only applied to follow TCP structure change and the detailed TCP structure was not derived because of the high tyrosine contents.

Figure 11 shows the influence of PEO and $CaCl_2$ on the CD spectra of PEY1. The structure of pure PEY1 resembled a random coil, whereas in the presence of Ca^{2+} the PEY1 structure was closer to that of a β-sheet. It is possible that the Ca^{2+} ions linked glutamic acid residues resulting in PEY1 folding. The addition of PEO N-10 further changed the structure of PEY1(Ca^{2+}) whereas PEO did not influence PEY1 structure in the absence of calcium ions.

The amount of added PEO (i.e. the PEO/PEY1 mass ratio) influenced the CD spectra. Figure 12 shows the CD reading at 229 nm as a function of the amount of PEO added to PEY1 or PEY1(Ca^{2+}). Without calcium, there was a small change in the CD reading at low PEO concentrations and the effect decayed with increasing PEO/PEY ratios. With calcium, PEO induced a much greater change in CD and this effect persisted to high PEO concentrations.

It is of interest to compare the CD spectra (Figure 12) and the thermal titrations (Figure 7) in order to relate heat effects to structure change. The binding was exothermic when the PEO/PEY1 ratio was below 0.1, and was endothermic when the ratio was between 0.1 and 0.2. At the same time, the CD reading of PEY1(Ca^{2+}) increased from -9116 to -4946 deg·cm^2·dmol^{-1} when the PEO/PEY1 ratio was below 0.1 and remained almost constant when the ratio was between 0.1 and 0.2. It is clear that the exothermic reaction corresponded to the structure change of the PEY1(Ca^{2+}) chains. In the absence of the PEY1(Ca^{2+}) structure change, the interaction of PEY1(Ca^{2+}) with PEO was an endothermic process.

Figure 13 summarizes the influence of PEO N-12K and $CaCl_2$ on PEYA CD spectra. The presence of PEO N-12K did not cause a detectable change in PEYA structure whereas Ca^{2+} decreased PEYA CD reading from 1250 to -1995 deg·cm^2·dmol^{-1}

at 229 nm. The further addition of PEO addition caused the CD reading change to -2613 deg·cm^2·dmol$^-$1 at 229 nm. Thus, it seems that Ca^{2+} ions led to PEYA folding, and that folded PEYA(Ca2+) further changed upon attachment to PEO.

The influence of pH on the ability of PEO to change the CD spectra of PKY1 is shown in Figure 14 . The CD results are shown as $\Delta\theta$ values which were calculated by subtracting the PKY1+PEO CD readings from the corresponding PKY1 CD reading at 229 nm. The CD results in Figure 14 are plotted against the heat effect from the first PEO injection. A good linear relationship was obtained, indicating the direct correlation between the magnitude of the exotherm and the change in CD spectra. Extrapolation to zero CD change gave an endothermic energy of 53 cal per mole of injected of C_2H_4O moieties, which perhaps is an indication of the enthalpy of the polypeptide attached to PEO in the absence of much structure change.

Discussion

Because the aqueous complex formation between PEO and water soluble tyrosine-containing polypeptides (TCP) is a complicated process, it is convenient to consider complex formation at three distance scales. The first distance scale corresponds to the size of an amino acid moiety and involves the interaction between the individual polymer segments. The major issues at this scale are the geometry of bonded segments and the corresponding energetics. The second distance scale corresponds to the length of a polypeptide molecule. The key features at this distance scale are the configuration of a complexed polypeptide and the fraction of amino acid residues directly bonded to PEO. The third distance scale corresponds to the size and shape of the overall complexes and can be micrometers. The focus of this work was to extend our knowledge of the interactions at the first and the second distance scales. The results of light scattering and viscosity measurements to characterize the overall size and density of the complexes will be presented in a future publication.

PEO/TCP Interactions at the Segmental Distance Scale

The energetics of complex formation were measured by isothermal titration calorimetry and circular dichroism (CD) was used to follow changes in the polypeptide configuration with complex formation. Two distinct behaviors were observed with and without calcium ions. Without calcium, the PEO/TCP interactions were endothermic (Figure 5) over the whole titration and there was only a small initial change in CD with complex formation. By contrast, with calcium present, the titrations were exothermic for about the first half and endothermic for the second. The polypeptide CD showed a large change over the exothermic portion of the titration. The origins of these effects are now considered.

It is proposed that three processes can occur simultaneously when PEO binds to TCP: 1) the attachment of PEO to TCP; 2) TCP conformation change; and, 3) the collapse of the complexed PEO coils resulting in an overall shrinkage of the complex.

Each of this these processes will have an associated heat effect. Without calcium, the CD indicated very little conformational change (process 2). Furthermore, dynamic light scattering results, to be presented in a future publication, show little evidence of process 3. Thus, without calcium the main effect is process 1, the initial attachment, and this is endothermic. This, in turn, suggests that the driving force for attachment must be the entropy gain associated with the release of water. [26]

In the presence of calcium, all three effects occur. The initial binding (process 1), as above, will be endothermic, however, in the first half of the titration this heat effect is masked by a large exotherm which we postulate is caused by the re-conformation of polypeptide. This is evidenced by the change in CD spectra (Figure 12) corresponding to exothermic part of the titration curve. Furthermore, from light scattering results to be published, it is known that the density of the overall complex is far greater than that of PEO. Therefore, process 3, the collapse of the peptide decorated PEO coils, also happens in the presence of calcium. Since the Flory-Huggins χ parameter of PEO in water is around +0.45[27], the corresponding heat effect will also be exothermic.[28]

The influence of pH on PKY1 titrations (Figure 10) and of PEO molecular weight (Figure 9) can be rationalized by the proposed heat effects – i.e. the collapse (folding) of polypeptide is exothermic and the binding of TCP to PEO is endothermic. Consider first Figure 10 which shows only an endotherm at high pH and only an exotherm at low pH. At high pH, most of the amine groups are not protonated and PKY1 will collapse before PEO is added, thus there is no complexation induced collapse. By contrast at low pH, the peptide will be highly expanded and so complex formation will include a substantial change in peptide configuration. Indeed, the linear correlation between CD change and the magnitude of the exotherm (Figure 14) emphasizes the link between structure change and the exothermic response.

It could be argued that it is difficult for a polypeptide to collapse when bonded to a large PEO coil. The results in Figure 9 show that the extent of the exotherm increases with decreasing PEO MW. We propose that this further supports the proposal that the exotherm results from the collapse of the polypeptide chains.

The observation that complex formation without calcium is an endothermic process suggests that complex formation is driven by hydrophobic interactions. Indeed, we have proposed that hydrophobic interactions are important in the interaction of PEO with synthetic phenolic polymers.[11] However, that conclusion seems to be contradicted in this work because the more hydrophobic polypeptide PKF1, which contains 50 mole% phenylalanine moieties, has no affinity for PEO, suggesting that PEO/TCP binding is not a simple hydrophobic interaction. The hydroxyl groups on the aromatic rings are required to enhance the PEO/TCP association.

From the earliest studies of PEO/phenolic polymer interactions it has been assumed that hydrogen bonding between polyether oxygens and phenolic hydroxyl

groups is the driving force for complex formation. [6] The formation of hydrogen bonds in water is usually exothermic, which contradicts our results without Ca^{2+}. Furthermore, Cong and coworkers used NMR to show that protons of PEO segments bonded to poly(vinyl phenol-co-potassium styrene sulfonate) sit near the π orbitals of the aromatic rings which is not consistent with hydrogen bonded structures.[11] Finally, isothermal titrations conducted in the presence of 1 M of urea, a known hydrogen bonding breaker, showed that PEO was binding to PEY1. [18] In summary, evidence does not support hydrogen bonding as a significant mechanism for complex formation between PEO and tyrosine containing polypeptides.

PEO/TCP Interactions at the Polypeptide Distance Scale

The issues at this distance scale include the effects of polypeptide composition, molecular weight and microstructure on complex formation with aqueous PEO. In a previous short communication we showed that oligomer peptide $(Glu, Tyr)_4$ (MW 1.1 kDa) does not interact with aqueous PEO whereas PEY1, which is poly(Glu, Tyr) (1:1) with a molecular weight of 36 kDa, does. Similarly, the results in Figure 8 show that the minimum PEO molecular weight for interactions with PEY1 is between 350 and 5000 kDa. The existence of a minimum molecular weight for complex formation is a common feature in polymer/polymer complexes.[29] The usual explanation is that with increasing molecular weight, the cost in translational entropy loss goes down whereas the binding energy per chain goes up.[30] Thus, the minimum molecular weights leading to complex formation reflect a balance of these effects.

Polypeptide composition had a large effect on complex formation. Comparison of the behaviors of PEY1, PEY4 and PEYA (see Table 1) is particularly interesting. Because the bindings of PEO/PEY1 and PEO/PEYA are endothermic without calcium, the area between the ITC curves and their corresponding baselines can be considered to be proportional to the total number of the phenolic groups that bind to PEO. Thus, for the same mass of PEY1 and PEYA, the number of the bound phenolic groups on PEY1 is approximately seven times greater than the number on PEYA. Furthermore, PEY4 did not interact with PEO at all. The obvious explanation for this ranking is the overall phenolic content. However, the average tyrosine number on each PEY1 chain (78) is only slightly higher than the numbers on each PEY1 chain (69) and PEY4 chain (51). Thus, the explanation lies elsewhere and we believe that it involves the polypeptide microstructure.

The polypeptides employed in this work were polydisperse with respect to molecular weight ($M_w/M_n \sim 1.6$). Furthermore, the copolymers will have a distribution of microstructure. If, as claimed by the supplier[13], the copolymers are statistical, the probability of a sequence of x tyrosine moieties is $P(x) = r_Y^{x-1}(1-r_Y)$ where r_Y is mole fraction of tyrosine. Furthermore, the number of sequences of length x in a chain of length n_Y is $n(x) = n_Y P(x)$. Figure 15 shows $n(x)$ as a function of x. Based on this calculation a PEY1 chain could have tyrosine block lengths as long as 6, whereas the

limiting block length for PEYA is 4 and for PEY4 is 3. Therefore, we propose that without the presence of calcium, tyrosine block lengths greater than 3 are required for complex formation. Indeed, 2D NMR gave direct evidence for closely spaced (i.e. < 0.5 nm) phenolic groups in PEY1 (Figure 3 and Figure 4).

Other evidence of microstructure effects includes the isothermal titration calorimetry results. The PEY1/PEO curve in Figure 5 shows a gradual decrease in heat effect with PEO addition. It is proposed that this reflects a range of polypeptide microstructures giving a range of interaction energies. Indeed, the corresponding capillary electrophoresis curve showed that 70% of PEY1 could not bind even in the presence of excess PEO.

As explained in the results section, the shape of the curve shown in Figure 7 could be explained by a range of interaction energies corresponding to a range of microstructures. Also, the observation that 70% PEY1 could not bind to PEO in the absence of calcium could reflect the absence of tyrosine blocks in the lower molecular weight fraction.

The requirement for short tyrosine blocks for PEO binding could be satisfied by the association of non-neighboring tyrosine residues. The positive influence of soluble calcium ions on complex formation could be explained by the calcium induced collapse of the polypeptide coils giving more active groups of associated tyrosine residues. The CD results showed a calcium-induced partial folding of PEY1.

We are interested in the interactions of high molecular weight PEO with tyrosine containing peptides because these systems are models for commercial flocculants systems based on mixtures of PEO and phenolic polymers. However, our results are also relevant to the use of PEO coated surfaces for protein repellant biomaterials. Specifically, our results indicate that only proteins with groups of four or more closely spaced tyrosine residues are likely to bind to PEO with a molecular weight greater than 350 Da.

Conclusions

The following conclusions are based on our studies of the interaction of high molecular weight PEO and tyrosine-containing polypeptides:

1. Without calcium, polypeptide binding to PEO is an endothermic process and there is no indication of significant binding-induced changes in the polypeptide configuration (CD). As much as 70% of PEY1 does not participate in binding even in the presence of excess PEO. We propose that polypeptide chains have only a few points of attachment to PEO without calcium.

2. With and without calcium PEY1 gives a stronger interaction with PEO than the more hydrophobic PEYA. Thus, nonspecific hydrophobic interactions do not

dominate complex formation. Indeed, phenylalanine based polypeptide (PKF1) showed no heat effect whatsoever when mixed with PEO.

3. With calcium, there is high affinity binding of PEO with PEY1 and PEYA and the complex formation coincides with a change in the polypeptide configuration. It is proposed that complex formation consists of three processes: 1) the attachment of polypeptide chains to PEO (endothermic); 2) the re-conformation of the polypeptide (exothermic); and, 3) the collapse of the supporting PEO framework (exothermic).

4. It is proposed that PEO/polypeptide binding sites involve more than three closely spaced phenolic groups. Calcium bridging of glutamic acid residues promotes the association of phenolic groups and thus complex formation.

5. The minimum PEO molecular weight for binding to tyrosine rich polypeptides is between 350 and 5000 Da. Previous work showed that minimum molecular weight of 1:1 poly(tyrosine-glutamic acid) for binding to high molecular weight PEO is between 1.1 and 36 kDa.[12] We propose that these limiting molecular weights correspond to the balance of translational entropy loss in the polymers and the gain in entropy associated with the release of bound water.

Table 1. The molecular weights of the tyrosine-containing polypeptides. M_{vis} is viscosity average molecular weight, M_w is weight average molecular weight, M_n is number average molecular weight, n_Y is the average number of tyrosine monomers on one polymer chain calculated based on M_w, M_w/M_n is molecular weight polydispersity. Data provided by Sigma.

Sample	Structure	M_{vis} (Da)	M_w (Da)	M_n (Da)	M_w/M_n	n_Y
PEY1	Poly(Glu, Tyr) (1:1)	36,100	24,500	15,312	1.6	78
PEY4	Poly(Glu, Tyr) (4:1)	31,300	38,800	24,250	1.6	51
PEYA	Poly(Glu, Tyr, Ala) (1:1:1)	40,000	26,700	16,688	1.6	69
PKY1	Poly(Lys, Tyr) (1:1)	128,000	72,000			
PKF1	Poly(Lys, Phe) (1:1)	41,500				

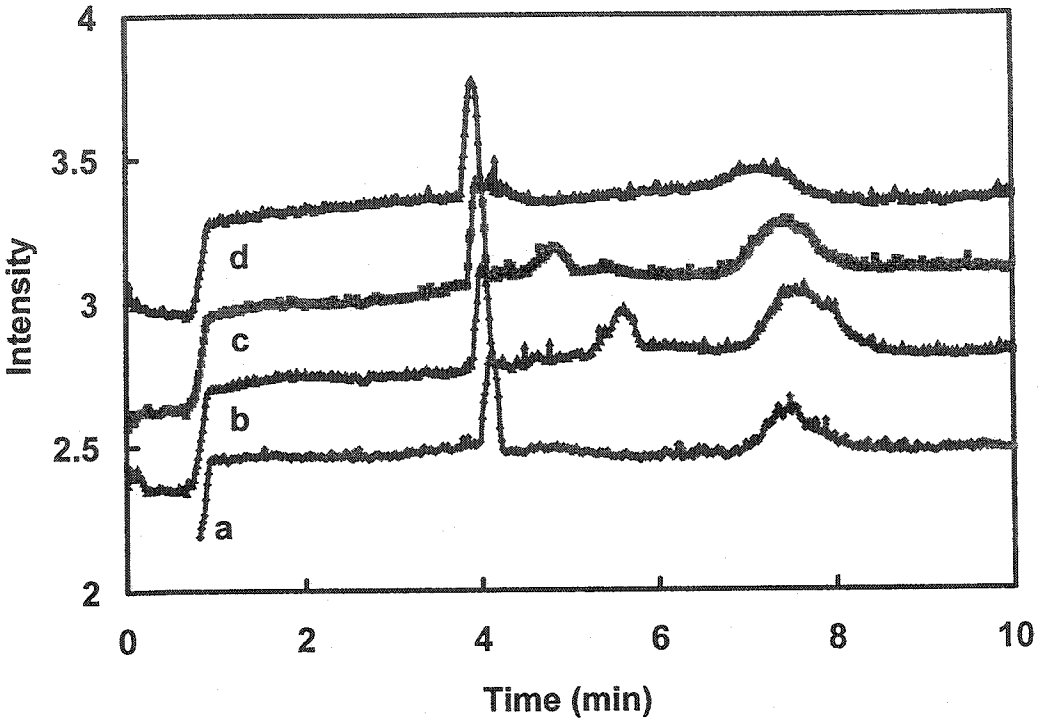

Figure 1. The capillary electrophoresis measurements of PEO 309/PEY1 in 0.01 M Tris buffer (pH=8) at 25°C. (a) [PEY1]=0.5 g/L; (b) [PEY1]=0.5 g/L, [PEO 309]=0.75 g/L; (c) [PEY1]=0.25 g/L, [PEO 309]=0.75 g/L; (d) [PEY1]=0.125 g/L, [PEO 309]=0.75 g/L. All the curves were shifted vertically for a better comparison.

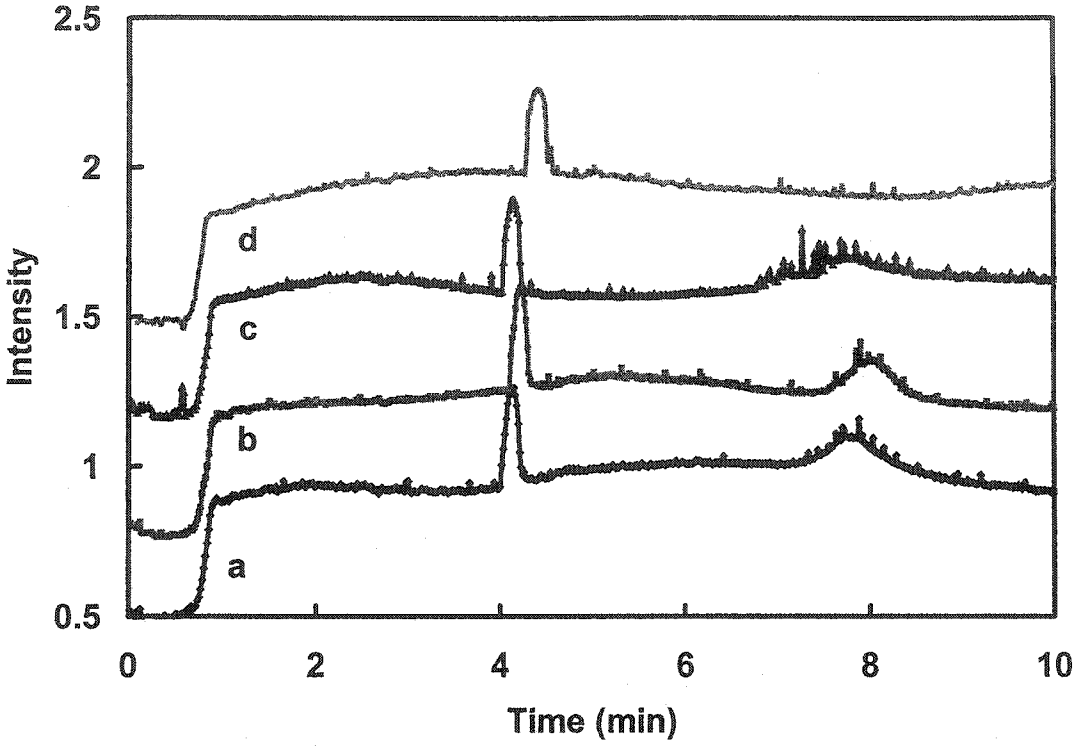

Figure 2. The capillary electrophoresis measurements of PEO 309/PEY1(Ca^{2+}) in 0.01 M Tris buffer (pH=8) at 25°C. (a) [PEY1]=0.5 g/L; (b) [PEY1]=0.5 g/L, [$CaCl_2$]=0.002 M; (c) [PEY1]=0.5 g/L, [PEO 309]=0.075 g/L, [$CaCl_2$]=0.002 M; (d) [PEY1]=0.5 g/L, [PEO 309]=0.125 g/L, [$CaCl_2$]=0.002 M. All the curves were shifted vertically for a better comparison.

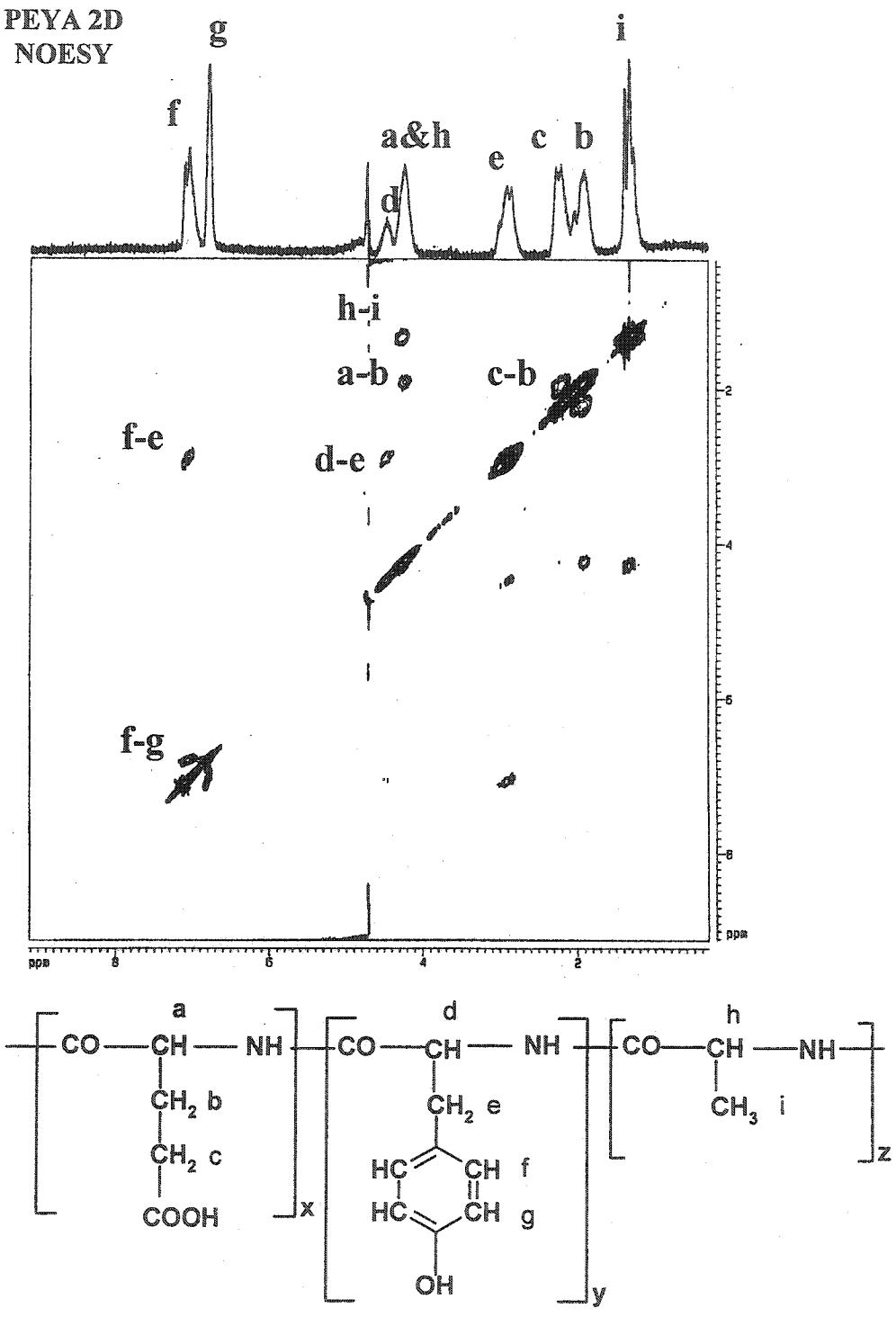

Figure 3. Two-dimensional NOESY NMR of PEYA at 30°C. Mixing time=0.1 s, [PEYA]=0.5 g/L.

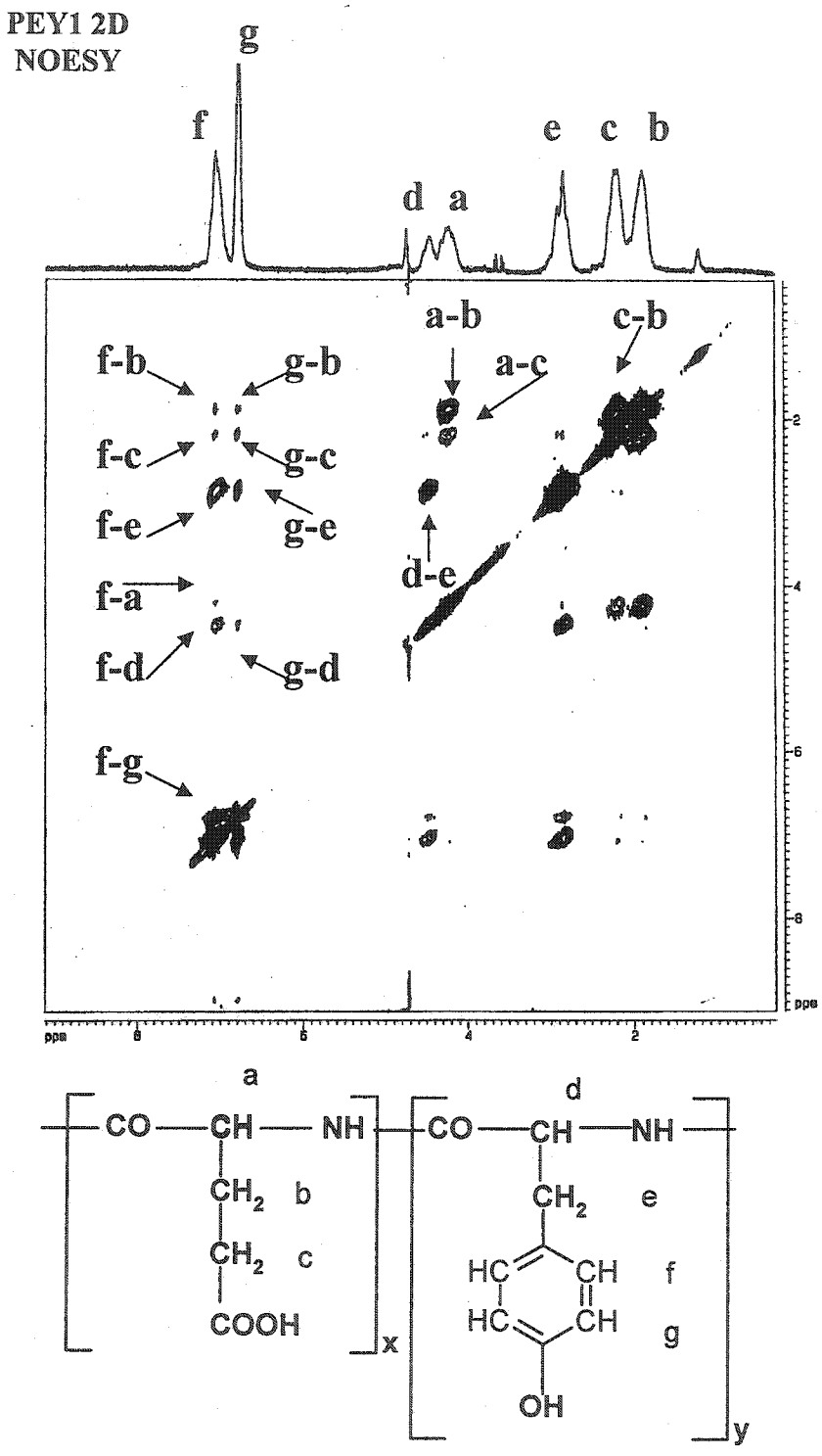

Figure 4. Two-dimensional NOESY NMR of PEY1 at 30°C. Mixing time=0.1 s, [PEY1]=1 g/L.

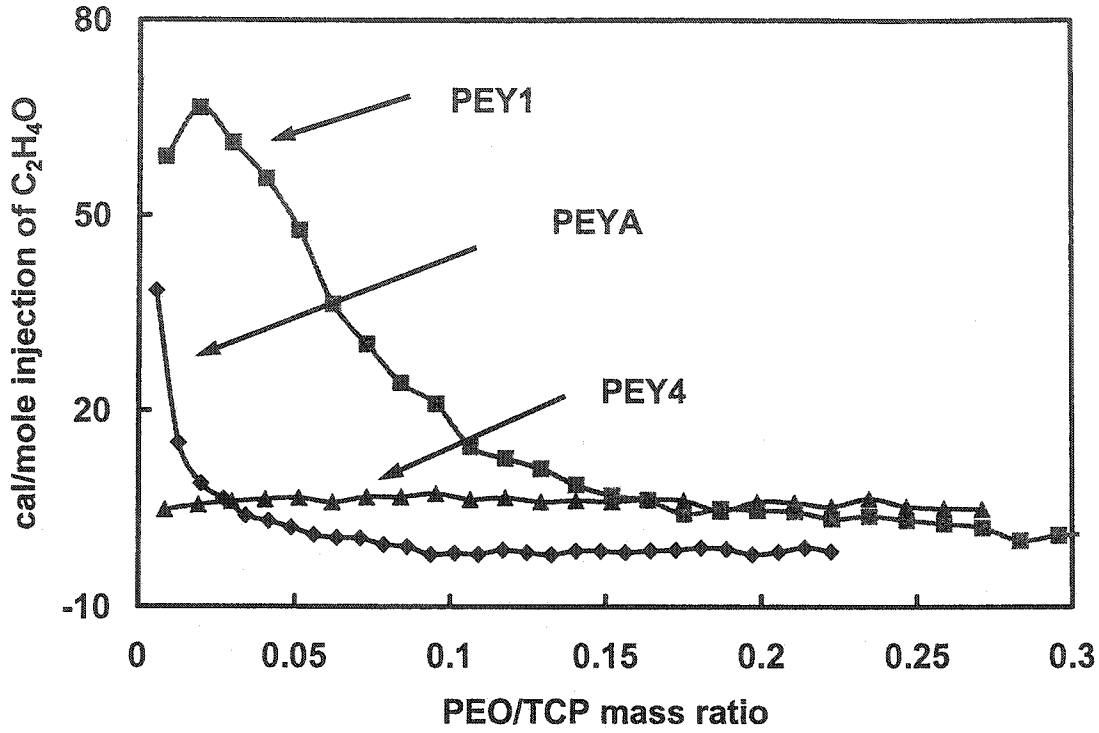

Figure 5. The isothermal titrations of TCP with PEO N-12K (MW=1 MDa) at 30°C. All the samples were prepared in buffer containing 0.01 mole/L Tris (pH=8). [PEY1]=0.4 g/L, [PEY4]=0.4 g/L, [PEYA]=0.6 g/L, [PEO N-12K]=0.6 g/L. 28 10-uL portions of PEO solution were injected into TCP solution during the titration. The duration of each injection was 20 s and the time interval between each two injections was 240 s.

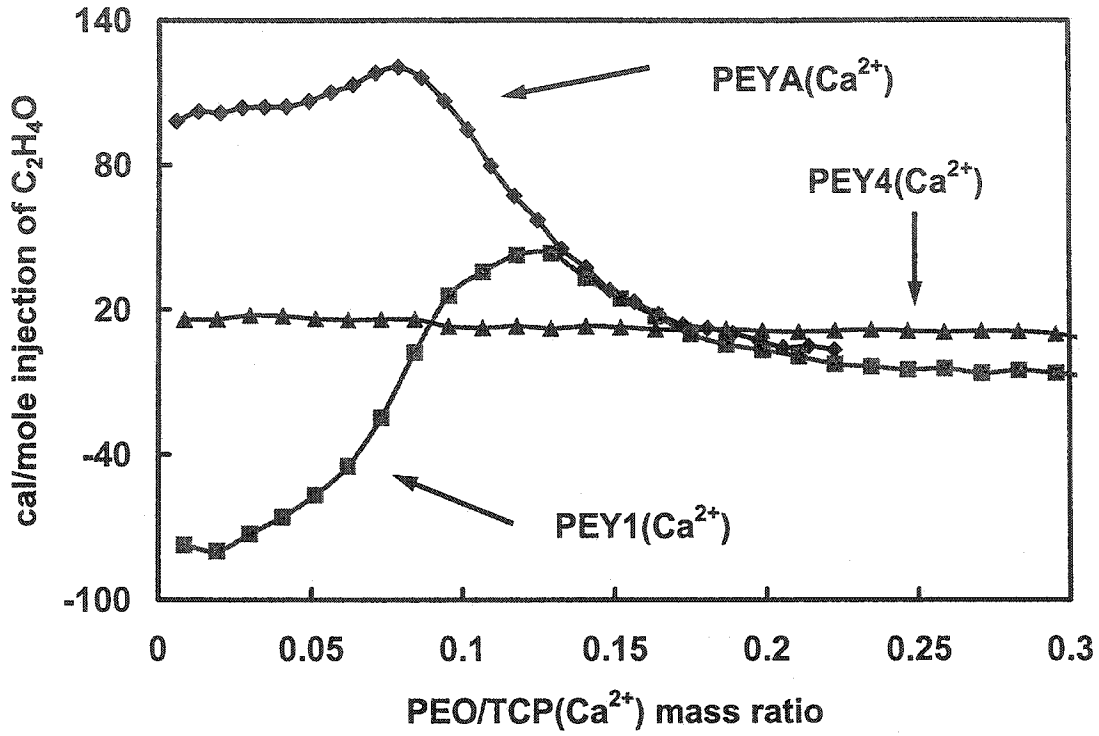

Figure 6. The isothermal titrations of TCP(Ca^{2+}) with PEO N-12K (MW=1 MDa) at 30°C. All the samples were prepared in buffer containing 0.01 mole/L Tris (pH=8) and 0.001 M $CaCl_2$. [PEY1(Ca^{2+})]=0.4 g/L, [PEY4(Ca^{2+})]=0.4 g/L, [PEYA(Ca^{2+})]=0.6 g/L, [PEO N-12K]=0.6 g/L. 28 10-uL portions of PEO solution were injected into TCP(Ca^{2+}) solution during the titration. The duration of each injection was 20 s and the time interval between each two injections was 240 s.

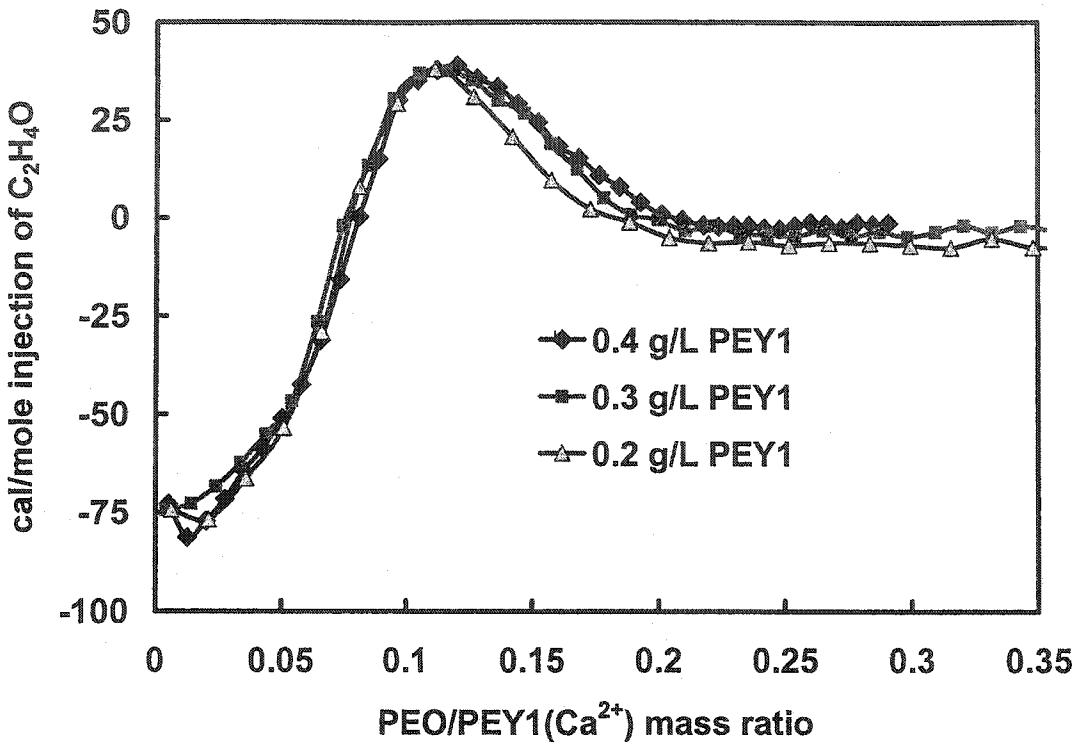

Figure 7. The isothermal titrations of PYE1(Ca^{2+}) with PEO N-12K (MW=1 MDa) at 30°C at different PEY1(Ca^{2+}) initial concentrations. All the samples were prepared in a buffer containing 0.01 mole/L Tris (pH=8) and 0.001 M $CaCl_2$. [PEO N-12K]=0.6 g/L. During the titration, 40 7-uL portions of PEO solution were injected into PEY1(Ca^{2+}) solution. The duration of each injection was 14 s and the time interval between each two injections was 300 s.

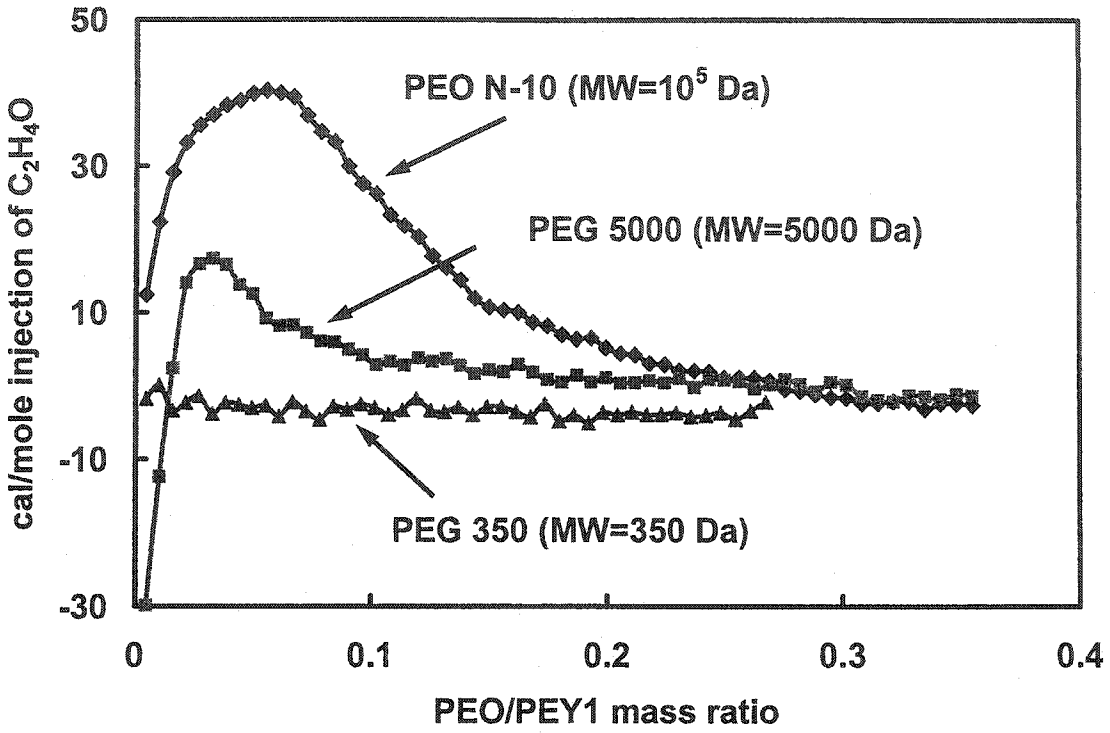

Figure 8. The isothermal titrations of PEY1 with PEO of different MW at 30°C. All the samples were prepared in buffer containing 0.03 mole/L Tris (pH=8). [PEY1]=0.5 g/L, [PEO]=0.8 g/L. 57 5-uL portions of PEO solution were injected into PEY1 solution during the titration. The duration of each injection was 10 s and the time interval between each two injections was 240 s.

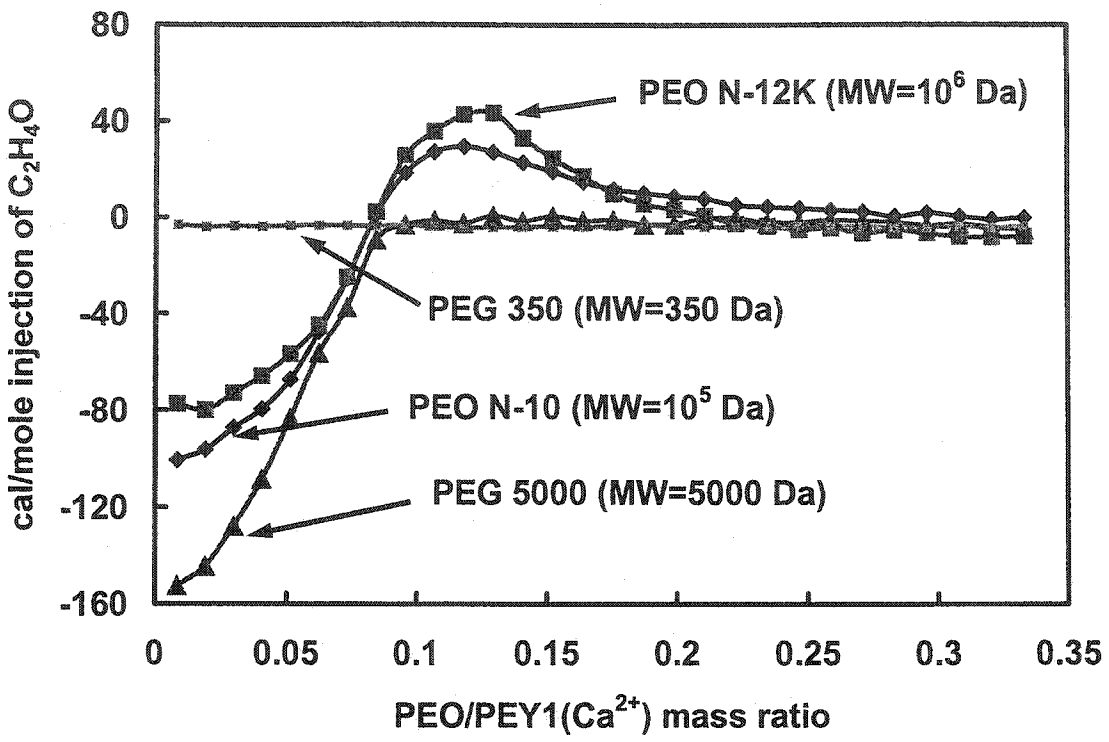

Figure 9. The isothermal titrations of TCP(Ca^{2+}) with PEO of different MW at 30°C. All the samples were prepared in buffer containing 0.01 mole/L Tris (pH=8) and 0.001 M $CaCl_2$. [PEY1(Ca^{2+})]=0.4 g/L, [PEO]=0.6 g/L. 28 10-uL portions of PEO solution were injected into TCP(Ca^{2+}) solution during the titration. The duration of each injection was 20 s and the time interval between each two injections was 240 s.

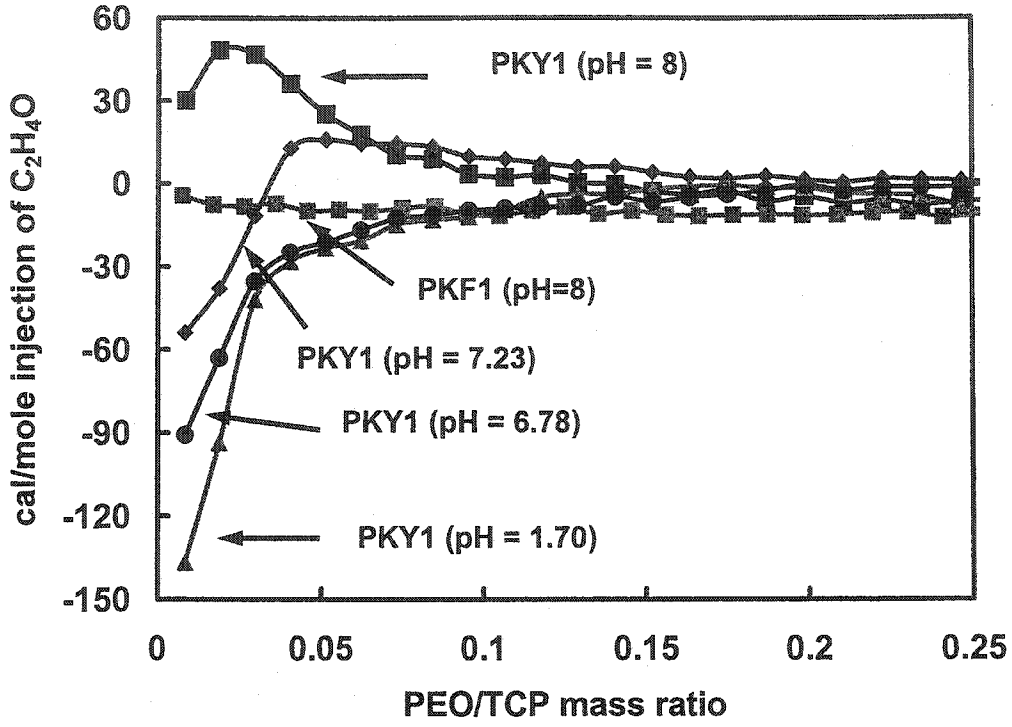

Figure 10. The isothermal titrations of TCP with PEO N-12K (MW=1 MDa) at 30°C at different pH. All the samples were prepared in buffer containing 0.01 mole/L Tris (except buffer with pH=1.70). Buffer with pH=1.70 was prepared by 0.02 M HCl. [TCP]=0.4 g/L, [PEO N-12K]=0.6 g/L. 28 10-uL portions of PEO solution were injected into TCP solution during the titration. The duration of each injection was 20 s and the time interval between each two injections was 240 s.

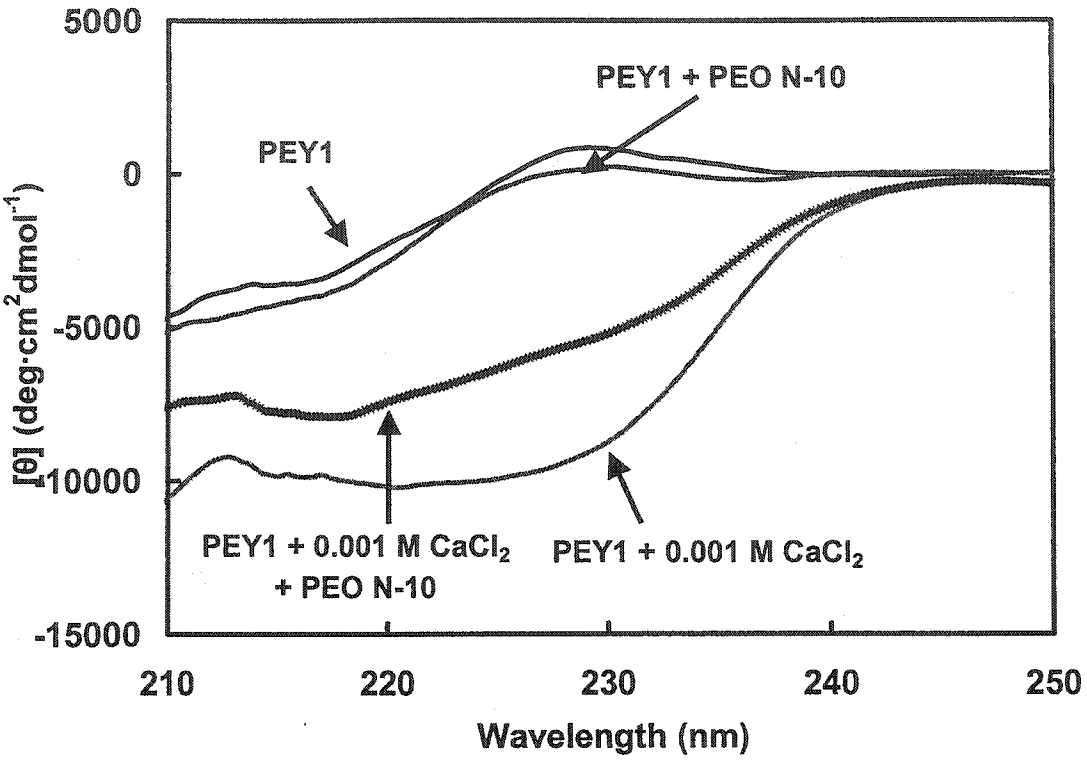

Figure 11. The effects of the presence of PEO N-10 and Ca^{2+} on PEY1 circular dichroism spectra at 25°C. [PEY1]=0.1 g/L, [PEO N-10]=50 mg/L, [$CaCl_2$]=0.001 M, pH was adjusted to 8 using 0.01 M Tris buffer.

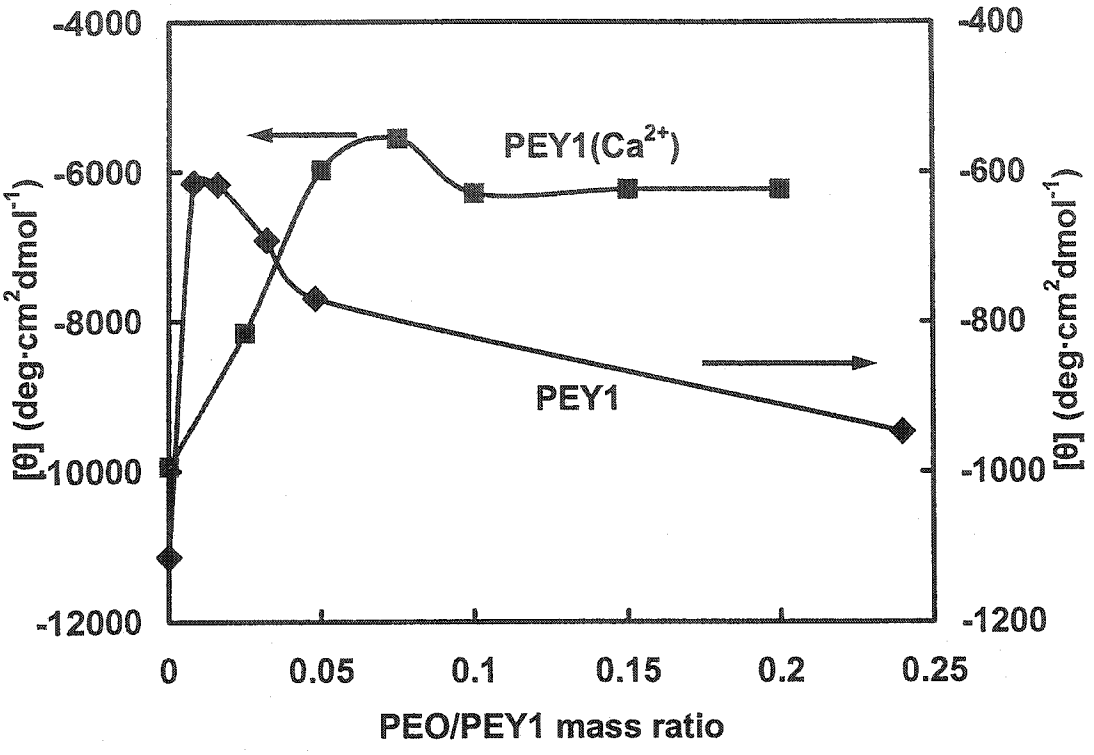

Figure 12. The mean residue ellipticities [θ] of PEY1 and PEY1(Ca^{2+}) as a function of PEO N-10/PEY1 ratio. The θ readings were recorded at 229 nm. For PEY1 measurements, [PEY1]=0.5 g/L, pH=8 (0.03 M Tris). For PEY1(Ca^{2+}) measurements, [PEY1(Ca^{2+})]=0.1 g/L, [$CaCl_2$]=0.001 M, pH=8 (0.01 M Tris).

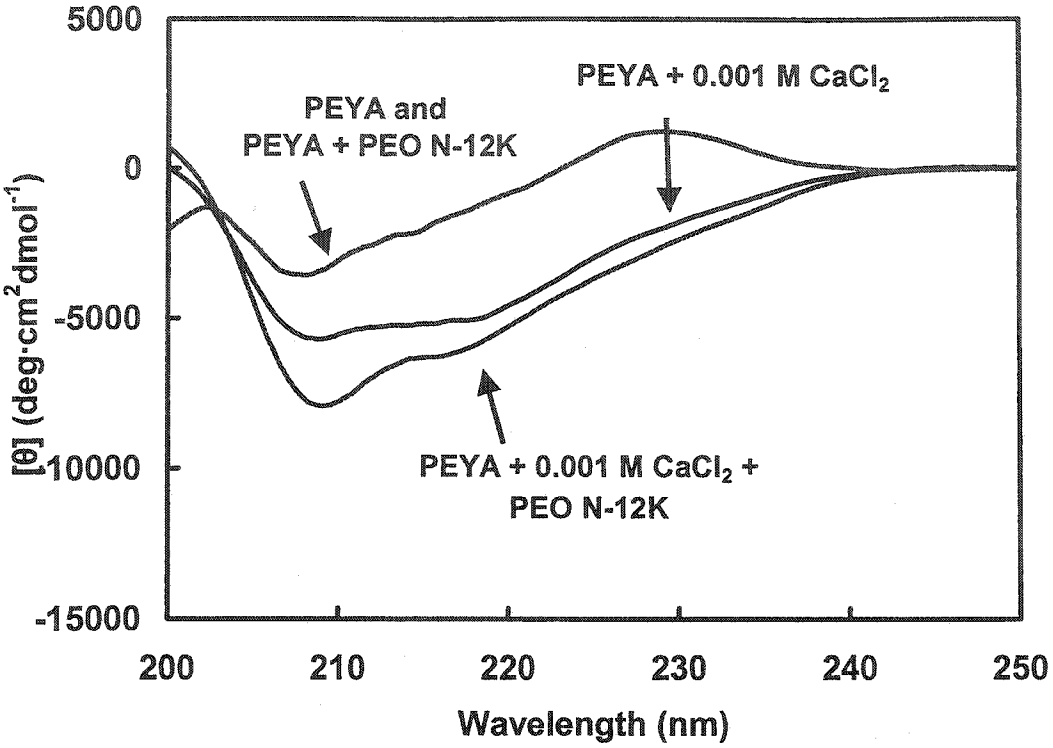

Figure 13. The effects of the presence of PEO N-12K and Ca^{2+} on PEYA CD spectra at 25°C. [PEYA]=0.1 g/L, [PEO N-12K]=50 mg/L, [$CaCl_2$]=0.001 M, pH was adjusted to 8 using 0.01 M Tris buffer.

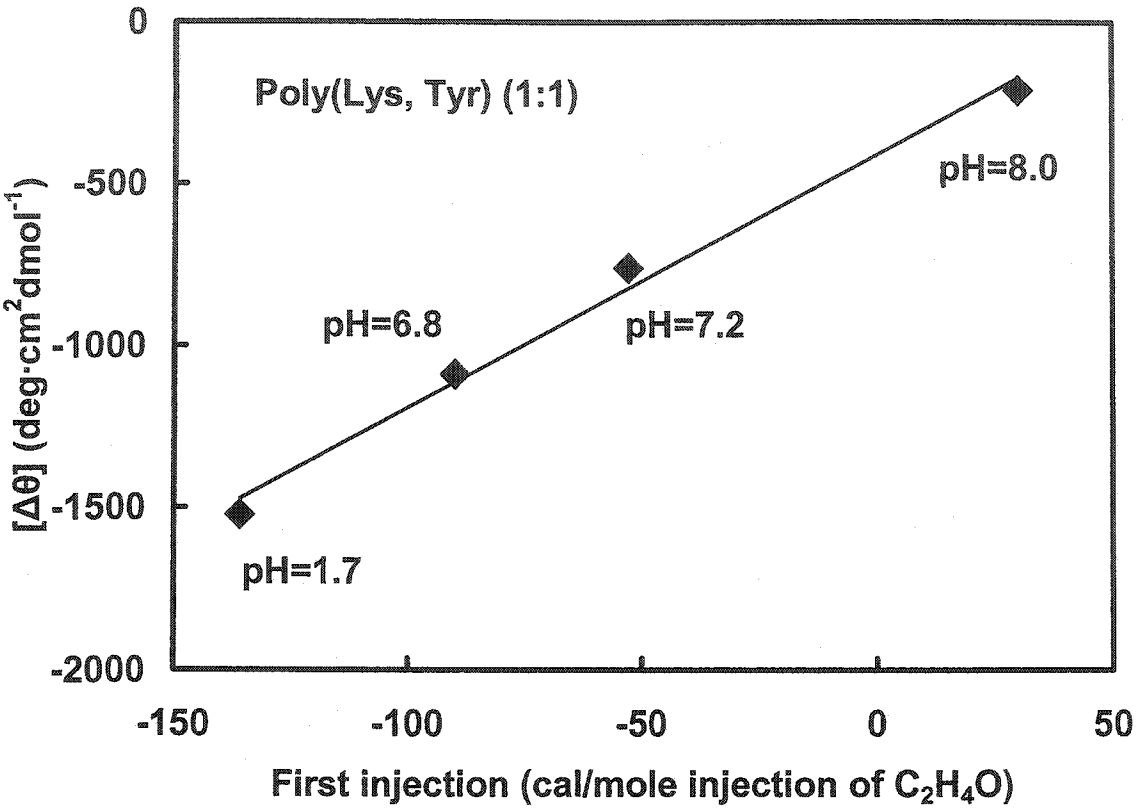

Figure 14. **The change PEY1 structure, measured by CD, as a function of heat released in the first injection of the isothermal titrations (Figure 10). [Δθ] was obtained by subtracting the PKY1+PEO N-12K [θ] readings at 229nm from the corresponding PKY1 [θ] readings without PEO. [PKY1]=0.1 g/L, [PEO N-12K]=0.05 g/L, solution pH was adjusted using 0.01 M Tris buffer except the solution of pH=1.70, which was adjusted using 0.02 M HCl.**

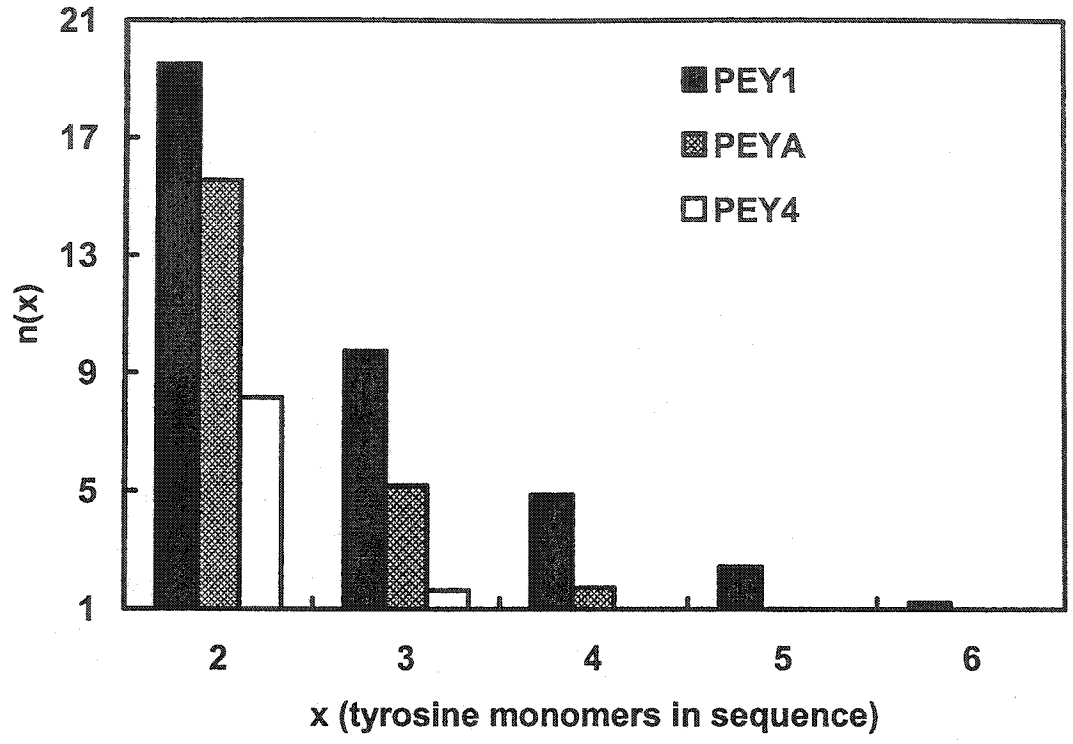

Figure 15. The calculated average number of tyrosine blocks of length x for three polypeptides assuming a random distribution of amino acid residues.

References

[1] Bailey, F. E.; Koleske, J. V. *Poly(ethylene oxide)*, Academic Press: New York, 1976.

[2] Carrard, J. P.; Pummer, H. U.S. Patent 4,070,236, 1973.

[3] Pelton, R. H.; Allen, L. H.; Nugent, H. M. *Svensk Papperstidning* **1980**, *83*, 251-258.

[4] Satterfield, B.; Stockwell, J. Eur. Pat. Appl. WO95/21296, 1995.

[5] Harris, J. M. *Poly(ethylene Glycol) Chemistry: Biotechnical and Biomedical Applications*, Plenum Press: New York, 1992.

[6] Stack, K. R.; Dunn, L. A.; Roberts, N. K. *Colloids and Surfaces* **1991**, *61*, 205-218.

[7] Carignan, A.; Garnier, G.; van de Ven, T. G. M. *Journal of Pulp and Paper Science* **1998**, *24*, 94-99.

[8] Gibbs, A.; Yang, Z.; Xiao, H.; Pelton, R. In *Fundamentals of Papermaking materials, Transactions of the Fundamental Research Symposium, 11th*, Cambridge, UK, 1997.

[9] Pelton, R.; Xiao, H.; Brook, M. A.; Hamielec, A. *Langmuir* **1996**, *12*, 5756-5762.

[10] Cong, R.; Pelton, R. H.; Russo, P.; Doucet, G. *Macromolecules* **2003**, *36*, 204-209.

[11] Cong, R.; Bain, A. D.; Pelton, R. H. *Journal of Polymer Science* **2000**, *38*, 1276-1284.

[12] Lu, C.; Pelton, R.; Valliant, J.; Bothwell S. ; Stephenson, K. *Langmuir* **2002**, *18*, 4536-4538.

[13] Blout, E. R.; Karlson, R. H. *Journal of the American Chemical Society* **1956**, *78*, 941-946.

[14] Laivins, G.; Polverari, M.; Allen, L. *Journal of Pulp and Paper Science* **2001**, *27*, 190-195.

[15] Lu, C.; Pelton, R. H. *PCC Flocculation using PEO and Tyrosine-containing Polypeptides*, to be submitted.

[16] Zhang, W.; Nilsson, S. *Macromolecules* **1993**, *26*, 2866-2870.

[17] Satoh, M.; Komiyama, J.; Iijima, T. *Biopolymers* **1982**, *21*, 1927-1931.

[18] Lu, C. Ph.D. Thesis, McMaster University.

[19] Lu, C.; Pelton, R. H. *The Supermolecular Structure of PEO and Tyrosine-containing Polypeptide Complex*, to be submitted.

[20] Rizo, J.; Bruch, M. D. *Structure Determination of Biological Macromolecules*, In *NMR Spectroscopy Techniques*; Bruch, M. D. Eds.; Marcel Dekker: New York, 1996.

[21] Bruch, M. D. *Multidimensional NMR Spectroscopy of Liquids*, In *NMR Spectroscopy Techniques*; Bruch, M. D. Eds.; Marcel Dekker: New York, 1996.

[22] Fisher, H. F.; Singh, N. *Methods in Enzymology* **1995**, *259*, 194-221.

[23] Dai, S.; Tam, K. C.; Li, L. *Macromolecules* **2001**, *34*, 7049-7055.

[24] Indyk, L.; Fisher, H. F. *Methods in Enzymology* **1998**, *295*, 350-364.

[25] Woody, R. W.; Dunker, A. K. *Aromatic and Cystine Side-Chain Circular Dichroism in Proteins*, In *Circular Dichroism and the Conformational Analysis of Biomolecules*, Fasman, G. D. Eds.; Plenum Press: New York, 1996.

[26] Florián, J.; Warshel, A. *Journal of Physical Chemistry B.* **1999**, *103*, 10282-10288.

[27] Brandrup, J.; Immergu, E. H. *Polymer Handbook*, John Wiley & Sons: New York, 1975.

[28] Hiemenz, P. C. *Polymer Chemistry: The Basic Concepts*, Marcel Dekker: New York, 1984.

[29] Tsuchida, E.; Abe, K. *Advances in Polymer Science* **1982**, *45*, 1-119.

[30] Williams, D. H.; Westwell, M. S. *Chemical Society Reviews* **1998**, *27*, 57-64.

Chapter 6 Supermolecular Structure of PEO/Tyrosine-containing Polypeptide Aqueous Complexes

Abstract

Poly(ethylene oxide) (PEO) and tyrosine-containing water soluble polypeptide (TCP) can form aqueous complexes. The supermolecular structure of the complexes was characterized in the presence of 0.001 M $CaCl_2$. It was found that the supermolecular structure depended on many variables, such as PEO molecular weight, PEO/TCP ratio, and shear rate. For PEO molecules with a molecular weight less than 2 MDa, the complexes aggregated to form dispersed colloidal particles. Increasing the PEO molecular weight increased the particle size. For PEO molecules with a molecular weight of 8 MDa, the complexes formed polymeric networks. A kinetics mechanism was proposed to account for the different supermolecular structures under the different experimental conditions. According to the proposed mechanism, three possible processes can take place once the polypeptide chains attach to the PEO chains. The first process is that the attached polypeptide chains function as bridges to couple PEO chains. The second process is the deactivation of the attached polypeptide chains by the PEO chains. The deactivated polypeptide chains cannot bridge PEO chains. It was proposed that the deactivation was induced by the encapsulation of TCP phenolic groups by PEO. The third process is the saturation of the PEO chains by the polypeptide chains when polypeptide is in excess. Once all the PEO chains are saturated, the aggregation of the complexes proceeds in a relatively slow rate compared to the aggregation before the PEO chains are saturated.

Introduction

In the papermaking industry, high molecular weight poly(ethylene oxide) (PEO) has been introduced successfully to improve filler retention.[1] However, the retention is only achieved in the presence of cofactors, which are the phenolic polymers capable of forming aqueous complexes with PEO.[2, 3] Common cofactors are kraft lignin[1], phenol formaldehyde resin[4], and poly(p-vinyl phenol).[5] It is accepted that the complex formation between PEO and a cofactor is necessary to cause effective filler retention.

Filler flocculation by PEO/cofactor is a rather complicated process.[6] During the flocculation, there are many possible interactions, such as PEO/cofactor complex formation, the adsorption of the PEO/cofactor complexes on the filler surface, and filler aggregation. A better understanding of the flocculation mechanism will promote a further development of the flocculation efficiency.

During the past two decades, the supermolecular structure of PEO/cofactor complexes has been studied by many researchers in order to gain insights about the flocculation mechanism. It was found that the complexes ranged from water soluble aggregates involving a few PEO molecules[7, 8] to macroscopic, visible precipitates[9, 10, 11]. Increasing PEO molecular weight may increase the PEO/cofactor complex size.[12] The complexes between PEO and some sulfonated kraft lignin adopted more extended structure than PEO.[13] On the other hand, the complexes between PEO and some phenol formaldehyde resins adopted more compact structure than PEO.[14]

However, many aspects of the PEO/cofactor complex formation mechanism still remain elusive. For example, it is not known whether the supermolecular structure of the PEO/cofactor complexes is a thermodynamically or kinetically controlled processes[15, 16] Furthermore, flocculation results suggest that PEO/cofactor complex structure is influenced by the hydrodynamic conditions under which the complexes are formed.[17] Thus, it is of interest to investigate the factors controlling the complex supermolecular structure. Our ultimate goal is to link complex structure to flocculation efficacy via the flocculation mechanism.

In this work, two tyrosine-containing polypeptides (TCP), poly(Glu, Tyr) (1:1) and poly(Glu, Ala, Tyr) (1:1:1), are used as model cofactors to study the supermolecular structures of the PEO/cofactor complexes. The two peptides have well-defined structures and are suitable for mechanistic study. From initial work we know that both peptides form aqueous complexes with PEO.[18]

PEO/cofactor flocculation is normally carried out in the presence of Ca^{2+} ions during the papermaking process because of the solubility of calcium carbonate. It has been shown that in some cases calcium ions may decrease the flocculation efficiency, and in other cases calcium ions may increase the flocculation efficiency.[19, 20, 21] Therefore, the experiments in this work were carried out in the presence of Ca^{2+} ions and the name

"TCP(Ca^{2+})" is used to represent tyrosine containing polypeptides dissolved in dilute (0.001 M) calcium chloride. The structures of PEO/TCP(Ca^{2+}) complexes were characterized by light scattering, viscometry, microscopy, and electrophoretic mobility apparatus. One of the most important results that emerged from this work was that the supermolecular structures of PEO/TCP(Ca^{2+}) complexes are controlled by kinetics. A kinetic mechanism is proposed to explain our results. The influence of complex supermolecular structure on flocculation will be discussed in a subsequent report.[21]

Experimental

Materials

PEO 309 (molecular weight (M)=8×10^6 Da), PEO 301 (M=4×10^6 Da), PEO N-12K (M=10^6 Da), PEO N-3000 (M=4×10^5 Da), and PEO N-10 (M=10^5 Da) were a gift from Union Carbide. Random copolymers L-poly(Glu, Tyr) (1:1) (PEY1) and L-poly(Glu, Tyr, Ala) (1:1:1) (PEYA) were purchased from Sigma. The viscosity-average molecular weights of PEY1 and PEYA are 36,100 Da and 40,000 Da respectively (provided by Sigma). PEO stock solutions were prepared by dissolving polymer (0.5 g/L) in water with slow end-to-end rotation for 24 hours. TCP stock solutions were prepared by dissolving peptides (1 g/L) in water under gentle shaking for 10 minutes. NaCl and $CaCl_2$ (BDH) were used without further purification. All the experiments were performed with water from a Millipore Milli-Q system fitted with one Super C carbon cartridge, two ion-exchange cartridges, and one Organex Q cartridge. .

Methods

Light Scattering

Dynamic light scattering was used to estimate the hydrodynamic diameters of PEO/TCP complexes. Measurements were made with a Lexel laser (wavelength 514 nm) equipped with a BI-9000 AT digital correlator (Brookhaven). The incident laser light power was 300 mw and the pinhole size of photo multiplier was 200. The correlation of the scattered light was measured at an angle of 90°. The hydrodynamic radii r_h of the highly scattering complexes in the presence of Ca^{2+} were calculated by the non-negatively constructed least-squares (regularized) method using software BI9000AT version 6.1, while the exponential method was used for the weakly scattering complexes prepared in the absence of Ca^{2+} and for pure PEO coils.

The molar masses of PEO/TCP complexes were estimated by intensity light scattering based on the count rate recorded at the 90°. The background light scattering was subtracted from all the measurements. Based on the Debye-Rayleigh light scattering theory[22], the apparent molar mass M_{app} of a polymer complex was given as

$$M_{app} = \frac{R_\theta}{P(\theta)Kc} \quad (1)$$

where R_θ, $P(\theta)$, K, and c are the Rayleigh ratio, the form factor, the optical constant, and the polymer solution concentration.[23] R_θ is defined as

$$R_\theta = \frac{i_s l^2}{I_0(1+\cos^2\theta)} \quad (2)$$

where i_s is the scattering intensity at a specific angle, l is the distance between the scattering centre and the detector, I_0 is the incident light intensity, and θ is the scattering angle. $P(\theta)$ is defined as

$$\frac{1}{P(\theta)} = 1 + \frac{1}{3}\overline{r_g^2}s^2 \quad (3)$$

where $\overline{r_g}$ is the radius of gyration, which can be estimated by the hydrodynamic radius determined from dynamic light scattering r_h. s is related to the laser wavelength λ and the scattering angle as

$$s = \frac{4\pi}{\lambda}\sin(\theta/2) \quad (4)$$

In this work, the $r_h^2 s^2$ values of all the complexes characterized are smaller than 1, within the valid range of Equation 3. The optical constant K is defined as

$$K = \frac{2\pi^2 n^2 (dn/dc)^2}{N_{av}\lambda^4} \quad (5)$$

where n is the refractive index of solvent water, dn/dc is the refractive index increment of the complex which can be estimated as

$$dn/dc = \frac{(dn/dc)_{PEO}c_{PEO} + (dn/dc)_{TCP}c_{TCP}}{c_{PEO} + c_{TCP}} \quad (6)$$

where c_{PEO} and c_{TCP} are the concentrations of PEO and TCP respectively. The refractive index increment of PEO $(dn/dc)_{PEO}$ was 0.145 mL/g[24] and the refractive index increment $(dn/dc)_{TCP}$ of PEY1 was 0.184 mL/g provided by Sigma.

Because the values of l and I_0 were un-known, the apparent molar masses of the complexes could not be determined directly. Thus, the complex molar masses $M_{complex}$ were calculated based on the known molecular weight of PEO N-12K (10^6 Da) M_{PEO} using equation (1)

$$\frac{M_{complex}}{M_{PEO}} = \frac{R_{\theta\,complex}}{P(\theta)_{complex} K_{complex} c_{complex}} \frac{P(\theta)_{PEO} K_{PEO} c_{PEO}}{R_{\theta\,PEO}} \quad (7)$$

The average coil densities of a complex was calculated as

$$\bar{\rho} = \frac{M_{complex}}{\frac{4}{3}\pi r_h^3 N_{av}} \quad (8)$$

where N_{av} is Avogadro's number.

In a typical light scattering experiment, 50 mg/mL TCP solution was first mixed with 0.001 M NaCl and 0.001 M $CaCl_2$ for 30 seconds. The stock PEO solution (0.5 g/L) was then added in one injection using a precision micro-pipette both under stirring and without stirring. The stirring was produced using a Fisher magnetic stirring bar (10 mm L×3 mm D) and a Fisher magnetic stirring plate (Thermix Stir model 120 MR). The RPM of the stirring plate was set to a scale of 3. When complex solutions were prepared without the stirring, they were let stand for 30 minutes before the simultaneous collections of complex size and light scattering intensity. When prepared under the stirring, complex solutions were first stirred for 15 minutes and then let stand for another 15 minutes before light scattering measurements were taken. It was believed that the stirring produced a higher intensity shearing rate. If necessary, NaCl concentration, $CaCl_2$ concentration, or the addition order of TCP and PEO was varied and will be specified in the following sections.

Optical Microscopy

A ZEISS Axioplan Universal microscope equipped with a QImaging Digital Camera was used to photograph PEO/TCP(Ca^{2+}) complexes. The sample was prepared by dropping PEO/TCP(Ca^{2+}) solution on a glass slide and covering it with a cover slip. Then, the sample was illuminated by a dark field light source.

Viscometry

The viscosities of PEO/PEY(Ca^{2+}) complexes were measured using a Stress Tech system (Reologica, Sweden) fitted with a concentric cylinder cup which had a total

volume of 16 mL. The viscosities were recorded as a function of time at constant shear rates at 25°C.

Electrophoretic Mobility

The electrophoretic mobilities of the PEO/TCP(Ca^{2+}) complexes were measured using Brookhaven ZetaPALS at 25°C. TCP solution was first mixed with 0.001 M $CaCl_2$ and 0.001 M NaCl. PEO N-12K (MW=10^6 Da) was then introduced without stirring and 2.5 hours were allowed for the complex solutions to mix entirely at room temperature. The reported mobility was the average of 10 cycles each consisting of 20 scans.

Results

This paper investigates the supermolecular structure of the complexes formed between high molecular weight PEO and two tyrosine containing polypeptides. PEY1 is a 1:1 random copolymer of glutamic acid and tyrosine with an average molecular weight of 36,100 Da. Previous work with isothermal titration calorimetry and capillary electrophoresis indicated that PEO is saturated with bound PEY1 when the mass ratio of PEO/PEY1 is 0.20 in the presence of calcium ions and 0.18 in the absence of calcium ions. PEYA is a 1:1:1 random terpolymer of glutamic acid , tyrosine and alanine with a molecular weight of 40,000 Da. The saturation ratio was 0.20 in the presence of calcium ions and 0.07 in the absence of calcium ions.[25]

Effect of PEO Molecular Weight

Figure 1 shows the hydrodynamic diameter of PEO N-12K (M=1 MDa) measured using dynamic light scattering. The PEO N-12K molecules had a bimodal size distribution with a large peak at around 80 nm and a small peak at around 660 nm. The presence of the peak at 660 nm was probably caused by the entanglement of the PEO chains as suggested by others.[26, 27] The light intensity average diameter was calculated to be 136 nm. For comparison, the hydrodynamic diameter of the PEO N-12K chains was also calculated to be 78 nm based on the equation proposed by Devanand et al.,

$$R_h = kM^{0.571} \quad (9)$$

where M is the molecular weight of PEO and k is 0.029 nm·$Da^{-0.571}$.[28] The radius calculated using the equation (9) is close to the experimental hydrodynamic radius of the well dissolved PEO chains as determined from dynamic light scattering.

Figure 1 also shows the distribution of the hydrodynamic diameters of PEO N-12K/PEY1 complexes. Like PEO alone, the complexes had a bimodal distribution with a large peak at around 70 nm and a small peak at around 580 nm. The average diameter of the complexes was 129 nm, which was slightly smaller than the value for PEO alone. According to the equation (7), the apparent molar mass of the PEO N-12K/PEY1

complexes was 1.4 MDa, which was lower than the total molar mass of two PEO N-12K chains. Thus, the PEO/PEY1 complexes appear to consist of individual PEO chains with many bound PEY1 molecules. We propose that the charge repulsion between the complexed peptides prevents the PEO chains from aggregating.

The presence of calcium resulted in mono-modal size distributions with highly scattering complexes. Figure 2-a shows the intensity average diameters of the complexes prepared in the presence of calcium ions. The PEO/PEY1 mass ratios were chosen to be 0.5 and 0.05, which corresponded to PEO in excess and PEY1(Ca^{2+}) in excess respectively. At the ratio of 0.5, the complex solutions were prepared both with and without stirring. At the ratio of 0.05, the complex solutions were prepared only without stirring. In general, the complex diameter increased with the increase of the PEO MW. At the same time, the complex diameter was sensitive to the level of shearing. At the PEO/PEY1 ratio of 0.5, the presence of the stirring decreased the complex diameter. An obvious explanation is that hydrodynamic forces tear apart the complexes. However, when the complexes prepared without stirring were stirred for five more minutes, their sizes and light scattering intensities remained unchanged. This suggests that the complexes were not fractured in the modest flows used in these experiments.

The apparent molar masses of the PEO/PEY1(Ca^{2+}) complexes were calculated from the light scattering intensities using the Debye-Rayleigh scattering theory (equation 7). Figure 2-b summarizes the effect of the PEO molecular weight on the complex molar mass. Increasing the PEO molecular weight increased the complex molar mass irrespective of the mixing methods or the PEO/PEY1 ratio. Meanwhile, the complexes mixed without stirring had higher molar masses than the complexes mixed with stirring. Moreover, the presence of stirring produced larger differences in the complex molar masses at the higher PEO molecular weights. Specifically, the PEO N-10 (M=100 kDa) chains produced complexes with a molar mass of 4.9 MDa without stirring and 4.5 MDa with stirring. In contrast, the PEO N-12K (M=1 MDa) chains produced complexes of 16 MDa without stirring and 10 MDa with stirring.

Because both the diameters and the apparent molar masses of the PEO/PEY1(Ca^{2+}) complexes were known, the average complex densities were calculated assuming the complexes were spherical. Figure 2-c shows the complex coil densities as a function of the PEO molecular weight. The complex coil densities decreased with the increase of the PEO molecular weight irrespective of the mixing methods and the PEO/PEY1 ratio. The complexes of the highest density corresponded to a PEO molecular weight of 100 kDa and the water content of these complexes was as low as 60%. The complexes mixed under the stirring had a higher coil densities than the complexes mixed without the stirring. Figure 2-c also shows the average coil densities of the uncomplexed PEO chains, which were calculated using the radius calculated from equation 11. The coil density of a PEO chain was about an order of magnitude lower than the coil density of the complexes. For instance, the coil density of PEO N-12K was

6.9 kg/m^3 and the coil density of the PEO N-12K/PEY1(Ca^{2+}) complexes prepared with stirring was 97 kg/m^2.

In summary, the dynamic and static light scattering results showed that the size of the PEO/PEY1(Ca^{2+}) complexes increased with the PEO molecular weight whereas the density decreased. Also, stirring during complex formation caused a decrease of the complex size and molar mass and an increase of the complex density.

Dynamic light scattering is normally suitable for the size determination of the colloidal particles less than 1 μm; However, the PEO/PEY1(Ca^{2+}) complexes were much larger than 1 μm when PEO molecular weights were above 2 MDa. As a result, visual light microscopy and viscometry were used to characterize large complexes. Figure 3 shows the microscopic image of the large aggregates withdrawn from the PEO N-60 (M=4 MDa)/PEY1(Ca^{2+}) complex solution, which was prepared with stirring. Some of the aggregates had the dimensions larger than 2 mm.

Lindström and coworkers were the first to report qualitative observations that viscosity increases with PEO/cofactor complex formation.[10] Later, Xiao et al. measured the viscosity increase when aqueous PEO 309 (M=8 MDa) was mixed with a phenol formaldehyde resin.[6] Before presenting new results it is instructive to consider the possible consequences of complex formation. In most cases, the chain length of the peptide is much lower than that of the PEO. Thus the peptides may be considered to be coupling or crosslinking agents for the long PEO chains. If a polypeptide couples two different PEO chains, the viscosity will increase, reflecting the increase of effective molecular weight.[29] On the other hand, crosslinking within an individual PEO coil will lower the permeability of the coil and will also contribute to coil shrinkage or collapse, both of which will lower viscosity.[30]

Figure 4 shows the viscosity of the PEO 309 (MW=8 MDa)/PEY1(Ca^{2+}) complex solution as a function of time. In this experiment, the PEY1(Ca^{2+}) solution of 31.2 mg/L was first sheared at 500 s^{-1}. Then, the concentrated PEO 309 solution (0.5 g/L) was added to the PEY1(Ca^{2+}) solution in one injection to give a final PEO concentration of 15.6 mg/L. The addition of the PEO solution increased the viscosity of the PEY1(Ca^{2+}) solution from 2.8 mPa·s to 4.5 mPa·s in 35 seconds. After which, the viscosity decreased slowly to 3.0 mPa·s. At the end of the measurements, some macroscopic elastic polymeric hydrogels larger than 5 mm were found on the wall of the viscometer. The results in Figure 4 suggest that two processes are operative. Initially, the peptide couples multiple PEO chains to increase viscosity; whereas, with time and stirring, the intra-chain crosslinking by bound polypeptide causes the complex to collapse.

Figure 4 also shows the viscosity change during the mixing of PEO 309 and PEY1 in the absence of calcium ions. The PEO 309 solution of 62.5 mg/L was first sheared at 175s^{-1}. The concentrated PEY1 solution (1 g/L) was then added to the PEO solution in one injection to give a final PEY1 concentration of 31.2 mg/L. The addition

of the PEY1 solution increased the viscosity of the PEO 309 solution from 2.0 mPa·s to 2.7 mPa·s in 22 seconds. Afterwards, the viscosity decreased to 2.3 mPa·s gradually. However, no macroscopic hydrogel formation was observed at the end of the measurements. We have shown that there was no aggregation between the PEO N-12K/PEY1 complexes in the absence of calcium ions (Figure 1) due to the charge repulsion between the PEY1 chains. It was possible that the PEO 309/PEY1 complexes aggregated slightly. However, the aggregated complexes were not stable and broke apart with time and shearing. Thus, the viscosity decreased after the initial increase and no macroscopic hydrogel was observed.

Previous results from isothermal titration calorimetry has shown that low molecular weight PEO N-10 (M=100 kDa) forms complexes with with PEY1(Ca^{2+}).[25] However, the complex formation from dilute solutions of PEO N-10 does not give measurable increases in viscosity. Figure 5 shows viscosity versus time curves for complexes made by mixing PEY1(Ca^{2+}) with mixtures of low (N-10) and high (309) molecular weight PEO. In this experiment, PEY1(Ca^{2+}), PEO 309 and PEO N-10 were first added into the viscometer. Then the complex solutions were sheared under 175 s^{-1} and the resulted viscosities were recorded. When the PEO 309 concentration and the PEY1(Ca^{2+}) concentration were fixed at 125 mg/L and 62.5 mg/L respectively, the increase of the PEO N-10 concentration decreased the maximum viscosity of the complex solution at the initial mixing stage. When the PEO N-10 concentration was increased to 187.5 mg/L, the complex solution showed no initial viscosity increase. It was clear that the presence of the low molecular weight (100 kDa) PEO chains could quench the initial viscosity increase during the mixing of PEY1(Ca^{2+}) and PEO 309.

van de Ven et al. found that the history of the PEO solution affects the filler flocculation efficiency by PEO/cofactor. They proposed that poorly-dissolved PEO solutions contain aggregates of entangled PEO chains which are more effective flocculants than the well-dissolved PEO chains.[31] As shown in Figure 6, three experiments were carried out to determine the influence of PEO 309 solution history on complex viscosity. In all three experiments, the PEO solution was first sheared at 175 s^{-1}. Then, the PEY1(Ca^{2+}) solution was added in one injection. In the first and the second experiments, the PEO solutions were pre-sheared under 600 s^{-1} and 400 s^{-1} for 650 seconds. In the third experiment, the viscosity was measured directly without pre-shearing the PEO solution. The results presented here indicate that increasing the shear rate used to pre-shear the PEO solution decreased the maximum viscosity during the initial mixing stage.

Effect of PEO/TCP Ratio

It has long been found that the PEO/cofactor ratio affects the filler flocculation significantly and that the best flocculation is normally obtained at an intermediate mass ratio of around 0.5.[6] Thus, it was of our interest to know how the PEO/PEY1 ratio affected the supermolecular structure of the PEO/PEY1(Ca^{2+}) complexes.

Figure 7 presents the light scattering intensities of the PEO N-12K (M=1 MDa)/PEY1($CaCl_2$) complex solutions as a function of time at two different PEO/PEY1 ratios. Because the light scattering intensity was directly related to the molar mass of the complex aggregates, Figure 7 reflects the kinetics of the complex aggregation. When the PEO/PEY1 ratio was 0.5, with PEO in excess, the complexes underwent a one-step aggregation. The light scattering intensity showed a fast initial increase and flattened out 50 seconds after the mixing of two components. When the PEO/PEY1 ratio was 0.05, with PEY1(Ca^{2+}) in excess, the complexes underwent a two-step aggregation. The light scattering intensity increased from 14 to 239 kcnts/s for the first 55 seconds. Then the light scattering intensity increased slowly from 239 to 392 kcnts/s for the next 20 minutes.

Figure 8 shows the hydrodynamic diameters, the apparent molar masses, and the average coil densities of the PEO N-12K/PEY1(Ca^{2+}) complexes as a function of the PEO/PEY1 mass ratio. It is important to note again that the mixing methods influenced the supermolecular structure. The stirring during the mixing of two components changed the size, the molar mass, and the coil density of the complexes at all the PEO/PEY1 ratios. It is clear that the complex structure was controlled by the mixing kinetics.

The complexes had the largest size at the intermediate PEO/PEY1 ratio. When the complexes were prepared without stirring, the largest diameter was 129 nm at a PEO/PEY1 ratio of 0.25. When the complexes were prepared with stirring, the largest diameter was 80 nm at a PEO/PEY1 ratio of 0.05. The highest molar mass of the complexes was also obtained at the intermediate PEO/PEY1 ratio. Without stirring, the complexes had a maximum molar mass of 38 MDa at a PEO/PEY1 ratio of 0.25. With stirring, the complexes had a maximum molar mass of 20 MDa at a PEO/PEY1 ratio of 0.05. Finally, the highest coil density was also obtained at the intermediate PEO/PEY1 ratio. When the ratio was too low, the complex possessed a high charge density which prevented the complex from collapsing. When the ratio was too high, there were not enough PEY1(Ca^{2+}) molecules which functioned as the cross-linkers to collapse the complexes.

We have shown that PEO 309 (MW=8 MDa) and PEY1(Ca^{2+}) formed macroscopic hydrogels, which could be characterized by viscometry. Figure 9 shows the ratio effect on the structure of the PEO 309/PEY1(Ca^{2+}) complexes. PEO 309 and $CaCl_2$ were first added into the viscometer and sheared at 175 s^{-1}. Then, the concentrated PEY1(Ca^{2+}) solution (1 g/L) was added to the PEO solution in one injection. In all the cases, the solution viscosity showed an initial maximum. At the same time, the highest viscosity maximum was obtained at an intermediate PEO/PEY1 mass ratio of 0.5.

It was shown in our previous report that the tri-polypeptide PEYA could form complexes with PEO without causing filler flocculation.[18] To explain the flocculation results, we used light scattering to characterize the PEO N-12K/PEYA(Ca^{2+}) complexes at different PEO/PEYA ratios and the results are shown in Figure 10. The

PEO/PEYA(Ca^{2+}) complexes were prepared with stirring. The largest PEO/PEYA(Ca^{2+}) complexes were obtained at an intermediate PEO/PEYA ratio of 0.25. Because only a fraction of PEYA(Ca^{2+}) molecules could bind to PEO N-12K[32], the fraction of the PEYA molecules in the complexes and the refractive index increment of the complexes could not be calculated exactly. Thus, the apparent molar mass of the complexes could not be derived using equation (7). The light scattering intensities of the complexes were plotted directly against the PEO/PEYA ratio as light scattering intensity was roughly proportional to complex aggregation level. As can be seen, the highest scattering intensity was observed at the PEO/PEYA ratio of 0.25. For comparison, Figure 10 also shows the light scattering intensities of the PEO N-12K/PEY1(Ca^{2+}) complexes. At all the PEO/TCP ratios, the light scattering intensities of the PEO/PEY1(Ca^{2+}) complexes were more than twice as high as the light scattering intensities of the PEO/PEYA(Ca^{2+}) complexes. At the ratio of 0.1, for instance, the light scattering intensity of the PEO/PEY1(Ca^{2+}) complexes was 389 kcnts/s and the light scattering intensity of the PEO/PEYA(Ca^{2+}) complexes was only 125 kcnts/s. It is clear that the PEO N-12K/PEYA(Ca^{2+}) complexes had a lower aggregation level than the PEO N-12K/PEY1(Ca^{2+}) complexes.

Figure 11 shows how the PEO/TCP ratio affected the electrophoretic mobility of the PEO N-12K/TCP(Ca^{2+}) complexes. According to the Ohshima's derivation, the electrophoretic mobility of a charged complex is directly proportional to the volume charge density of the complex.[33] The mobility of the PEO/PEY1(Ca^{2+}) complexes increased exclusively from -1.32 to -0.14 (μm/s)/(V/cm) when the PEO/PEY1 ratio was increased from 0.05 to 1. Thus, increasing the PEO/PEY1 ratio decreased the volume charge density of the complex. In contrast, the mobility of the PEO/PEYA(Ca^{2+}) complexes showed a minimum of -0.90 (μm/s)/(V/cm) at a PEO/PEYA ratio of 0.1.

Effects of NaCl Concentration and Addition Order

Sodium ions are present in the papermaking process and the PEO/cofactor flocculation was often found to be sensitive to NaCl concentration.[34] In our following report we will show that the flocculation of precipitated calcium carbonate by PEO/TCP depended on NaCl concentration.[21] Figure 12 shows the effect of NaCl concentration on the structure of the PEO N-12K/PEY1(Ca^{2+}) complexes. In this experiment, $CaCl_2$ and NaCl were first added to a 50 mg/L PEY1 solution and the resulting solution was stirred for 30 seconds. The NaCl concentration was varied from 0.001 M to 0.12 M. Then, the concentrated PEO solution (0.5 g/L) was added in one injection. The apparent molar mass of the complexes decreased from 11 MDa to 5.8 MDa when the NaCl concentration was increased from 0.001 M to 0.06 M. Further increasing the NaCl concentration to 0.12 M increased the molar mass slightly to 6.9 MDa. At the same time, the hydrodynamic diameters of the complexes remained at around 75 nm irrespective of the NaCl concentration.

To further elucidate the complex aggregation mechanism, the PEO N-12K/PEY1(Ca^{2+}) complexes were prepared using two different addition orders of PEY1, $CaCl_2$, and PEO. One was prepared using the normal order, in which PEY1 was first mixed with $CaCl_2$ and then PEO was added. In the other, PEO and PEY1 were premixed and then $CaCl_2$ was added. As shown in Table 1, the complexes prepared by the normal addition order had a larger size and a higher molar mass than complexes prepared with the second addition order. This experiment further confirms that the PEO/TCP(Ca^{2+}) complex structure was controlled by the mixing kinetics.

Discussion

Proposed Mechanism of Complex Aggregation

High molecular weight PEO and some water soluble tyrosine-containing polypeptides (TCP) form aqueous complexes which can flocculate many colloidal particles, such as precipitated calcium carbonate.[18] The flocculation is a complicated process because many interactions are possible. To understand the mechanism behind the flocculation, the mechanism of the complex formation between PEO and TCP are explored in this paper. Because free Ca^{2+} ions are often present during the flocculation process, most of the characterizations of the complexes are carried out in the presence of 0.001 M $CaCl_2$.

One of the most important observations is that the structure of the PEO/TCP(Ca^{2+}) complexes is controlled kinetically. We have shown that changing the mixing method changed the structure of the complexes. Specifically, both the mixing order and the degree of the shearing during the mixing changed the aggregation level of the complexes. Meanwhile, the aggregation level of the PEO/TCP(Ca^{2+}) complexes was also influenced by many other variables, such as the molecular weight of PEO, the mass ratio of PEO/TCP, and the NaCl concentration.

We propose that the major features of PEO/TCP(Ca^{2+}) complex formation and evolution can be explained by three processes schematically illustrated in Figure 13. In the first process, labeled *complex aggregation*, the attached TCP(Ca^{2+}) chains function as bridges to couple the PEO chains, resulting in complex molar masses that are more than ten times higher than the molar masses of the individual PEO chains (see Figure 2) . The resulting aggregates also have a much higher density than the parent PEO coils (see Figure 2). Furthermore, the densification or collapse occurs with time, as evidenced by a decrease in viscosity (Figure 4).

The second process schematically illustrated in Figure 13 is called *TCP(Ca^{2+}) deactivation* – this is a new concept which we have invoked to explain our results. It is proposed that the TCP(Ca^{2+}) chains bound to the first PEO chain rearrange so that the polypeptide is no longer able to bind to the second PEO molecule. The deactivation is caused by the encapsulation of all the active phenolic groups by the first PEO chain. The active phenolic groups are defined as those phenolic groups that can bind to PEO. It was

proposed in our previous report that the affinity between PEO and the phenolic goups depends on TCP microstructure and a block must have at least four tyrosine groups in order to bind to PEO. The evidence for deactivation includes the colloidal complex size prepared using excess low molecular weight PEO (MW≤1 MDa). Without the deactivation process the complex size would have grown infinitely until all the polymers were consumed.

The third process shown in Figure 13is called *PEO saturation,* which occurs when TCP(Ca^{2+}) is in excess. Once all the PEO chains were saturated, PEY1(Ca^{2+}) could not couple different PEO chains. It might be expected that the bound charged groups would stabilize peptide-saturated PEO; however, the results in Figure 7 show that the polypeptide-rich complexes slowly aggregate. In the following paragraphs, the major observations are rationalized in terms of the three proposed processes.

Rationalization of Experimental Observations

Effect of PEO/TCP Ratio

The interplay of the three processes in Figure 13 can be illustrated by considering the effect of PEO/TCP ratio. When PEO is in excess, the aggregation of the complexes is competing with the deactivation of the TCP(Ca^{2+}) chains by PEO. The aggregation can proceed until all the TCP(Ca^{2+}) chains are deactivated. Increasing the ratio of PEO/TCP increases the probability of deactivation, leading to a decreased molar mass of the complexes. This effect was also reflected in the rheological behavior of the PEO 309/PEY1(Ca^{2+}) complexes; increasing the PEO/PEY1 ratio decreases the amplitude of the viscosity maximum (see Figure 9). On the other hand, when PEO is added to an excess of TCP(Ca^{2+}), there will be some rapid initial complex aggregation, however, PEO saturation will limit coupling of PEO chains. The corresponding kinetic behavior is shown in Figure 7, which suggests a rapid initial complex aggregation followed by a slow aggregation of polypeptide saturated complexes.

Effect of PEO Molecular Weight

According to the Rouse model, the characteristic relaxation time of a single flexible chain in a solvent is proportional to the square of chain length.[35] It seems reasonable to propose that the rate of a PEO coil folding in deactivations also decreases with PEO chain length. As a result, the complex aggregation level increases with the PEO molecular weight.

In addition, the PEO 309 (MW=8 MDa) stock solution was prepared by gentle end-to-end rotation for 24 hours. It was possible that the PEO 309 solution contained entangled PEO aggregates. The entanglements can further decrease the encapsulation rate. Therefore, the PEO 309/PEY1(Ca^{2+}) complexes could aggregate to form a polymeric network, which in turn increased the solution viscosity dramatically. When

the PEO 309 solution was pre-sheared at 600 s^{-1} for 650 seconds, the entanglements broken down to the individual polymer chains. Thus, the solution viscosity increased to a smaller maximum.

Effect of Shear Rate

The results summarized in Figure 8 show that smaller complexes with a lower molecular weight were formed in the presence of higher intensity mixing. We propose that the smaller complexes observed with increased mixing intensity actually reflects an increase in the rate of deactivation. One could imagine that flow induced motions of the large PEO coils would enhance the rate of polypeptide encapsulation.

Effect of Salt Concentration

The presence of calcium ions increases the size, the molar mass and the density of the complexes. Although PEY1 binds to PEO in the absence of calcium ions, there is no evidence for complex aggregation. It is possible that the strong electrostatic repulsion between the PEY1 chains prevents the PEO/PEY1 complexes from aggregating. When the Ca^{2+} ions are added to the PEY1 solution, around 60% of the carboxyl groups on the PEY1 chains bind with the Ca^{2+} ions.[32] Therefore, the charge repulsion is decreased, allowing the PEO/PEY1(Ca) complexes to aggregate.

Increasing NaCl concentration from 0.001 M to 0.06 M lowered the aggregation level of the PEO/PEY1(Ca^{2+}) complexes (see Figure 12). The exact mechanism is unknown. We speculate that the increase of Na^{+} concentration may interfere with the binding between PEO and PEY1(Ca^{2+}), resulting in a increased deactivation rate of the PEY1(Ca^{2+}) molecules.

Effect of Addition Order

The size, the molar mass, and the density of the complexes depended on the addition order of PEY1, PEO and $CaCl_2$. Table 1 shows the complexes prepared by the two addition orders. In the normal order, PEY1 was first mixed with $CaCl_2$ and then PEO was added. In the changed order, PEY1 and PEO were first mixed and then $CaCl_2$ was added. It is clear that the complexes prepared by the normal order aggregated to a higher molar mass than the complexes prepared by the changed order.

The addition order effect can be explained by the deactivation of PEY1 by PEO in the absence of calcium. When PEO is first mixed with PEY1, many active phenolic groups will be encapsulated by PEO without causing any aggregation. It was shown in our previous report that more phenolic groups on PEY1(Ca^{2+}) can bind to PEO since the association between PEY1 and calcium led the polypeptide to fold into a microstructure favorable to the binding. Thus, when calcium is added to the PEO/PEY1 complexes, some inactive phenolic groups become active, causing the complexes to aggregate.

However, the aggregation proceeds to a lower molar mass, because less active phenolic groups are available to couple the complexes.

Effect of TCP Structure

The PEO N-12K/PEY1(Ca^{2+}) complexes were larger, denser and had a higher molecular weight than the PEO N-12K/PEYA(Ca^{2+}) complexes when the two complexes were prepared under the same conditions. It was shown in our previous work that a PEY1(Ca^{2+}) chain had more active phenolic groups than a PEYA(Ca^{2+}) chain. Thus, longer time is expected to deactivate a PEY1(Ca^{2+}) chain than a PEYA(Ca^{2+}) chain. As a result, PEO/PEY1(Ca^{2+}) complexes can aggregate to a higher molecular weight with a denser structure.

Conclusions

1. PEY1 and PEO form aqueous complexes, and in the absence of calcium ions there is no aggregation of the individual PEO chains decorated with the PEY1 chains. In the presence of calcium ions, the complexes consist of aggregates containing multiple PEO and PEY1 molecules.

2. The structures of the aqueous PEO/TCP(Ca^{2+}) complexes are kinetically controlled and depend upon the balance of complex aggregation, deactivation and saturation (see Figure 13 for definitions).

3. It is proposed that deactivation - a process by which a polypeptide attached to PEO rearranges so that it is no longer able to couple to another PEO molecule or cluster - explains some of the most important features of the PEO/cofactor complexes including:

a) Lower molecular weight PEO leads to a lower complex molar mass because the deactivation rate is too fast to permit the development of large complexes.

b) Complex size and molecular weight decreases with mixing intensity during complex formation because shear forces enhance deactivation.

c) The presence of lower molecular weight PEO inhibits the formation of large complexes with high molecular weight PEO (Figure 5). The reason low molecular weight PEO interferes is that the polypeptide bound to it is rapidly deactivated and cannot participate in complex formation.

d) Increasing PEO/TCP ratio can decrease the complex molar mass because increasing PEO/TCP ratio increases the probability of the TCP deactivation by PEO.

Table 1. The effect of addition order on the structures of the PEO/PEY1(Ca^{2+}) complexes mixed under stirring. [PEO N-12K]=25 mg/L, [PEY1]=50 mg/L, [NaCl]=0.001 M, [$CaCl_2$]=0.001 M, T=25°C.

Addition order	NaCl→PEY1→$CaCl_2$→PEO	NaCl→PEY1→PEO→$CaCl_2$
Complex hydrodynamic diameter (nm)	100	59
Complex light scattering intensity (kcnts/s)	473	159
Complex apparent molar mass (MDa)	16	6.7
Complex coil density (kg/m^3)	49	103

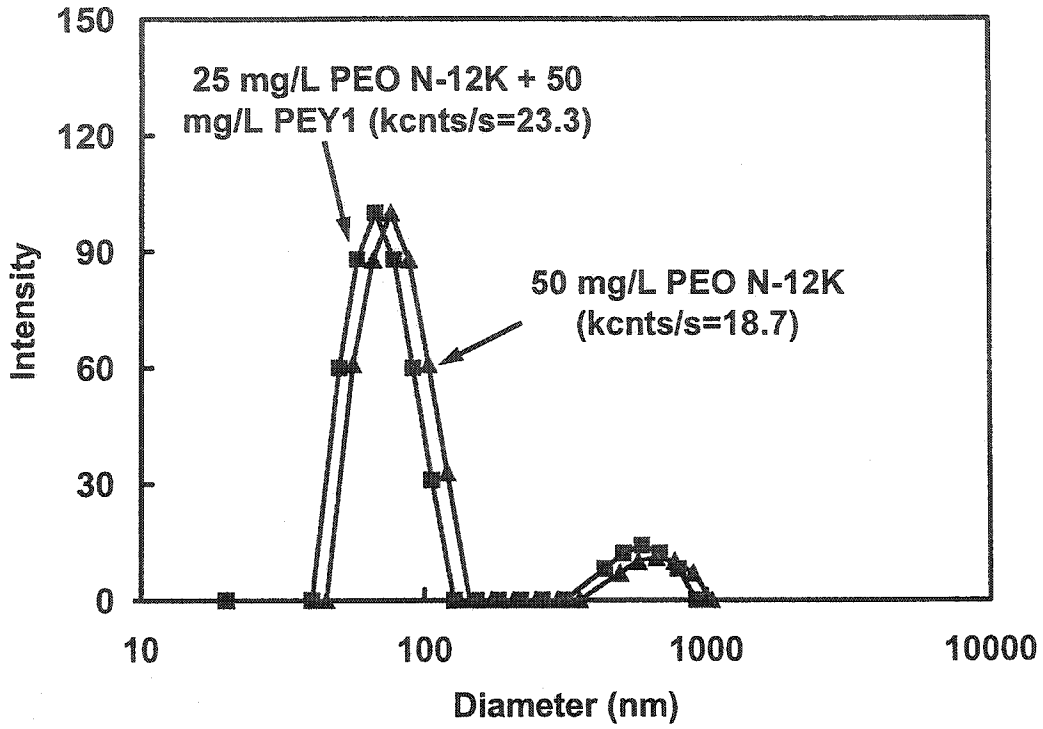

Figure 1. The hydrodynamic diameters of PEO N-12K and PEO N-12K/PEY1 measured by dynamic light scattering. T=25°C.

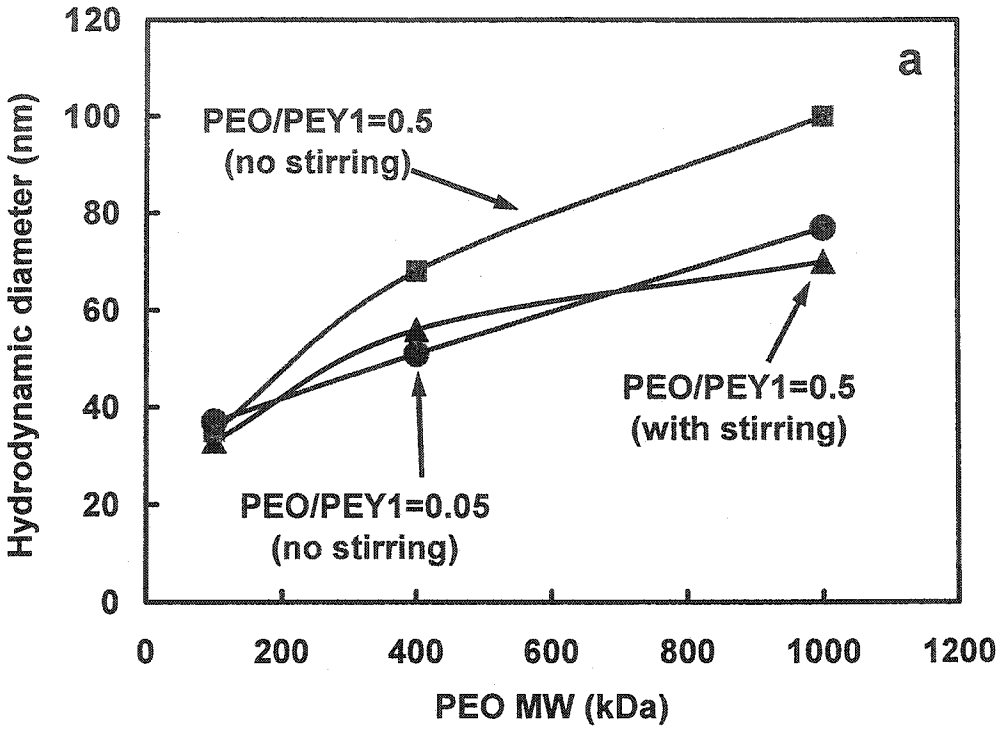
a
Hydrodynamic diameter (nm)
120
100
80
60
40
20
0
PEO/PEY1=0.5
(no stirring)
PEO/PEY1=0.5
(with stirring)
PEO/PEY1=0.05
(no stirring)
0
200
400
600
800
1000
1200
PEO MW (kDa)

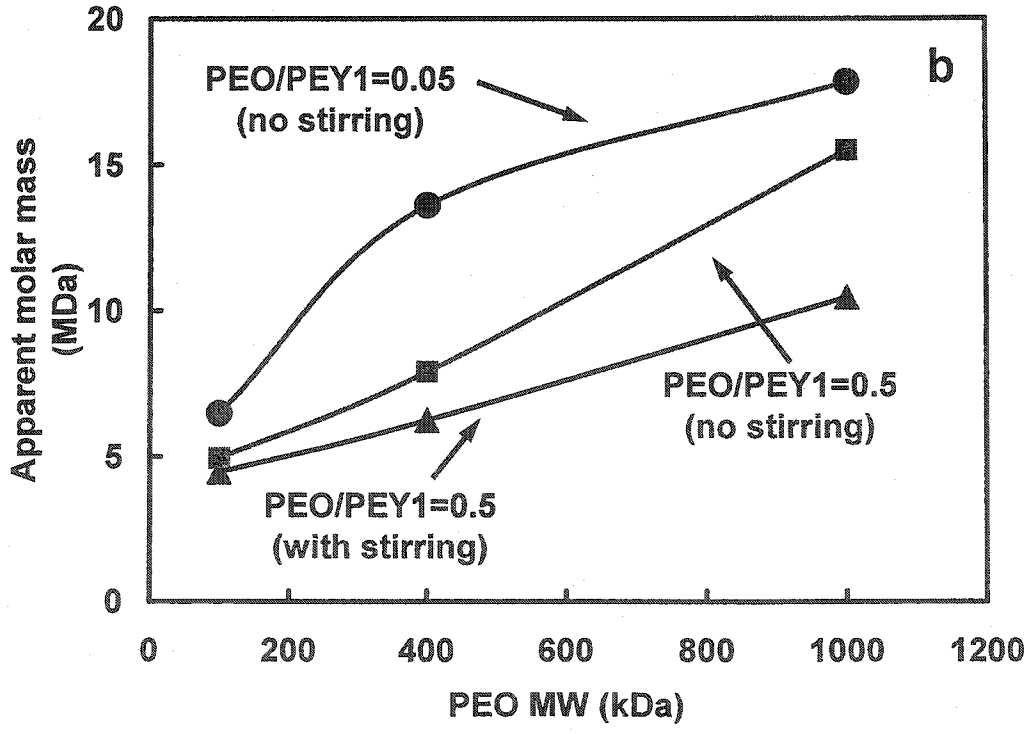
b
Apparent molar mass (MDa)
20
15
10
5
0
PEO/PEY1=0.05
(no stirring)
PEO/PEY1=0.5
(no stirring)
PEO/PEY1=0.5
(with stirring)
0
200
400
600
800
1000
1200
PEO MW (kDa)

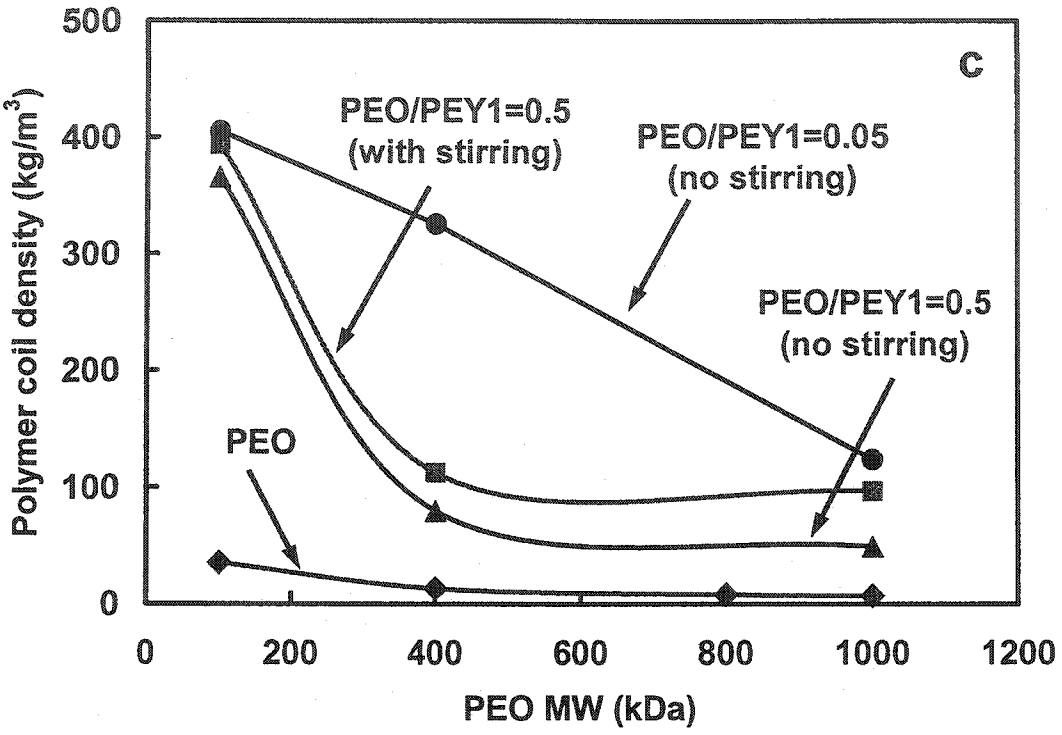

Figure 2. The average hydrodynamic diameter, the apparent molar mass, and the density of PEO/PEY1(Ca^{2+}) complexes as a function of PEO molecular weight. [PEY1]=50 mg/L, [NaCl]=0.001 M, [$CaCl_2$]=0.001 M, T=25°C. PEY1 was first mixed with NaCl and $CaCl_2$. The PEO solution (0.5 g/L) was then added in one injection.

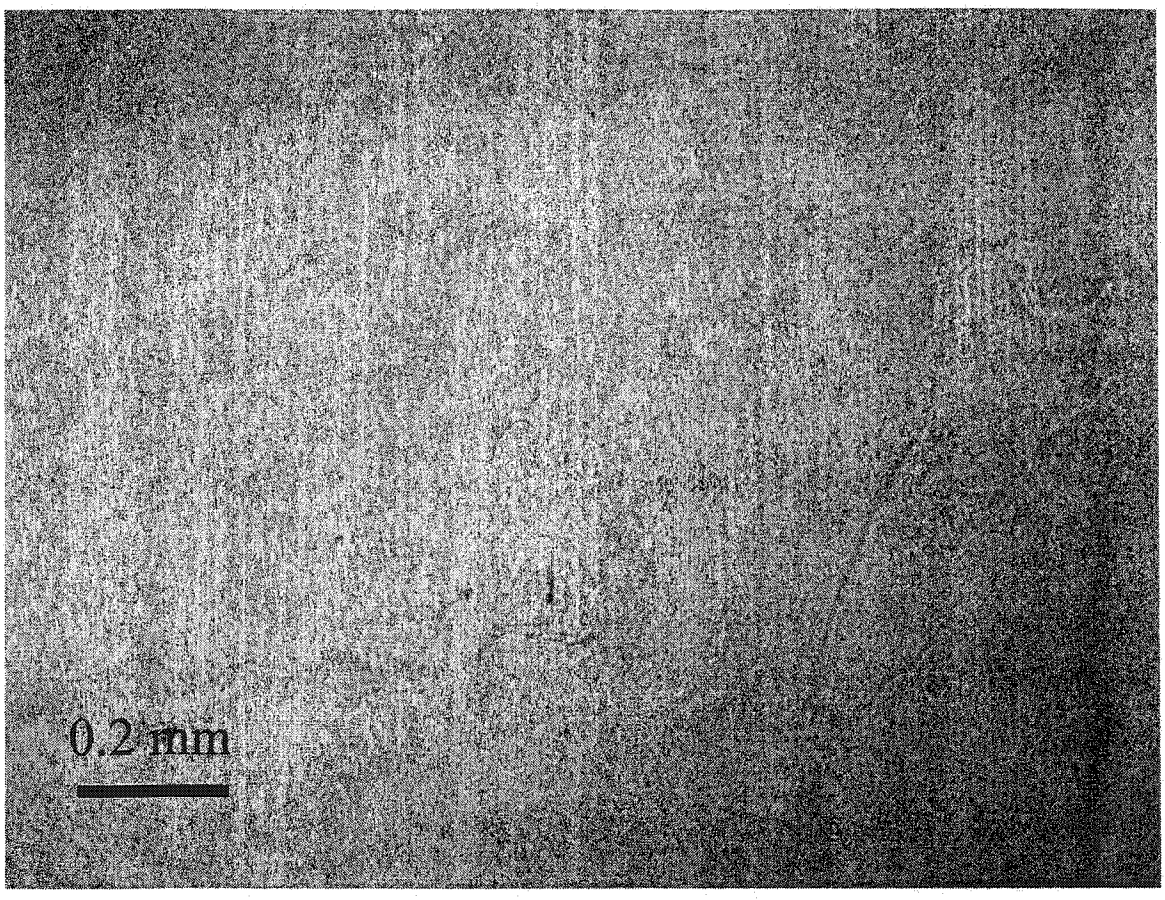

Figure 3. The microscopic image of PEO 301/PEY1(Ca^{2+}) complexes. [PEO 301]=25 mg/L, [PEY1]=50 mg/L, [$CaCl_2$]=0.001 M, [NaCl]=0.001 M, T=25°C. PEY1 was first mixed with NaCl and $CaCl_2$. The PEO solution (0.5 g/L) was then added in one injection under stirring.

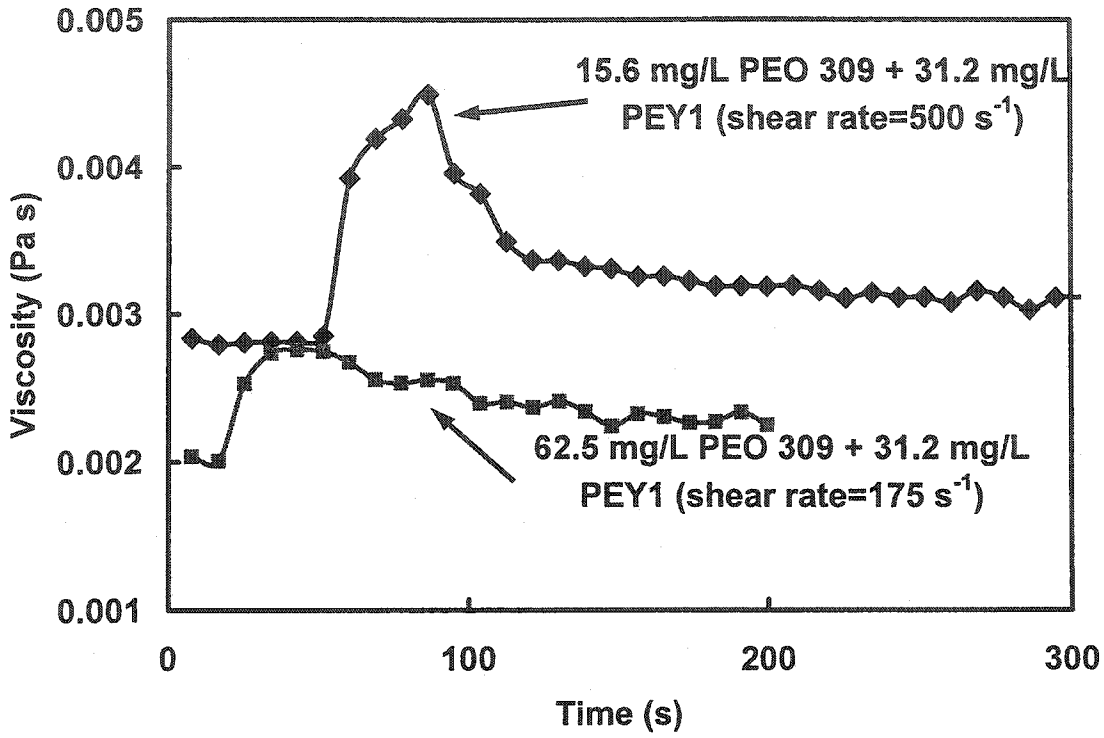

Figure 4. The viscosities of the PEO 309/PEY1(Ca^{2+}) solution and the PEO 309/PEY1 solution as a function of time. T=25°C, [NaCl]=0.001 M. In the absence of $CaCl_2$, the PEY1 solution (1 g/L) was introduced to the PEO 309 solution in one injection 20 seconds after the shearing (175 s^{-1}) was started. In the presence of 0.001 M $CaCl_2$, the PEO 309 solution (0.5 g/L) was introduced to the PEY1(Ca^{2+}) solution in one injection 50 seconds after the shearing (500 s^{-1}) was started.

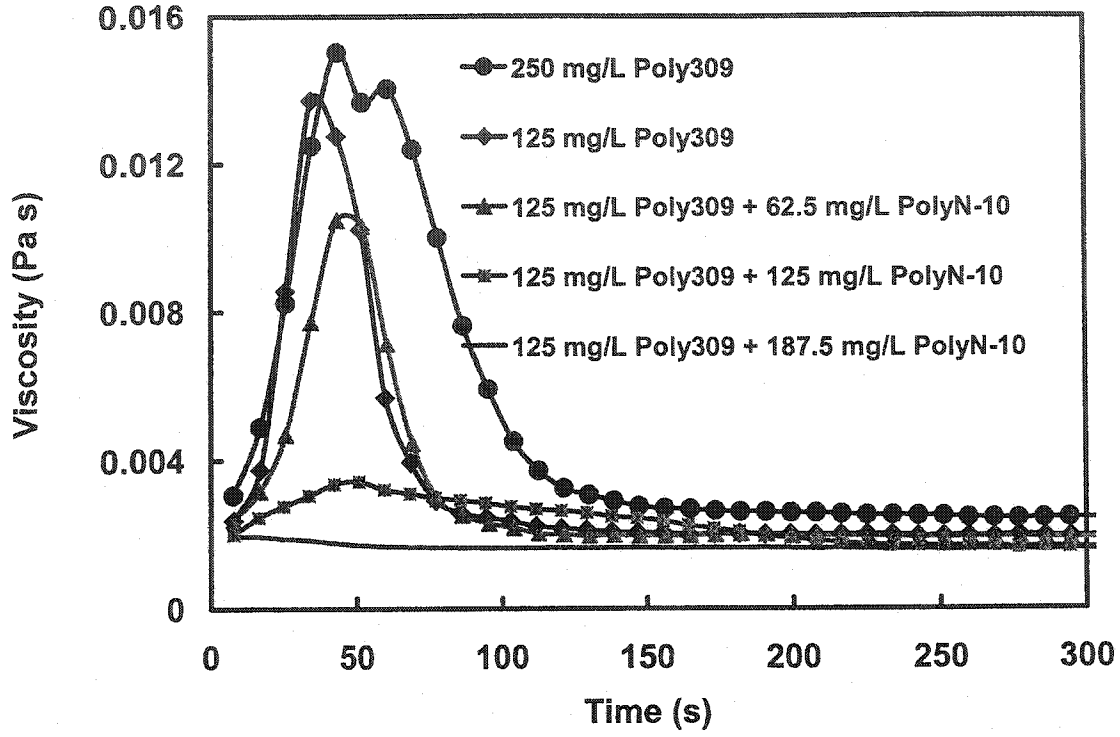

Figure 5. The viscosities of the PEO/PEY1(Ca^{2+}) solutions as a function of time. [PEY1]=62.5 mg/L, [NaCl]=0.001 M, [$CaCl_2$]=0.001 M, T=25°C, shear rate=175 s^{-1}. PEY1, NaCl, $CaCl_2$, and PEO were introduced into the viscometer first, and then the shearing was started.

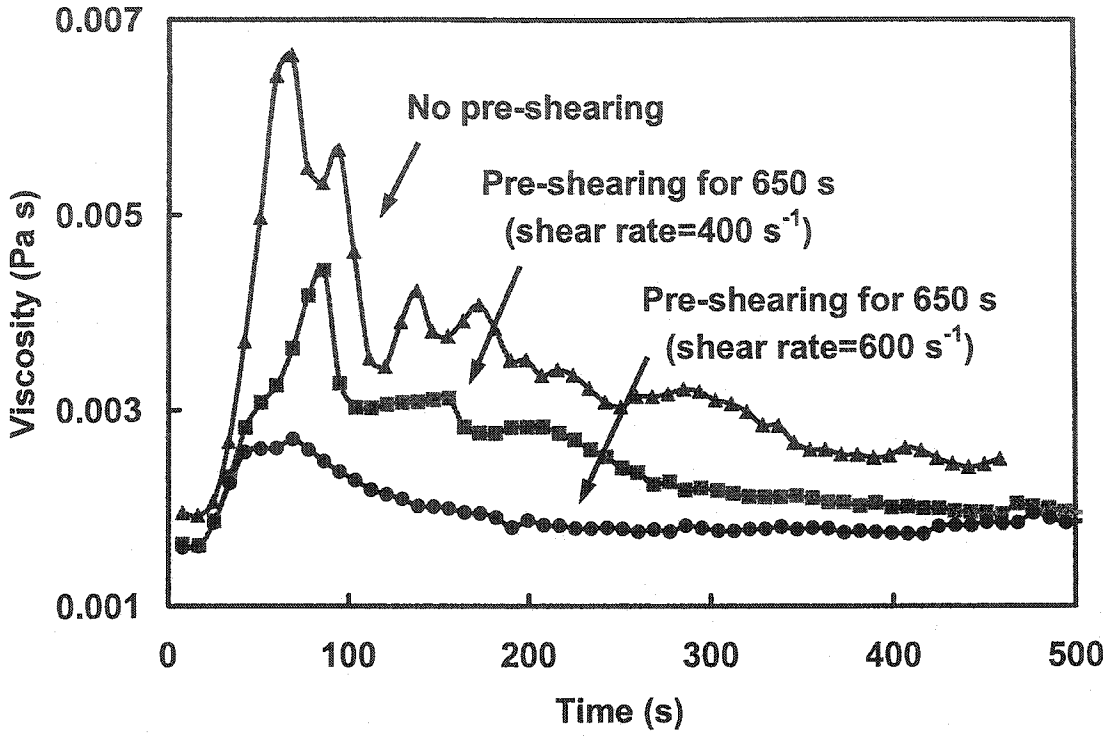

Figure 6. The viscosities of the PEO 309/PEY1(Ca^{2+}) solutions as a function of time. [PEO 309]=62.5 mg/L, PEY1(Ca^{2+})=31.2 mg/L, [NaCl]=0.001 M, [$CaCl_2$]=0.001 M, T=25°C, shear rate=175 s^{-1}. PEO was mixed with NaCl and $CaCl_2$. PEO solutions were then pre-sheared under various shear rates. Finally, the PEY1 solution (1 g/L) was introduced in one injection 20 seconds after the shearing (175 s^{-1}) was started.

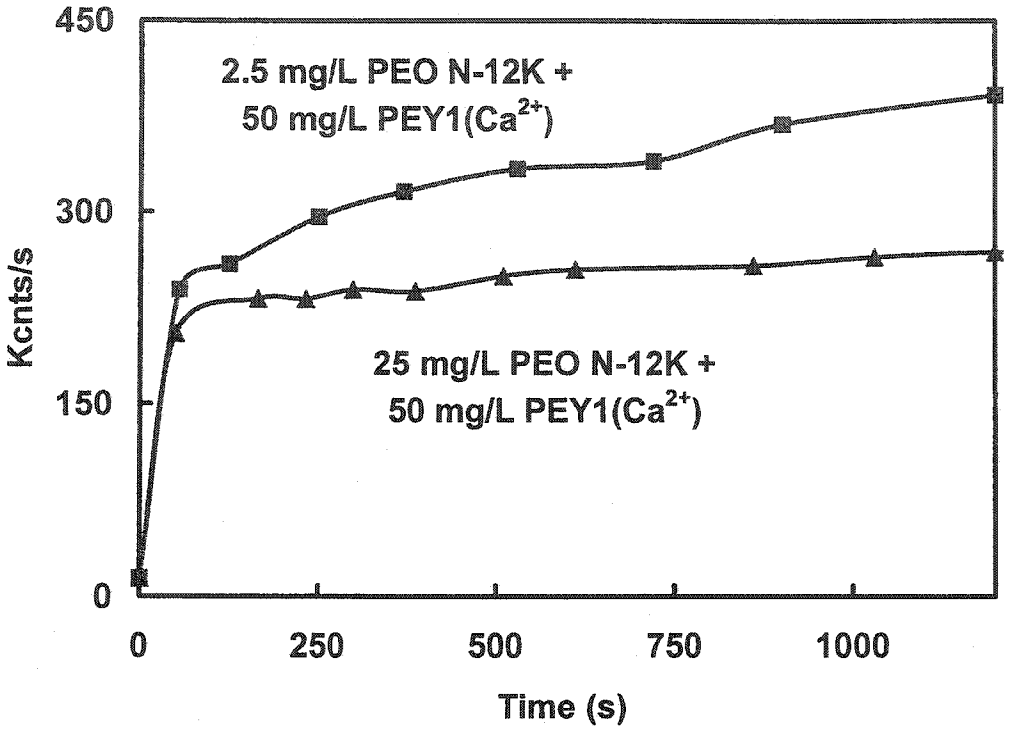

Figure 7. **The light scattering intensities of PEO N-12K/PEY1(Ca^{2+}) solutions as a function of time. [NaCl]=0.001 M, [$CaCl_2$]=0.001 M, T=25°C. PEY1 was first mixed with NaCl and $CaCl_2$. The PEO solution (0.5 g/L) was then added in one injection under stirring.**

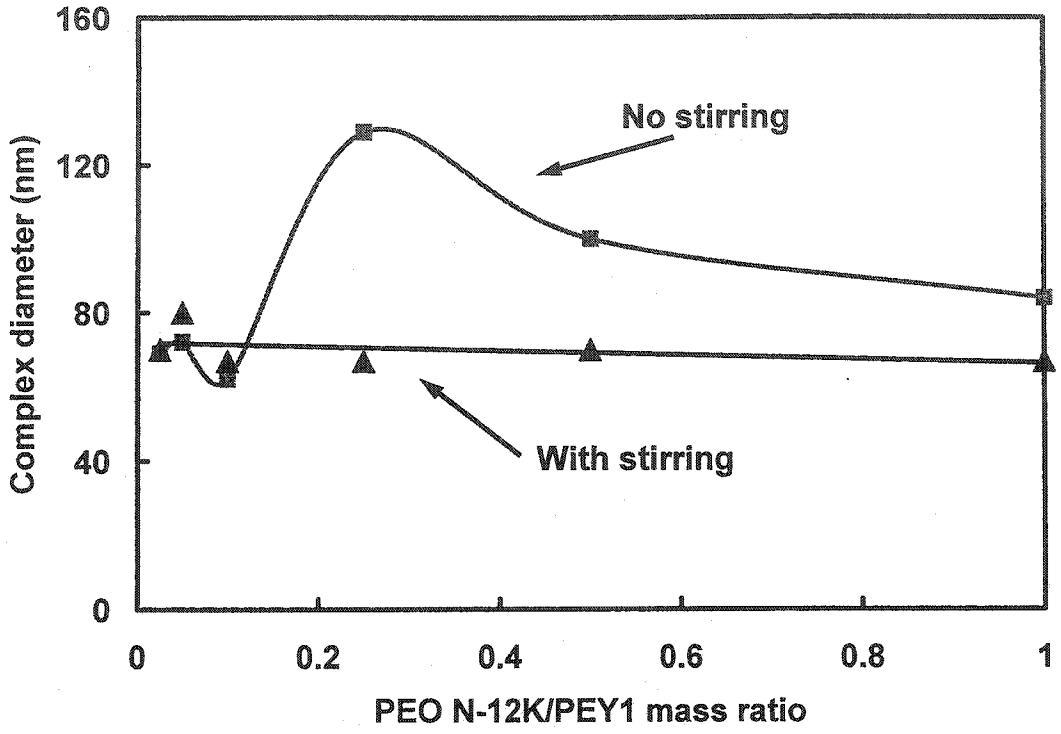
160
120
80
40
0
Complex diameter (nm)
No stirring
With stirring
0
0.2
0.4
0.6
0.8
1
PEO N-12K/PEY1 mass ratio

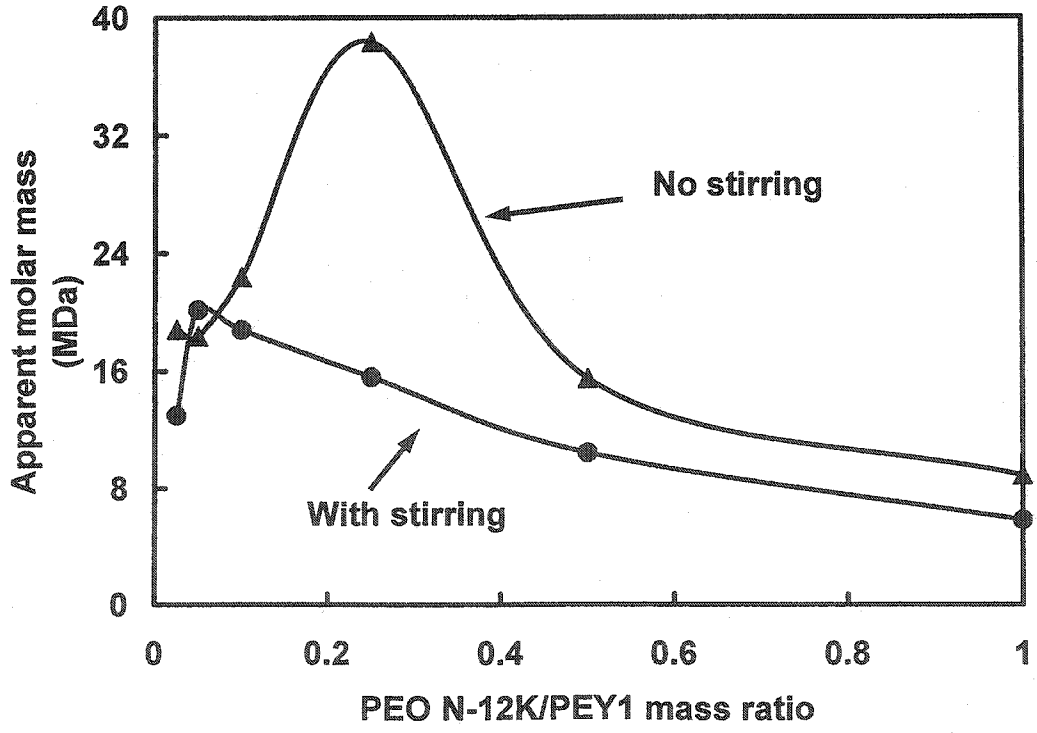
40
32
24
16
8
0
Apparent molar mass (MDa)
No stirring
With stirring
0
0.2
0.4
0.6
0.8
1
PEO N-12K/PEY1 mass ratio

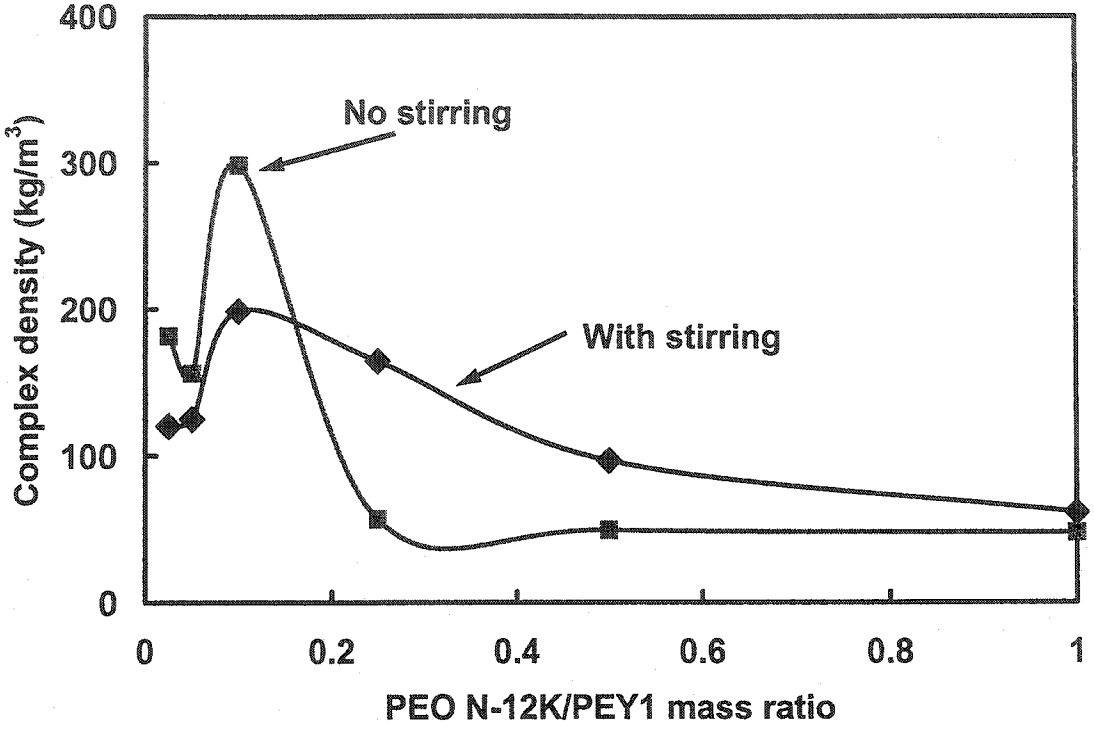

Figure 8. The hydrodynamic diameter, the apparent molar mass, and the density of PEO N-12K/PEY1(Ca^{2+}) complexes as a function of the PEO N-12K/PEY mass ratio. [PEY1]=50 mg/L, [NaCl]=0.001 M, [$CaCl_2$]=0.001 M, T=25°C. PEY1 was first mixed with NaCl and $CaCl_2$. The PEO solution (0.5 g/L) was then added in one injection.

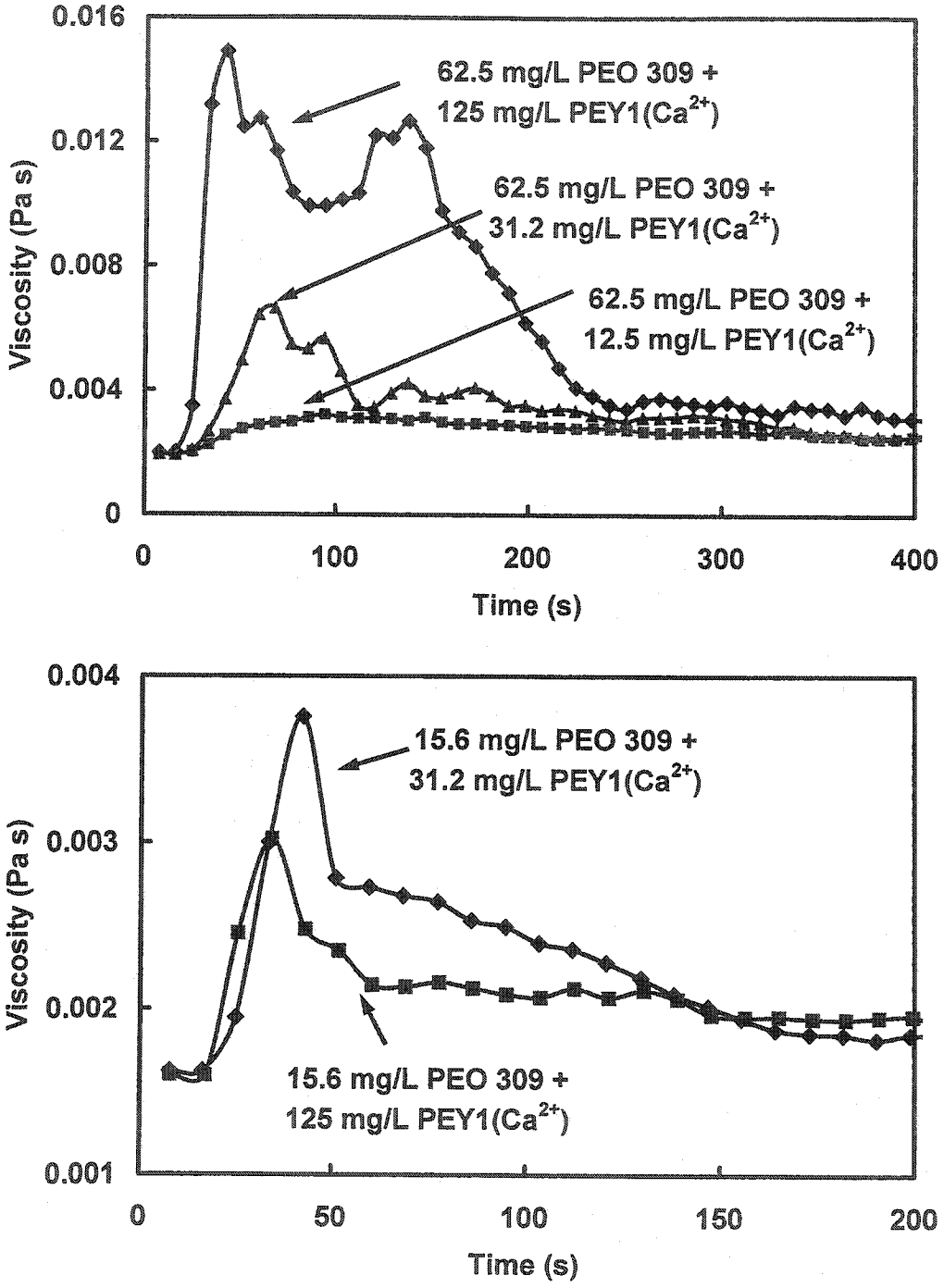

Figure 9. The viscosities of PEO 309/PEY1(Ca^{2+}) complex solutions as a function of time. [NaCl]=0.001 M, $CaCl_2$=0.001M, T=25°C, shear rate=175 s^{-1}. PEO was premixed with NaCl and $CaCl_2$. PEY1 was introduced 20 seconds after the shearing was started.

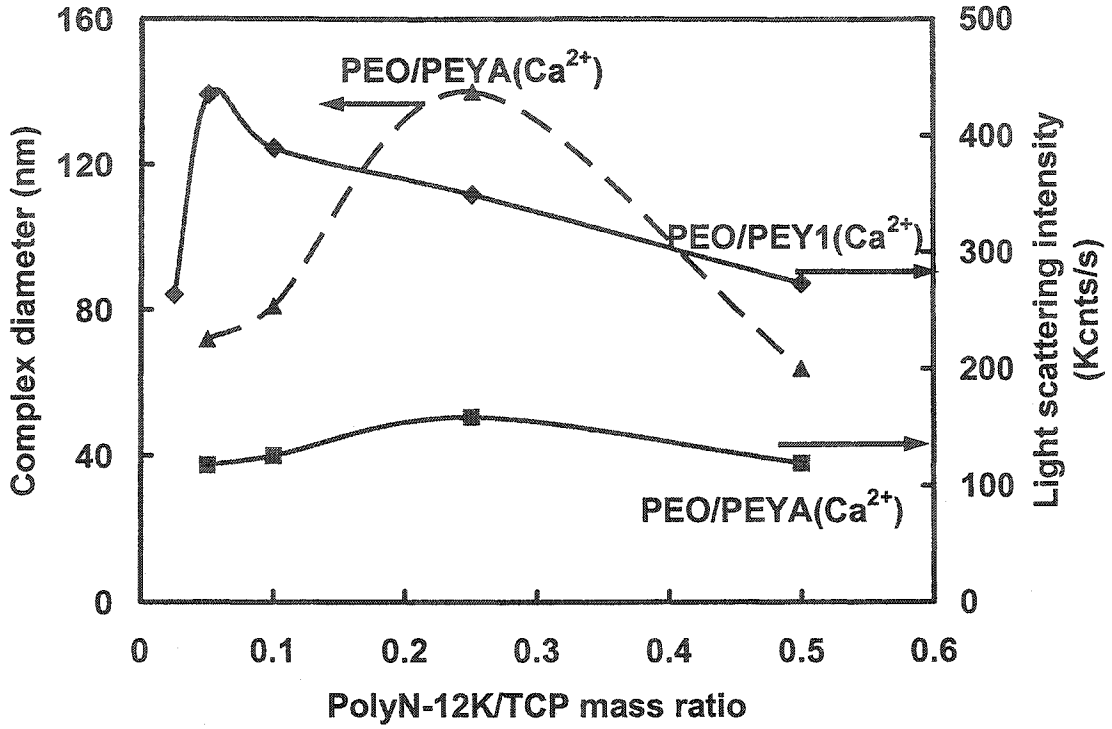

Figure 10. Light scattering intensities and hydrodynamic diameters of PEO N-12K/TCP(Ca^{2+}) complexes. [PEYA]=50 mg/L, [PEY1]=50 mg/L, [NaCl]=0.001 M, [$CaCl_2$]=0.001 M, T=25°C. PEY1 or PEYA was first mixed with NaCl and $CaCl_2$. The PEO solution (0.5 g/L) was then added in one injection under stirring.

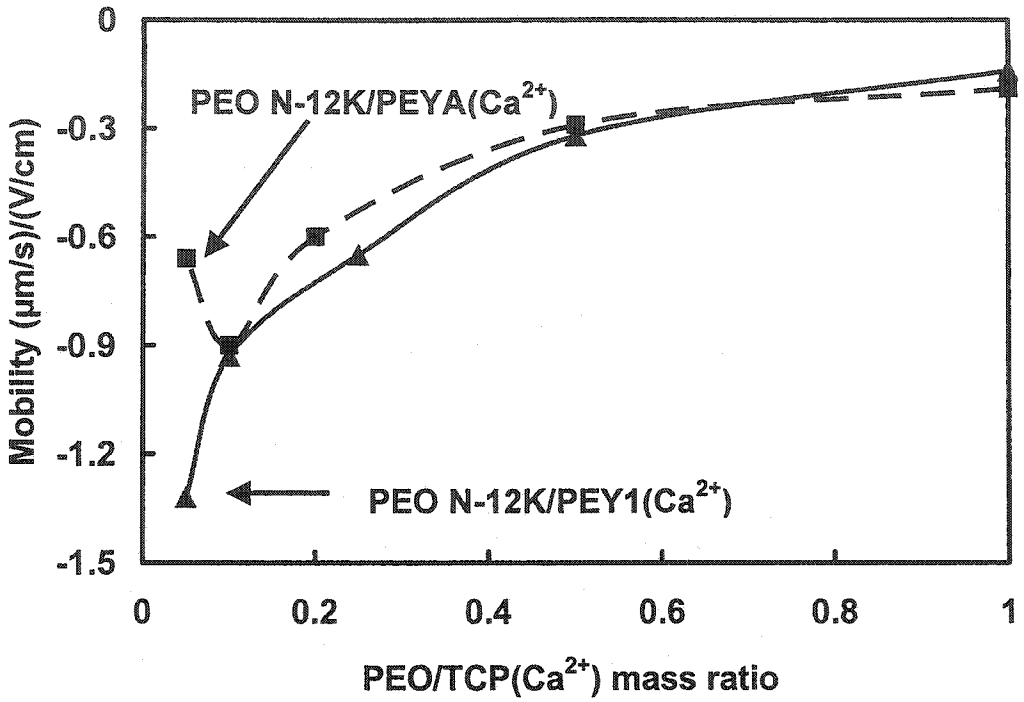

Figure 11. The electrophoretic mobilities of PEO N-12K/TCP(Ca^{2+}) complexes. [PEY1]=200 mg/L, [PEYA]=100 mg/L, [NaCl]=0.001 M, [$CaCl_2$]=0.001 M, T=25°C. PEY1 or PEYA was first mixed with NaCl and $CaCl_2$. The PEO solution (0.5 g/L) was then added in one injection the absence of stirring.

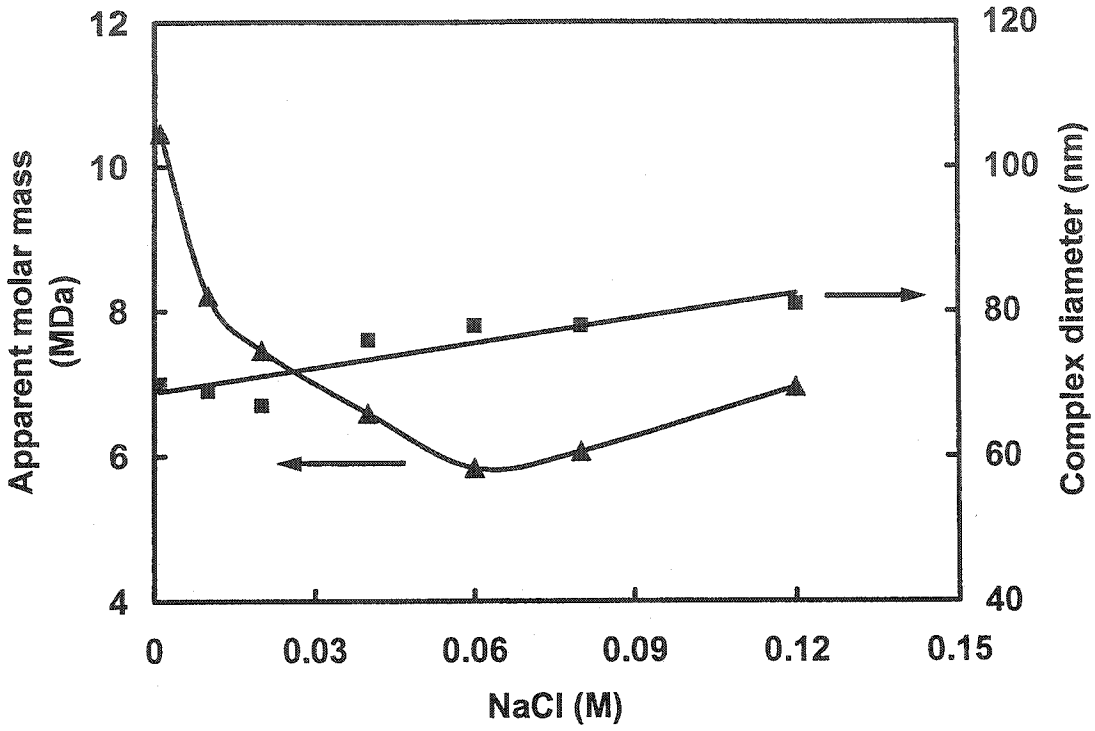

Figure 12. The effect of NaCl concentration on the apparent molar mass of PEO N-12K/PEY1(Ca^{2+}) complexes. [PEO N-12K]=25 mg/L, [PEY1]=50 mg, [$CaCl_2$]=0.001 M, T=25°C. PEY1 was first mixed with NaCl and $CaCl_2$. The PEO solution (0.5 g/L) was then added in one injection under stirring.

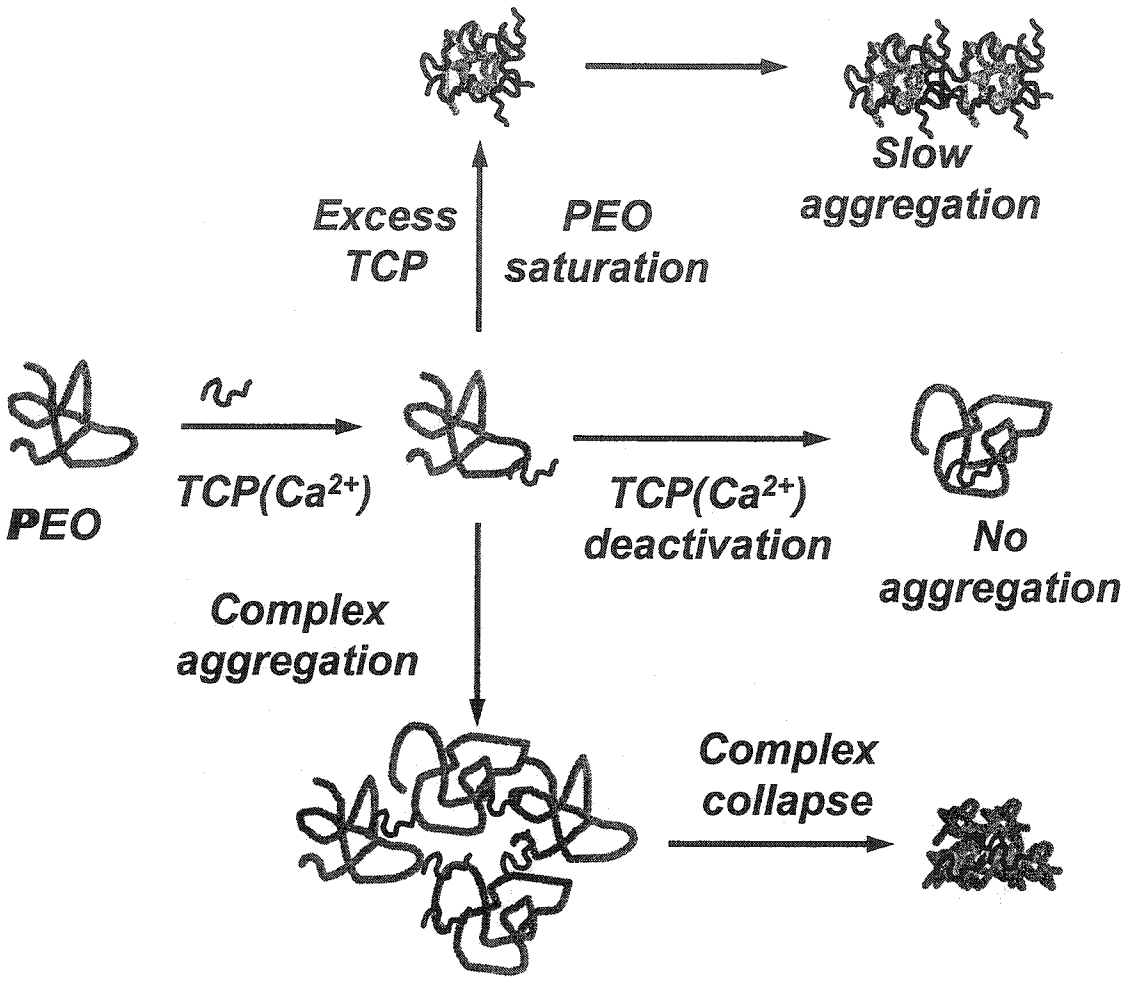

Figure 13. Schematic illustration of the aggregation mechanism of PEO/TCP(Ca^{2+}) complexes.

References

[1] Pelton, R. H.; Allen, L. H.; Nugent, H. M. *Sven. Paperstidn.* **1980**, *83*, 251.

[2] Carrard, J. P.; Pummer, H. *U.S. Patent* 4,070,236, 1973.

[3] Satterfield, B.; Stockwell, J. *Eur. Pat. Appl.* WO95/21296, 1995.

[4] Pelton, R. H.; Tay, C. H.; Allen, L. H. *Journal of Pulp and Paper Science* **1984**, *10*, 5.

[5] Echt, E. *European Patent Application*, 621 369 A1, 1994.

[6] Xiao, H.; Pelton, R. H.; Hamielec, A. *Journal of Pulp and Paper Science* **1996**, *22*, J475.

[7] Cong, R.; Bain, A. D.; Pelton, R. H. *Journal of Polymer Science B* **2000**, *38*, 1276.

[8] van de Ven, T. G. M. *Journal of Pulp and Paper Science* **1997**, *23*, J447.

[9] Xiao, H.; Pelton, R. H.; Hamielec, A. *Journal of Polymer Science* **1995**, *35*, 2605.

[10] Lindström, T.; Glad-Nordmark, G. *J. Colloid Interface Sci.* **1984**, *97*, 62.

[11] Stack, K. R.; Dunn, L. A.; Roberts, N. K. *Colloids and Surfaces* **1991**, *61*, 205.

[12] Cong, R.; Pelton, R. H.; Russo, P.; Doucet, G. *Macromolecules* **2003**, *36*, 204.

[13] Carignan, A.; Garnier, G.; van de Ven, T. G. M. *Journal of Pulp and Paper Science* **1998**, *24*, 94.

[14] Stack, K. R.; Dunn, L. A.; Roberts, N. K. *Journal of Wood Chemistry and Technology* **1993**, *13*, 283.

[15] Dautzenberg, H. *Macromol. Symp.* **2000**, *162*, 1.

[16] Bakeev, K.N.; Izumrudov, V. A.; Kuchanov, S, I.; Zezin, A, B.; Kabanov, V. A. *Macromolecules* **1992**, *25*, 4249.

[17] Gibbs, A.; Pelton, R. H. *Journal of Pulp and Paper Science* **1999**, *25*, 267.

[18] Lu, C.; Pelton, R. H.; Valliant, J.; Bothwell S. ; Stephenson, K. *Langmuir* **2002**, *18*, 4536.

[19] Gibbs, A.; Yang, Z.; Xiao, H.; Pelton, R. In *Fundamentals of Papermaking materials, Transactions of the Fundamental Research Symposium, 11th*, Cambridge, UK, 1997..

[20] Laivins, G.; Polverari, M.; Allen, L. *Journal of Pulp and Paper Science* **2001**, *27*, 190.

[21] Lu, C.; Pelton, R. H. The Mechanism of PCC Flocculation with PEO and Tyrosine-containing Polypeptides, private communication.

[22] Elias, H. G. *The Study of Association and Aggregation via Light Scattering*, in *Light Scattering from Polymer Solutions*, Huglin, M. B., Eds., Academic Press: New York, 1972.

[23] Hiemenz, P. C.; Rajagopalan, R. *Principles of Colloid and Surface Chemistry*, Marcel Dekker: New York, 1997.

[24] Huglin, M. B. *Specific Refractive Index Increment*, in *Light Scattering from Polymer Solutions*, Huglin, M. B., Eds., Academic Press: New York, 1972.

[25] Lu, C.; Srokowski, E.; Pelton, R. H., Complex Formation between PEO and Tyrosine-containing Polypeptides, private communication.

[26] Brown, W. *Macromolecules* **1984**, *17*, 66.

[27] de Gennes, P. G. *Pure and Applied Chemistry* **1992**, *64*, 1585.

[28] Devanand, K.; Selser, J. C. *Macromolecules* **1991**, *24*, 5943.

[29] Hara, M.; Wu, J.; Lee, A. H. *Macromolecules* **1988**, *21*, 2214.

[30] Hiemenz, P. C. *Polymer Chemistry: The Basic Concepts*, Marcel Dekker, New York, 1984.

[31] Kratochvil, D.; Alince, B.; van de Ven, T. G. M. *Journal of Pulp and Paper Science* **1999**, *25*, 331.

[32] Lu, C., PhD Thesis, Appendix 1, McMaster University.

[33] Ohshima, H. *Journal of Colloid and Interface Science* **1994**, *163*, 474.

[34] Pelton, R. H.; Xiao, H.; Brook, M. A.; Hamielec, A. *Langmuir* **1996**, *12*, 5756.

[35] Rouse, P. E., *J. Chem. Phy.* **1956**, *21*, 1273.

Chapter 7 PCC Flocculation with PEO/Tyrosine-containing Polypeptide Dual-component Flocculants

Abstract

High molecular weight poly(ethylene oxide) (PEO) was applied in conjunction with L-poly(Glu, Tyr) (1:1) (PEY1) to flocculate the aqueous suspensions of precipitated calcium carbonate (PCC). The association between PEY1 and calcium ions (PEY1(Ca^{2+})) was required to induce the flocculation. The flocculation efficiency depended on many experimental conditions, such as PEO molecular weight, PEO/PEY1 ratio, and shear rate. Xiao and Pelton's complex bridging flocculation mechanism was extended to take into consideration the PEO/PEY1(Ca^{2+}) complex formation mechanism. According to the extended flocculation mechanism, multilayers of the PEO/PEY1(Ca^{2+}) complexes adsorb on the PCC surface to induce PCC bridging flocculation. When the complexes adsorb on the PCC surface, three processes occur simultaneously. The first process is the bridging of PCC by the adsorbed complexes. The second process is the deactivation of PEY1(Ca^{2+}) by PEO – this is a new concept developed in this work. It was proposed that the deactivation was induced by the encapsulation of TCP phenolic groups by PEO. The third process is the saturation of PEO by PEY1(Ca^{2+}) when PEY1(Ca^{2+}) is in excess. The flocculation proceeds until either all the PEY1(Ca^{2+}) chains are deactivated or all the PEO chains are saturated.

Introduction

Flocculants are often required in the papermaking process to incorporate colloidal sized fillers and fines into the paper sheet. Cationic polymers, which can bridge the anionic fillers and fines, are commonly used to induce an effective flocculation.[1] However, the efficiency of cationic polymers is often hindered due to the interaction with largely present dissolved and colloidal anionic substances (DCS). Thus, neutral poly(ethylene oxide) (PEO) of high molecular weight (MW) was introduced to replace cationic flocculants.[2] However, the PEO flocculation is only achieved in the presence of cofactors, which are water soluble phenolic polymers capable of forming complexes with PEO.[3, 4]

During the past two decades, many researchers have made contributions to understanding the mechanism of PEO/cofactor flocculation. Pelton's group first proposed a complex bridging mechanism.[5] According to this mechanism, PEO/cofactor complexes function as bridges to flocculate colloidal particles and the adsorption of the complexes is necessary for an effective flocculation. Both Stack and van de Ven's groups found that neither PEO nor cofactor could adsorb on some surfaces, whereas the PEO/cofactor complexes could.[6, 7] Filler flocs induced by cofactor and high MW PEO showed remarkable elasticity, which was considered as an important indicator of floc survivability in turbulent flow.[8]

The PEO/cofactor flocculation is a complicated process due to the presence of many components and the explanations of many flocculation observations still remain elusive. Both the flocculation rate and the steady state flocculation extent were reported to increase with increasing PEO molecular weight.[5] The entanglement of PEO molecules increases the flocculation rate.[9] PEO of 10^6 Da induces poor or no filler flocculation, even though the average size of the complexes was (70 nm) larger than the thickness (40 nm) of the two electrical double layers around the PCC surface.[10] Flocculation also depends on the ratio of PEO/cofactor and the best condition was often found at an intermediate ratio.[5] At a fixed PEO/cofactor ratio, the flocculation extent increases with increasing concentrations of PEO and cofactor.[5] Generally speaking, the mechanism that prevents complete flocculation remains unknown.

The understanding of the flocculation mechanism was largely hampered by using commercial cofactors most of which are phenolic resins with complicated structures. Recently, we discovered that a polypeptide L-poly(Glu, Tyr) (1:1) (PEY1) with a well-defined structure can be used as a model cofactor.[11] The mechanism of PEO/PEY1 complex formation was studied in our previous report[10] and summarized in the following paragraph.

In the absence of soluble calcium ions, PEY1 molecules can attach to PEO molecules without inducing the aggregation of the PEO molecules. In the presence of soluble calcium ions, the structures of PEO/PEY1 complexes are controlled kinetically. The PEY1 molecules associate with calcium ions (PEY1(Ca^{2+})) and function as bridges to couple PEO molecules. During the same time, the PEY1(Ca^{2+}) chains will also

undergo deactivation, a process by which a polypeptide attached to PEO rearranges so it is no longer able to couple to another PEO molecule.

The objective of this work was to extend Xiao and Pelton's complex bridging flocculation mechanism to account for complex formation. In this work, precipitated calcium carbonate, a common papermaking filler, was flocculated under varying conditions, such as PEO MW and PEO/PEY1 ratio. Flocculation rates and steady state flocculation extents were determined using a photometric dispersion analyzer, and the interactions between PCC and the PEO/PEY1 complexes were characterized using an electrophoretic mobility apparatus. The experimental results were then rationalized using the extended flocculation mechanism.

Experimental

Materials

PEO 309 (molecular weight (MW)=8×10^6 Da), PEO 301 (MW=4×10^6 Da), PEO N-60 (MW=2×10^6 Da), and PEO N-12K (MW=10^6 Da) were obtained from Union Carbide. Random L-polypeptide poly(Glu, Tyr) (1:1) (MW=36.1 kDa) (PEY1) was purchased from Sigma in the form of sodium salt. PEO stock solutions were prepared by dissolving polymer (0.5 g/L) in water with gentle end-to-end rotation for 24 hours. PEY1 stock solutions were prepared by dissolving peptides (1 g/L) in water under gentle shaking for 10 minutes. Precipitated calcium carbonate (PCC) (Albacar HO, Specialty Minerals Inc.) consists of the aggregates of scalenohedral needles with a mean particle size of 1.34 μm (Brookhaven Disk Centrifuge), and a specific surface area of 10.0 m^2/g (nitrogen adsorption). Dextran sulfate (DS) (MW=10,000 Da) was purchased from Sigma in the form of sodium salt with an average of 2.3 sulfate groups per glucose residue. NaCl and $CaCl_2$ (BDH) were used without further purification. All the experiments were performed with water from a Millipore Milli-Q system fitted with one Super C carbon cartridge, two ion-exchange cartridges, and one Organex Q cartridge.

Methods

Photometric Dispersion Analyzer

PCC flocculation was monitored using a photometric dispersion analyzer (PDA) (Rank Brothers, Cambridge, UK). In a typical flocculation experiment, PCC, PEY1, and PEO were added sequentially. The addition order and time intervals between additions were varied. The total suspension volume was 200 mL. The suspension was stirred at 475 rpm using a three-bladed propeller (55 mm diameter). If a different rpm was used, it will be specified in the following sections. The suspension was circulated through the PDA at a rate of 45 mL/min. An amplified DC output and an amplified AC output were recorded simultaneously. The amplified DC output was proportional to the transmitted light intensity and converted to the relative turbidity of the suspension by the following relationship

$$\tau_r = \ln\left(\frac{V_w}{V_t}\right) \Big/ \ln\left(\frac{V_w}{V_{t=0}}\right) \qquad (1)$$

where V_w was the output voltage for water, $V_{t=0}$ was the output voltage for the PCC suspension and V_t was the output voltage at time t during flocculation. The amplified AC output is proportional to the root mean square of transmitted light intensity. The ratio of the amplified AC output to the amplified DC output is defined as R_{rms}.

The steady state flocculation extent was derived by assuming that the relative turbidity at the steady state was proportional to the concentration of un-flocculated colloidal particles. The initial flocculation rate was derived from R_{rms} as follows. Consider a suspension containing N_1 primary PCC particles. PCC aggregation rate by a polymeric flocculant is given by the following equation[12],

$$dN_m / dt = \left[\frac{1}{2}\sum_{i=1}^{i=m-1} k_{i,m-i} N_i N_{m-i} - \sum_{i=1}^{\infty} k_{im} N_i N_m\right] E \qquad (2)$$

where N_m, N_i and N_j are the number concentrations of PCC aggregates containing m, i, and j primary PCC particles respectively, E is the flocculation efficiency which gives the fraction of collisions leading to effective particle aggregations, and k is PCC-PCC collision rate constant. At the initial stage of flocculation, k is assumed to be equal to the collision rate of two primary PCC particles k_1[13] which is given as follows,

$$k_1 = \sqrt{\frac{8\pi}{15}}(r_1 + r_1)^3 G \qquad (3)$$

where r_1 is radius of primary PCC molecule, and G is shear rate. The decreasing rate of total PCC particle concentration, irrespective of PCC aggregates size, $\sum_{i=1}^{\infty} N_i$, can be obtained from equation (2) as

$$d\sum_{i=1}^{\infty} N_i / dt = -\frac{1}{2} k_1 E (\sum_{i=1}^{\infty} N_i)^2 \qquad (4)$$

Equation (4) can be solved to obtain

$$\frac{1}{\sum_{i=1}^{\infty} N_i} - \frac{1}{N_0} = \frac{1}{2} E k_1 t \qquad (5)$$

$$n_N = N_0 \Big/ \sum_{i=1}^{\infty} N_i \qquad (6)$$

where n_N is the number-average number of primary PCC particles in one aggregate at time t. Therefore, $1/\sum_{i=1}^{\infty} N_i$ is a linear function of time with a slope of $\frac{1}{2}Ek_1$, which is defined as the PCC initial flocculation rate. Information about $1/\sum_{i=1}^{\infty} N_i$ can be obtained experimentally from R_{rms}.[14, 15] According to the Gregory's derivation as

$$R_{rms} = (\sum_{i=1}^{\infty} N_i L / A)^{\frac{1}{2}} C \qquad (7)$$

where L is the path length of the incident light, A is the cross-section area of the incident light, and C is the average scattering cross section of the PCC aggregates and given as

$$C = \pi R^2 Q \qquad (8)$$

where R is the average radius of PCC aggregates, and Q is the scattering coefficient of PCC aggregates and can be assumed constant. R can be estimated from r_1 based on two extreme geometries. One is that PCC primary particles comprising the aggregates coalesce to form spheres of the same total volume, and the other are chain-like aggregates which tend to align with the flow. The chain-like aggregates were proposed by Gregory to be nearer to the real shape.[14] By assuming the geometry of chain-like aggregates, C is given as

$$C = n_N \pi r_1^2 Q \qquad (9)$$

Equation (7) can therefore be rewritten by inserting equation (9) and (6)

$$R_{rms} = (\sum_{i=1}^{\infty} N_i)^{-\frac{1}{2}} \pi r_1 N_0 Q (L/A)^{\frac{1}{2}} \qquad (10)$$

Equation (10) suggests that R_{rms}^2 is directly proportional to $1/\sum_{i=1}^{\infty} N_i$. The initial slope ($k_R$) of R_{rms}^2 versus time is directly proportional to $\frac{1}{2}Ek_1$ according to equation (5) and can be used to evaluate flocculation rate. A higher k_R value suggests a faster flocculation.

Electrophoretic Mobility

The adsorption of polymer on PCC particles was monitored by the change in electrophoretic mobility of PCC particles determined using a Brookhaven ZetaPALS instrument at 25°C. According to Ohshima's derivation, the mobility of a particle in an electrical field is proportional to the volume charge density of the adsorbed polymer layer.[16] Thus, the change in mobility can reflect the adsorption of polymer on the particle

surface. The reported mobility was the average of 10 cycles, where each cycle contained 20 scans.

Results

Polymer Adsorption on PCC Surfaces

The adsorption of PEO/cofactor complexes on particle surface is required for an effective flocculation.[4] The understanding of polymer adsorption at the solid/liquid interface is necessary for studying the PEO/cofactor flocculation mechanism.

In this work, 500 mg/L PCC mixed with 10 mg/L dextran sulfate (DS) was used as a target colloid suspension for flocculation. DS was added to mimic the dissolved and colloidal anionic substances in the pulp suspension. The anionic DS molecules adsorbed on positively charged PCC surface at neutral pH, and the adsorption amount was estimated by measuring the electrophoretic mobilities of the PCC particles. Based on Ohshima's derivation, the particle electrophoretic mobility is directly proportional to the particle surface charge density, which is in turn related to the amount of the adsorbed polyelectrolyte.[16] When the PCC mobility was plotted against the concentration of the added DS, the DS concentration at which the PCC mobility reached the most negative value corresponds to the saturation of the surface with DS. Figure 1 shows the PCC mobility as a function of DS concentration, which were normalized to the PCC surface area. The pH was adjusted to 7.8 by the addition of HCl. The PCC mobility decreased with the increase of DS concentration until reached a minimum value of -2.10 $m^2 V^{-1} s^{-1} \times 10^{-8}$ at 0.3 mg/m^2 DS, corresponding to the maximum DS adsorption amount. In the following paragraphs, "PCC+DS" was used to represent the PCC particles covered with DS.

Figure 1 also shows the PCC mobility as a function of PEY1 concentration at pH 7.8. PEY1 is negatively charged and thus adsorbed on the PCC surface. The maximum PEY1 adsorption amount was around 0.4 mg/m^2.

The adsorption of PEO 309 (MW=8 MDa) on the PCC surface was measured using tannic acid method.[17] There was no detectable PEO adsorption. PEO 309 was also not able to flocculate PCC particles. Thus, we believe that PEO does not adsorb onto the PCC surface as suggested by other researchers.[18]

The adsorptions of PEO and PEY1 on the PCC+DS surface were also measured at pH 7.8 in this work. No detectable PEO adsorbed on PCC+DS surface as measured using the tannic acid method. PEY1 adsorption was determined by measuring the concentration of free PEY1 in the solution using a UV spectrometer. No detectable amounts of PEY1 adsorbed on the PCC+DS surface. It is possible that charge repulsion prevented PEY1 from adsorbing.

Table 1 shows the changes of PCC and PCC+DS mobilities upon the consecutive additions of PEY1 and PEO. The suspensions remain colloidal stable under the experimental conditions. The PCC mobility changed from +0.60 to -2.15 and then to -0.61 $m^2 V^{-1} s^{-1} \times 10^{-8}$ upon the sequential additions of PEY1 and PEO N-12K (MW=1

MDa), indicating the consecutive adsorptions of two polymers. The mobility of PCC+DS remained at around -2.15 $m^2 V^{-1} s^{-1} \times 10^{-8}$ upon the addition of PEY1. The subsequent addition of PEO changed the mobility to -0.83 $m^2 V^{-1} s^{-1} \times 10^{-8}$, suggesting that the complexes adsorbed on the PCC+DS surface even though neither PEY1 nor PEO adsorbed.

In summary, PEO did not adsorb on the PCC surface, while both PEY1 and PEO/PEY1(Ca^{2+}) complexes adsorbed. PEO/PEY1(Ca^{2+}) complexes adsorbed on the PCC+DS surface even though neither PEO nor PEY1 adsorbed.

Effect of Soluble Calcium Ions on PCC Flocculation

Soluble calcium ions are often present in the pulp suspensions. Figure 2 shows the effect of soluble calcium ions on the PCC flocculation induced by PEO 309 (MW=8 MDa) and PEY1 at pH 9.8. In this experiment, 5 mg/L PEY1 and 2.5 mg/L PEO were added to the PCC suspension sequentially. The calcium concentration was adjusted by $CaCl_2$ and EDTA. The first jump in relative turbidity occurred upon the addition of PCC to the flocculation vessel, which contained only dilute electrolyte. After the relative turbidity of the PCC suspension reached one (the steady state), PEY1 was introduced. PEY1 did not induce flocculation and the relative turbidity shows no significant change. However, flocculation occurred upon the subsequent addition of PEO, giving a decrease in relative turbidity. Without the additions of $CaCl_2$ and EDTA, PEO/PEY1 flocculated the PCC suspension. The relative turbidity of the suspension decreased to a minimum of 0.67 and the initial flocculation rate was 0.49 s^{-1}. When 0.0004 M EDTA was added to the PCC suspension, removing the free calcium ions, PEO/PEY1 did not induce flocculation. Whereas, the addition of 0.0005 M $CaCl_2$ enhanced the flocculation. The relative turbidity of the suspension decreased to 0.22 and the initial flocculation rate was 0.93 s^{-1}. Figure 2 also shows PCC+DS flocculation, in which 10 mg/L DS was premixed with PCC and then $CaCl_2$, PEY1, and PEO 309 were added sequentially. The steady state relative turbidity was 0.21 and the initial flocculation rate was 1.2 s^{-1}.

It is well known that changing the concentration of soluble calcium ions will vary the zeta potential of PCC.[19] Thus, it is important to know whether the removal of the free calcium ions can prevent the adsorption of PEO/PEY1 complexes, therefore inhibiting flocculation. Table 2 shows the influence of dissolved calcium ions on the adsorption of PEO/PEY1 complexes determined by measuring the mobility of PCC. At pH 9.7, the mobility of PCC is -0.46 $m^2 V^{-1} s^{-1} \times 10^{-8}$. The addition of 0.0005 M $CaCl_2$ reversed the PCC mobility to +0.57 $m^2 V^{-1} s^{-1} \times 10^{-8}$. In contrast, the addition of 0.0004 M EDTA decreased the PCC mobility to -1.26 (μm/s)/(V/cm). The sequential additions of PEY1 and PEO in the presence of EDTA changed the PCC mobility to -3.27 and -1.44 $m^2 V^{-1} s^{-1} \times 10^{-8}$ accordingly. It is clear that the removal of the free calcium ions did not prevent the adsorption of PEO/PEY1 complexes.

PCC Flocculation

Figure 3 shows the effect of the PEO/PEY1 ratio on PCC flocculation at pH 7.8. 10 mg/L PEY1 and various amount of PEO N-60 (MW=2 MDa) were added

sequentially. We have known from our previous report that the binding between PEO and PEY1(Ca^{2+}) was an irreversible process (high affinity binding) and PEY1(Ca^{2+}) was saturated with bound PEO molecules at a PEO/PEY1 mass ratio of 0.2 (mass saturation ratio).[20] Two important features can be generalized from Figure 3. (1) An intermediate PEO/PEY(Ca^{2+}) mass ratio of 0.25 gave the highest initial flocculation rate of 0.12. (2) Different PEO/PEY1 ratios corresponded to different flocculation behaviors. When the PEO/PEY1 mass ratio was 0.5, higher than the mass saturation ratio, the initial flocculation rate was 0.029 s^{-1}. The relative turbidity decreased to 0.81 in about 100 seconds and then flattened out. When the mass ratio was 0.05, lower than the mass saturation ratio, the initial flocculation rate was 0.007 s^{-1}. The relative turbidity decreased slowly to 0.71 in 350 seconds without reaching a steady state.

Figure 4 shows the effect of PEO N-60/PEY1 concentration on PCC flocculation at fixed PEO/PEY1 ratios. When the mass ratio was 0.05, increasing the PEY1 concentration from 10 mg/L to 50 mg/L increased the initial PCC flocculation rate significantly from 0.007 to 1.5 s^{-1}. The relative turbidity suggested a two-step flocculation at 50 mg/L of PEY1, with a fast initial decrease for around 30 seconds and a continuing slow decrease for more than 200 seconds. When the mass ratio was 0.25, increasing the PEY1 concentration from 10 mg/L to 45 mg/L increased the initial flocculation rate from 0.12 to 1.9 s^{-1}. The steady state relative turbidity decreased from 0.30 to 0.06 in 30 seconds and flattened out, suggesting a one-step flocculation.

It is noteworthy that PCC flocculation highly correlated with the aggregation of PEO/PEY1(Ca^{2+}) complexes.[10] The highest aggregation levels of both PCC and the complexes occurred at intermediate PEO/PEY1 mass ratios around 0.2. When the mass ratio was below the saturation ratio, both PCC and the complexes aggregated in two steps with a fast initial aggregation and a continuing slow aggregation. When the mass ratio was above the saturation ratio, both PCC and the complexes aggregated in only one step.

Figure 4 also suggests that PEO/cofactor flocculation behaves differently from the conventional bridging flocculation induced by single-component flocculant. For conventional bridging flocculation, the highest flocculation rate occurs at an intermediate flocculant concentration. If the flocculant concentration is much higher than the concentration necessary to saturate the colloid surfaces, the colloids will be sterically stabilized. However, increasing the PEO/PEY1 concentration only led to an increased initial flocculation rate and no steric stabilization was observed even when the PEY1 concentration was one tenth of the PCC concentration.

It is well recognized that a higher PEO molecular weight leads to a higher PEO/cofactor flocculation extent.[21] Figure 5 shows the PEO MW effect on PCC flocculation with a PEO/PEY1 mass ratio of 0.5. As expected, when PEO MW was increased from 1 to 8 MDa, the initial flocculation rate increased from almost 0 to 1.4 s^{-1} and the steady state relative turbidity decreased from 1 to 0.24. In our previous report, we have shown that a higher PEO molecular weight leads to a higher PEO/PEY1(Ca^{2+}) aggregation level.[10] Thus, the PCC flocculation extent correlated closely to the complex aggregation level from the aspect of PEO molecular weight.

Figure 6 shows the effects of shear rate and NaCl concentration on PCC flocculation. Xiao et al. reported that increasing the shear rate can increase PEO/cofactor flocculation extent.[5] Our experiments confirmed Xiao's results. Both the initial flocculation rate and the steady state flocculation extent were enhanced when propeller rpm was increased from 330 to 475. On the other hand, increasing NaCl concentration from 0.001 M to 0.04 M decreased both the initial flocculation rate and the steady sate flocculation extent. Since the molar mass of PEO/PEY1(Ca^{2+}) complexes decreased with the increase of NaCl concentration, the PCC aggregation level also correlated to the complex aggregation level from the aspect of NaCl concentration. However, the shear rate showed opposite effects on the PCC flocculation extent and the complex aggregation level. Increasing the shear rate decreased the complex molar mass.

Figure 7 shows PCC flocculation by the premixed PEO/PEY1(Ca^{2+}) complexes to elucidate the flocculation mechanism. In a typical experiment, PEO and PEY1 was mixed in the presence of 0.0007 M $CaCl_2$ and then 2ml of 50 g/L PCC was added in one injection to give a final PCC concentration of 0.5 g/L. The relative turbidity increased significantly upon the addition of PCC. Since PCC mixing was competing with PCC flocculation, the relative turbidity began to decrease before reaching one. The steady state relative turbidity of the PCC suspension flocculated with 5 mg/L PEO N-12K and 10 mg/L PEY1(Ca^{2+}) was around 0.67, suggesting that PCC can be flocculated by the premixed PEO N-12K/PEY1(Ca^{2+}) complexes. In comparison, there was no PCC flocculation using the normal addition order in which 10 mg/L PEY1 and 5 mg/L PEO N-12K were added to the PCC suspension sequentially (Figure 5). In addition, PCC suspensions were also flocculated by the premixed PEO N-60/PEY(Ca^{2+}) complexes at a high PEO/PEY1 mass ratio of 0.375 and a low PEO/PEY1 mass ratio of 0.1. It is clear that the complexes could adsorb on the PCC surface and induce a flocculation irrespective of PEO/PEY1 ratio.

PCC+DS Flocculation

In the papermaking process, PCC flocculation is normally carried out in the presence of many anionic dissolved and colloidal substances, which can adsorb on the PCC surface and interfere with the flocculation. In this work, DS was added to PCC suspensions to simulate anionic dissolved and colloidal substances.[22]

Figure 8 shows the initial flocculation rates of PCC+DS flocculation experiments with different PEO N-60/PEY1 mass ratios. The intermediate PEO/PEY1 ratio of 0.25 gave the highest k_R value of 0.027 s^{-1}. Figure 8 also shows the initial rates of PCC flocculation experiments (from Figure 3). It is clear that the addition of DS reduced the flocculation rate at all PEO/PEY1 ratios.

Figure 9 shows PCC+DS flocculation by premixed PEO N-60/PEY1(Ca^{2+}) complexes. No flocculation was observed at the PEO/PEY1 mass ratios of 0.375 and 0.1. For comparison, Figure 9 also shows the PCC+DS flocculation results using the normal addition order in which PEY1 and PEO were added to PCC+DS suspensions sequentially. PCC+DS could be flocculated under normal addition order. The initial

flocculation rates were 0.063 s^{-1} and 0.011 s^{-1} at the PEO/PEY1 mass ratios of 0.1 and 0.375 respectively.

In Table 3, the adsorption of premixed PEO N-60/PEY1(Ca^{2+}) complexes on PCC+DS surfaces were investigated by measuring the electrophoretic mobilities of PCC+DS. The mobility of PCC+DS was -2.30 $m^2 V^{-1} s^{-1} \times 10^{-8}$. At the PEO/PEY1 mass ratio of 0.05, the PCC+DS mobility remained unchanged in the presence of the premixed complex. At a higher PEO/PEY1 mass ratio of 0.375, the PCC+DS mobility increased to -1.12 $m^2 V^{-1} s^{-1} \times 10^{-8}$. Previously we have shown that the complex charge density decreased with the increase of PEO/PEY1 ratio.[10] Thus, there was probably no complex adsorption at the ratio of 0.05 due to the charge repulsion between the particles and the complexes. At the ratio of 0.375, the charge repulsion was reduced and the complexes adsorbed on the PCC+DS surface.

Figure 10 shows the effect of the addition order of PEO 309 and PEY1 on PCC+DS flocculation. When PEY1 was added 60 seconds before PEO 309, the relative turbidity dropped to 0.19 with a high initial flocculation rate of 1.7 s^{-1}. When PEO 309 was added 5 seconds before the addition of PEY1, the initial flocculation rate decreased to 0.50 s^{-1} and the steady state relative turbidity increased to 0.28. When PEO 309 was added 260 seconds before the addition of PEY1, the initial flocculation rate further decreased to 0.11 s^{-1} and the steady state relative turbidity further increased to 0.55. Figure 10 also shows the PCC+DS flocculation by premixed PEO 309/PEY1 complexes. PCC and DS were mixed in the flocculation vessel first. 2 mL of PEO 309/PEY1 solution premixed in the absence of Ca^{2+} was then added to PCC+DS suspension to give a total volume of 200 mL. The relative turbidity only dropped to 0.81 at the steady state.

Discussion

The objective of this work is to extend our knowledge of PEO/cofactor flocculation mechanism. Xiao et al. proposed a complex bridging mechanism, in which PEO/cofactor complexes function as bridges to induce flocculation. However, the mechanism that prevents the complete flocculation still remains unknown. To facilitate the study of the flocculation mechanism, we employed a well-defined polypeptide cofactor L-poly(Glu, Tyr) (1:1) (PEY1) and investigated the mechanism of PEO/PEY1(Ca^{2+}) complex formation in our previous work.[10] In the following paragraphs, we will extend the complex bridging mechanism by correlating complex formation to PCC flocculation. After which, many flocculation observations will be rationalized based on the extended mechanism.

Complex Formation Mechanism

PEO/PEY1(Ca^{2+}) complex formation and evolution can be summarized into three processes.[10] In the first process, called *complex aggregation*, the attached PEY1(Ca^{2+}) molecules (active peptides) function as bridges to couple PEO chains. The second process is *peptide deactivation* - this is a new concept which we have invoked to explain the finite complex size. The PEY1(Ca^{2+}) chains bound to PEO rearrange so that the polypeptide is no longer able to bind to another PEO molecule. The deactivation is

caused by the encapsulation of all the active phenolic groups by the first PEO chain. The active phenolic groups are defined as those phenolic groups that can bind to PEO. It was proposed in our previous report that the affinity between PEO and the phenolic groups depends on TCP microstructure and a block must have at least four tyrosine groups in order to bind to PEO.[20] The third process is *PEO saturation* which occurs when PEY1(Ca^{2+}) is in excess. PEO chains saturated with bound PEY1(Ca^{2+}) chains aggregate slowly. We define the unbound PEO segments as active PEO segments.

Proposed Flocculation Mechanism

Xiao et al. proposed that the complex formation and the flocculation occur simultaneously.[5] Our experiments in this work confirmed their statement. PCC flocculation was normally carried out by adding PEY1 and PEO to the PCC suspension sequentially (normal addition order). Both Figure 7 and Figure 9 shows that the flocculation using the normal addition order reached a different steady state extent than the flocculation induced by the premixed PEO/PEY1(Ca^{2+}) complexes. In other words, complex formation affects PCC flocculation and the two processes occur simultaneously using the normal addition order. Thus, the PCC flocculation mechanism must take into account the complex formation mechanism.

In Figure 11, we propose a flocculation mechanism by considering the complex formation mechanism. When PEY1 is first added to the PCC suspension, PEY1 associates with dissolved calcium ions. Some of the PEY1(Ca^{2+}) chains are consumed to saturate the PCC surface, and the rest of PEY1(Ca^{2+}) chains remain free in water. Upon the addition of PEO, PEO and PEY1(Ca^{2+}) form complexes. At the same time, the complexes adsorb on the PCC surface. Once the complexes adsorb, three processes can occur. In the first process, labeled *PCC flocculation*, the adsorbed complexes function as bridges to flocculate PCC particles. The bridging occurs mostly through the attachment of the active PEO segments on one PCC particle to the active PEY1(Ca^{2+}) chains on another PCC particle. The second process is *complex deactivation*, in which the active peptides are deactivated by PEO and thus is not able to attach to the active PEO segments on another PCC. Finally, PCC particles are sterically stabilized by the deactivated complexes, which refer to the complexes with only deactivated PEY1(Ca^{2+}) molecules. The third process is called *complex saturation*, which occurs when PEY1(Ca^{2+}) is in excess. In this process, the complexes contain PEO molecules saturated with PEY1(Ca^{2+}) (saturated complex). Since the saturated complexes aggregate slowly, the PCC particles covered with the saturated complexes also aggregate slowly.

Xiao et al. pointed out that the complexes can build up multilayer on particle surface.[5] For clarity, Figure 11 only shows one layer of complexes on PCC surface for the *complex deactivation* process and the *complex saturation* process. However, in reality the complexes could have grown to multilayers until the surfaces were covered entirely by the deactivated complexes or the saturated complexes.

If we ignore the slow PCC flocculation when PEO is saturated by PEY1(Ca^{2+}), the collision efficiency E as proposed in equation (2) can be written as

$$E = 2\alpha \frac{\sigma_{PEY1}}{\sigma_{ttl}} \frac{\sigma_{PEO}}{\sigma_{ttl}} \quad (11)$$

where α is a constant resulting from charge repulsion between two approaching PCC particles, σ_{PEY1} is the PCC surface area covered with the active PEY1(Ca^{2+}) chains, σ_{PEO} is the surface area covered with the active PEO segments, and σ_{ttl} is the total surface area. It is clear from the equations (2) and (11) that the fastest flocculation occurs when the surface is covered half by the active peptides and half by the active PEO segments. The flocculation rate changes with time since both σ_{PEY1} and σ_{PEO} change with time. Flocculation proceeds until all the complexes are either deactivated or saturated. In addition, the flocculation rate can also be affected by shear rate and PCC surface charge density through the terms k_1 and α respectively. In the following paragraphs, many flocculation observations will be rationalized according to the proposed flocculation mechanism.

The Rationalization of Flocculation Observations

We have shown in Figure 2 that dissolved calcium ions are required to induce an effective PCC flocculation by PEO/PEY1. In the absence of calcium ions, the complexes contain individual PEO molecules with bound PEY1.[10] The strong electrostatic repulsion prevents the complexes from aggregating. When PEY1 and PEO 309 are added to PCC suspension sequentially in the absence of calcium ions, complex adsorption competes with PCC bridging by adsorbed complexes. Since the aggregation rate is largely hindered by the strong electrostatic repulsion between the adsorbed PEY1 chains, most PCC particles are stabilized by one layer of complexes before the flocculation can occur. However, in the presence of Ca^{2+} ions, around 60% of the carboxyl groups on PEY1 bind with Ca^{2+} ions[23] and PEO 309/PEY1(Ca^{2+}) complexes aggregate. Thus, the complexes can build up a multilayer on the PCC surface and function as the bridges to couple PCC particles.

The interplay of the three processes in Figure 11 can be applied to explain the PEO/PEY1 ratio effect on PCC flocculation. When PEO is in excess, PCC flocculation competes with complex deactivation. The fastest flocculation occurs when the PCC surface is covered half by active PEO segments and half by active PEY1(Ca^{2+}) molecules. The flocculation proceeds until all the complexes are deactivated. When the PEO/PEY1 ratio is above the optimal flocculation ratio, increasing the ratio increases the probability of PEY1(Ca^{2+}) deactivation by PEO and thus decrease PCC flocculation rate. When the PEO/PEY1 ratio is below the optimal ratio, decreasing the ratio increases the electrostatic repulsion between the adsorbed complexes, also leading to a decreased flocculation rate. When PEY1 is in excess, PCC flocculation is competing with the complex saturation process. Before PEO is saturated by PEY1(Ca^{2+}), the flocculation proceeds at a fast rate through the attachment of active PEO on one particle to active PEY1(Ca^{2+}) on another particle. Once PEO is saturated, PCC aggregates at a relatively

slow rate since the saturated complexes aggregate slowly. Indeed, Figure 4 shows clearly that PCC flocculation was a two-step process when PEY1(Ca^{2+}) was in excess.

Since the earliest flocculation studies with PEO/phenolic resin combinations, it has been known that flocculation efficacy is a strongly increasing function of PEO molecular weight in the range 0.5 MDa to 8 MDa. The reason for this extreme sensitivity has never been adequately explained. For example, PEO N-12K (MW=1 MDa) and PEY1(Ca^{2+}) form the complexes with an average diameter of 70 nm, which is larger than the thickness of two electrical double layers around the PCC particles (40 nm). However, the sequential addition of PEY1 and PEO N-12K gives no flocculation (Figure 5).

We propose that PEO of lower molecular weight gives a faster PEY1(Ca^{2+}) deactivation rate. At the initial stage of flocculation, PEO N-12K/PEY1(Ca^{2+}) complexes adsorb on the PCC surface with active PEY1(Ca^{2+}) chains. However, the complexes are too small to penetrate two electrical double layers and induce flocculation. With time, the adsorbed complexes build up a multilayer. At the same time, most of the active PEY1(Ca^{2+}) chains become deactivated, resulting in no flocculation. When PEO 309 (MW=8 MDa) is used, the PEY1(Ca^{2+}) deactivation rate is decreased. Thus, the adsorbed complexes can grow far beyond the two electrical double layers and at the same time remain active to cause flocculation.

Figure 6 shows that increasing shear rate could increase both the flocculation rate and the steady state flocculation extent. However, we found in our previous report that increasing the shear rate increases the deactivation rate of PEY1(Ca^{2+}) by PEO. An obvious explanation is that a higher shear rate leads to a higher PCC collision rate. The net result is that increasing shear rate has a higher effect on the PCC collision rate than on the PEY1(Ca^{2+}) deactivation rate and the flocculation is improved.

It was shown in our previous report that increasing NaCl concentration from 0.001 M to 0.04 M can increase the deactivation rate of PEY1(Ca^{2+}) by PEO. Thus, the PCC flocculation efficiency is reduced.

Figure 8 shows that PCC+DS flocculation has a lower flocculation rate than PCC flocculation. When PCC surfaces are covered with DS, the electrostatic and steric repulsions between DS and PEO/PEY1(Ca^{2+}) complexes decrease both the adsorption rate and the surface maximum coverage of the complexes. According to the equations (2) and (11), PCC flocculation rate is directly proportional to the square of the surface coverage by the complexes as both σ_{PEY1} and σ_{PEO} are proportional to the surface maximum coverage of the complexes. Thus, the flocculation rate decreases with the presence of DS on the PCC surface.

Figure 10 shows that adding PEO 309 (MW=8 MDa) before PEY1 leads to a lower flocculation rate than adding PEY1 before PEO 309. We speculate that this addition order effect relates to the dissolving property of PEO. PEO 309 stock solution was prepared by dissolving in water for 24 hours under gentle mixing. It is possible that many of the PEO chains remained entangled.[9] The entanglements can further decrease the PEY1(Ca^{2+}) deactivation rate. We have shown in our previous paper that pre-

shearing PEO 309 broke the entanglements and increase the PEY1(Ca^{2+}) deactivation rate.[10] Thus, when PEO 309 is added to the PCC+DS suspension first, PEO 309 entanglements are broken down, leading to a increased PEY1(Ca^{2+}) deactivation rate and a reduced flocculation rate.

Finally, we believe that the carboxyl groups on a cofactor assist the cofactor to adsorb on PCC+DS surface. For the past several years, we have carried out PCC flocculation tests using many cofactors, including PEY1, polystyrene-core polyvinyl phenol-shell particle, poly(vinyl phenol-co-styrene sulfonate potassium), and phenolic resin (commercial cofactor Oxirez from Ciba). All the above cofactors were negatively charged and were able to adsorb on a positively charged PCC surface, allowing an effective PCC flocculation. However, we found that only PEY1 could flocculate PCC+DS effectively.[11, 24] One of the most important differences between PEY1 and the other cofactors is that the charge groups on PEY1 are carboxyl groups, whereas on the others the charge is from sulfonate or sulfate groups. The charge repulsion between DS and sulfonate/sulfate groups prevent the adsorption of PEO/cofactor complexes. On the other hand, carboxyl groups have a high affinity to calcium ions[25], [26] and facilitate PEO/PEY1 complexes to adsorb on PCC+DS surface.

Conclusions

1. A new flocculation mechanism was proposed by combining Xiao et al's complex bridging flocculation mechanism and the PEO/PEY1(Ca^{2+}) complex aggregation mechanism. The new mechanism can be summarized into three processes:
    a. PCC flocculation - this process was adopted from Xiao et al's mechanism. PEO/PEY1(Ca^{2+}) complexes function as bridges to couple PCC particles.
    b. Complex deactivation – this is a new concept. When PEO is in excess, PEO/PEY1(Ca^{2+}) complexes undergo deactivation, in which PEY1(Ca^{2+}) loses the ability to couple PEO molecules. PCC flocculation proceeds until PCC surface is saturated with the deactivated complexes. This process prevents the flocculation from reaching completion.
    c. Complex saturation – this is a new concept. When PEY1 is in excess, PEO is saturated with PEY1(Ca^{2+}). Since the saturated complexes aggregate slowly, the PCC particles covered with the saturated complexes also aggregate slowly.
2. In the absence of soluble calcium ions, PCC particles are stabilized with PEO/PEY1 complexes, resulting in no flocculation.
3. Poorly dissolved PEO solution contains entanglements which decreases the deactivation rate of PEY1(Ca^{2+}). Pre-shearing the poorly dissolved PEO solution before adding PEY1 breaks down the entanglements, resulting in a reduced flocculation rate.
4. Carboxyl groups on a cofactor have a high affinity to calcium ions and facilitate the adsorption of PEO/cofactor complexes on the PCC+DS surface.

Table 1. PCC mobilities in different polymer solutions. [NaCl]=0.001 M, T=25°C, pH was adjusted to 7.8 using HCl. NaCl, HCl, and PCC were premixed. Required polymer solutions were added in the order as indicated in the table. Mobility error bar is one standard deviation of 10 measurement cycles.

Samples	Mobility ($m^2 V^{-1} s^{-1} \times 10^{-8}$)
500 mg/L PCC	+0.60 ± 0.01
500 mg/L PCC → 2.5 mg/L PEO N-12K	+0.56 ± 0.02
500 mg/L PCC → 5 mg/L PEY1	-2.15 ± 0.05
500 mg/L PCC → 5 mg/L PEY1 → 2.5 mg/L PEO N-12K	-0.61 ± 0.01
500 mg/L PCC → 10 mg/L DS	-2.17 ± 0.02
500 mg/L PCC → 10 mg/L DS → 5 mg/L PEY1	-2.15 ± 0.04
500 mg/L PCC → 10 mg/L DS → 2.5 mg/L PEO N-12K	-2.20 ± 0.04
500 mg/L PCC → 10 mg/L DS → 5 mg/L PEY1 → 2.5 mg/L PEO N-12K	-0.83 ± 0.03

Table 2. Ca^{2+} depletion on PCC mobility at 25°C. Required components were added in the order as indicated in the table. The mobility error bar is one standard deviation of 10 measurement cycles.

Samples	Mobility ($m^2\ V^{-1}\ s^{-1} \times 10^{-8}$)
500 mg/L PCC + 0.002 M Na^+ + 0.0004 M EDTA (pH=9.8)	-1.26 ± 0.05
500 mg/L PCC + 0.002 M Na^+ + 0.0004 M EDTA → 5 mg/L PEY1 (pH=9.8)	-3.27 ± 0.04
500 mg/L PCC + 0.002 M Na^+ + 0.0004 M EDTA → 5 mg/L PEY1 → 2.5 mg/L PEO 309 (pH=9.8)	-1.44 ± 0.08
125 mg/L PCC + 0.002 M Na^+ (pH=9.7)	-0.46 ± 0.04
125 mg/L PCC + 0.002 M Na^+ + 0.0005 M $CaCl_2$ (pH=9.7)	+0.57 ± 0.03
125 mg/L PCC + 0.002 M Na^+ + 0.0005 M $CaCl_2$ → 10 mg/L DS (pH=9.8)	-2.66 ± 0.05

Table 3. PCC mobilities with the pre-mixed PEO/PEY(Ca^{2+}) complex solution. T=25 °C, pH=7.5. The mobility error bar is one standard deviation of 10 measurement cycles.

Samples	Mobility ($m^2\ V^{-1}\ s^{-1} \times 10^{-8}$)
500 mg/L PCC + 0.001 M NaCl + 0.0007 M $CaCl_2$ + 10 mg /L DS	-2.30 ± 0.05
30 mg/L PEY + 1.5 mg/L PEO N-60 + 0.0007 M $CaCl_2$ → 500 mg/L PCC + 10 mg/L DS	-2.29 ± 0.02
15 mg/L PEY + 1.5 mg/L PEO N-60 + 0.0007 M $CaCl_2$ → 500 mg/L PCC + 10 mg/L DS	-2.00 ± 0.03
5 mg/L PEY + 1.875 mg/L PEO N-60 + 0.0007 M $CaCl_2$ → 500 mg/L PCC + 10 mg/L DS	-1.12 ± 0.02

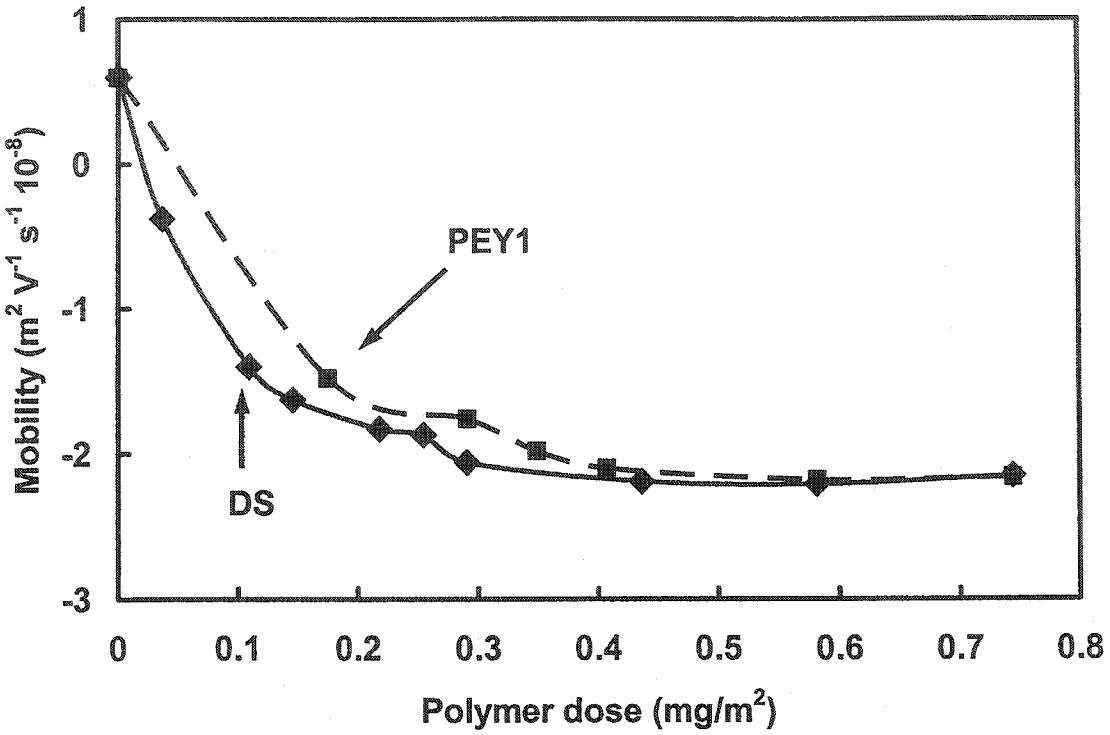

Figure 1. **PCC electrophoretic mobilities as a function of DS/PEY1 concentration. [PCC]=0.5 g/L, [NaCl]=0.001 M, pH=7.8, T=25°C. pH was adjusted by addition of HCl. The concentration unit of the added polymers is normalized to PCC surface area and is defined as mass of adsorbed polymer per m^2 of the PCC particle surface.**

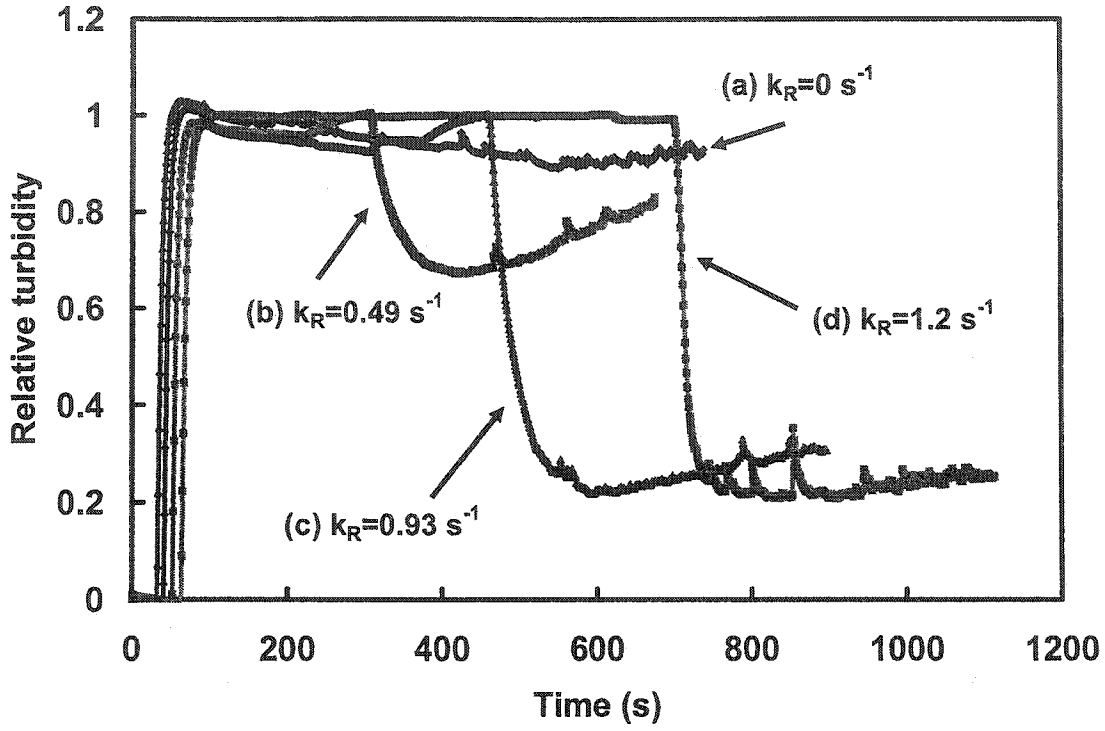

Figure 2. **Ca^{2+} effect on PCC flocculation by PEO 309/PEY1. [PCC]=0.5 g/L, [PEO]=2.5 mg/L, [PEY1]=5 mg/L, T=25°C, pH was adjusted by the addition of NaOH and [Na^+] was adjusted by the addition of NaCl. PCC was first premixed with the salts. PEY1 and PEO were added sequentially with an interval of 60 seconds. (a) [EDTA]=0.0004 M, [Na^+]=0.002 M, pH=9.8; (b) [Na^+]=0.002 M, pH=9.8; (c) [Na^+]=0.002 M, [$CaCl_2$]=0.0005 M, pH=9.8; (d) [Na^+]=0.002 M, [$CaCl_2$]=0.0005 M, pH=9.7, [DS]=10 mg/L, DS was premixed with PCC before the PEY1 addition.**

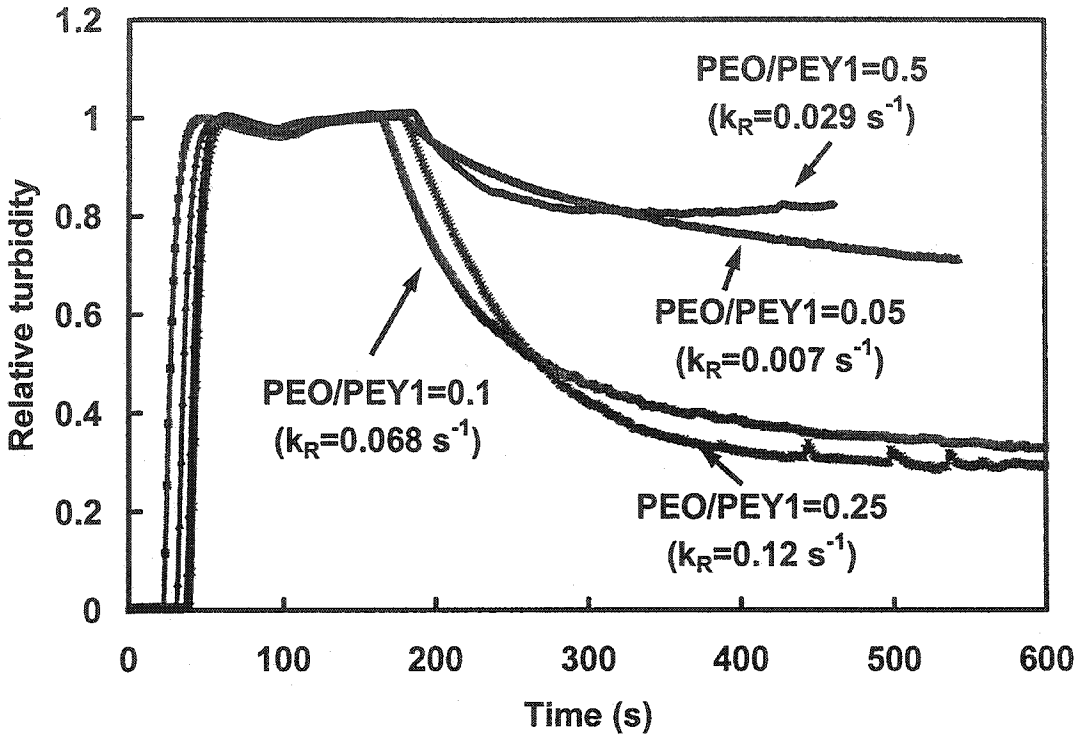

Figure 3. **PCC flocculation with different PEO N-60/PEY1(Ca^{2+}) mass ratios. [PCC]=0.5 g/L, [NaCl]=0.001 M, [PEY(Ca^{2+})]=10 mg/L, pH was adjusted to 7.8 by the addition of HCl, T=25°C. PCC was premixed with salt before the addition of PEY1. PEO was introduced around 60 s after the addition of PEY1 to initiate the flocculation.**

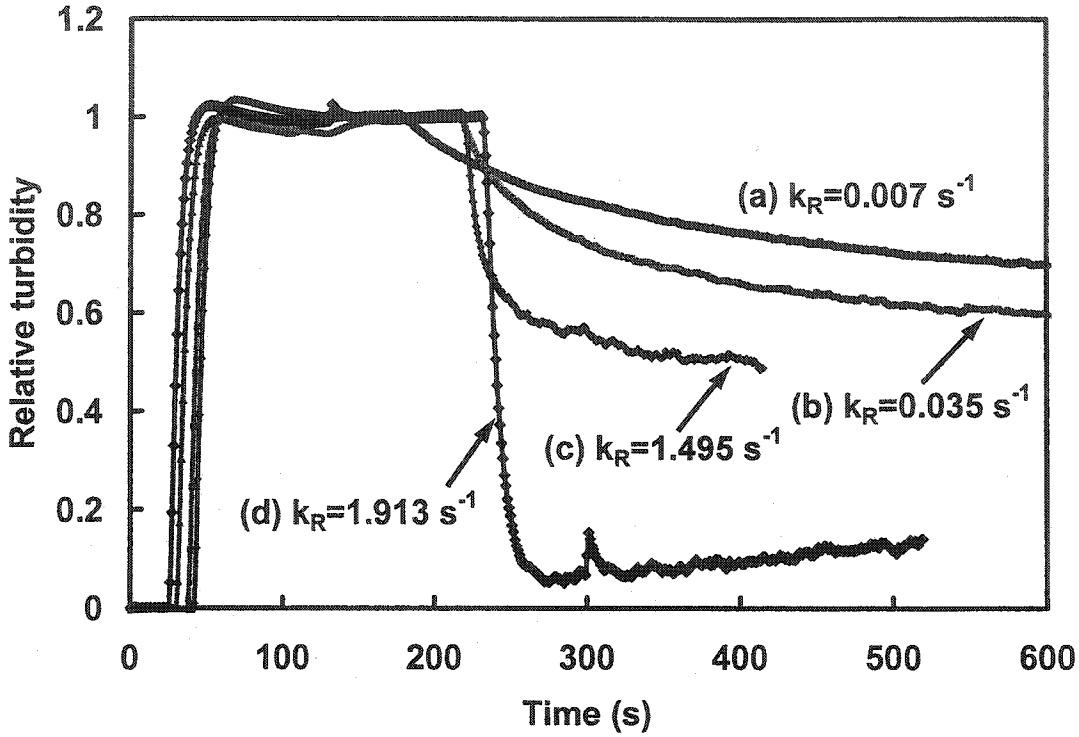

Figure 4. **PEO N-60/PEY1(Ca^{2+}) concentration effect on PCC flocculation at a constant PEO/PEY1(Ca^{2+}) mass ratio of 0.05. The pH was adjusted to 7.8 by the addition of HCl, T=25°C, [PCC]=0.5 g/L. PCC was premixed with salt before the addition of PEY1. PEO was introduced more than 60 s after the addition of PEY1 to initiate the flocculation. (a) [PEO]=0.5 mg/L, [PEY1]=10 mg/L; (b) [PEO]=1 mg/L, [PEY1]=20 mg/L; (c) [PEO]=2.5 mg/L, [PEY1]=50 mg/L; (d) [PEO]=11.25 mg/L, [PEY1]=45 mg/L.**

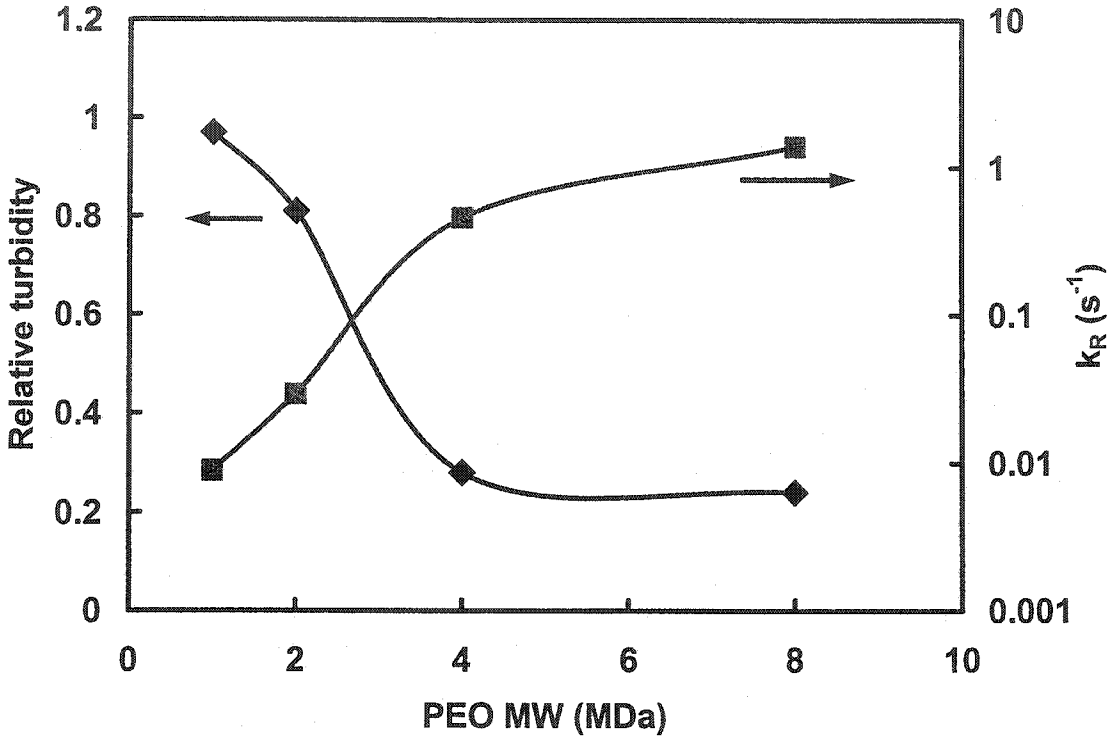

Figure 5. **PCC flocculation with PEO of different MWs. [PCC]=0.5 g/L, [NaCl]=0.001 M, [PEY1(Ca^{2+})]=10 mg/L, [PEO]=5 mg/L, pH was adjusted to 7.8 by the addition of HCl, T=25°C. PCC was premixed with salt before the addition of PEY1. PEO was introduced more than 60 s after the addition of PEY1 to initiate the flocculation.**

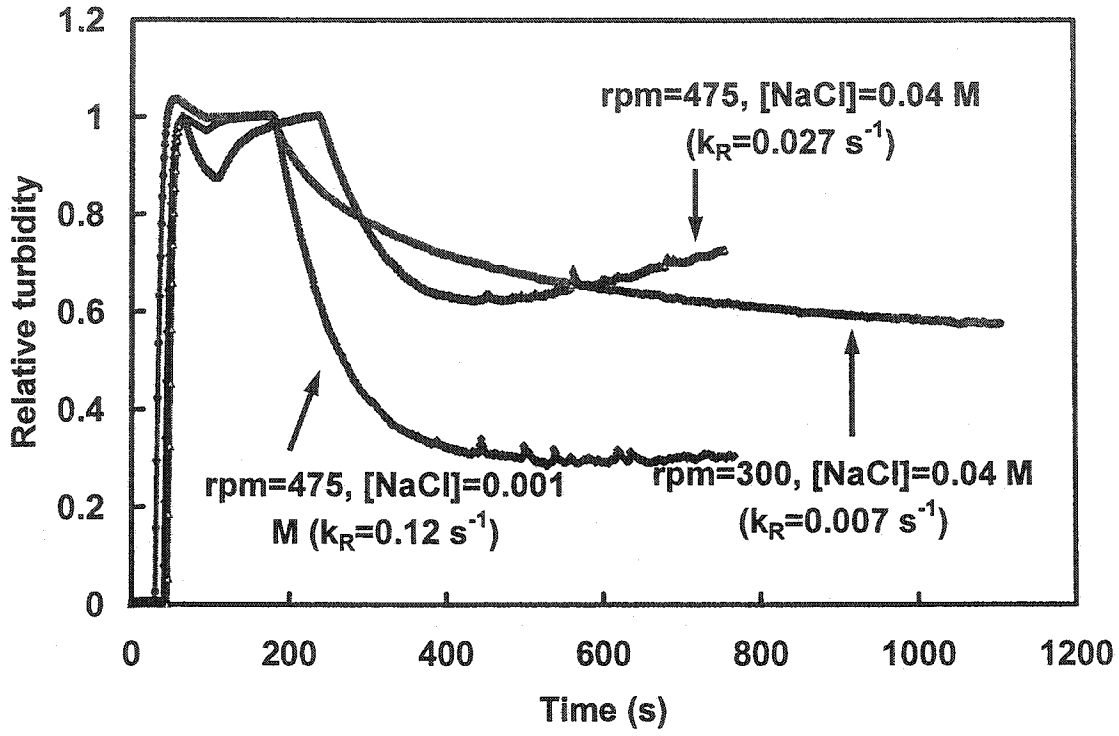

Figure 6. **The effects of NaCl concentration and shear rate on PCC flocculation. [PCC]=0.5 g/L, [PEY1(Ca^{2+})]=10 mg/L, [PEO N-60]=5 mg/L, pH was adjusted to 7.8 by the addition of HCl, T=25°C. PCC was premixed with salt before the addition of PEY1. PEO was introduced more than 60 s after the addition of PEY1 to initiate the flocculation.**

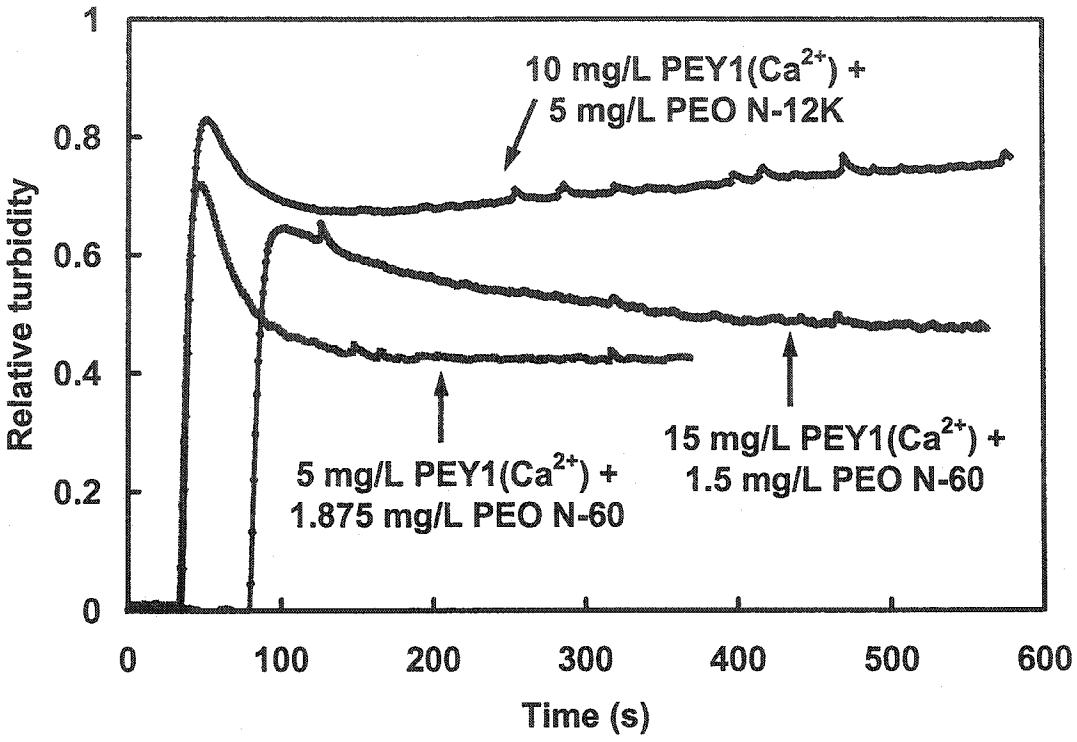

Figure 7. **PCC flocculation by pre-mixed PEO/PEY1(Ca^{2+}). pH was adjusted to 7.8 by the addition of HCl, T=25°C. PEO and PEY1 were premixed in the presence of 0.0007 M $CaCl_2$ for 5 minutes. 2 mL of 50 g/L PCC was then added to give a total volume of 200 mL.**

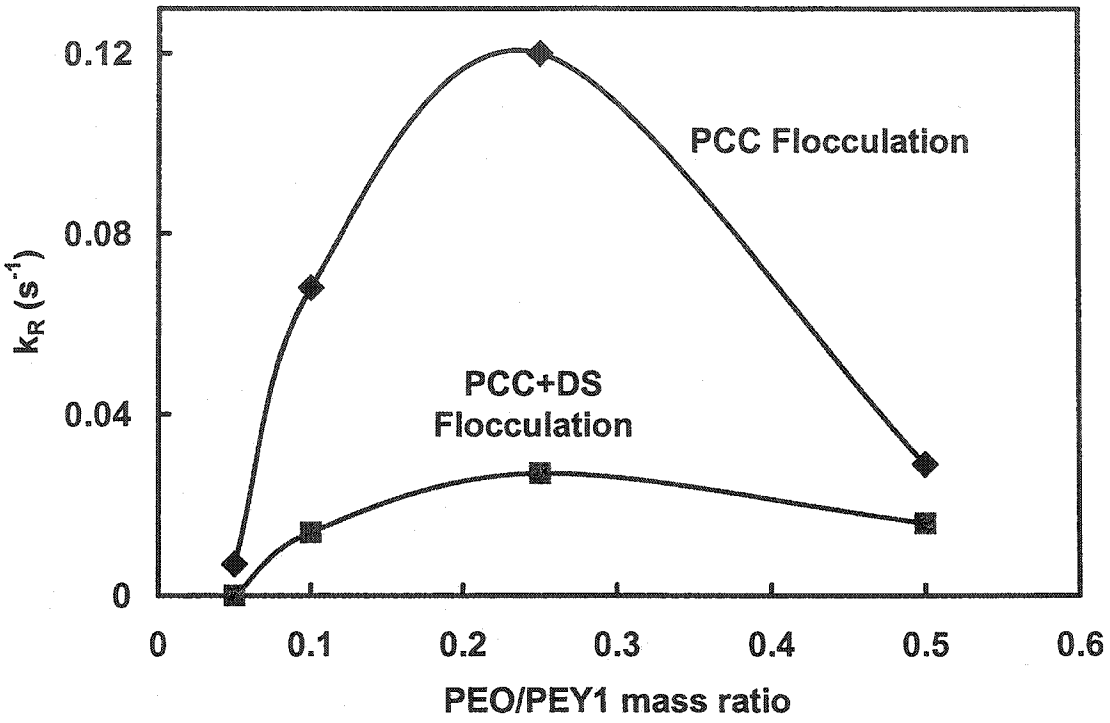

Figure 8. **The initial flocculation rates of PCC and PCC+DS versus PEO/PEY1 mass ratio. For PCC+DS flocculation, PCC was premixed with DS before the additions of PEY1 and PEO. [PCC]=0.5 g/L, [PEY1]=10 mg/L, [NaCl]=0.001 M, pH was adjusted to 7.8 by the addition of HCl, T=25°C. PEO was introduced more than 60 s after the addition of PEY1 to initiate the flocculation.**

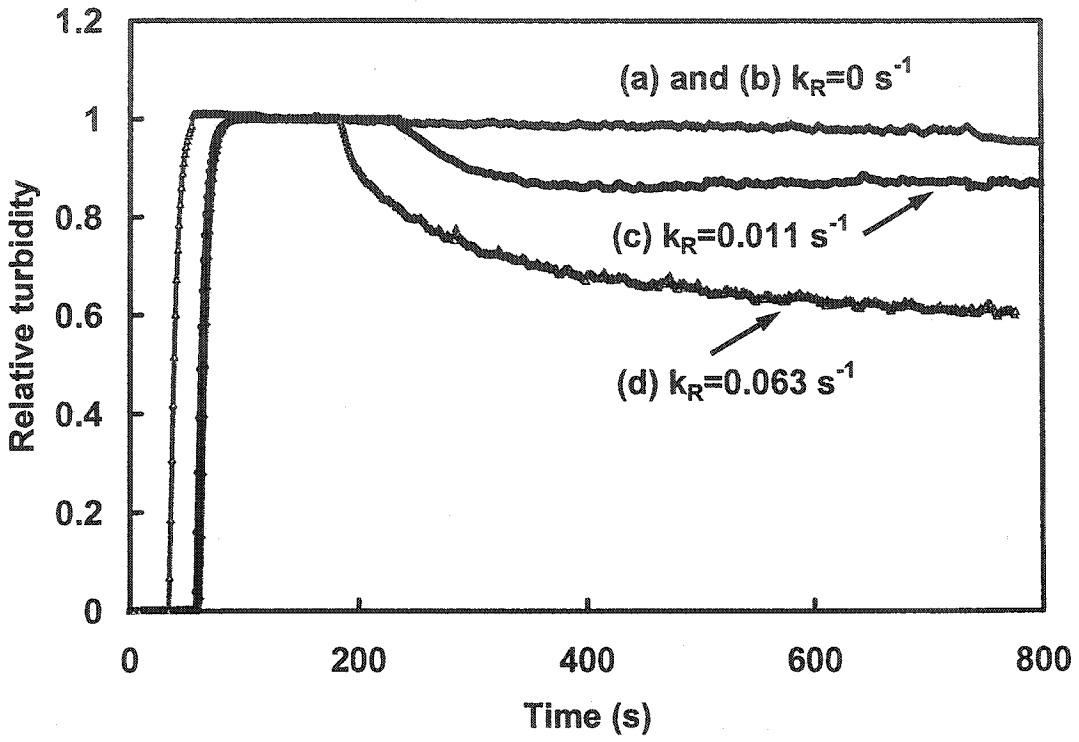

Figure 9. **PCC+DS flocculation with premixed PEO/PEY1(Ca^{2+}) at 25°C. (a) 15 mg/L PEY1 and 1.5 mg/L PEO N-60 were premixed in the flocculation testing vessel in the presence of 0.001 M NaCl and 0.0007 M $CaCl_2$. Premixed PCC and DS were added to give 0.5 /L PCC and 10 mg/L DS; (b) 5 mg/L PEY1 and 1.875 mg/L PEO N-60 were premixed in the flocculation testing vessel in the presence of 0.001 M NaCl and 0.0007 M $CaCl_2$. Premixed PCC and DS were added to give 0.5 g/L PCC and 10 mg/L DS; (c) 0.5 g/L PCC, 0.001 M NaCl, 0.0007 M $CaCl_2$, and 10 mg/L DS were premixed in the flocculation testing vessel. 1.875 mg/L PEO N-60 was added more than 60 seconds after the addition of 5 mg/L PEY1 to initiate flocculation; (d) 0.5 g/L PCC, 0.001 M NaCl, and 10 mg/L DS were premixed in the flocculation testing vessel and pH was adjusted to 7.8 using HCl. 1.5 mg/L PEO N-60 was added more than 60 seconds after the addition of 15 mg/L PEY1 to initiate the flocculation.**

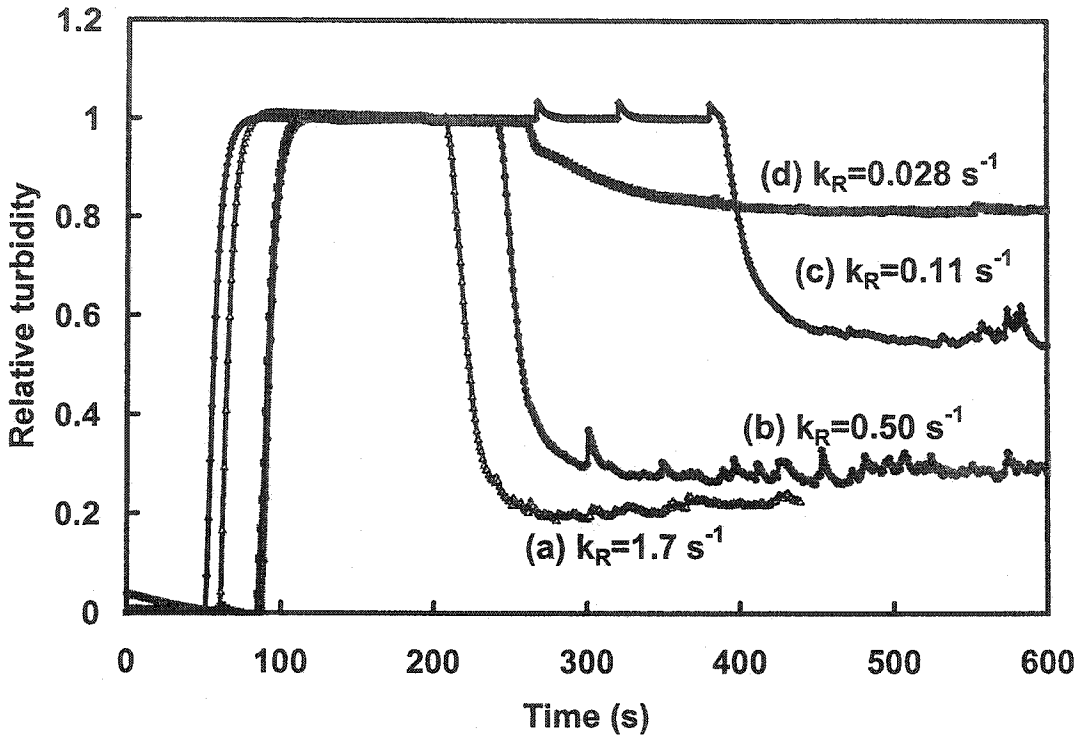

Figure 10. Effect of PEO/PEY1 addition order on PCC+DS flocculation at 25°C. 0.5 g/L PCC, 0.001 M NaCl, and 10 mg/L DS were premixed in the flocculation testing vessel. pH was adjusted to 7.8 by HCl. [PEO 309]=2.5 mg/L, [PEY1=5 mg/L. (a) PEO 309 was added 60 seconds after the addition of PEY1 (b) PEY1was added 5 seconds after the addition of PEO 309; (c) PEY1was added 260 seconds after the addition of PEO 309; (d) PEY1and PEO 309 were premixed and introduced into flocculation vessel to initiate flocculation.

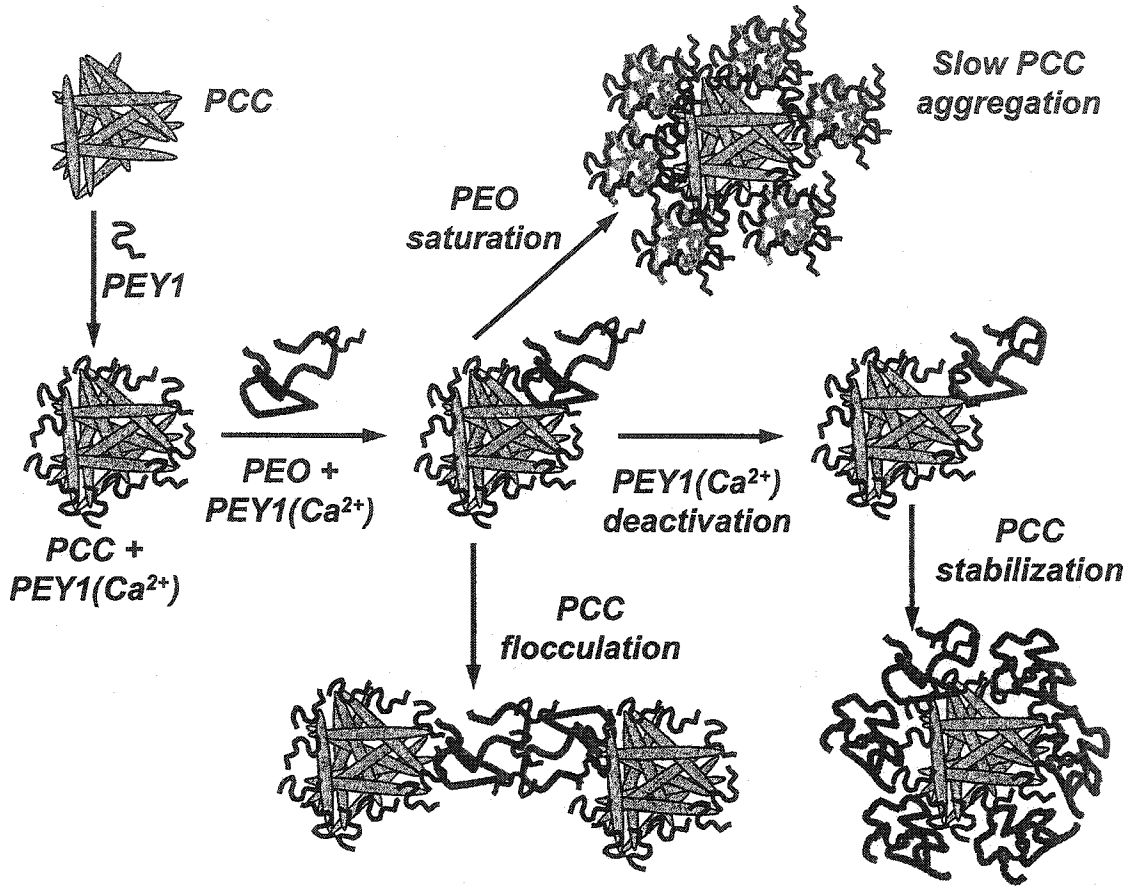

Figure 11. The schematic illustration of PCC flocculation by PEO and PEY1.

References

[1] Neimo, L. *Papermaking Chemistry*, Fapet Oy, Helsinki, 1999.

[2] Pelton, R. H.; Allen, L. H.; Nugent, H. M. *Svensk Papperstidn.* **1980**, *83*, 251.

[3] Carrard, J. P.; Pummer, H. *U.S. Patent* 4,070,236, 1973.

[4] Xiao, H.; Pelton, R. H.; Hamielec, A. *Journal of Colloid and Interface Science* **1995**, *175*, 166.

[5] Xiao, H.; Pelton, R. H.; Hamielec, A. *Journal of Pulp and Paper Science* **1996**, *22*, J475.

[6] van de Ven, T. G. M. ; Alince, B. *Journal of Pulp and Paper Science* **1996**, *22*, J257.

[7] Stack, K. R.; Dunn, L. A.; Roberts, N. K. *Colloids and Surfaces A* **1993**, *70*, 23.

[8] Gibbs, A.; Pelton, R. H. *Journal of Pulp and Paper Science* **1999**, *25*, 267.

[9] Kratochvil, D.; Alince, B.; van de Ven, T. G. M. *Journal of Pulp and Paper Science* **1999**, *25*, 331.

[10] Lu, C.; Pelton, R. H. The Supermolecular Structures of PEO/Tyrosine-containing Polypeptides, personal communications.

[11] Lu, C. ; Pelton, R. H. ; Valliant, J. ; Bothwell, S. ; Stephenson, K. *Langmuir* **2002**, *18*, 4538.

[12] Lu, C.; Pelton, R. H. *Langmuir* **2001**, *17*, 7770.

[13] Saffman, P. G.; Turner, J. S. *J. Fluid Mech.* **1956**, *1*, 16.

[14] Gregory, J.; Nelson, D. W. *A New Optical Method for Flocculation Monitoring*, in *Solid-Liquid Separation*, Gregory, J. Eds., Ellis Horwood: Chichester, 1984, p172.

[15] Gregory, J. *Journal of Colloid and Interface Science* **1985**, *105*, 357.

[16] Ohshima, H. *Journal of Colloid and Interface Science* **1994**, *163*, 474.

[17] Attia, Y. A.; Rubio, J. *Br. Polym. J.* **1975**, *7*, 135.

[18] van de Ven, T. G. M. *Journal of Pulp and Paper Science* **1997**, *23*, J447.

[19] Foxall, T.; Peterson, G.; Rendall, H. M.; Smith, A. L. *Journal of Chemical Society Faraday Transaction* **1979**, *75*, 1034.

[20] Lu, C.; Srokowski E.; Pelton, R. H. *Aqueous Complex Formation between Poly(ethylene oxide) and Tyrosine-containing Polypeptides*, private communication.

[21] Pelton, R. H.; Allen, L. H.; Nugent, H. M. *Pulp Paper Can.* **1980**, *81*, 54.

[22] Gibbs, A.; Pelton, R. H.; Cong, R. *Colloids and Surfaces A* **1999**, *159*, 31.

[23] Lu, C. PhD Thesis, Appendix 1, McMaster University.

[24] Lu, C.; Pelton, R. H. *Journal of Colloid and Interface Science* **2002**, *254*, 101.

[25] Zhang, W.; Nilsson, S. *Macromolecules* **1993**, *26*, 2866.

[26] Satoh, M.; Komiyama, J.; Iijima, T. *Biopolymers* **1982**, *21*, 1927.

Chapter 8 Concluding Remarks

Dual-component flocculants are commonly employed in the papermaking process to incorporate fillers and fines into the paper sheet. At present, three main types of dual-component flocculants are used: (1) a high charge density low molecular weight cationic polymer followed by a low charge density high molecular weight anionic polymer (polyelectrolyte complex flocculants); (2) a low charge density high molecular weight cationic polymer followed by an anionic colloidal particle (microparticle flocculants); (3) an anionic phenolic polymer (cofactor) followed by high molecular weight PEO. This thesis deals with the PEO/cofactor flocculation mechanism.

For the past two decades, many researchers have made contributions to understanding the mechanism of PEO/cofactor flocculation. Xiao et al. proposed the complex bridging mechanism to explain many flocculation observations. According to the complex bridging mechanism, PEO and cofactor form aqueous complexes, which can adsorb on the colloid surface and function as bridges to flocculate colloids (see Figure 3 in Chapter 1). Both the complex formation and the complex adsorption are necessary for an effective flocculation. van de Ven et al. further proposed that the association between PEO and cofactor decreases PEO configurational entropy, facilitating the adsorption of PEO on fiber and filler surfaces.

However, two important issues about the PEO/cofactor flocculation mechanism still remain to be resolved. (1) The complex formation is essential for an effective flocculation. Thus, it is necessary to understand the complex formation mechanism and incorporate it to the complex bridging flocculation mechanism. (2) The extent of PEO/cofactor flocculation depends on many experimental conditions and rarely reaches one hundred percent. However, the mechanism that prevents complete flocculation is still unknown.

Three major challenges to understanding the PEO/cofactor flocculation mechanism have inhibited previous researchers:

1. Most commercial cofactors are phenolic resins prepared by condensation polymerization. The complicated structures and the broad molecular weight distribution of such cofactors hinder the characterization of PEO/cofactor complexes.
2. New methods were required to investigate some aspects of PEO/cofactor complexes, such as the energetics of complex formation and the structures of bonded cofactors.
3. The need to understand the links between complex structure and the flocculation mechanism.

The objectives of this work were: (1) to develop well defined model cofactors; (2) to extend our knowledge of the PEO/cofactor flocculation mechanism.

The major contributions of this work include:

1. For the first time, polypeptides were used as papermaking flocculants. Specifically, tyrosine-containing polypeptides (TCP) were used as model cofactors to study the

mechanism of PEO/cofactor flocculation. Compared to the commercial cofactors prepared by condensation polymerization, TCP cofactors have well-defined structures and are suitable for mechanistic studies. Furthermore, PEO/TCP aqueous complexes are stable at a broad pH range (from pH 2 to pH 10) and may be used as new biomaterials for drug delivery, bio-sensor, and many other applications.

2. For the first time, circular dichroism (CD) and isothermal titration calorimetry (ITC) were applied to study PEO/TCP complex formation. TCP cofactors are optically active and circular dichroism was able to detect TCP secondary structure change upon complex formation with PEO. ITC was used to measure the energetics of PEO/cofactor binding, providing direct evidence of TCP structure effects on binding affinity.
3. PEO/TCP complexes were characterized at three distance scales. The first distance scale corresponds to the size of an amino acid moiety and involves the interaction between the individual polymer segments. The second distance scale corresponds to the length of a polymer chain. The third distance scale corresponds to the size and shape of the overall complexes. Furthermore, the characterization of the complexes was carried out in the presence of 0.001 M $CaCl_2$ because soluble calcium ions are present in many papermaking suspensions and because the presence of soluble calcium ions was found to increase PEO/TCP flocculation extent.
    a. At the segmental distance scale, the driving force of the binding between PEO and TCP phenolic groups was the entropy gain associated with release of water. More hydrophobic polypeptides containing phenylalanine moieties did not bind to PEO, suggesting non-specific hydrophobic interactions did not dominate complex formation.
    b. At the polymer chain distance scale, the association between PEO and TCP was a high affinity binding. TCP chains have only a few points of attachment to PEO and such points involve more than three closely spaced phenolic groups. At the same time, the minimum PEO molecular weight for binding to tyrosine rich polypeptides is between 350 and 5000 Da and the minimum molecular weight of 1:1 poly(tyrosine-glutamic acid) for binding to high molecular weight PEO is between 1.1 and 36 kDa.
    c. The supermolecular structure of aqueous PEO/TCP complexes in the presence of calcium ions depends upon many experimental conditions, such as the shearing rate, the PEO molecular weight, and the PEO/TCP ratio. A kinetic mechanism was proposed to control the supermolecular structure. According to this mechanism, TCP act as crosslinkers to couple PEO molecules. To account for the finite complex size, two new concepts, TCP deactivation and PEO saturation (see Figure 13 in Chaper 6 for definitions), were introduced in this work. During complex formation, PEO coupling competes with TCP deactivation by PEO or PEO saturation by TCP and increasing the rates of TCP deactivation and PEO saturation decreases the molar mass of PEO/TCP complexes.

4. The complex bridging flocculation mechanism of Xiao et al. was extended by taking into consideration TCP deactivation and PEO saturation (see Figure 13 in Chapter 7 for details). In this mechanism, filler particles are flocculated by PEO/cofactor complexes. Meanwhile, flocculation competes with TCP deactivation and PEO saturation. Complexes with only deactivated TCP or saturated PEO stabilize filler particles sterically. The extended complex bridging flocculation mechanism can also be applied to explain microparticle flocculation and polyelectrolyte complex flocculation.
5. A latex-based cofactor with polystyrene-core poly(vinyl phenol)-shell (PS-PVPh) was prepared by the surfactant-free emulsion polymerization of p-acetoxystyrene monomer in the presence of polystyrene seed particles followed by base hydrolysis.
6. The maximum PEO adsorption on the PS-PVPh particle surface is over six times greater than that adsorbed on the polystyrene surface. PS-PVPh particles are almost completely flocculated over a broad range of PEO concentrations in contrast to polystyrene latex. An extension of the spreading model of Pelssers et al. coupled with standard treatments of polymer adsorption kinetics and coagulation kinetics gives good predictions of the maximum extent of flocculation for polystyrene latex. It was not necessary to invoke spreading to simulate the PS-PVPh particle flocculation curves.
7. PS-PVPh particles enhance the ability of PEO to flocculate polystyrene latex. When composite particles are added after PEO, they bridge together PEO coated particles and aggregates. When composite particles are added before PEO, they act as bridging agents and adsorb PEO in an extended configuration ideal for flocculation.

Appendix 1 Supplementary Materials for Chapter 5

Experimental

Potentiometric Titration

To determine the binding fraction of Glu groups on PEY1 with Ca^{2+} ions, potentiometric titrations were carried out using a calcium ion selective electrode (ISE) (Thermo-Orion) and an automatic Burette (Man-Tech) controlled by software PC-Titrate version 2.0 (Man-Tech). 50 mL peptide solution containing 160 mg/mL peptide and 0.001/0.04 M NaCl was introduced to the titration vessel and thermo stated at 25°C. 0.1 M $CaCl_2$ was gradually added to the titration beaker using precision step motor under gentle stirring and the corresponding electrode voltage was recorded by computer. Background titrations were conducted by titrating 0.001M and 0.04 M NaCl solutions with $CaCl_2$ in the absence of peptides. The fraction of bound Glu groups was derived accordingly by assuming one Ca^{2+} ion bound with two Glu groups.

Results

Capillary Electrophoresis of PEO/PEYA(Ca2+) Complexes

Figure 1 shows capillary electrophoresis results of PEO 309/PEYA(Ca^{2+}) complexes. PEYA is a 1:1:1 terpolymer of tyrosine, alanine and glutamic acid. Unlike PEY1, there is only one peak corresponding to free PEYA molecules when PEYA and PEO 309 were mixed in the absence of calcium ions. Thus, there was no interaction between PEO and PEYA or the fraction of PEO bound PEYA was below detection limit. In the presence of 0.002 M $CaCl_2$, The peak corresponding to the free PEYA chains was present even when the PEO 309/PEYA(Ca^{2+}) mass ratio was 0.5, which was much higher than the PEO/PEYA(Ca^{2+}) mass saturation ratio of 0.2 determined from ITC. It seems that some PEYA(Ca^{2+}) molecules were not able to bind with PEO even when PEO was in large excess. Increasing the $CaCl_2$ concentration to 0.005 M reduced the peak intensity of the free PEYA molecules. The decreased PEYA peak intensity suggests that a greater fraction of PEYA(Ca^{2+}) attached to PEO 309. Furthermore, the complexes did not show a corresponding peak since they formed visible macroscopic gels, which was too large to enter capillary.

PEO Proton NMR

The NMR chemical shift of pure PEO proton was 3.71 ppm. The change of the PEO proton chemical shift in the presence of PEY1 was used to understand the PEO/PEY1 binding mechanism. Figure 2 shows PEO N-10 (MW = 100 kDa) one-dimensional proton spectra in the presence of PEY1. The PEY1 concentration was fixed at 0.5 g/L and the PEO concentration was varied from 5 mg/L to 25 mg/L. For curves b, c, and d, PEO was added to PEY1 solution in one injection. Decreasing the PEO/PEY1 mass ratio from 0.05 to 0.01 resulted in a PEO proton peak shift from 3.44 to 3.38 ppm. It is well known that aromatic rings can generate ring current effects. When a proton is close to the edge of the aromatic ring, its chemical shift moves to a higher frequency. When the proton is close to the top or the bottom of the ring, its chemical shift moves to a

lower frequency. PEO associates with the phenolic groups from the top and the bottom of the aromatic rings, thus the PEO proton chemical shift moved to a lower frequency. Decreasing PEO/PEY1 ratio decreased the average distance between PEO and phenolic groups, and thus the chemical shift of the PEO proton moved a greater position to the lower frequency.

In curve (a) of Figure 2, PEO N-10 was added to PEY1 in two injections. For the first injection, PEO was added to PEY1 solution to give 5 mg/L PEO. After 10 minutes, more PEO was added to give a final PEO concentration of 200 mg/L. The final PEO/PEY1 mass ratio of 0.4, which was higher than the mass saturation ratio of PEO/PEY1 (0.18). The PEO chemical shift split into two peaks. The narrow peak at 3.71 ppm was assigned to free PEO and the broad peak at 3.66 ppm was assigned to complexed PEO. However, there was no proton peak observed at 3.38 ppm, which corresponded to the peak at the PEO/PEY1 ratio of 0.05 before the addition of the second shot of PEO. It was possible that the average distance between PEO and PEY1 was controlled by the thermodynamics. When more PEO was added in the second shot, the average distance between PEO of the first shot and phenolics groups decreased to reach a more stable structure.

Ca2+ Binding to TCP

It is well known that polyGlu has high affinity to Ca^{2+} under aqueous conditions at neutral pH.[1,2] Figure 3 and Figure 4 confirmed above conclusions. Figure 3 shows the raw titration curves at 0.001 M/0.04 M NaCl. It is clear that more $CaCl_2$ solution was required for PEY1 solution to reach the same ISE voltage than that pure NaCl solution, indicating the binding between Ca^{2+} and PEY1. The binding fraction of Glu groups by Ca^{2+} ions as a function of $CaCl_2$ concentration is presented in Figure 4. At the low NaCl concentration of 0.001 M, the binding fraction showed a rapid increase to 50% at a low $CaCl_2$ concentration of 0.0001 M. Then, the binding fraction increased slowly to 60% when the $CaCl_2$ concentration was increased to 0.001 M. When the NaCl concentration was increased to 0.04 M, Na^+ ions competed with Ca^{2+} ions for the binding with Glu groups and the Glu binding fraction by Ca^{2+} increased slowly to 35% when $CaCl_2$ concentration was increased to 0.001 M..

It is important to know whether TCP(Ca^{2+}) can self-aggregate or not in order to under the complex formation mechanism. The self-aggregation of TCP(Ca^{2+}) was monitored by the light scattering intensity at 90 degree and the results are shown in Figure 5 and Figure 6. The scattering intensities of 50 mg/L PEY1(Ca^{2+}) and 50 mg/L PEYA(Ca^{2+}) at a 90 degree angle increased linearly from 5 kilo counts per second (kcnts/s) to 22 kcnts/s and 15 kcnts/s respectively 10 minutes after the addition of 0.001 $CaCl_2$. Higher $CaCl_2$ concentrations increased the rate of polypeptide aggregation. It was possible that the Ca^{2+} ions functioned as the bridges to couple peptide molecules.

Thermal Titration of PEY1 with PEO in 1 M Urea

Urea is known as an effective hydrogen bonding broker and was often used to verify the existence of hydrogen bonding between polymer complexes.[3] In Figure 7, the

thermal titration of PEY1 with PEO was carried out in 1 M urea to determine whether the binding between PEO and PEY1 phenolic groups was driven by hydrogen bonding or not. The positive binding peak in Figure 7 suggests the PEO/PEY1 complexes were not interrupted by urea and the driven force of PEO/ PEY1 binding was not hydrogen bonding.

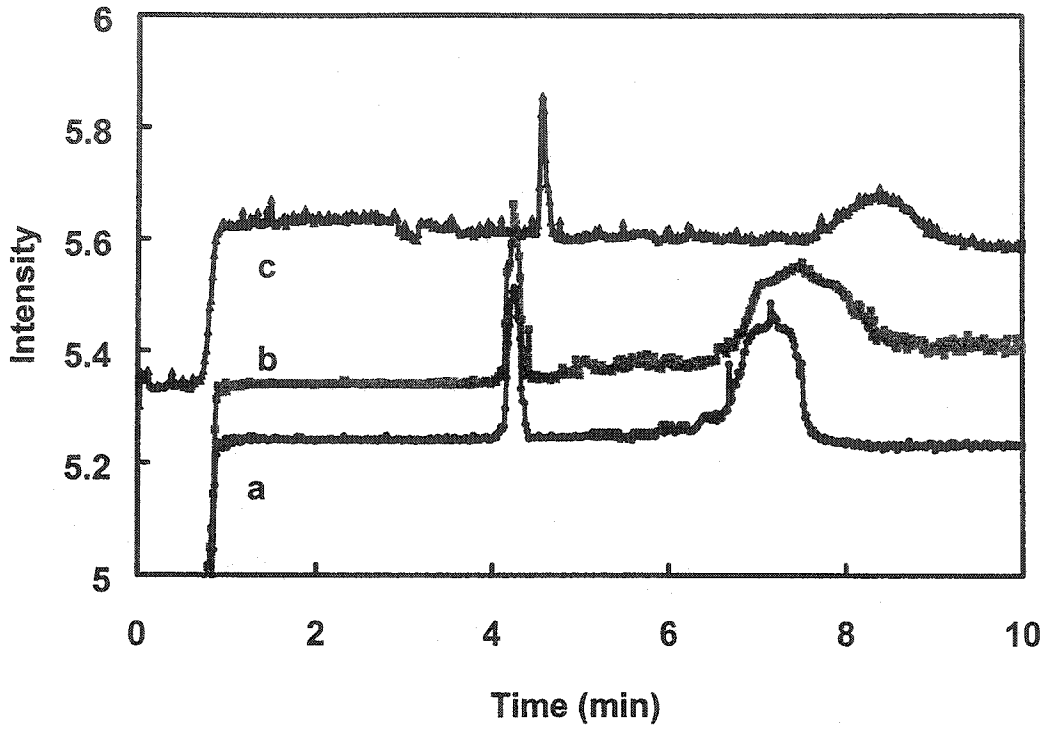

Figure 1. **The capillary electrophoresis measurements of PEO 309/PEYA(Ca^{2+}) in 0.01 M Tris buffer (pH=8) at 25°C. (a) [PEYA]=0.75 g/L; (b) [PEYA]=0.75 g/L,[PEO 309]=0.375 g/L, [$CaCl_2$]=0.002 M; (c) [PEYA]=0.5 g/L, [PEO 309]=0.375 g/L, [$CaCl_2$]=0.01 M.**

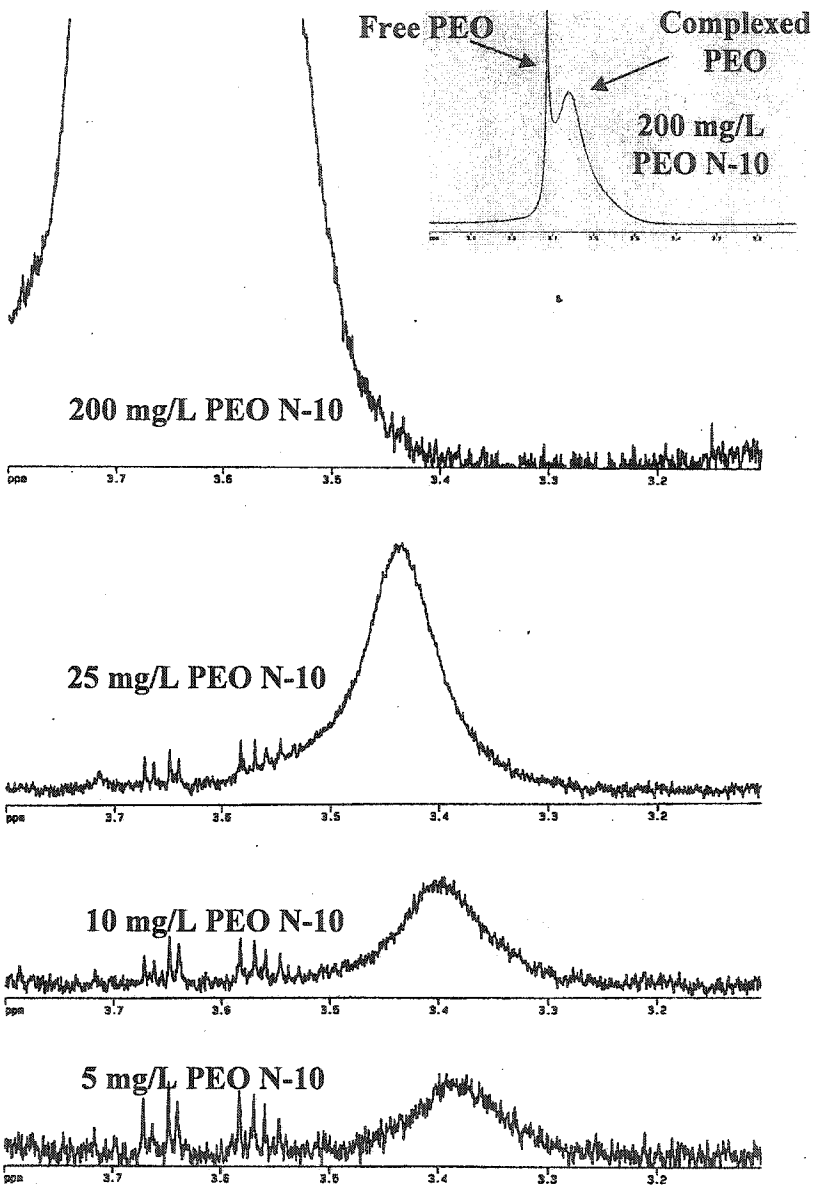

Figure 2. **One-dimensional proton NMR of PEO N-10 with different PEO N-10/PEY1 ratio at 30°C. [PEY1]=0.5 g/L. PEO was added to PEY1 in one injection and the final PEO concentrations were 5, 10, and 25 mg/L. For complex solution containing 200 mg/L PEO, PEO was first added in one injection to give a PEO concentration of 5 mg/L. After the complex solution was left stand for 10 minutes, a second injection of PEO was introduced to give a final PEO concentration of 200 mg/L.**

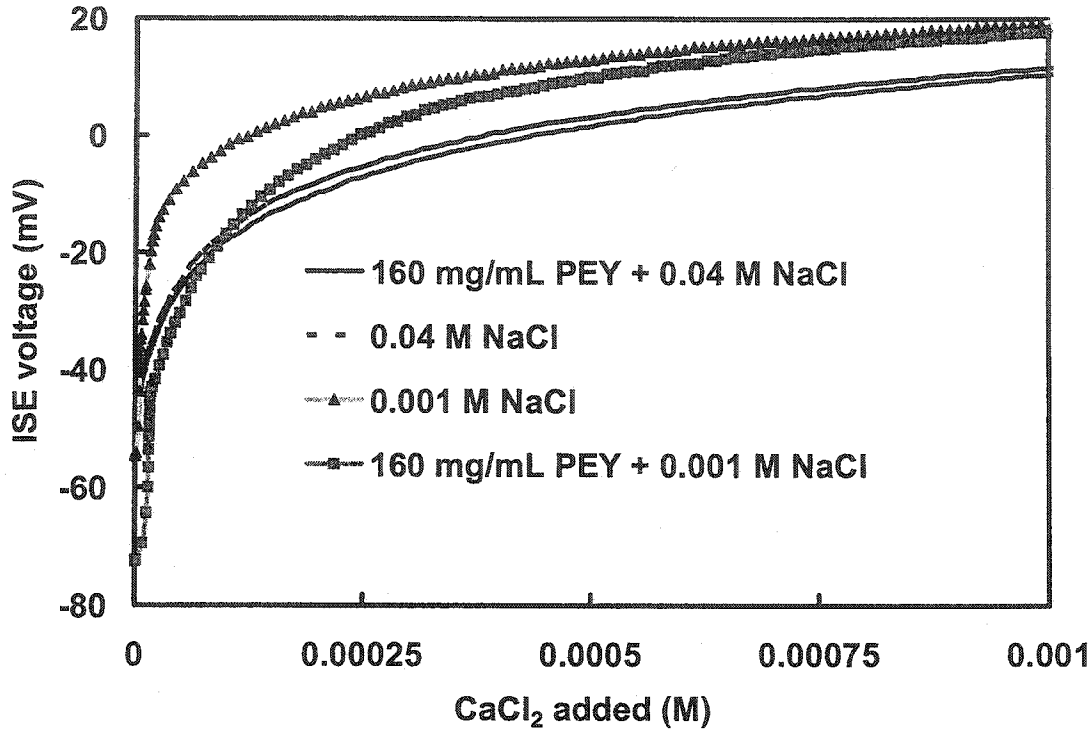

Figure 3. Potentiometric titration of 160 mg/mL PEY with 0.1 $CaCl_2$ at 25°C using a Ca^{2+} ion selective electrode.

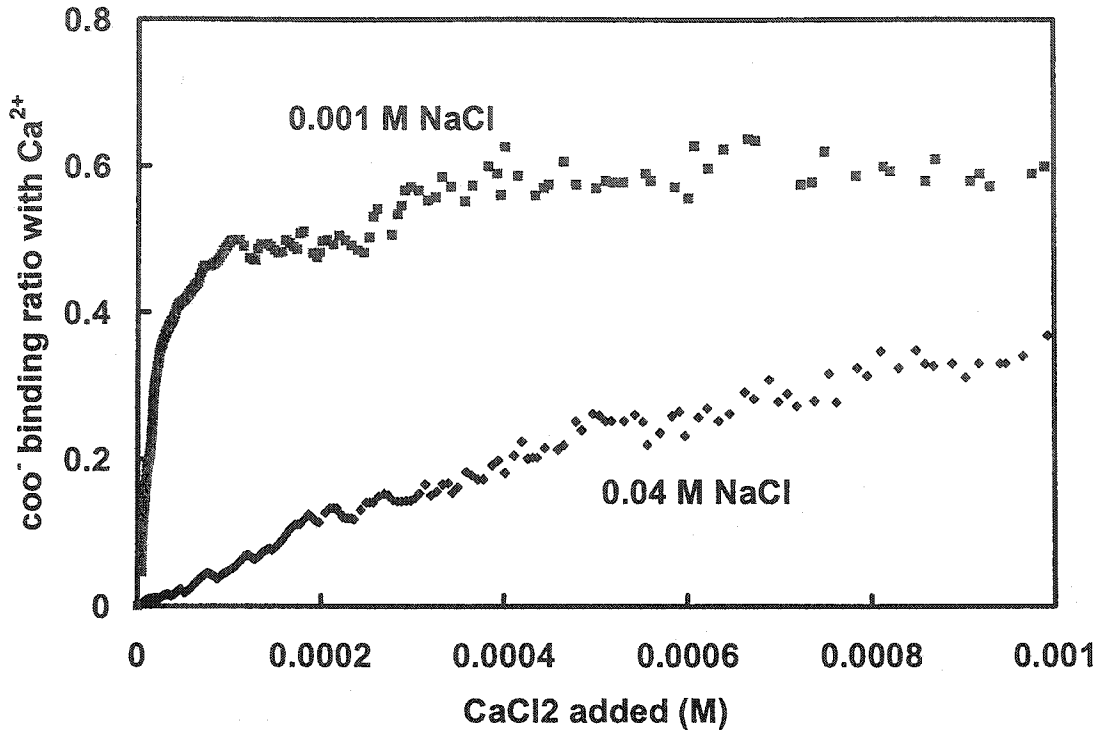

Figure 4. The binding fraction of PEY1 with Ca^{2+} ions as a function of $CaCl_2$ concentration at different NaCl concentrations at 25°C.

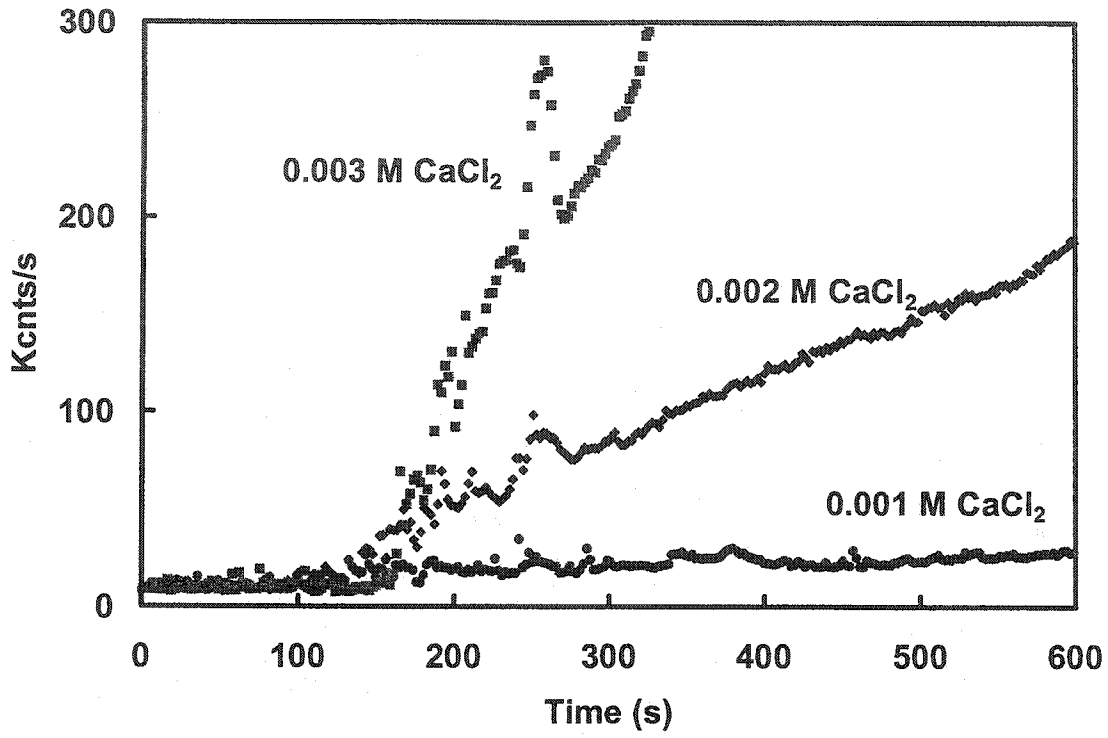

Figure 5. **Light scattering intensities of PEY1(Ca^{2+}) solutions as a function of time at different $CaCl_2$ concentrations. [PEY1]=50 mg/L, [NaCl]=0.001 M, T=25°C, $CaCl_2$ was added at 110th second for the 0.001 M $CaCl_2$ solution, at 140th second for the 0.002 M $CaCl_2$ solution, and at 160th second for the 0.003 M $CaCl_2$ solution.**

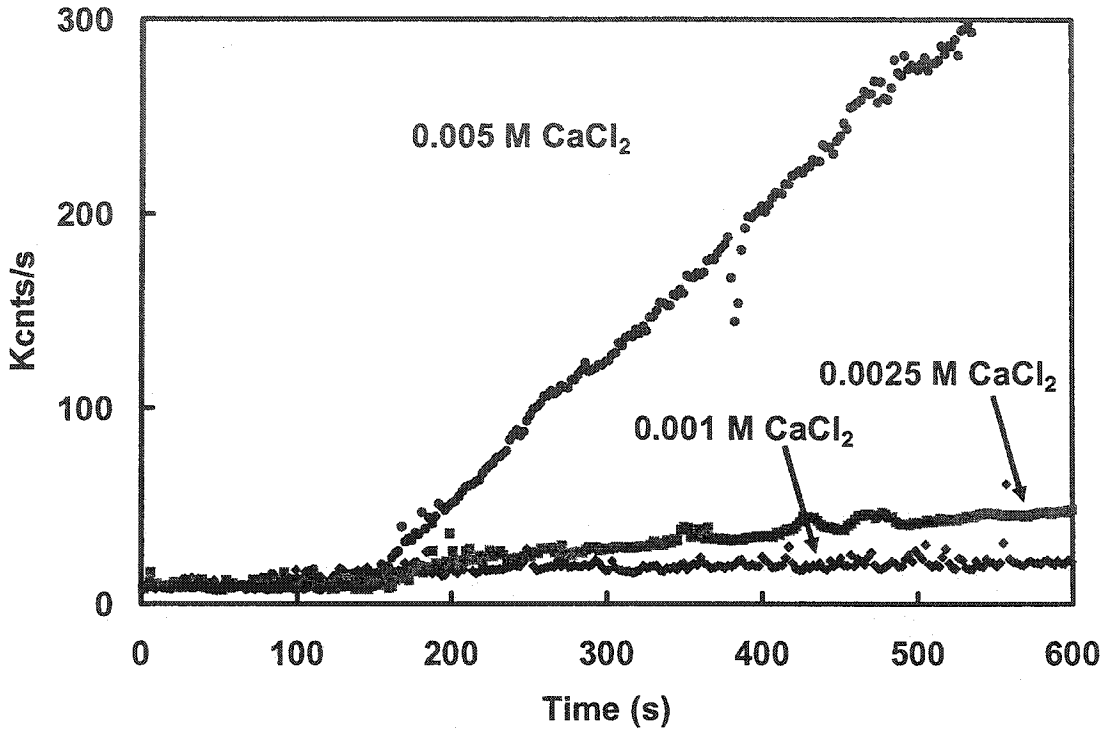

Figure 6. **Light scattering intensities of PEYA(Ca^{2+}) solutions as a function of time at different $CaCl_2$ concentrations. [PEYA]=50 mg/L, [NaCl]=0.001 M, T=25°C, $CaCl_2$ was added at 85th second for the 0.001 M $CaCl_2$ solution, at 150th second for the 0.002 M $CaCl_2$ solution, and at 150th second for the 0.003 M $CaCl_2$ solution.**

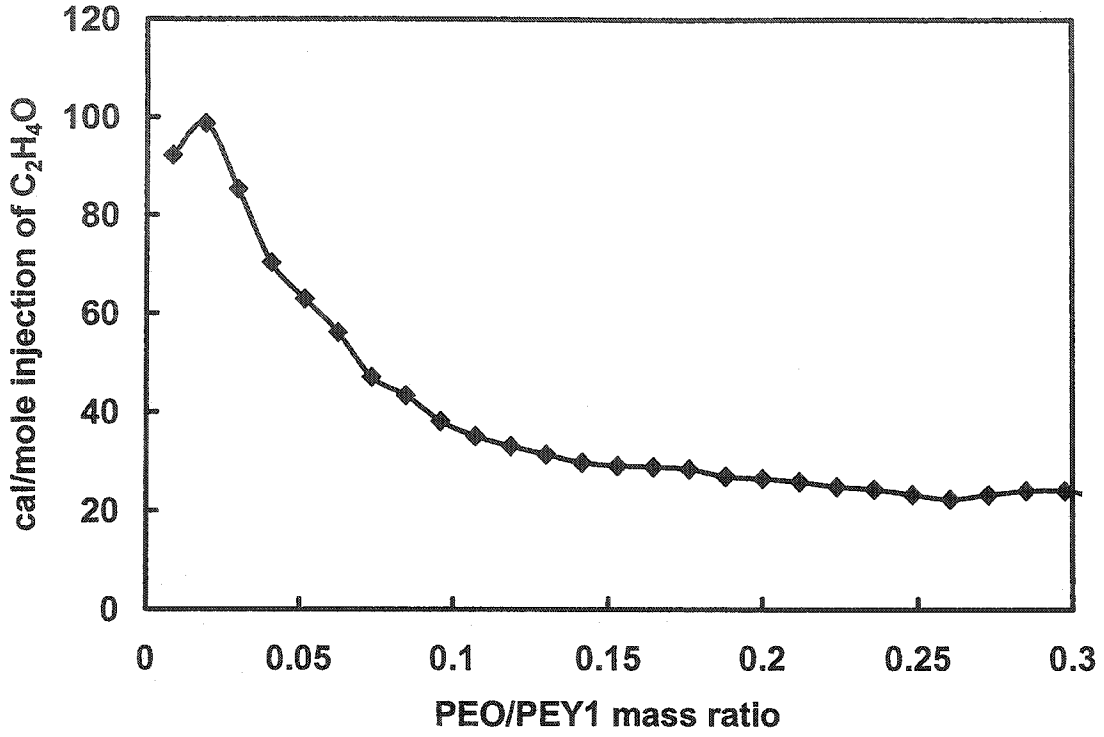

Figure 7. **ITC titrations of PEY1 with PEO N-10 (MW=100 kDa) in the presence of 1 M urea at 30°C. The sample was prepared in a buffer containing 0.01 mole/L Tris (pH=8) and 1 M urea. [PEY1]=0.4 g/L, [PEO]=0.6 g/L. 28 10-uL portions of PEO solution were injected into PEY1 solution during titration. The duration of each injection was 20 s and the time interval between each two injections was 240 s.**

References

[1] Zhang, W.; Nilsson, S. *Macromolecules* **1993**, 26, 2866.

[2] Satoh, M.; Komiyama, J.; Iijima, T. *Biopolymers* **1982**, 21, 1927.

[3] Ilman, F.; Tanaka, T.; Kokufuta, E. *Nature* **1991**, 349, 400.

Appendix 2 Supplementary Materials for Chapter 6 and Chapter 7

Results

Figure 1 shows the effect of $CaCl_2$ concentration on the supermolecular structure of PEO N-12K/PEYA(Ca^{2+}) complexes. In this experiment, $CaCl_2$ was first added to a 50 mg/L PEYA solution and the resulted solution was stirred for 30 seconds. $CaCl_2$ concentrations were chosen to be 0.001 M, 0.0025 M, and 0.005 M. At the end of 30 seconds, the light scattering intensity of the PEYA solution increased from around 9 to 13, 18, and 38 kcnts/s respectively. Then, the concentrated PEO solution (0.5 g/L) was added to PEYA(Ca^{2+}) solutions in one injection and the solutions was stirred for another 30 minutes. It can be seen that increasing the $CaCl_2$ concentration increased both the hydrodynamic diameter and the light scattering intensity of the PEO/PEYA(Ca^{2+}) complexes. It appears that the association between the carboxyl groups on PEYA and calcium ions caused the aggregation of PEYA(Ca^{2+}). A higher Ca^{2+} concentration led to larger PEYA(Ca^{2+}) aggregates before the addition of PEO. Upon the addition of PEO, the larger PEYA(Ca^{2+}) aggregates resulted in a higher aggregation level of the PEO/PEYA(Ca) complexes.

Figure 2 shows the effect of $CaCl_2$ concentration on PCC+DS flocculation by PEO and PEYA at the pH of 7.8. In the absence of $CaCl_2$, the sequential additions of PEO and PEYA induce no flocculation. When 0.001 M $CaCl_2$ M was added, the PCC suspension was flocculated slightly and the relative turbidity decreased to 0.92 at the steady state. When the $CaCl_2$ concentration was further decreased to 0.0025 M and 0.005M, the steady state relative turbidity decreased to 0.80 and 0.58. It is clear that increasing $CaCl_2$ concentration increased the flocculation extent. By comparing Figure 1 and Figure 2, we found the flocculation extent of PCC+DS correlated closely to the aggregation level of PEO/PEYA(Ca^{2+}) complexes form the aspect of the $CaCl_2$ concentration.

Figure 3 shows the effect of PEO molecular weight on PCC flocculation by PEO and PEY1. This figure corresponds to the original flocculation results of Figure 5 in Chapter 7. Figure 4 shows the effect of PEO/PEY1 ratio on PCC+DS flocculation. This figure corresponds to the original flocculation results of Figure 8 in Chapter 7.

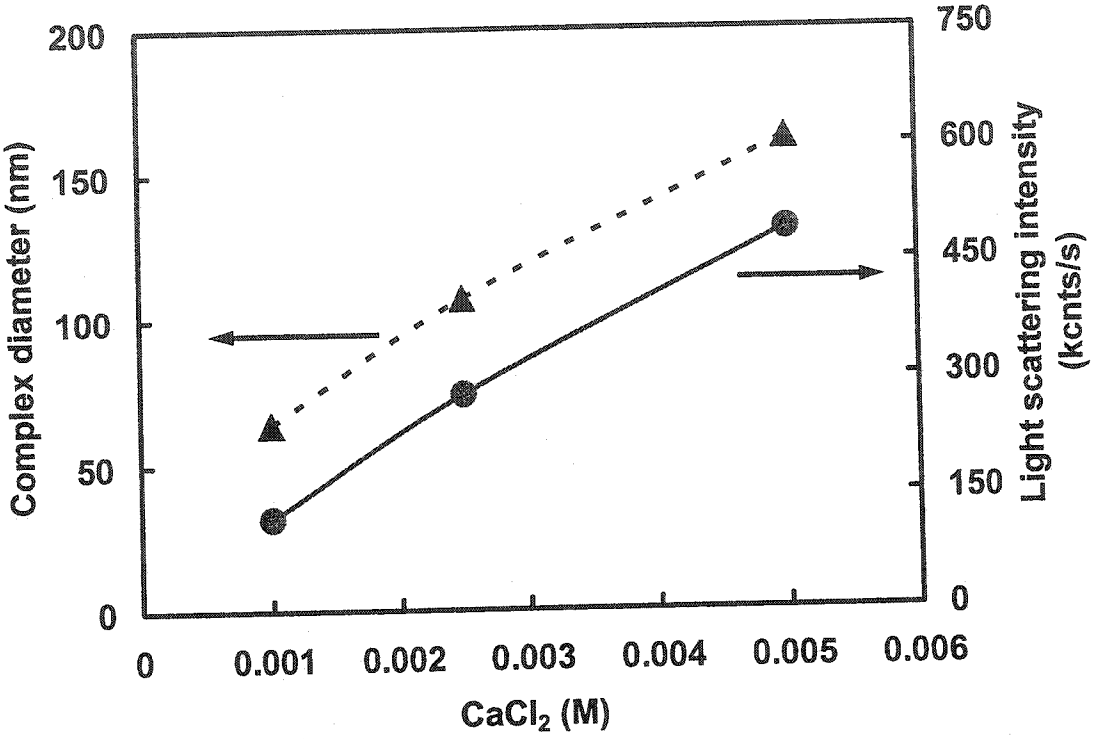

Figure 1. **The effect of $CaCl_2$ concentration on the supermolecular structure of PEO N-12K/PEYA(Ca^{2+}) complexes. [PCC]=0.5 g/L, [PEYA]=50 mg/L, [PEO N-12K]=25 mg/L, [NaCl]=0.001 M, [$CaCl_2$]=0.001 M, T=25°C. PEYA was first mixed with NaCl and $CaCl_2$. The PEO solution (0.5 g/L) was then added in one injection under stirring.**

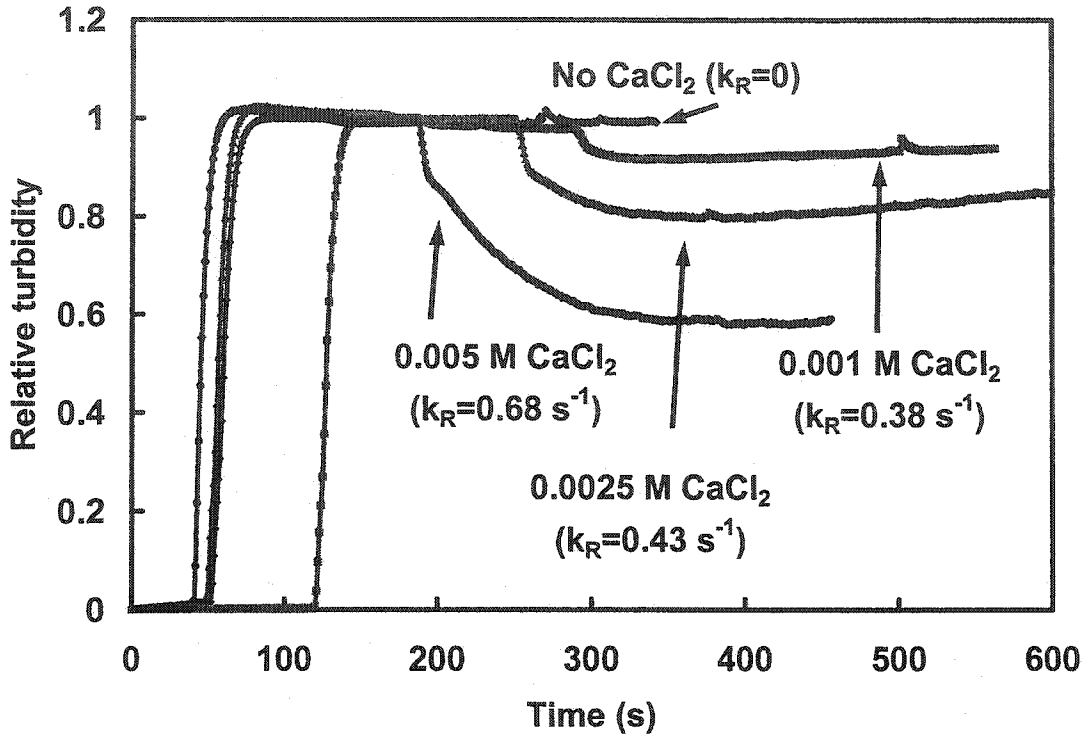

Figure 2. **The effect of $CaCl_2$ concentration on PCC+DS flocculation by PEO 309 and PEYA. [PCC]=0.5 g/L, [PEO 309]=5 mg/L, [PEY1]=10 mg/L, [NaCl]=0.001 M, pH was adjusted to 7.8 by the addition of HCl, T=25°C. PEO was introduced more than 60 s after the addition of PEY1 to initiate the flocculation.**

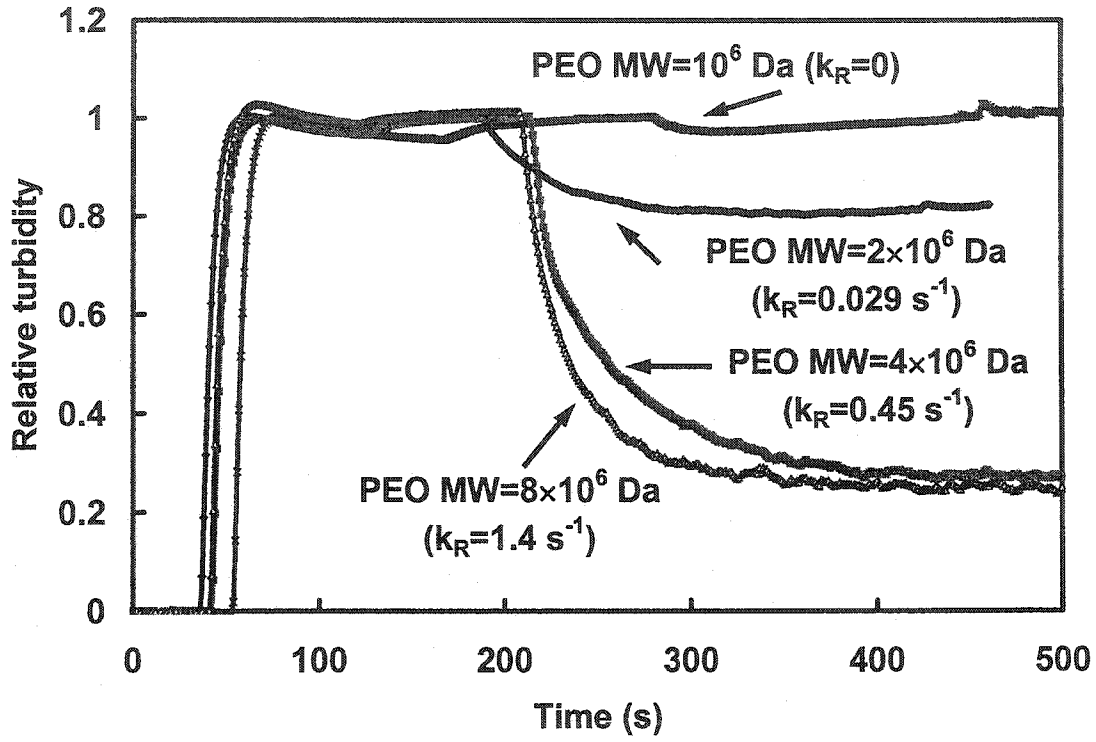

Figure 3. **PCC flocculation with PEO of different MWs. [PCC]=0.5 g/L, [NaCl]=0.001 M, [PEY1(Ca^{2+})]=10 mg/L, [PEO]=5 mg/L, pH was adjusted to 7.8 by the addition of HCl, T=25°C. PCC was first premixed with salt before the addition of PEY1. PEO was introduced more than 60 s after the addition of PEY1 to initiate the flocculation.**

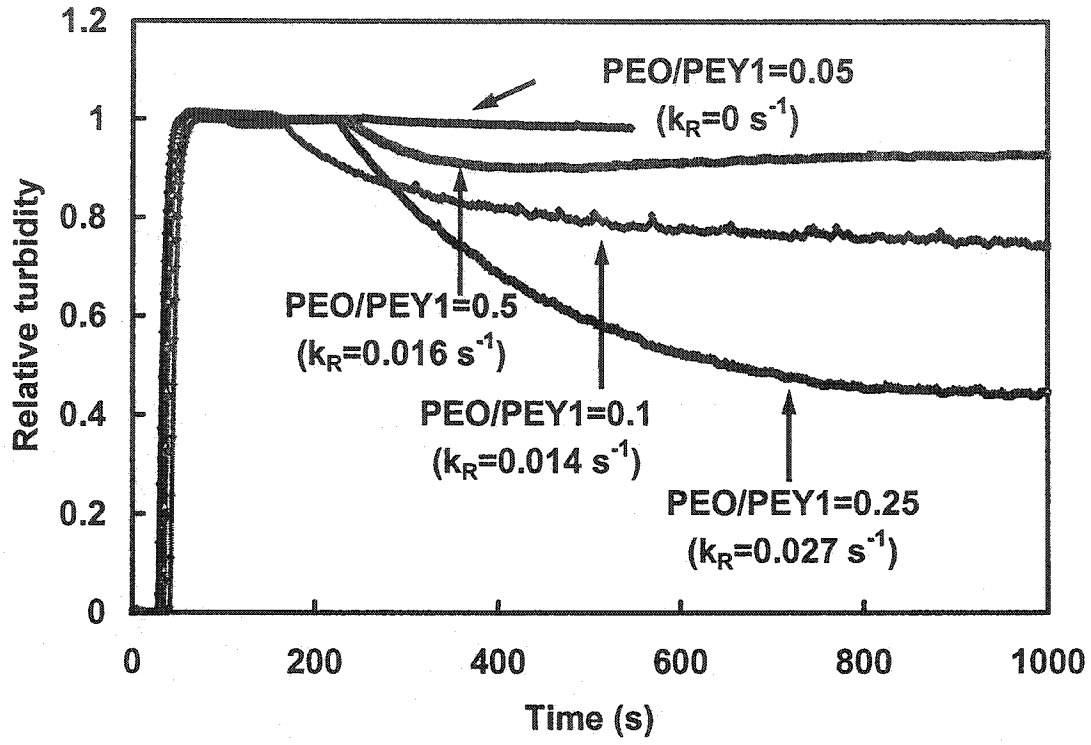

Figure 4. **PCC+DS flocculation as a function of PEO/PEY1 mass ratio. PCC was premixed with DS before the additions of PEY1 and PEO. [PCC]=0.5 g/L, [PEY1]=10 mg/L, [NaCl]=0.001 M, pH was adjusted to 7.8 by the addition of HCl, T=25°C. PEO was introduced more than 60 s after the addition of PEY1 to initiate the flocculation.**